Novel roles of hepatitis C virus NS5A domain I in virus genome replication and assembly

Shucheng Chen

Submitted in accordance with the requirements for the degree of Doctor of Philosophy

The University of Leeds

Faculty of Biological Sciences

School of Molecular and Cellular Biology

October 2022

The candidate confirms that the work submitted is her own and that appropriate credit has been given where reference has been made to the work of others.

Acknowledgements

After more than four years of graduate studies in University of Leeds, I have to say that I harvested a lot from science and the life in a different country. I really appreciate this fantastic experience and thanks everyone who joined this long journey with me!

Firstly, I am incredibly grateful for my supervisor Prof. Mark Harris for giving me the opportunity to study in this laboratory! His patient supervision, excellent guidance and helpful comments gave me the confidence and bravery to complete my project. This project would not be possible without him. I am extremely grateful for the professional and excellent guidance he offered to me.

A special thanks to Greg Towers and Sophie Ridewood from UCL for kindly providing a series of host factors silenced constructs. I would also like to thank all my colleagues at the Garstang 9.47 and especially in the Harris group. They always showed me kind and warm-hearted help when I struggled.

Furthermore, I would like to thank an important person of my life: my partner Kaiwen. I am so lucky to have him in my PhD and my life. He companied me to come through all the hard time during this four-year. His caring love and constant encouragement made me a better person. He is the most shining star in this long night for me.

A big thanks to my parents who are the firmest refuge of mine. Although they are in China and far away from me during my PhD, they constantly care about me every time, every day. My mom is my best friend, she understands me, supports me and gives me the power whenever I was lost. It has been three years since our last reunion but I believe we will see each other very soon!

Finally, I would like thank the China Scholarship Council and University of Leeds Scholarship for funding this project and my life in UK. I would like also thank UK Medical Research Council for funding HCV studies in our lab.

Abstract

Hepatitis C virus NS5A is a multifunctional phosphoprotein comprised of three domains (DI, DII and DIII). DI and DII have been shown to function in genome replication, whereas DIII plays a role in virus assembly. A previous study in our lab demonstrated that DI in genotype 2a (JFH1) also participates in virus assembly, exemplified by the V67A/P145A mutant which exhibited no defect in genome replication, but blocked infectious virus production (Yin et al., 2018).

Here I extend this analysis to identify another five conserved and surface exposed residues proximal to V67/P145 (I52, G70, M72, P141 and E148), which shared the same phenotype in genome replication, and two additional residues proximal to P145 (C142 and E191), which exhibited the same phenotype in viral assembly.

The partially defective mutants (I52, G70, M72 P141 and E148) in replication were further investigated in genotype 3a (DBN3a), the phenotype of four mutants in DBN3 NS5A DI was consistent with JFH1 mutants. In parallel, to investigate the mechanism underpinning this replication role of domain I, we assessed the involvement of cyclophilin A (CypA). The CsA sensitive assay, CypA silenced Huh7.5 cell lines and GST pulldown assay all displayed the association between JFH1 NS5A DI and CypA. Additionally, the interaction of CypA and NS5A DI inhibited the activation of NF-κB pathway to allow HCV replication but not assembly. However, DBN3a replication was completely dependent on CypA, whose association with NS5A DI was not detected.

Further phenotypic analysis of C142A and E191A revealed changes in the abundance of dsRNA, the size and distribution of lipid droplets (LD) and the colocalisation between NS5A and LDs compared to wildtype. Additionally, to investigate the mechanism(s) underpinning this role of DI, we assessed the involvement of the interferon-induced double-stranded RNA-dependent protein kinase (PKR). In PKR-knockout cells, C142A and E191A exhibited levels of infectious virus production, LD size and colocalisation between NS5A and LD that were indistinguishable from wildtype. Co-immunoprecipitation and *in vitro* pulldown experiments confirmed that wildtype NS5A domain I (but not C142A or E191A) interacted with PKR. We further showed that the assembly phenotype of C142A and E191A was restored by ablation of interferon regulatory factor-1 (IRF1), a downstream effector of PKR.

These replication data revealed a complex interplay between NS5A domain I and CypA and this interaction protected HCV replication through inhibiting the NF-κB pathway. In additional, the assembly data suggested a novel interaction between NS5A DI and PKR that functions to evade an antiviral pathway which blocks virus assembly through IRF1.

Abbreviations

A	Ala, alanine
aa	Amino Acid
AH	Amphipathic helix
ALT	Alanine aminotransferase
ANXA2	Annexin A2
Apo	Apolipoprotein
AST	Aspartate aminotransferase
Bin1	Bridging integrator 1
BOC	Boceprevir
CHC	Chronic hepatitis C
CKII	Casein kinase II
CKIα	Casein kinase I
CLDN1	Claudin 1
CMV	Cytomegalovirus
Co-IP	Co-immunoprecipitation
CoVs	Coronaviruses
CREs	Cis-acting RNA elements
CsA	Cyclosporin A
Cyp	Cyclophilin
CypA	Cyclophilin A
CypB	Cyclophilin B
CypD	Cyclophilin D
CypI	Cyclophilin inhibitors
Cys	Cysteine
DAA	Direct-acting antiviral
DAPI	4’,6’-diamidino-2-phenylindole dihydrochloride
DBN3a	Genotype 3

DCV	Daclatasvir
DEPC	Diethyl pyrocarbonate
DGAT1	Diacylglycerol acyltransferase 1
DI	Domain I
DII	Domain II
DIII	Domain III
DMEM	Dulbecco’s Modified Eagles Medium
DMVs	Double membrane vesicles
dsRBM	DsRNA binding motif
dsRNA	Double-stranded RNA
E. coli	Escherichia coli
EC50	Half maximal effective concentration
EGF	Epidermal growth factor
eIF2α	Eukaryotic initiation factor 2
ER	Endoplasmic reticulum
ERK	Extracellular regulated kinase
ESCRT	Endosomal sorting complex required for the transport
FAPP2	Four-phosphate adaptor protein 2
FBS	Foetal bovine serum
GAGs	glycosaminoglycans
GBV-B	GB virus B
GCN2	General control nonderepressible kinase 2
GFP	Green fluorescent protein
GLB	Glasgow Lysis Buffer
GPS2	G protein pathway suppressor 2
GST	Glutathione Sepharose 4B
HAV	Hepatitis A virus
HBV	Hepatitis B virus
HCC	Hepatocellular carcinoma
HCV	Hepatitis C virus
HDL	High-density lipoproteins

HDV	Hepatitis D virus
HEK-293T	Human embryonic kidney 293T
HEV	Hepatitis E virus
hpe	Hours post-electroporation
HRI	Heme-Regulated eIF2 alpha kinase
HRS	Hepatocyte growth factor–regulated tyrosine kinase substrate
HS	Heparan sulfate
HSPGs	Heparan sulfate proteoglycans
huh7	Human hepatocellular carcinoma cell line 7
Huh7.5	Human hepatocellular carcinoma cell line 7.5
HVR	Hypervariable regions
IDUs	Injection drug use
IFN	Interferon
IL-I	Interleukin 1
IPTG	Isopropyl β-D-1-thiogalactopyranoside
IRES	Internal ribosomal entry site
IRF1	Interferon regulatory factor-1
IRF-3	Interferon regulatory factor 3
ISDR	Interferon sensitive determinant region
ISGs	Interferon stimulated genes
ISRE	IFN-stimulated response element
IU/mL	Infectious units per mL
JACop	Just-Another Co-localisation Plugin
JFH1	Genotype 2a
LB	Lysogeny broth
LCS	Low-complexity sequences
LDL	Low-density lipoproteins
LDL-R	LDL receptor
LDs	Lipid droplets
LDV	Ledipasvir
LVPs	Lipoviroparticles

maLDs	Microsome-associated LDs
MAPK	Mitogen-activated protein kinase
MFI	Mean fluorescence intensity
MHC-I	Major histocompatibility complex I
mJFH-1	Infectious virus of JFH1
MMVs	Multimembrane vesicles
MOPS	3-(n-morpholino)propanesulfonic acid
mSGR-luc-JFH1	JFH1 Sub-genomic replicons
MTP	Microsomal triglyceride transfer protein
MW	Membranous web
NAP1L1	Nucleosome assembly protein 1-like protein 1
NFAT	Nuclear factor of activated T-cells
NF-κB	Nuclear factor kappa B
NLPs	Nucleocapsid-like particles
NMR	Nuclear magnetic resonance
NPC1L1	Niemann-Pick C1-like 1 cholesterol absorption receptor
NS	Non-structural
NS2	Non-structural 2
NS3	Non-structural 3
NS4A	Non-structural 4A
NS4B	Non-structural 4B
NS5A	Non-structural 5A
NS5B	Non-structural 5B
OCLN	Occludin
ORF	Open reading frame
OSBP	Oxysterol binding protein
PCR	Overlap extension polymerase chain reaction
PePHD	PKR-eIF2α phosphorylation homology domain
PERK	PKR-like Endoplasmic Reticulum Kinase
PFA	Paraformaldehyde
PH	Pleckstrin homology

PI4KA	Phosphatidylinositol 4-kinase IIIα
PI4KIIIα	Phosphatidylinositol-4-kinase IIIα
PI4P	Phosphatidylinositol 4-phosphate
PKA	Protein kinase A
PKR	Double-stranded RNA-dependent protein kinase
PLA1A	Phosphatidylserine-specific phospholipase A1
PLB	Passive lysis buffer
Plk1	Polo-like kinase 1
PPIase	Peptidyl-prolyl isomerase
PSTPIP2	Proline-serine-threonine phosphatase interacting protein 2
PVDF	Polyvinylidene fluoride microporous membranes
RASs	Resistance-associated substitutions
RBD	RNA binding domain
RBV	Ribavirin
RC	Replicase complexes
RdRp	RNA-dependent RNA polymerase
RIG-I	Retinoic acid-inducible gene I
RLU	Relative light units
RT	Room temperature
SGR	Subgenomic replicon
SGR-luc-DBN3a	DBN3a Sub-genomic replicons
SH3	Src homology 3
SMV	Simeprevir
SOCS3	Suppressor of cytokine signalling 3
SOF	Sofosbuvir
SR-BI	Scavenger receptor class B type I
STAT	Signal transducer and activator of transcription
SVR	Sustained virological response
TBS-T	Tris-buffered saline with Tween-20
TIP47	Tail-interacting protein of 47 kDa
TIRAP	Toll-interleukin 1 receptor domain-containing adaptor protein

TLR-3	Toll-like receptor-3
TLR4	Toll-like receptor 4
TMDs	Transmembrane domains
TNF	Tumour necrosis factor-alpha
TRAF	TNF receptor-associated factor
TVR	Telaprevir
UIM	Ubiquitination interacting motif
UTR	Untranslated region
VAP	Vesicle-associated membrane protein-associated protein
VEL	Velpatasvir
VLDL	Very low-density lipoprotein
WT	Wild-type

Table of Contents

Table of Figures

Table of Tables

Chapter 1 Introduction

1.1 Hepatitis C virus (HCV)

1.1.1 General Introduction

Viral hepatitis is caused by five viruses categorized by different alphabet letters, including hepatitis A, B, C, D and E (HAV-HEV) (Mohsen and Levy, 2017). HAV and HEV are believed to share the epidemiological spread through contaminated food and water (Webb et al., 2020). HBV is mainly spread by percutaneous or mucosal surface contact with infected blood, which is associated with sexual or Mother-to-child transmission (Shepard et al., 2006). The infection of HDV is generally dependent upon hepatitis B infection due to the requirement of HBV surface antigen. The coinfection of HBV and HDV results in a more severe and complicated course of the disease (Urban et al., 2021).

Hepatitis C virus (HCV) infection causes disease and inflammation in the liver. It has been a widely concerned public health issue worldwide for the last 30 years. HCV is the primary causative agent of non-A, non-B hepatitis which was first diagnosed in 1975 (Feinstone et al., 1975) and finally identified in the serum of a chimpanzee infected with non-A, non-B hepatitis patient sera (Choo et al., 1989).The virus typically transmits via blood products of infected individuals during transfusion, injection drug use, organ transplantation, hemodialysis, or accidental exposure (Chen and Morgan, 2006). Unsafe healthcare practices and injection drug use (IDUs) remain the primary route of transmission (Organization, 2017). HCV is one of the leading causative agent of chronic liver diseases, including cirrhosis, hepatocellular carcinoma (HCC) and liver cancer (Lim et al., 2012, Wang et al., 2021). Due to the unavailability of prophylactic vaccines and limited clinical treatment protocols, HCV is far from being eradicated and has gradually become a global health burden (Deuffic-Burban et al., 2007) Until 2019,

it infected around 58 million individuals worldwide (Chan et al., 2021), which has decreased by 13 million since 2015 (Naggie, 2019). Although several studies have stated that the incidence of HCV infection has decreased since the second half of the 20th century, there were still 1.5 million new HCV infections per year (Organization, 2021).

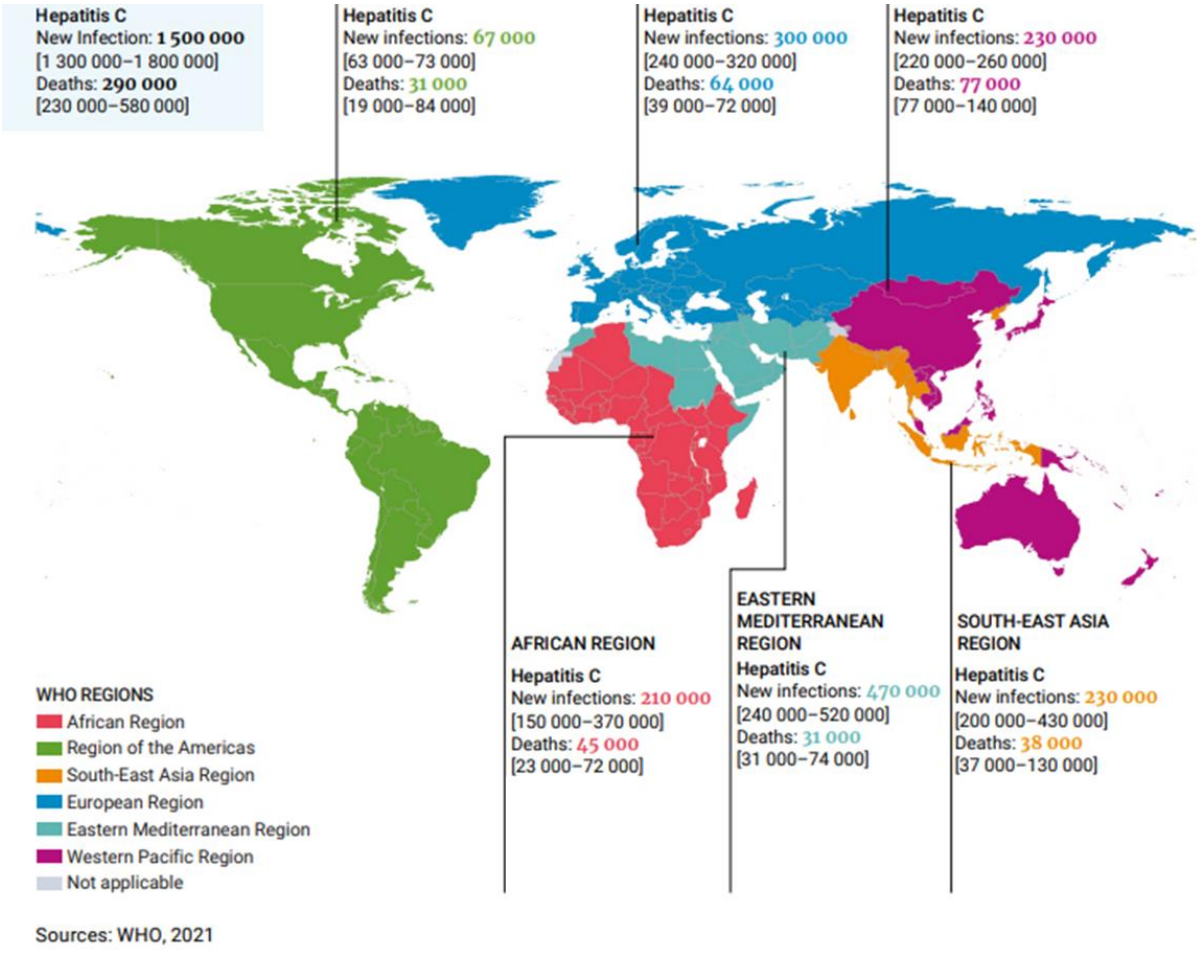

Fig 1.1 Incidence of HCV infection in WHO region (2019).

According to the statistics of 2019, the estimated number of persons newly infected (N=1.5 million) surpassed the persons dying from end-stage HCV infection (N=290 000) and being treated with DAAs (N=940 000), indicating that the global epidemic may continue to expand (Organization, 2021).

1.1.2 Classification

HCV is an enveloped virus belonging to the genus Hepacivirus and within the Flaviviridae family. Before 2011, Genus Hepacivirus was considered to contain only two members: HCV and GB virus B (GBV-B). GBV-B was originally described in association with acute hepatitis in 1967 (Deinhardt et al., 1967) and was finally identified in 1995 from New World monkeys (Simons et al., 1995). GBV-B exhibited high similarity and correlation with HCV (25–30% amino acid homology) based on the same liver pathology and infections. However, it has not been found in infected humans (Stapleton et al., 2011). More divergent hepaciviruses have been described recently, which showed similar genome structures with HCV and GBV-B. However, these hepaciviruses discovered after 2011 are not human pathogens, as they were isolated from other species such as bats and rodents (Quan et al., 2013, Firth et al., 2014, Drexler et al., 2013, Kapoor et al., 2013), Old World monkey (Lauck et al., 2013), cow (Corman et al., 2015, Baechlein et al., 2015), dog (Kapoor et al., 2011), horse (Burbelo et al., 2012) and graceful catshark (Hartlage et al., 2016). Besides Hepacivirus, Flavivirus, Pestivirus, and Pegivirus are also included in the Flaviviridae family (Fig 1.2A).

HCV exhibits an extensive genetic heterogeneity and a complex taxonomic structure, with 7 major genotypes and 67 subtypes having been identified (Smith et al., 2014) (Fig 1.2B). To date, subtypes 1a, 1b, 2a, 2b, 2c, 3a, 4a, 4d, 5a and 6a are widely known and studied globally. The diversity of nucleotide level between HCV genotypes is approximately 30%, while the various of nucleotide sequence in each subtype about 15% (Simmonds et al., 1993, Bukh et al., 1995). In addition, the isolates from the same subtype also vary by about 10% (Martinez and Franco, 2020). The variability of HCV genome is mainly distributed within the membrane glycoproteins E1 and E2 (Argentini

et al., 2009). The hypervariable regions 1 and 2 (HVR1 and HVR2) of the E2 protein exhibited 50% sequence homology among 7 different genotypes (Le Guillou-Guillemette et al., 2007). In contrast, the regions which contribute to translation and replication or some structured domains including 5'-untranslated region (UTR) and 3'-UTR are highly conserved. Particularly, the 5'-UTR showed 90% sequence homology among different strains (Bukh et al., 1992, Piñeiro and Martinez-Salas, 2012). In addition, the core protein is the most conserved viral protein, with 81%-88% nucleotide sequence identity between different isolates (Davis, 1999, Simmonds et al., 1994).

HCV distribution and prevalence vary according to different geographical regions of the world, the variation is also generally displayed among different groups of a community (Idrees, 2008, Lavanchy, 2011) (Fig 1.2C). Genotype 1-3 are the most common genotype and distributed worldwide. Subtype 1a is most common detected in the United States and Northern Europe, while subtype 1b, which contributes to 70% of cases of HCV infection, exhibits a global distribution with a high prevalence in South Europe (Nouroz et al., 2015, Martinez and Franco, 2020). Genotype 2a and 2b are endemic in North America, Japan and Europe, while genotype 2c is most prominent in Northern Italy (Hnatyszyn, 2005). Genotype 3a and 3b, the most common subtypes of Genotype 3, are distributed globally (Sievert et al., 2011, Welzel et al., 2017). Genotype 3a was originally emerged and transmitted in the Indian subcontinents, including the northern part of India and Pakistan (Idrees and Riazuddin, 2008, Sievert et al., 2011, Singh et al., 2004, Sood et al., 2012). It has been exported to transmission chains in South Asia, Europe, and North America (Xu et al., 2022). Genotype 3b is distributed widely in Asia, including China, India, Malaysia and Thailand (Shah et al., 2021). Genotype 4 is mainly found in the Middle East and Central Africa, whereas 4d is a primary subgenotype caused by IDUs, which was originally identified in Denmark

(Bukh et al., 1993, Bukh et al., 1994). Genotype 5 and Genotype 6 is identified almost exclusively throughout in South Africa and Southeast Asia, respectively (Simmonds, 2001, Zein, 2000). Additionally, the newly appeared genotype 7 was demonstrated in seven patients in the Democratic Republic of the Congo (Murphy et al., 2015). Among 7 genotypes, genotypes 1 and 3 are the most primary prevalence, which are responsible for 83.4 million cases (46%) and 54.3 million cases (30%) of all infections, respectively (Messina et al., 2015). The share of genotypes 2, 4, and 6 is totally about 23%, whereas the proportion of genotypes 5 only contains 1%.

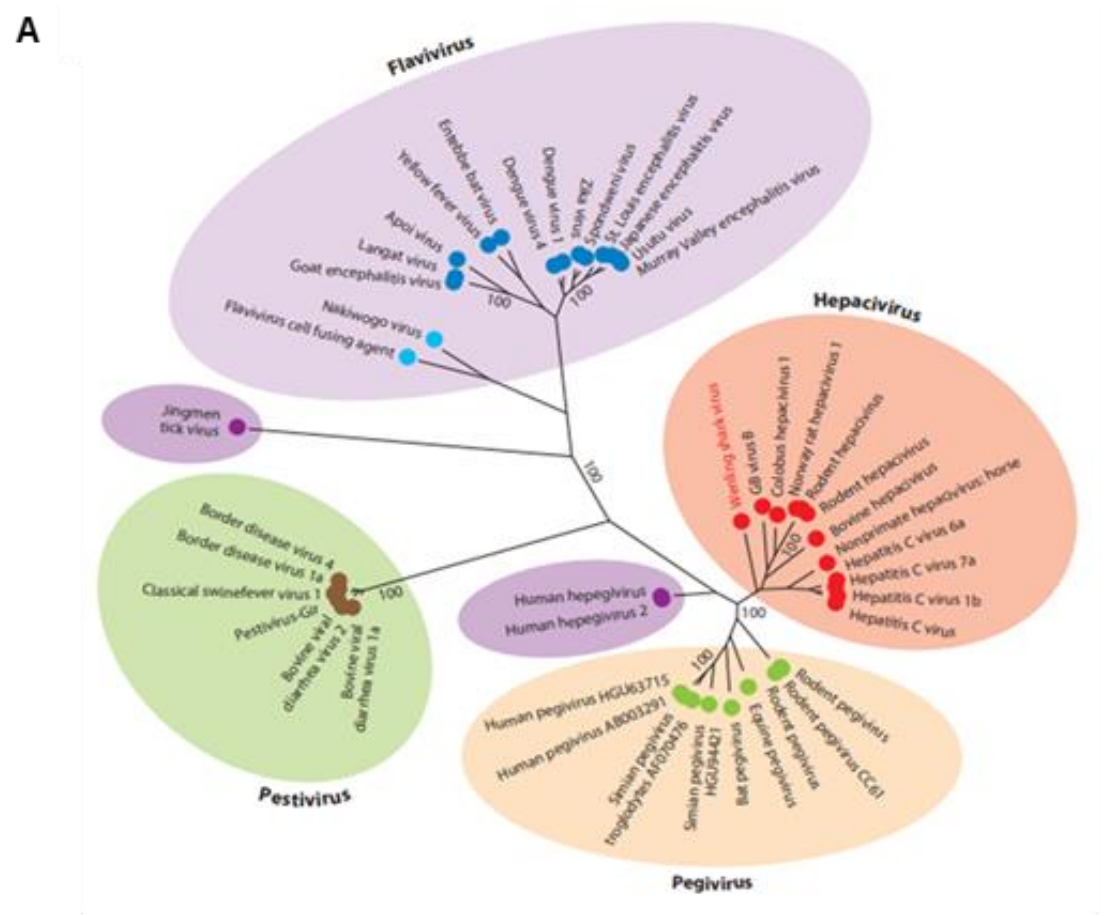
A
Flavivirus
Entebbe bat virus
Yellow fever virus
Apoi virus
Langat virus
Goat encephalitis virus
Dengue virus 4
Dengue virus 1
Ilheus virus
Spondweni virus
St. Louis encephalitis virus
Japanese encephalitis virus
Usutu virus
Murray Valley encephalitis virus
Kokiwogo virus
Flavivirus cell fusing agent
100
100
Jingmen tick virus
Hepacivirus
Wenling shark virus
GB virus B
Colobus hepacivirus 1
Norway rat hepacivirus 1
Rodent hepacivirus
Rodent hepacivirus
Bovine hepacivirus
Nonprimate hepacivirus: horse
Hepatitis C virus 6a
Hepatitis C virus 7a
Hepatitis C virus 1b
Hepatitis C virus
100
100
Border disease virus 4
Border disease virus 1a
Classical swinefever virus 1
Pestivirus Giraffe 1
Bovine viral diarrhea virus 2
Bovine viral diarrhea virus 1a
100
Pestivirus
Human hepeghivirus
Human hepegivirus 2
100
Human pegivirus HGU63715
Human pegivirus AB001291
Simian pegivirus troglodytes AF070476
Simian pegivirus HGU94421
Bat pegivirus
Equine pegivirus
Rodent pegivirus
Rodent pegivirus CC61
Pegivirus

B

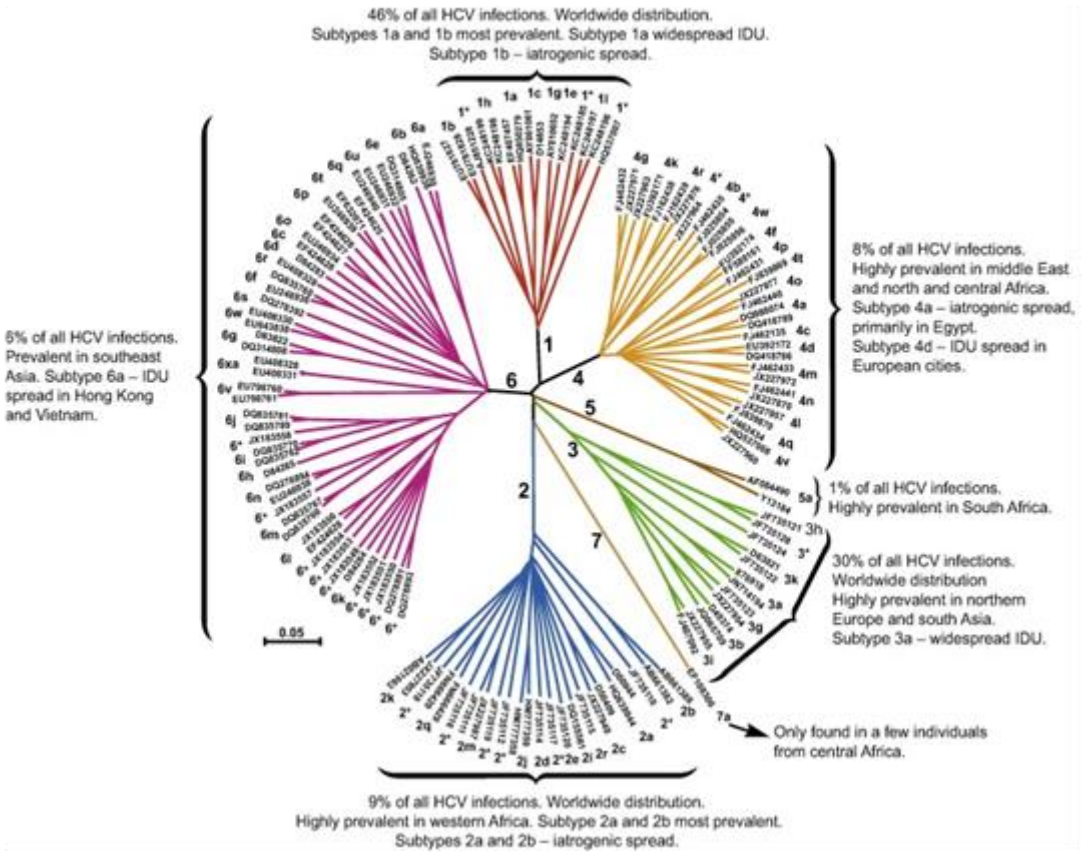
46% of all HCV infections. Worldwide distribution.
Subtypes 1a and 1b most prevalent. Subtype 1a widespread IDU.
Subtype 1b – iatrogenic spread.
6% of all HCV infections.
Prevalent in southeast Asia. Subtype 6a – IDU spread in Hong Kong and Vietnam.
8% of all HCV infections.
Highly prevalent in middle East and north and central Africa.
Subtype 4a – iatrogenic spread, primarily in Egypt.
Subtype 4d – IDU spread in European cities.
1% of all HCV infections.
Highly prevalent in South Africa.
30% of all HCV infections.
Worldwide distribution
Highly prevalent in northern Europe and south Asia.
Subtype 3a – widespread IDU.
Only found in a few individuals from central Africa.
0.05
9% of all HCV infections. Worldwide distribution.
Highly prevalent in western Africa. Subtype 2a and 2b most prevalent.
Subtypes 2a and 2b – iatrogenic spread.

C

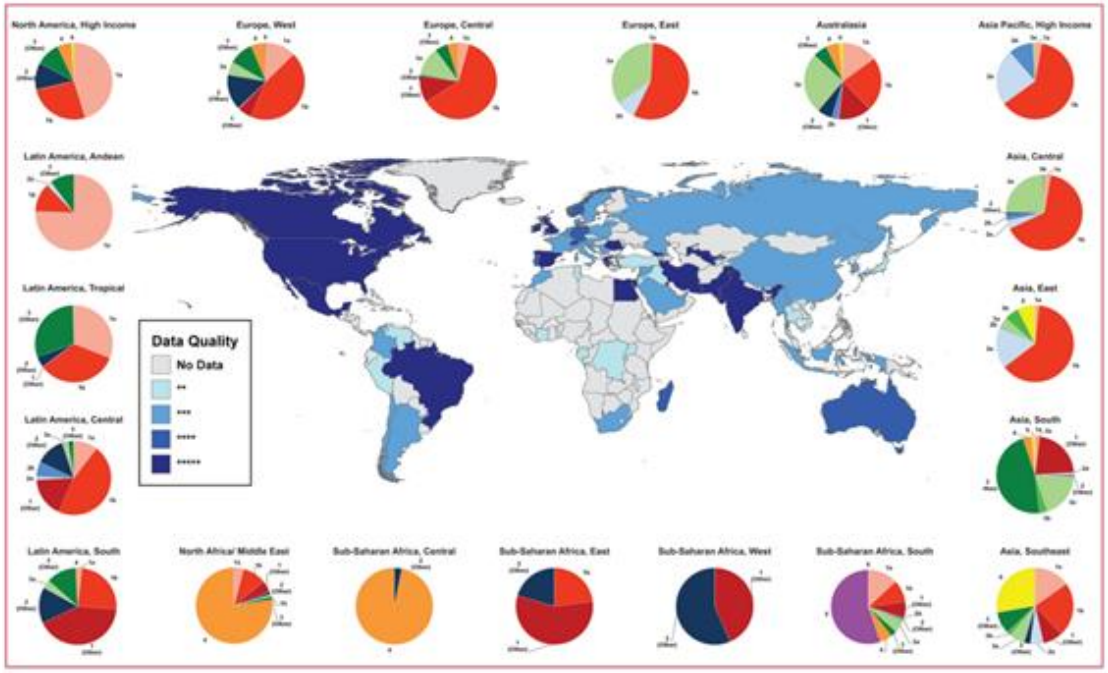

Fig 1.2 HCV Classification and distribution.

(A) All four genera and related viruses of the family Flaviviridae (Hartlage et al., 2016). **(B)** The genotypes are categorized into seven major genotypes and 67 subtypes using phylogenetic analysis of the nucleotide sequences analysis. The prevalence and distribution of subgenotypes are also indicated (Bukh, 2016). **(C)** The prevalence and distribution of HCV genotypes in the global burden of disease areas (Hnatyszyn, 2005).

1.1.3 Epidemiology and Pathology

HCV is predominantly a blood-borne virus, indicating that blood contact and production is the most efficient transmission route (Feinstone et al., 1975). It can also be transmitted through heterosexual contact or birth to an infected mother, but the transmission risk is lower (Martinez and Franco, 2020). IDUs also pose a transmission risk, and it is the cause of 80 % of acute infection in developed countries (Wilkins et al., 2015, Sy and Jamal, 2006). Additionally, blood transfusion has become a new transmission route due to the use of unsterilized injection needles (Klevens et al., 2012, Su et al., 2010). Some rare conditions can also transmit HCV, including using

unsterilized instruments for nose and ear piercing, acupuncture or tattoos (Alter, 2007). However, the virus cannot be transmitted by saliva, such as by sharing drinks or food with an HCV-infected patient (Bennett et al., 2019). Although HCV infects humans and is transmitted through various modes, the origin of HCV infection in humans is still unclear.

The virus usually appears in blood within two weeks after first exposure. Alanine aminotransferase (ALT) and aspartate aminotransferase (AST), which are specific biomarkers of severe liver damage, and are also able to predict the progression of liver fibrosis during chronic HCV infection (Aqib et al., 2021). In addition, HCV-specific antibodies can be detected 20–150 days after exposure (Busch, 2001, Cox et al., 2005, Page-Shafer et al., 2008). 15-30% of infected individuals enter into the acute phase after an incubation period of 2–12 weeks, which is generally asymptomatic and infrequently diagnosed. However, some non-specific symptoms such as lethargy, fatigue, and myalgia weakness appear with acute infection. Some patients even have more pronounced symptoms, such as jaundice, which may be associated with increased ALT (Orland et al., 2001, Marcellin, 1999). After the acute phase, the infection of 18-34% of patients is spontaneously cleared within 6-12 months (Page et al., 2009, Dore et al., 2010, Grebely et al., 2010), and viral RNA cannot be detected in blood (Grebely et al., 2014, Micallef et al., 2006).

The acute infection frequently transfers to chronic hepatitis C (CHC) with the persistence of un-cleared virus and viraemia after half a year. The development rate of CHC is associated with differences in infected individuals, including age, gender and ethnicity. Additionally, co-infection with HIV and HBV, excessive intake of alcohol and jaundice development also accelerate the transformation progression (Chen and Morgan, 2006). CHC generally has slow disease progression with long persistent

hepatic inflammation. After long-term infection over 20-30 years, 10–20% of infected individuals develop the disease progression of liver fibrosis and cirrhosis (Seeff, 2009, Westbrook and Dusheiko, 2014). Serious cirrhosis is the primary cause of HCC, hepatic decompensation and death.

1.1.4 Therapies

The treatment of all CHC-infected patients should be considered in several aspects, including the genotype, the extent and development of cirrhosis, complication and adverse effects. HCV therapy aims to reduce mortality and complications associated with CHC and finally cure liver disease (Miller et al., 2014). The success of the cure of CHC infection is marked by a sustained virological response (SVR) indicating HCV RNA cannot be detected in serum or polymerase chain reaction with a sensitive assay (lower limit of detection of ≤15 IU/mL) at 12 or 24 weeks after cessation of treatment (Cornberg et al., 2019).

Interferon (IFN) alpha was the first drug found to have bioactivity against HCV infection, while the therapy with limited efficiency with 6% SVR (Fried and Hoofnagle, 1995, Davis et al., 1989). Afterwards, nucleotide analogue ribavirin (RBV), pegylated interferon 2b alfa and pegylated interferon 2a alfa were included in the treatment for HCV before 2003 (Li and De Clercq, 2017). Before the direct-acting antiviral (DAA) development in 2011, combination therapy with pegylated interferon-α and RBV was consistently considered the predominant therapy for HCV infection (Fried et al., 2002). The double therapies increased the HCV cure rates of genotype 1 to above 50% (Fig 1.3A) and achieved 70% and 80% cure rates for genotype 2 and 3, respectively (Liang and Ghany, 2013).

DAAs cure most HCV infections, and the virological response achieves 95% in most genotypes (Ansaldi et al., 2014). The development of DAAs is rapid, and ten therapies were approved between 2011 and 2016 (Geddawy et al., 2017). The generation of NS3/4A protease inhibitors telaprevir (TVR) and boceprevir (BOC) in 2011 were the first DAA to be developed. Their combination with pegylated interferon and RBV leads to SVR rates in approximately 65–75% of HCV genotype 1 infections (Bacon et al., 2011, Poordad et al., 2011, Jacobson et al., 2011) (Fig 1.3A).

To improve the DAAs treatment effectiveness, NS5B polymerase inhibitor sofosbuvir (SOF) was developed. Sofosbuvir is a pyrimidine nucleotide analogue which can be phosphorylated within the cell, leading to the early termination of HCV RNA strand synthesis (Li and De Clercq, 2017). SOF rarely has resistance. Only one resistance case was reported in vivo (Keating and Vaidya, 2014). The triple-combination treatment with SOF, pegylated interferon 2a alfa and RBV achieved almost 90% effectiveness against the viral diseases with genotypes 1 and 4 (De Clercq, 2013, Lawitz et al., 2013) (Fig 1.3A). Additionally, an oral regimen of SOF and RBV enhances the SVR rates of 95% and 82% of patients infected with genotypes 2 and 3, respectively (Jacobson et al., 2013). The successfully treated effectiveness of the SOF/RBV combination also enabled the IFN treatment to become history. With the generation of all-oral treatment, IFN-free and RBV-free oral regimens provide more toleration, and the SVR rate also increases to 90–95% (Rockstroh, 2015) (Fig 1.3A).

Due to the high effectiveness of SOF in HCV infections, it was identified by WHO as essential medicine and generally participated in combination therapies with other new DAAs. DAAs were classified into three groups based on the different targets of HCV non-structural (NS) proteins: the NS3/4A protease inhibitors (BOC, TVR, Simeprevir, asunaprevir, grazoprevir and paritaprevir), NS5A inhibitors (daclatasvir, ledipasvir

(LDV), ombitasvir, elbasvir and velpatasvir (VEL)), NS5B nucleotide inhibitors (SOF). Non-nucleoside polymerase inhibitors (dasabuvir) (Asselah and Marcellin, 2012, Herbst and Reddy, 2013) (Fig 1.3B).

Daclatasvir (DCV), an inhibitor of the N-terminus of HCV NS5A, directly acts in both viral RNA replication and assembly. The DCV treatment for adult patients with CHC has been approved in the United States, Europe and Japan, demonstrating the composability with other DAAs (Degasperi et al., 2015, Majumdar et al., 2016). Moreover, the combination of DCV and NS3/4A protease inhibitors asunaprevir also enhanced the SVR rates >90% in HCV genotype 1b infected individuals (Chayama et al., 2014, Chayama et al., 2012).

Patients who are infected with HCV genotype 3 less responsive to some DAAs treatments which have a superior clinical efficacy for other genotypes (Kanwal et al., 2014, Andriulli et al., 2008). The serious situation was partially alleviated when DCV and sofosbuvir SOF were shown to be efficacious against genotype 3 (Chan et al., 2017, Kattakuzhy et al., 2016). However, despite improvements in the treatment , resistance is still reported in about 10% of the patients. Furthermore, the high resistance rates are more likely due to the contribution of genotype 3 (Dore et al., 2015, Lawitz et al., 2013, Nelson et al., 2015). Therefore, it is urgent to solve the problems of resistance rates of genotype 3 and generate more effective DAAs.

Although current therapy combinations are appropriate for most CHC infection with HCV different genotypes, the resistance-associated substitutions (RASs) the patients face is the major problems that need to be solved (Lawitz et al., 2015). Currently, the new second DAAs with well tolerance are developing and generating, which allows the DAAs combinations to create higher cure effectiveness.

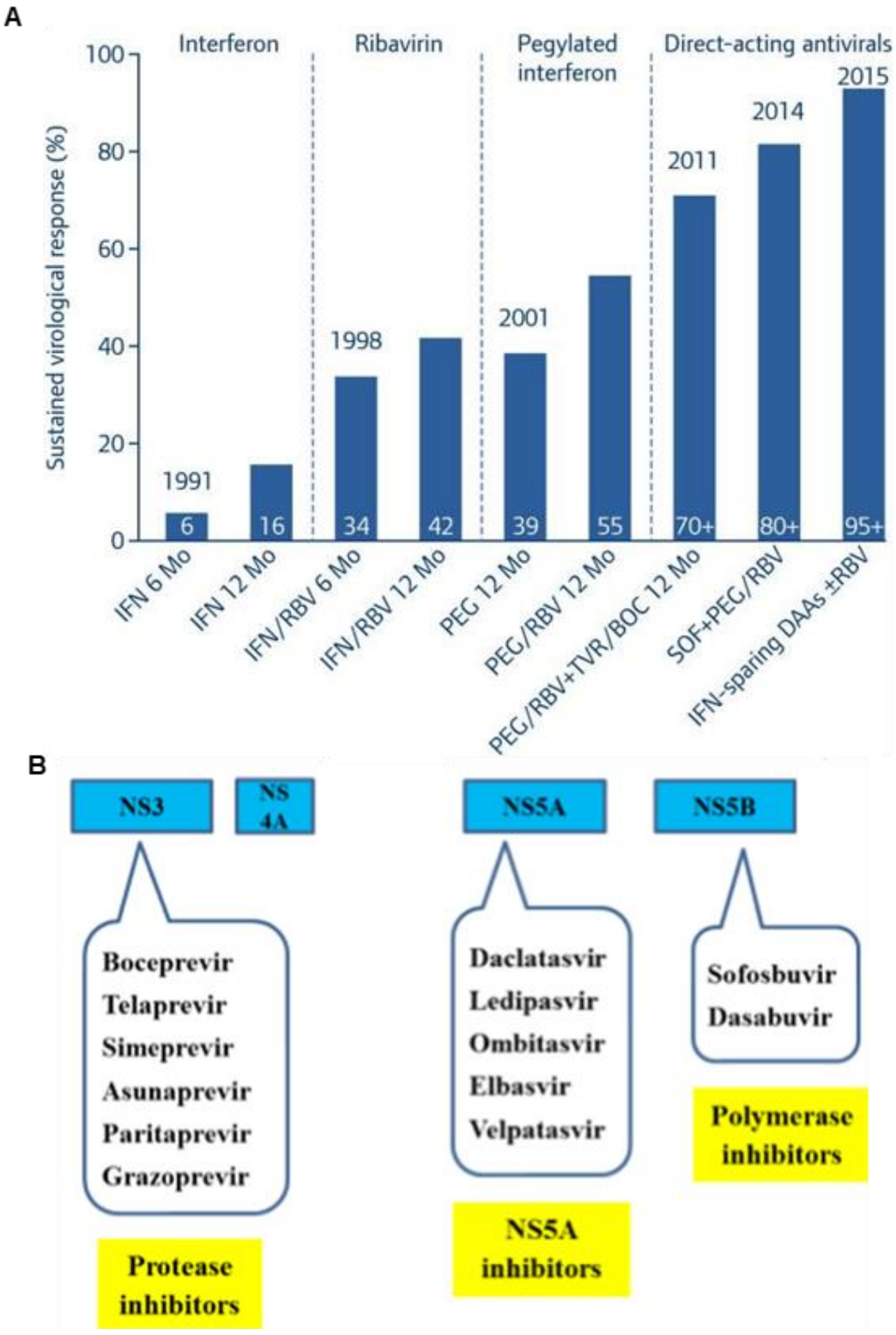

Fig 1.3 The treatment of CHC infection: IFN, RBV and DAAs.

(A) The development of the therapies with HCV genotype 1 infection (Rockstroh, 2015). **(B)** The summary of DAAs with different targets (Geddawy et al., 2017).

1.2 Molecular virology of HCV

1.2.1 Genomic organisation

The HCV RNA genome contains approximately 9600 nucleotides and is comprised of a 5′ UTR, a single open reading frame (ORF) encoding a single polyprotein of 3000 amino acids (aa), and a 3′-UTR (Hoffman et al., 2015). An internal ribosomal entry site (IRES) that is located within the 5′-UTR mediates the translation of this single ORF in a cap-independent manner (Hoffman and Liu, 2011, Scheel and Rice, 2013). The 3′ UTR, the initiation site for the synthesis of the negative-strand RNA during viral replication, consists of three distinct regions: a short genotype-specific variable region, the poly (U/UC) tract and the X-tail which is composed of three stem-loops (Song et al., 2006). Further, it is involved in virus translational regulation by an undefined mechanism (Bradrick et al., 2006, Bung et al., 2010). The polyprotein is processed co- and post-translationally by cellular signalases and viral proteases into 10 viral proteins: the structural proteins, core, E1 and E2, and p7 and the non-structural proteins NS2, NS3, NS4A, NS4B, NS5A and NS5B (Fig. 1.4). Apart from NS2, the other NS proteins are necessary and sufficient for genome replication and form a membrane-associated replicase complex in association with cellular factors (Lavanchy, 2009, Reiss et al., 2011). Most non-structural proteins are well characterised: NS3 has NTPase/RNA helicase and serine protease activities with NS4A as its cofactor and is involved in HCV RNA replication and viral particle assembly (Murray et al., 2008, Zhu and Briggs, 2011). NS5B is the viral RNA-dependent RNA polymerase.

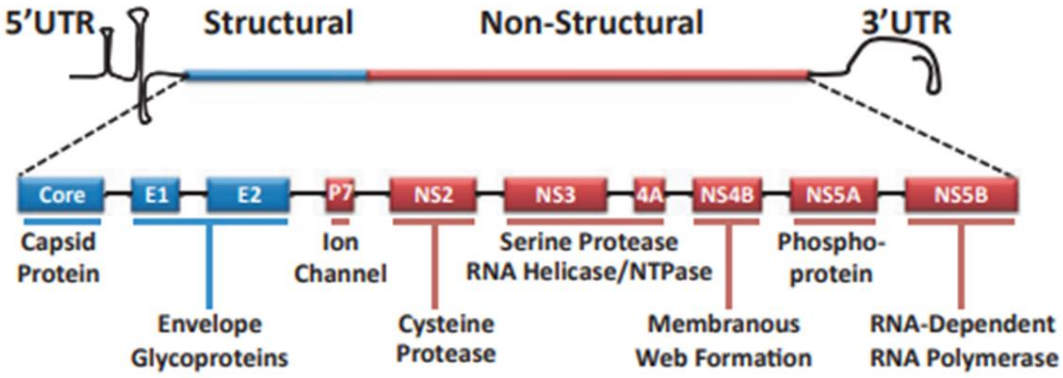

Fig 1.4 HCV genome structure and viral protein functions.

The HCV genome contains a single large open reading frame of 3000 amino acids flanked by 5' and 3' UTRs, encoding a polyprotein which can be cleaved into ten individual proteins (Poordad and Dieterich, 2012).

1.2.2 Structural proteins

1.2.2.1 Core protein

The core protein is an RNA-binding protein, which forms nucleocapsids to directly encapsulate and protect HCV genomic RNA during virus infections (Polyak et al., 2006). It is a 21kDa protein that contains 191 aa from the N-terminus of the polyprotein (Yasui et al., 1998). The mature core protein is dimeric alpha-helical and consists of 3 distinct predicted domains based on different amino acid compositions and hydrophobicity (McLauchlan, 2000).

The hydrophilic Domain I contains 117aa, rich in numerous positive charges and basic residues, and occupies approximately two-thirds of the length of the core. The function of Domain I was demonstrated that involved in RNA binding, nuclear localization (Suzuki et al., 2005, Suzuki et al., 1995, Chang et al., 1994) and oligomerization necessary for particle formation (Kunkel and Watowich, 2002, Klein et al., 2005, Nakai et al., 2006). Half of the N-terminus in the core protein is predominant for the formation

of nucleocapsids. It was demonstrated that the 75 N-terminal residues of the core protein were sufficient to assemble nucleocapsid-like particles (NLPs) in vitro (Majeau et al., 2004). To further identified the essential residue, the mutational analysis in a cell-free system observed that two clusters within the N-terminal 68 amino acids were associated with the generation of NLPs (Klein et al., 2005). Additionally, research in 2007 also revealed that NLPs formation used 1-82 N-terminal aa of core protein and the successful generation of NLPs caused by global positive charge (Fromentin et al., 2007). Three basic clusters can be further divided from Domain I due to aa charge distribution: the basic domain I (2–23 aa), the basic domain II (38–74 aa), and the basic domain III (101–121 aa) (Gawlik and Gallay, 2014).

Compared with Domain I, Domain II and III are hydrophobic, which play the roles in virus particle productions with lipid droplets and the anchor of endoplasmic reticulum (ER), respectively (Hourioux et al., 2007, Ogawa et al., 2009). Since the function of Domain II and III, the core protein was also considered to participate in the viral lifecycle besides its role in viral nucleocapsid formation. The location of HCV core protein in the cytoplasm is primary at the ER, lipid droplets (LDs) and mitochondria (Mani et al., 2022). At the beginning of the core protein release, signal peptidase separates core protein from E1 glycoprotein in the ER lumen (Santolini et al., 1994). After further cleavage in the C-terminal region of the core protein by the signal peptide peptidase within the transmembrane region, a mature core protein is generated and targeted to LDs (Kopp et al., 2010, McLauchlan et al., 2002, Pene et al., 2009). In HCV-infected cells, rapid synthesis of core protein leads to more transportation to the LDs assembly site, which enhances the formation of LDs and may further involve in the process of steatosis (Moriya et al., 1998, Moriya et al., 1997, Barba et al., 1997). Furthermore, core protein also demonstrated the role of interacting with mitochondria

to facilitate reactive oxygen species productions (Korenaga et al., 2005), which may result in the function of core protein in stimulating or inhibiting apoptosis (Kountouras et al., 2003, Chou et al., 2005, Meyer et al., 2005). In addition to this function, core protein also was revealed to play the roles in modulation of immune cell differentiation and dual-directional regulation of inflammatory cytokine releases and hepatic angiogenesis (Tu et al., 2012, Dolganiuc et al., 2003, Hassan et al., 2009).

1.2.2.2 E1 and E2 Envelope Glycoproteins

E1 and E2 are two highly glycosylated proteins of HCV embedded on the surface of the virion and play an essential role in the virion envelope. These two envelope glycoproteins are cleaved and released from the polyprotein by signal peptidase (Dubuisson et al., 2002), whereas their activation is independent of the cleavage (Vieyres et al., 2010). E1 and E2 are type-I transmembrane proteins which interact with each other to assemble as a noncovalent heterodimer, including two N-terminal ectodomains (160 and 334aa) and a short C-terminal transmembrane domain (30aa). The ectodomains of E1 and E2 were considered to indirectly contribute to the proper folding of glycoproteins (Michalak et al., 1997). The transmembrane domain is rich in hydrophobic aa and functions in membrane anchoring, heterodimer complex formation and ER localization (Cocquerel et al., 2000, Cocquerel et al., 1998)

These two glycoproteins contain a range of intramolecular disulphide bonds and N-linked glycans after the modification of post-translation (Vieyres et al., 2010). The disulphide bonds assist in forming more stable covalent complexes of E1 and E2 on the surface of the virion. In addition, the N-linked glycosylation responds to the synthesis of multi-subunit complexes, which is essential for virus entry into host cells (Naderi et al., 2014, Cocquerel et al., 2006). E1 and E2 are involved in the whole

process of virus entry, including cell attachment, binding with cellular receptors, endocytosis and fusion. E2 protein has been identified to contain two Hypervariable regions (HVR1 and HVR2), which showed huge diversity of aa sequences among different HCV genotypes and subgenotypes (Weiner et al., 1991). 1-27aa of E2 ectodomains was referred to as HVR1, a globally basic region with positively charged residues. This character leads to the interaction with negatively charged factors on the cell surface, which is critical for cell recognition and attachment (Callens et al., 2005). HVR1-deleted virus disrupted the high dependence on scavenger receptor class B type I (SR-BI), which is a HCV receptor and essential for HCV entry (Prentoe et al., 2014). Notably, HVR1 is responsible for masking many neutralising epitopes. The loss of this domain resulted in the dramatic increase of antibody-mediated neutralisation and higher sensitivity of virus to various neutralising antibodies (Bankwitz et al., 2010, Prentoe et al., 2016). Additionally, HVR2 has also been demonstrated to regulate the interaction with the E2 receptor (Roccasecca et al., 2003). However, the role of E1 is not completely clear. The only function identified is the association with intra-cytoplasmic virus-membrane fusion (Rosa et al., 1996, Flint and McKeating, 2000).

1.2.3 Non-structural protein

1.2.3.1 P7

The p7 protein, a small polypeptide with 63aa, is regarded as the connection between structural and NS proteins (Lin et al., 1994, Mizushima et al., 1994). This polytopic membrane protein is also released by signal peptidase cleavage and comprises two transmembrane domains connected by a short cytoplasmic loop (Carrère-Kremer et al., 2002). The N- and C-termini of the P7 protein are exposed to the lumen of the ER in the cytosol (Carrère-Kremer et al., 2002, Lin et al., 1994). The re-initiation sequence

of translocation in the C-terminus is considered to be a signal peptide during the fusion process with a reporter protein (Carrere-Kremer et al., 2004). Additionally, the role of p7 in membrane structure is emerged due to the barely accessible residues on the exposed N- and C-termini, and this function is associated with the ER, mitochondrial and plasma membranes (Carrère-Kremer et al., 2002, Griffin et al., 2005, Griffin et al., 2004). p7 protein belongs to the viroporin family but is not involved in RNA replication (Gonzalez and Carrasco, 2003). The mainly co-localisation partner of P7 is the E2 protein. The other interactions also were detected in NS2, NS3 and NS5A (Vieyres et al., 2013), practically the interaction with NS2, which recruits core protein to the proposed site from LD at the stage of assembly (Boson et al., 2011, Tedbury et al., 2011). Furthermore, the p7 polypeptide also was observed as a calcium ion channel in artificial lipid membranes (Griffin et al., 2003, Pavlović et al., 2003, Premkumar et al., 2004). The suppression of ion channel activity of P7 might be a new antiviral method for HCV infections.

1.2.3.2 NS2

NS2 is a non-glycosylated and integral transmembrane protein of 23 kDa with several stretches of hydrophobic aa. Although the membrane topology of NS2 is not fully understood, the two internal signal-like sequences at 839–883aa and 928–960aa infer the four putative transmembrane segments in NS2, which associates with the E2 membrane (Santolini et al., 1995, Yamaga and Ou, 2002).

The release of NS2 requires a protease to separate NS2 and NS3 junction. The NS2/NS3 protease comprises the C-terminal domain of NS2 (94–217 aa) and the first 180 residues of NS3 (Lindenbach and Rice, 2001), which has been identified as a zinc-dependent metalloprotease and cysteine proteinase (Grakoui et al., 1993a,

Grakoui et al., 1993b, Hijikata et al., 1993, Pallaoro et al., 2001). The separation of the NS2/NS3 connection is necessary for RNA replication (Jones et al., 2007, Kolykhalov et al., 2000, Welbourn et al., 2005), whereas NS2 has been demonstrated that not a member of the replication complex (Blight et al., 2000, Lohmann et al., 1999) and is easily degraded by protein kinase casein kinase 2 (Franck et al., 2005). Therefore, the N-terminus of NS3 might be the beginning site of replication but not NS2. Additionally, the zinc dependency may also result from the N-terminus of NS3 due to the zinc ion of the NS3 protease domain, which can maintain the stability of protein structure (Kim et al., 1996, Love et al., 1996).

In addition to the role in the activity of NS2/NS3 protease, NS2 has also been revealed to have a potential role in modulating cellular gene transcription (Dumoulin et al., 2003). Furthermore, the NS2 functions in HCV assembly and release were also demonstrated, whereas the mechanism still needs to be further determined (Kalinina et al., 2002, Lindenbach et al., 2005, Pietschmann et al., 2006). NS2 also enable it to interact with host proteins, such as liver-specific pro-apoptotic CIDE-B, and can act as an inhibitor to suppress CIDE-B-induced apoptosis (Erdtmann et al., 2003). More mechanisms with these functions of NS2 still need to be further investigated.

1.2.3.3 NS3/NS4 complex

NS3 is a multifunctional protein with a molecular weight of 70 kDa. NS3 is mainly responsible for the cleavage of non-structural protein region (NS3/4A, NS4A/4B, NS4B/5A and NS5A/5B junction) from polyprotein in HCV infected cells to generate viral RNA replication complex (Lindenbach and Rice, 2005), which is attributed to the zinc-dependent serine protease domain occupying approximately first 188aa at the N-terminus (Kim et al., 1995). The zinc ion in this protease domain is necessary for the

structural and folding stability of the enzyme (De Francesco et al., 1996, Lee and Lim, 2008, Urbani et al., 1998).

In addition to the dependence on zinc ions, the more stable and effective activity of NS3 protease also requires the binding of NS4A. NS4A is a small protein of 8kDa and contains a hydrophobic N-terminal domain which has been identified as the requirement of NS3 for ER targeting (Wölk et al., 2000).NS4A also contains serine proteinase cofactor activity sites at the central portion of NS4A (21-30aa), resulting in the NS3/NS4 protease stably located at ER membrane and accurate targeting to the NS protein junction (Bartenschlager et al., 1995, Lin et al., 1995, Tanji et al., 1995a). Moreover, NS3/NS4A protease activity is also revealed to be involved in inhibiting the dsRNA-dependent innate immune response. It has been shown that the activity of dsRNA-dependent interferon regulatory factor 3 (IRF-3) was disrupted by NS3/NS4A which also antagonised the cellular RNA helicase retinoic acid-inducible gene I (RIG-I) pathway (Heim and Thimme, 2014, Horner and Gale, 2013, Meylan et al., 2005, Sumpter Jr et al., 2005). Additionally, NS3/NS4A also inhibits the IRF-3 upstream factor Toll-like receptor-3 (TLR-3) by cleaving the TRIF adaptor (Li et al., 2005). Hence, the NS3-4A protease is reported to play essential roles in the replication and persistence of HCV (Morikawa et al., 2011).

The C terminus of NS3 encodes an RNA helicase/NTPase domain of 442aa (Kim et al., 1995). The NS3 helicase is a DExH/D-box RNA helicase which belongs to the helicase superfamily-2, containing a conserved Asp-Glu-Cys-His motif in the ATP binding site (Raney et al., 2010, Tai et al., 1996). This helicase activity requires the NS3 dimerisation and then contributes to the duplex RNA unwinding using an ATP-dependent manner (Serebrov and Pyle, 2004). Moreover, the function in dsRNA unwinding of this helicase is enhanced by interacting with serine protease at N-

terminal (Frick et al., 2004). The NS3 helicase also acts on RNA binding, and the connection with NS4 enhances RNA activity (Pang et al., 2002). The function of the NS3 helicase in the HCV life cycle is not totally understood, but current research has shown that the random translocation of NS3 helicase exploiting the energy of NTP hydrolysis was essential for the formation of helicase for the next cycle (Levin et al., 2005). Additionally, NS3 helicase may be involved in the onset of RNA replication through unwinding positive and/or negative strand RNA or promoting the formation of replicase complex (Li et al., 2021). Furthermore, 40–54 aa in C-terminal, an α-helix mainly with a negative charge, has been reported to interact with other NS proteins and to modulate HCV replication and assembly (Lindenbach et al., 2007, Phan et al., 2011).

1.2.3.4 NS4B

The NS4B protein is a highly hydrophobic NS protein of 27kDa with 261 aa residues, which has been identified to play a critical role in virus replication (Dvory-Sobol et al., 2010, Gouttenoire et al., 2010a, Zając et al., 2019). It is an integral membrane protein which is considered most likely to possess four transmembrane domains in the central sites with 70-190 aa (Hügle et al., 2001, Lundin et al., 2003). The rest of NS4B comprises an N-terminal portion (1-69aa) in the ER lumen and a C-terminal portion (191-261aa) in the cytoplasm, which both contain two amphipathic helices (Gouttenoire et al., 2009b, Hdoufane et al., 2022, Lundin et al., 2003).

NS4B is referred to as a membrane anchor for the replication complex and is located at ER or ER-derived membrane (Egger et al., 2002, Elazar et al., 2004, Gretton et al., 2005, Hügle et al., 2001, Lundin et al., 2003). NS4B has also been identified to facilitate RNA replication by inducing the formation of membranous structures (Egger

et al., 2002). Additionally, NS4B showed similar protein membrane segments with other NS proteins, indicating it may play a role in the generation of replicase complex (Brass et al., 2008, Gouttenoire et al., 2009a, Moradpour et al., 2004a, Penin et al., 2004a). The nucleotide-binding motif of NS4B is able to hydrolyse GTP and to further affect HCV replication (Einav et al., 2004). Moreover, the NTPase activity NS4B has also been identified to play a role in virus assembly (Einav et al., 2004, Jones et al., 2009, Thompson et al., 2009).

1.2.3.5 NS5A

NS5A is a large membrane-associated protein with 447 aa residues and harbours two forms with molecular weights of 56 and 58 kDa, respectively. These two forms are generated by differential phosphorylation: basal (56 kDa) and hyperphosphorylation (58 kDa). Basal phosphorylation is distributed in the central and C-terminal parts of NS5A, while hyperphosphorylation concentrates on the central part, indicating four serine residues 225, 229, 232 and 235. (Kandangwa and Liu, 2019, Tanji et al., 1995b). It has been demonstrated that all NS proteins upstream of NS5A are involved in the phosphorylation of NS5A protein (Oliver Koch and Bartenschlager, 1999). However, the role of NS5A phosphorylation in the virus life cycle still needs to be further investigated. NS5A has been reported to play roles in virus replication, assembly and interaction with cellular factors. These roles of NS5A protein will be described in more detail in Section 1.3.

1.2.3.6 NS5B RNA-Dependent RNA Polymerase

NS5B is a hydrophilic membrane protein of 68 kDa with 591 aa residues, and the first 530aa N-terminal composes of a catalytic domain of the NS5B portion (Moradpour and Penin, 2013). Since the existence of conserved GDD sequence motif, which is a

defining feature with all viral RNA-dependent RNA polymerases (RdRp), NS5B is endowed with the characters of RdRp and is the central catalytic enzyme of the HCV RNA replication (Sesmero and Thorpe, 2015, Yamashita et al., 1998). NS5B participates in the whole process of RNA synthesis, using the genome as a template to form a complementary negative-strand RNA which is acted on a second template to generate positive-strand RNA. In addition to the GDD motif sequence, the N-terminal of NS5B also contains the RdRp classical “fingers, palm and thumb” structure (Bressanelli et al., 1999, Lesburg et al., 1999). The palm domain contains the active site of the polymerases, while the interaction between fingers and thumb domain forms a groove with a catalytic site allowing the direct target with positive- and negative-strand HCV RNAs (Lesburg et al., 1999). The highly flexible β-hairpin loop in the thumb domain also assisted modulate the RNA template binding and the onset of RNA synthesis (Appel et al., 2006). However, the detailed dsRNA unwinding process in this structure is still unclear.

NS5B is also regarded as a tail-anchored protein due to the α-helical transmembrane domain in the C-terminal region (Ivashkina et al., 2002, Schmidt-Mende et al., 2001). This domain encodes 21 aa residues and is responsible for membrane connection and cytosolic orientation of ER with the exposed catalytic domain (Moradpour et al., 2004a, Schmidt-Mende et al., 2001). C-terminus is not necessary for RdRp activity but is indispensable for HCV RNA replication (Moradpour et al., 2004a). The connection of the catalytic domain and the transmembrane domain results in a conformational alteration, which probably associates with the formation of replicase complex by binding with host cell factors, such as hVAP-33 (Gao et al., 2004, Schmidt-Mende et al., 2001).

NS5B has also been reported to interact with Human vesicle-associated membrane protein-associated protein (VAP) subtype B (Hamamoto et al., 2005), retinoblastoma tumour suppressor (Munakata et al., 2005), Cyclophilin B (Watashi et al., 2005), Nucleolin (Kusakawa et al., 2007), Chaperonin (Inoue et al., 2011) and human oestrogen receptor alpha (Hillung et al., 2012). Recent research also revealed the interaction of NS5B with the cellular kinase Akt which can modulate the RNA-dependent RNA polymerase (RdRp) activity of NS5B and HCV infection (Sabariegos et al., 2021, Valero et al., 2016).

1.3 NS5A

1.3.1 Structure of NS5A

NS5A protein is composed of an N-terminal amphipathic α-helix (1-30aa) that allows NS5A to anchor on the ER, a structured domain 1 (DI), and two intrinsically disordered domains (DII and DIII) interconnected by two low-complexity sequences (LCS-1 and -2) (Fig 1.5A) (Ross-Thriepland and Harris, 2015).

The AH structure of the NS5A N-terminal region is regarded as a membrane anchor allowing NS5A to embed into the cytosolic leaflet of the membrane (Brass et al., 2002, Penin et al., 2004a). The AH contains a tryptophan-rich hydrophobic side buried in the membrane and a polar/charged side exposed to the cytosol. This membrane localization is parallel to the lipid bilayer, which is mediated by the hydrophobic side of the AH (Fig 1.5B). In addition to the role of targeting and binding with ER membrane, AH also plays a critical role in replicase complex formation (Elazar et al., 2003). moreover, the structure-function analysis for AH demonstrated an absolutely conserved residue on the surface of the membrane, indicating that AH might also associate with protein-protein interactions (Moradpour et al., 2005).

Following the AH, NS5A was divided into three distinct domains I, II and III. NS5A DI is a highly conserved structure with a zinc-binding domain which is coordinated by a unique motif of 4 fully conserved cysteine residues (Cys 39, Cys 57, Cys 59, and Cys 80). four different conformations of DI from genotypes 1a and 1b were observed by X-ray crystallography, with the same monomeric unit but exhibiting different dimeric arrangements (Lambert et al., 2014, Love et al., 2009, Tellinghuisen et al., 2005). More introduction to the structure and function of DI will be described in Section 1.3.2.

Compared with DI, DII and DIII are intrinsically disordered, natively unfolded and less conserved (Penin et al., 2004b, Tellinghuisen et al., 2004). However, nuclear magnetic resonance (NMR) and circular dichroism have demonstrated a propensity of both domains to form secondary structures (Feuerstein et al., 2012, Hanoulle et al., 2009b, Liang et al., 2007). In addition, an NMR analysis for the entire disordered region of NS5A (residues 191–447) from genotype 1b has shown numerous transient secondary and tertiary structures in DII and DIII (Sólyom et al., 2015). DII has been reported to contain a short structural motif (PW-turn) embedded in a proline-rich sequence (Dujardin et al., 2019). DIII contains a small amphipathic α-helical structural element exhibiting a pronounced asymmetrical distribution of the hydrophobic residues (Verdegem et al., 2011). Recently, The 3D structure of the highly disordered DII-III regions was predicted (Li et al., 2022) using the online I-TASSER server (Roy et al., 2010, Yang and Zhang, 2015). The structure showed the highest homology with the maltose-binding periplasmic protein (PDB ID 3OSR) (Li et al., 2022).These structures are strongly suggested to play important roles in the HCV cycle.

The three domains are separated by two short LCSs. LCS I is rich in serine clusters and eight highly conserved serine residues have been identified by mass spectrometry, reverse genetics and phospho-proteomics. Six serine residues 222, 225, 229, 232,

235 and 238 inhibited critical roles in NS5A phosphorylation, which is associated with HCV replication and assembly (Chong et al., 2016, Fridell et al., 2013, Kanazawa et al., 2004, Masaki et al., 2014). Moreover, a sequential phosphorylation cascade, “S229-S232-S235-S238”, has been identified (Hsu et al., 2018). LCSII is a proline-rich region composed of three polyproline motifs. The existence of highly conserved PxxP motifs in this region allows the binding with Src homology 3 (SH3) domains of host proteins (Mayer, 2001, Tan et al., 1999).

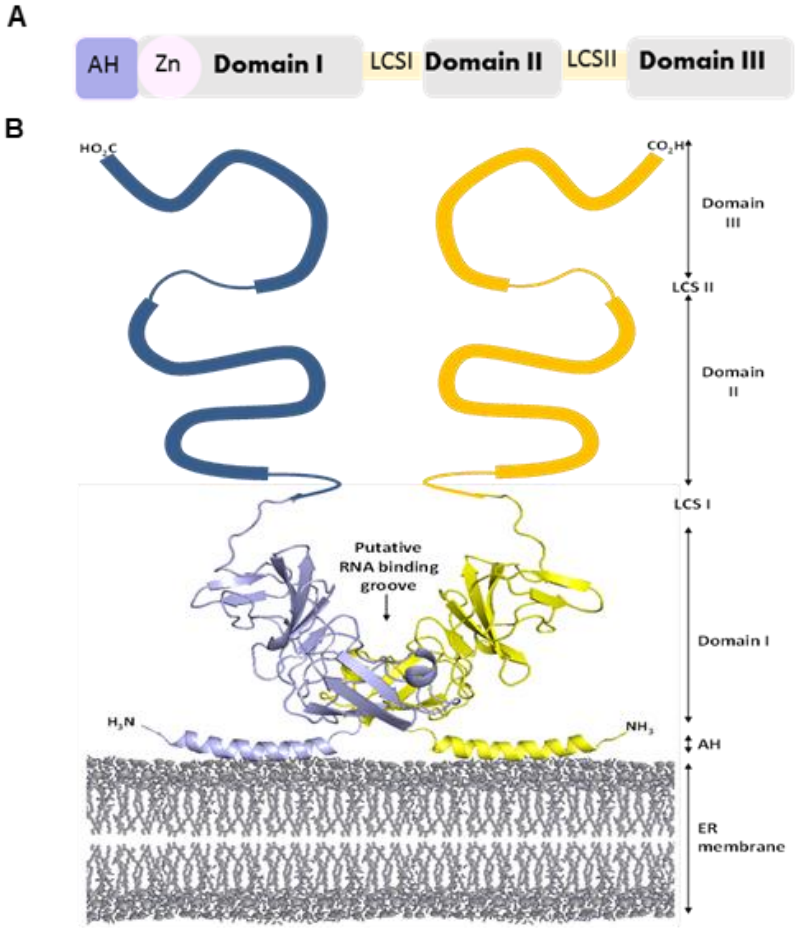

Fig 1.5 The structure of NS5A.

(A) NS5A contains three domains (I, II and III) connected by two low-complexity sequences (LCS I and LCS II). A 33aa amphipathic helix (AH) and a highly ordered domain I associated with a zinc ion. **(B)** Model of the structure of NS5A. The two domain I manners form the dimeric conformation observed by (Tellinghuisen et al., 2005), which anchored the membrane by AH (Douglas Ross-Thriepland, 2013).

1.3.2 Structure of NS5A DI

NS5A DI is highly conserved and consists of a basic N-terminal subdomain IA (36-100aa) and a predominantly acidic C-terminal subdomain IB. Subdomain IA contains an N-terminal extended loop lying which was connected with a 3-stranded anti-parallel β-sheet (B1-B3) (Fig 1.6A). An α-helix structure in B3 also has been identified as AH2. These structures of subdomain IA form a 4-cysteine zinc coordination site (Cys 39, Cys 57, Cys 59, and Cys 80) which have previously been shown to be absolutely required for HCV RNA replication (Tellinghuisen et al., 2005). The structure of NS5A has been shown to rely on zinc atoms based on the location of the zinc coordination site and their biochemical characterization (Tellinghuisen et al., 2004). The connection between subdomain IA and subdomain IB is a proline-rich region. Subdomain IB mainly consists of 2 anti-parallel β -sheets: B4-B7 and B8-B9 near the C-terminus (Fig 1.6A). A disulphide bond connecting the side chains of the conserved residues Cys 142 and Cys 190 has been observed near the C-terminus, referring to a covalent linked B6-B9 (Fig 1.6B).

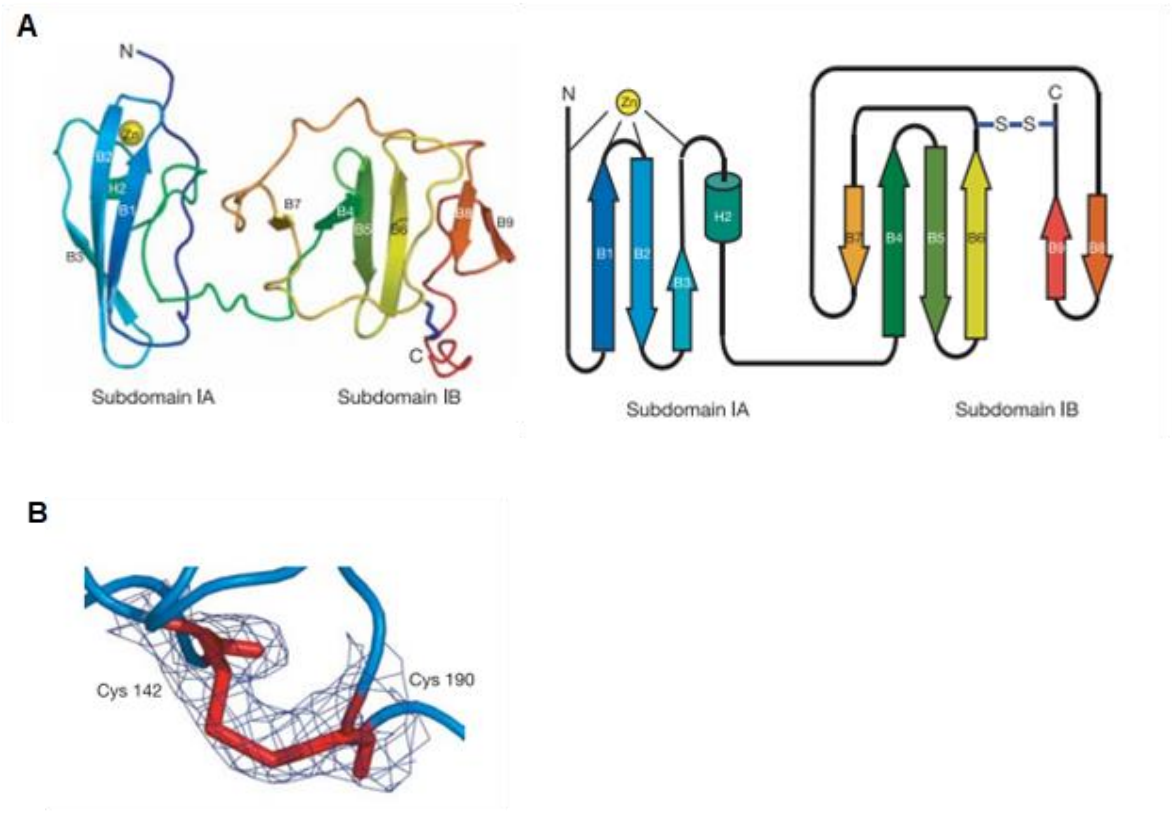

Fig 1.6 The structure of Subdomain IA and IB into NS5A DI.

(A) Ribbon diagram and topology organization model of the structure of domain I including N terminus (blue) to C terminus (red). The coordinated zinc atom is shown in yellow. The C-terminal disulphide Cys142-Cys190 bond is shown in blue. (**B)** The model of the disulphide bond in subdomain 1B, Cys 142 and Cys 190 are labelled in red (Tellinghuisen et al., 2005).

X-ray crystallography showed that NS5A DI is a highly structured, zinc-binding domain containing a three-dimensional structure that shows two different dimeric conformations when lacking an AH peptide (Love et al., 2009, Tellinghuisen et al., 2005). The first crystal structure of NS5A DI from genotype 1b was determined more than 17 years ago (Fig 1.7A). This structure (residues 36-198) (PDB accession code: 1ZH1) is an asymmetric unit, also known as a “clam-like” dimer, composed of two identical DI monomers in a dimeric conformation maintained by disulphide bonds. This structure accommodates a large, positively charged groove, proposed as a putative

RNA binding groove. N-terminal amphipathic helix on a phospholipid membrane of this structure which was computationally analyzed by surface potential plots and NMR, showed that NS5A would be anchored to the membrane in a way that the putative RNA binding groove was projected outwards in a manner that could facilitate the binding of RNA, as seen in Fig. 1.5B. The location of the zinc-binding site in the structure of domain I combined with a disulphide bond towards the C-terminus indicates both the zinc and disulphide bond contribute to the maintenance of the NS5A fold (Tellinghuisen et al., 2005).

The second crystal structure of NS5A DI from genotype 1b (33-202) exhibited an altered dimer structure of two parallel monomers which was described in 2009 (Love et al., 2009) (PDB accession code: 3FQM) (Fig. 1.7B). The monomers are related by a two-fold-symmetry axis that runs parallel to their length. As same as the previous structure, the two N termini are found on the same end of the dimer, implying a colocalization of the two amphipathic N-terminal helices. Moreover, the zinc-binding site displays the same coordination geometry. However, unlike the previous structure, there is no overlap between the two monomer-monomer interface surfaces, and in fact, the two regions are on opposite sides of the monomer. In addition, an interesting difference is the disulphide bond between Cys 142 and Cys 190 reported by Tellinghuisen, which is not present in this structure. Although these side chains are adjacent to each other, the distance between them does not allow the formation of a covalent bond. The two altered structural forms of DI now available may be indicative of the multiple roles emerging for NS5A in viral RNA replication and viral particle assembly (Love et al., 2009).

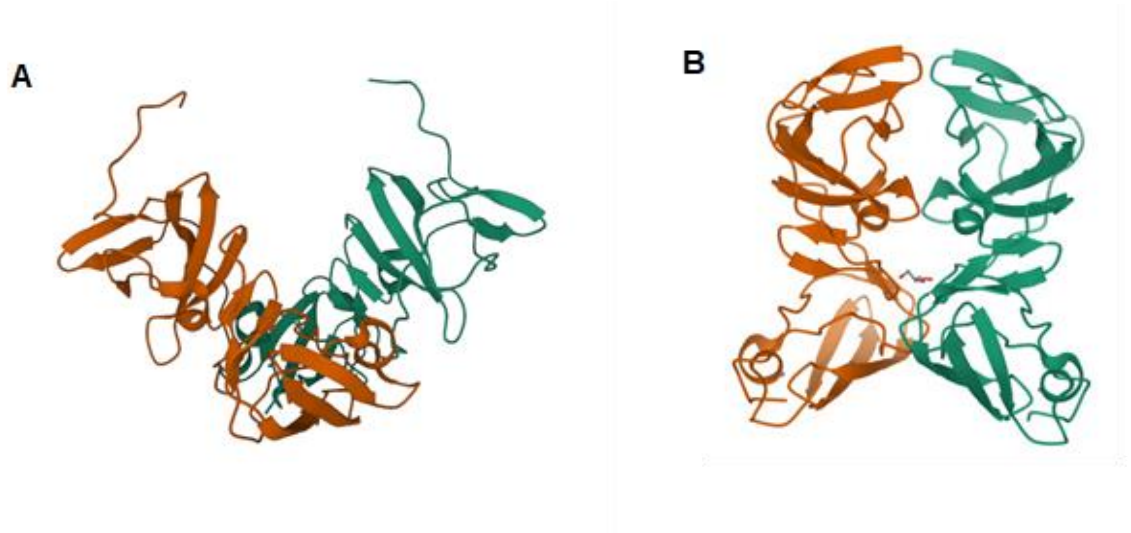

Fig 1.7 Two dimeric conformations of NS5A domain I from genotype 1b.

The monomers are shown in green and amber. **(A)**1ZH1, the first crystal structure of NS5A domain I from genotype 1b. (PDB DOI: 10.2210/pdb1ZH1/pdb) **(B)** 3FQM, the second genotype 1b dimer NS5A domain I crystal structure (PDB DOI: 10.2210/pdb3FQM/pdb) (Love et al., 2009, Tellinghuisen et al., 2005).

1.3.3 Function of NS5A in HCV infection

NS5A is a multifunctional protein and has been identified to be involved in the process of viral replication and assembly. These two roles are relatively independent. The functional regions for viral RNA replication have been mapped to AH, DI and DII, whereas the function region for assembly is largely targeted to DIII.

The main function of AH is ER membrane localization. Furthermore, G418 resistance colonies and mutants in the AH region both abrogated RNA replication, indicating the critical role in maintaining membrane-associated replicase complexes and modulating HCV replication (Elazar et al., 2003, Penin et al., 2004a).

Domain I was considered to be involved exclusively in genome replication, whereas recent research revealed the novel role of NS5A DI in virus particle assembly (Yin et al., 2018). The mechanism of NS5A DI to affect assembly still needs to be further

investigated, but the function of affecting replication has been indicated in a different region. The 4-cysteine zinc coordination site in DI subdomain IA is comprised of 4 fully conserved cysteine residues (Cys 39, Cys 57, Cys 59, and Cys 80), which has been identified to be necessary for HCV replication (Tellinghuisen et al., 2004). Numerous pieces of evidence have demonstrated the existence of the disulphide bond (Cys142 and Cys 190) in subdomain IB. However, the role of the disulphide bonds in HCV infections is still not clear, as they are dispensable for HCV replication (Tellinghuisen et al., 2004). The disulphide bond in the C- terminus of DI might alter the arrangement of domains II and III to further switch the different conformation of NS5A in the HCV life cycle (Tellinghuisen et al., 2005). Hence, the two dimer forms of are proposed to exhibit different functions in the HCV life cycle caused by the difference in construction and disulphide bond. These altered conformations might randomly transform based on different roles of NS5A in viral RNA replication and particle assembly. The wide groove of “claw-like” dimer 1ZH1 with the orientation of back to the membrane accommodates single stranded RNA or dsRNA, proposing to be an RNA binding region (Tellinghuisen et al., 2005). Numerous NS5A dimers may build a ‘basic railway’ which allow viral RNA to moves on intracellular membranes and modulate its different function during HCV replication (Moradpour et al., 2005). The “back-to-back” dimer 3FQM is considered to be associated with viral particle assembly due to the deficiency with the structure groove and disulphide bond, whereas the evidence is still insufficient.

Domain II also has been identified to be involved in viral RNA replication through mutagenesis analysis. A deletion of the C-terminal 35aa, resulted in complete abrogation of replication. However, the N-terminus did not affect virus replication (Appel et al., 2008). Additionally, a mutagenesis analysis using subgenomic replicon (SGR) genotype 1b displayed small deletions (8–15 residues) of the C- terminus also

completely inhibited replication (Tellinghuisen et al., 2008b). Furthermore, the mutagenesis analysis for DII 309-338aa in genotype 2a demonstrated multiple residues in DII were essential for virus replication but not particle release (Ross-Thriepland et al., 2013).

Domain III has been identified to be dispensable for HCV RNA replication, whereas it plays a critical role in viral particle assembly and production. The deletion of all highly conserved residues or the large insertions in this region only slightly affects RNA replication (Appel et al., 2005). The combination of deletion and alanine scanning mutagenesis has also demonstrated that domain III is not required for the function of NS5A in HCV RNA replication (Tellinghuisen et al., 2008b). However, the role of domain III in virus replication may occur in the early stage, resulting in delayed replication kinetics in genotype 2a HCV clone (Hughes et al., 2009). Additionally, domain III is a highly flexible and tolerant domain. To date, several sites in domain III have been identified to tolerate the insertion of green fluorescent protein (GFP), which does not affect HCV replication (Appel et al., 2005, Liu et al., 2006, Moradpour et al., 2004b). Domain III is also involved in the modulation of NS5A basal and hyperphosphorylation. The deletion and mutation analysis has been shown to reduce the NS5A phosphorylation, whereas it only induces a slight decrease in HCV replication (Appel et al., 2005). Therefore, the function of domain III is focused on viral particle assembly and production. The insertion analysis with a heterologous sequence into the coding region of domain III has been identified to suppress virus production (Schaller et al., 2007). In addition, the mutagenesis analysis in genotype 1a and 2a have also identified the association with virus assembly and production (Appel et al., 2008, Kim et al., 2011, Tellinghuisen et al., 2008a). Moreover, the deletions in domain III disrupt the colocalization with lipid droplets which is the

indicated site for HCV particle assembly, further affecting the formation of the virus particle (Appel et al., 2008).

1.3.4 NS5A-Host interaction

NS5A, as a multifunctional protein, is associated with HCV RNA replication and viral particle production through interaction with other viral proteins and cellular factors. Over 132 human proteins have been listed to be involved in the interaction with NS5A, associating with the cellular pathways in the immune system, cellular signalling, cell adhesion, cellular growth and death (Tripathi et al., 2013). Sixty proteins have been identified to participate in the HCV life cycle, and the interaction with NS5A mainly concentrates on the unstructured domains II and III.

1.3.4.1 Host factors required for replication

The alteration of the NS5A phosphorylation pattern is likely to associate with RNA replication via regulating interactions with cell factors (Appel et al., 2005, Evans et al., 2004). The basal and hyperphosphorylation of NS5A have been reported to be modulated by several kinases. The α isoform of casein kinase I (CKIα) is induced by a phosphorylation event at the 3 positions with a typical (pS/pT) XXS sequence, which can phosphorylate NS5A on serine residues in the LCS I domain based on a phosphorylation cascade from S229 to S232, then S235 and finally S238 (Hsu et al., 2018, Quintavalle et al., 2007). Casein kinase II (CKII) is involved in modulating NS5A phosphorylation on Ser 457 in Domain III, and this phosphorylation site is considered to play the essential role in virus particle assembly in genotype 2a (Tellinghuisen et al., 2008a). Polo-like kinase 1 (Plk1), a serine-threonine kinase, is also regarded as an NS5A phosphokinase to modulate both P56 and P58. The interaction of PlK1 and NS5A has been identified, and the knockdown of Plk1 reduces HCV RNA replication

(Chen et al., 2010).

Some factors have been identified to interact with NS5A in an S225 phosphorylation-dependent interaction model. The nucleosome assembly protein 1-like protein 1 (NAP1L1) has been demonstrated to be one S225 phosphorylation-dependent interaction factor with NS5A, associating with the HCV RNA replication and affecting the distribution of replication complexes throughout the cytoplasm (Goonawardane et al., 2017). Vesicle-associated membrane protein-associated protein A (VAP-A) is also revealed to interact with NS5A to modulate phosphorylation and HCV replication (Evans et al., 2004). Moreover, the interaction between NS5A and VAP-A is considered to be indirect and requires the involvement of G protein pathway suppressor 2 (GPS2) (Xu et al., 2013). The S225 phosphorylation target of this interaction also plays an essential role in “membranous web” (MW) formation and distribution (Goonawardane et al., 2017). Additionally, VAP-B has also been reported to interact with NS5A and forms homo- and heterodimers with VAP-A to regulate HCV replication (Hamamoto et al., 2005). Bridging integrator 1 (Bin1), a factor associated with membrane curvature and trafficking, is also reported to interact with NS5A dependent on S225 in the LCSI domain (Goonawardane et al., 2017).

HCV replication modulated by NS5A phosphorylation might also require the involvement of the LCSII domain. LCSII contains two polyproline motifs (PXXP motifs) which can effectively bind with the SH3 domain-containing proteins. Grb2, a cellular adaptor protein responsible for the mitogen-activated protein kinase (MAPK) signalling, can interact with NS5A via PXXP motifs. This interaction contributes to reducing the extracellular regulated kinase 1 (ERK1) and ERK2 phosphorylation and then further inhibit the epidermal growth factor (EGF) signalling and MAPK mitogenic pathway (Tan et al., 1999). Bin1 also contains the SH3 domain to interact with NS5A LCSII (Nanda

et al., 2006). Based on the interaction between Bin 1 and S225 in LCSI, S225 phosphorylation might induce a conformation alteration in NS5A that buried polyproline motif, or the interaction might establish in multiple sites in NS5A. In addition, the catalytic subunit of cAMP-dependent protein kinase A (PKA) can phosphorylate Threonine 356 in domain III which is close to the polyproline motif of NS5A, leading to changes in the conformational sampling of this SH3 binding determinant (Cordek et al., 2014).

In addition, phosphatidylinositol 4-kinase IIIα (PI4KA) is also one of the NS5A-interacting proteins. The disruption of PI4KA has been demonstrated to modify the NS5A localization and maintain the morphology of the HCV-induced MW by enhancing the expression of phosphatidylinositol 4-phosphate (PI4P) (Berger et al., 2009, Tai et al., 2009). In addition, PI4KA activity is involved in the formation of basally phosphorylated NS5A, and the knockdown of PI4KA reduces the HCV RNA replication (Siu et al., 2016). Furthermore, cyclophilin A and B have been revealed to interact with NS5A to promote RNA replication (Foster et al., 2010, Verdegem et al., 2011).

1.3.4.2 Host factors required for assembly

The role of NS5A in HCV assembly is mainly focused on domain III. The CK-mediated phosphorylation is also modulating the assembly process (Tellinghuisen et al., 2008a). The hyperphosphorylation modulated by CKIα is likely to be involved in the Core/NS5A interaction and recruitment to LDs, suggesting to play an essential role in nucleocapsid assembly (Masaki et al., 2014). CKII was also reported to modulate HCV assembly through phosphorylating the serine residue in NS5A domain III (Secci et al., 2016). The inhibitor of CKII reduces the HCV particle production of genotype 2 but does not affect RNA replication (Tellinghuisen et al., 2008a).

In the process of HCV assembly, diacylglycerol acyltransferase 1 (DGAT1) was found to interact with NS5A and recruits NS5A onto the surface of LDs. This interaction was also found to enhance the binding between NS5A and the core. However, the catalytically inactive mutant in DGAT1 only inhibits the localization of NS5A to LDs but not core, suggesting a direct role of DGAT1 in modulating HCV particle production via NS5A (Camus et al., 2013). A tail-interacting protein of 47 kDa (TIP47) has also been revealed to bind with NS5A via its N-terminal PAT domain. The silence of TIP47 expression completely abrogates the viral replication and production (Ploen et al., 2013). In addition, TIP47 also interacts with the α-helical domain of NS5A and further integrates LD membranes into the membranous web (MV) to facilitate HCV production (Vogt et al., 2013). NS5A DI has been reported to interact with Oxysterol binding protein (OSBP) and then colocalize to the Golgi compartment. The deletion in the pleckstrin homology (PH) domain of OSBP N-terminal results in the loss of location to the Golgi apparatus and HCV production, indicating the function of OSBP in HCV infection (Amako et al., 2009).

Phosphatidylserine-specific phospholipase A1 (PLA1A) has also been identified to modulate HCV assembly. The loss of PLA1A only affects the HCV assembly of genotype 2a, but not other steps of the HCV lifecycle (viral entry, translation and replication). PLA1A can interact with NS2/NS5A and further stabilizes its structure during HCV infection. Additionally, PLA1A plays an essential role in the stabilization of the replicase complex associated with NS5A and further facilities the interaction between viral proteins to enhance HCV assembly (Guo et al., 2015). Rab18 also can facilitate the fusion of LDs and ER membranes through colocalizing with NS5A on LDs surface in HCV-infected cells. This binding is likely to facilitate the physical interaction of NS5A with other viral proteins and host factors associated with LDs (Salloum et al.,

2013). Annexin A2 (ANXA2) is also regarded as a host factor to affect viral assembly. The loss of ANXA2 displayed no effect on RNA replication but had a significant reduction of virus titre. It has been reported that NS5A Domain III requires the direct recruitment of ANXA2, suggesting the role of ANXA2 associated with NS5A to facilitate the HCV viral particle formation (Backes et al., 2010).

The interaction between NS5A and apolipoproteins is essential for the process of HCV particles production. Apolipoprotein (Apo) A1 has been demonstrated to interact with NS5A and colocalize NS5A in the Golgi apparatus (Shi et al., 2002). The colocalisation of Core, NS5A and ApoJ was also found on the surface of LDs. The interaction complex can further enhance the binding of these two viral proteins with LDs (Lin et al., 2014). ApoE was considered only interact with NS5A but not with other viral proteins to affect viral assembly and production. The assembly-defective mutagenesis analysis showed reduced expression of ApoE–NS5A interaction, indicating the role of this interaction in HCV infection (Benga et al., 2010).

1.4 Life cycle of HCV

1.4.1 HCV virus particle composition

HCV particles are membrane enveloped of 40–80 nm in diameter, which lacks an obvious form of symmetry or surface features but exhibits a heterogeneous morphology (Bradley et al., 1985, Catanese et al., 2013, Gastaminza et al., 2010, He et al., 1987, Merz et al., 2011). The viral particle contains a nucleocapsid formed by the core protein, which is surrounded by ER-derived lipid bilayer. This structure envelopes the viral RNA and allows the insertion of E1 and E2 glycoproteins, which are involved in virus binding and entry (Fig1.8) (Lindenbach and Rice, 2013).

HCV particles generally have a low buoyant density ranging from 1.03 to 1.25g/mL

(Catanese et al., 2013). Higher-density particles are less infectious and can be neutralized by anti-human IgG. In contrast, *in vivo* inoculation into chimpanzees demonstrated that the HCV particles with lower buoyant density had the most infectivity (Bradley et al., 1991, Hijikata et al., 1993). Additionally, serum-derived HCV and HCVcc particles showing high specific infectivity have buoyant densities of ≤1.10 g/ml (Hijikata et al., 1993, Lindenbach et al., 2005), which is distinct from the characteristics of other enveloped RNA virus with most highly infectivity in the high density. It has been demonstrated that HCV infection is associated with lipids and lipoprotein metabolism in the hepatocytes, suggesting a more complex structure of infectious HCV particles.

The characteristic feature of HCV particles is the association with host lipoproteins. The low-density HCV particles with high infectivity are tightly associated with VLDL or low-density lipoproteins (LDL), forming the lipoviroparticles (LVPs) (Andre et al., 2002, Nielsen et al., 2006, Thomssen et al., 1992). LVPs have been identified to contain abundant cholesterol and triglycerides, and some Apos have been found on the rough surfaces of LVPs such as ApoB (ApoB-100 and ApoB-48), ApoA-I, ApoE-54, and ApoCs (Catanese et al., 2013, Gastaminza et al., 2008, Meunier et al., 2008, Piver et al., 2017). Notably, these Apo are much easier to be labelled by antibody compared with E1 and E2. Apo is involved in the lipoprotein structure, lipoprotein clearance and lipoprotein metabolism (Ramasamy, 2014, Sundaram and Yao, 2012). HCV can exploit Apo to entry and rapid multiplication in hepatocytes and further assist the virus in evading antibody neutralization (Aizawa et al., 2015). However, the more specific structure of LVPs and the interactions between lipoproteins, Apo, and the HCV viral particles still needs to be further investigated.

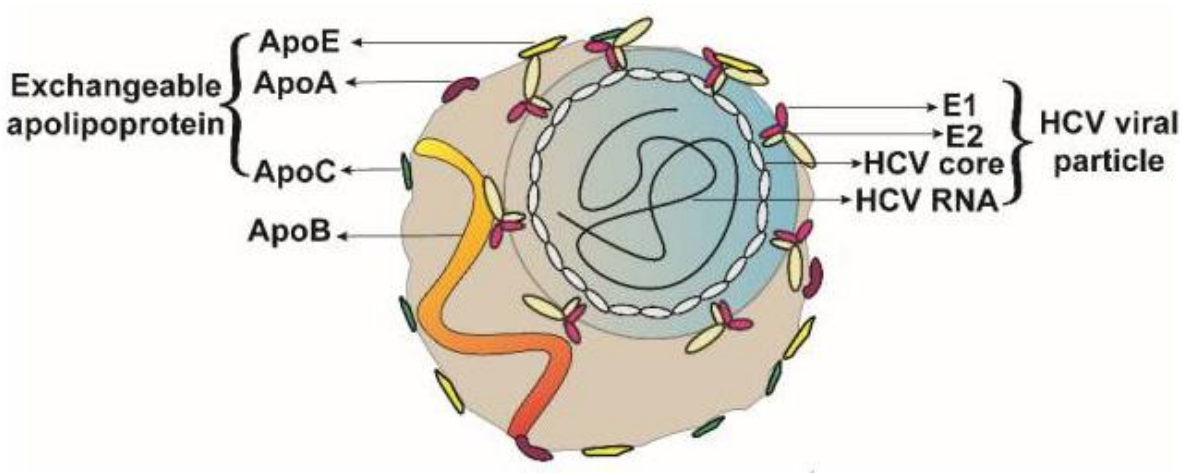

Fig 1.8 Structure model of the HCV LVP.

HCV viral particle (blue circle) contains a nucleocapsid formed by core protein and enveloped by an ER-derived membrane embedded with E1 and E2. This structure jointly surrounds and protects positive-stranded viral RNA. The lipid components (brown shape) contain VLDL and LDL, which are associated with different Apo (ApoA, ApoB, ApoC and ApoE). These two structures constitute a hybrid particle LVP (Gong and Cun, 2019).

1.4.2 HCV entry

The process of HCV LVP entry to the cells is complicated, associating with several receptors, co-receptors and host factors. This process is composed of three steps: viral attachment, receptor-mediated endocytosis and host cell endosomal membranes fusion (Fig1.9) (Ansaldi et al., 2014, Hajarizadeh et al., 2013, Mohd Hanafiah et al., 2013).

Viral attachment requires the involvement of glycoprotein, Apo at the surface of LVP and various factors on the cell surface. HCV LVP firstly attaches to the cells via the low-affinity interaction with the LDL receptor (LDL-R) and glycosaminoglycans (GAGs) present on heparan sulfate (HS) proteoglycans (HSPGs) (E Karangelis et al., 2010). ApoE, syndecan 1 and syndecan 4 have been demonstrated to be responsible for this

interaction (Jiang et al., 2013, Lefèvre et al., 2014, Shi et al., 2013). Interestingly, glycoproteins E1 and E2 are not involved in this process, even though they have also been found to bind with GAGs (Xu et al., 2015). LDL-R can transport the cholesterol-rich LDL into cells through clathrin-mediated endocytosis (Sorrentino et al., 2013). However, the specific role of the cell surface proteins involved in HCV entry still needs to be further confirmed. In addition to these two attachment receptors, five factors on the cell surface also participate in HCV particle entry, including scavenger receptor class B type I (SR-BI), tetraspanin CD81, claudin 1 (CLDN1), occludin (OCLN) and Niemann-Pick C1-like 1 cholesterol absorption receptor (NPC1L1). After HCV LVP initially interacts with LDLR and GAGs, SR-BI as a co-receptor binds with high-density lipoproteins (HDL), ApoB-containing lipoproteins and oxidized forms of LDL (Dreux et al., 2009, Scarselli et al., 2002). These interactions facilitate lipoprotein metabolism through the absorption and delivery of cholesterol from these lipoproteins (Acton et al., 1996). SR-BI has also been identified to bind with E2 protein on HepG2 cells following the loss of CD81 expression (Scarselli et al., 2002).

Following the stable attachment on cells, CD81 and the tight junction proteins CLDN1 and OCLN mediate clathrin-dependent endocytosis to promote cellular internalization. CD81 can interact and prime with E2 protein to promote low pH activation during virus entry (Sharma et al., 2011). This interaction guides HCV LVP to the tight junctions to interact with CLDN1 (Harris et al., 2010). Various transduction pathways are involved in this movement process, including EGFR, Ras and Rho GTPases (Brazzoli et al., 2008, Lupberger et al., 2011, Zona et al., 2013). OCLN, as a tight junction protein, plays a role in the post-attachment step of HCV entry between GAGs and SR-BI interaction and endosomal acidification (Sourisseau et al., 2013). However, the exact interaction between OCLN and HCV LVP is still unclear. NPC1L1 was also identified

as an additional HCV entry factor caused by abundant cholesterol in HCV particles. The role of NPC1L1 in HCV entry appears to associate with cholesterol uptake (Jia et al., 2011).

The viral fusion process is a low-pH mediated manner modulated by the interaction between E2 and CD81. Notably, the process might be facilitated via ApoC-I, which is an exchangeable apolipoprotein in HDL (Dreux et al., 2007, Meunier et al., 2008). ApoC-I interacts with E2 in an SR-BI or CD81-independent manner, which has been identified to enhance the pH-dependent fusion rates (Dreux et al., 2007). After host cell endosomal membrane fusion, virus RNA is released into the cytosol for further translation and replication.

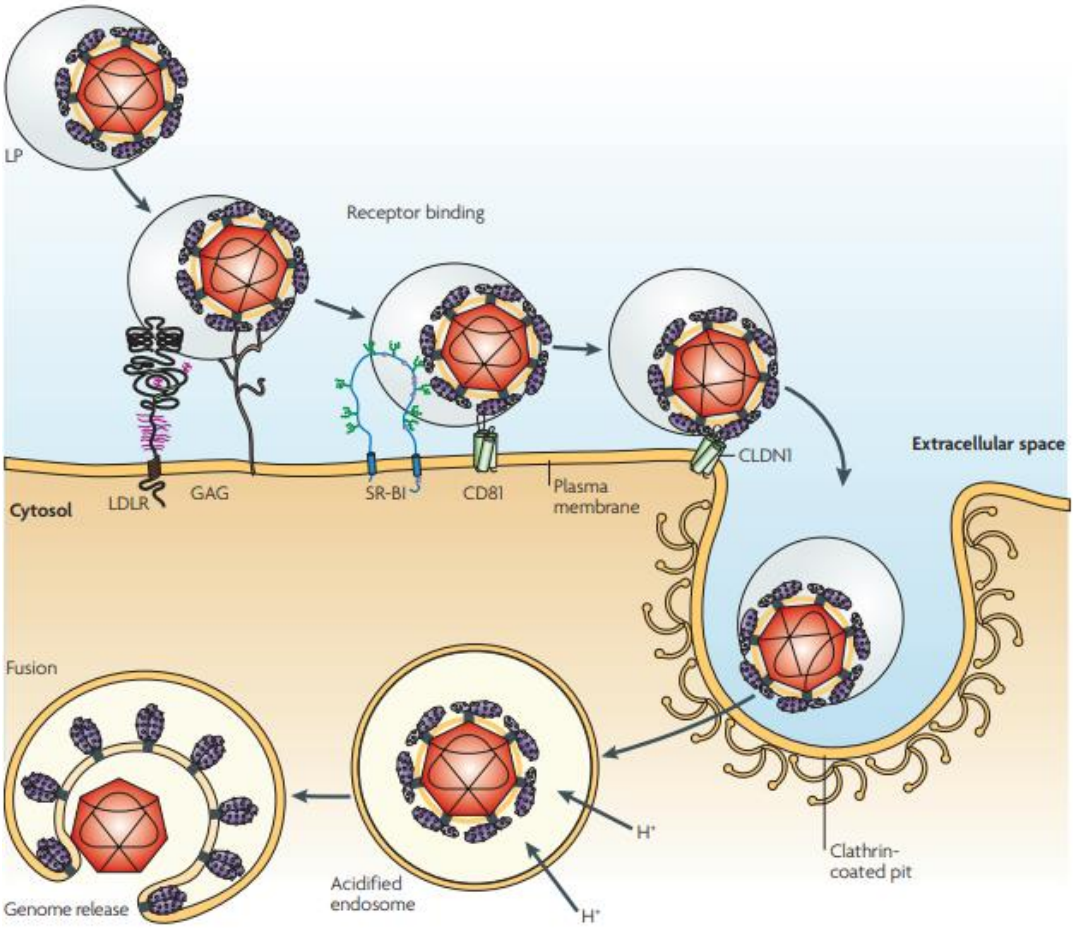

Fig 1.9 The current model of HCV entry.

Step1: Viral attachment. HCV LVP interacts with GAGs on HSPG, LDLR and SR-BI, inducing the exposure of the CD81 binding site of E2 protein. Step2: clathrin-dependent endocytosis. The E2 and CD81 interaction guide HCV LVP to the tight junctions to interact with CLDN1, associating with EGFR, Ras and Rho GTPases. Step 3: Host cell endosomal membranes fusion in a low pH manner (Moradpour et al., 2007).

1.4.3 RNA replication

Once viral RNA is released into the cytosol, it is translated into polyprotein by the ribosome binding with 5′UTR IRES (Lindenbach et al., 2005). This process is facilitated by various elements in the 3′UTR and cis-acting RNA elements (CREs) in the protein-

coding region (Adams et al., 2017). The translation process produces an approximately 3000 aa long polyprotein precursor, which is cleaved by host and viral proteases into three structural proteins and seven non-structural proteins (Dubuisson and Cosset, 2014), which are described in 1.2.1.

HCV RNA replication is also a complicated process that requires several steps, suggesting the role of several viral and cellular proteins (Lohmann, 2013). Non-structural proteins NS3 to NS5B are necessary and sufficient for HCV replication. Upon the polyprotein cleavage in the cytosol, NS3/4A, NS4B, NS5A and NS5B constitute the viral RC which is then closely connected with ER membranes. NS2 is considered not to be one component of viral RC and not essential for RNA replication. However, NS2/NS3 junction is likely to endow NS2 with a similar function to NS3 (Madan et al., 2014). NS2 appears to indirectly modulate the replication due to the replication requirement of NS3. Together with cellular factors, the viral RC remodels ER membrane to form the viral replication organelles termed the membranous web (MW) (Miller and Krijnse-Locker, 2008, Paul and Bartenschlager, 2015).

Double membrane vesicles (DMVs) and multimembrane vesicles (MMVs) are the main components of MV. Purified DMVs, with an average diameter of ~150 nm, contain activated viral replicase, indicating the truth replication organelles are DMVs and play an essential role in HCV replication (Paul et al., 2013, Romero-Brey et al., 2015). It contains all NS proteins and dsRNA required for RNA replication (Ferraris et al., 2013, Ferraris et al., 2010, Gosert et al., 2003, Paul et al., 2013). In addition, abundant DMVs were found when RNA replication achieved a peak in HCV-infected cells (Romero-Brey et al., 2012). Notably, expression of HCV replicase proteins NS3–5B in the absence of genome can induce DMVs, whereas NS4B and NS5A are considered the most important inducer (Egger et al., 2002, Gouttenoire et al., 2009a). The

mutagenesis analysis in NS3–5B polyprotein has identified that the self-interaction of NS4B plays an important role in DMV induction (Gouttenoire et al., 2010b, Paul et al., 2011). Moreover, NS4B can regulate membrane integrity in vitro, suggesting potentially membrane activity in vivo (Palomares-Jerez et al., 2012). NS5A can interact with the PPIase region of CypA to facilitate the formation of viral RC (Madan et al., 2014). In addition, proline-serine-threonine phosphatase interacting protein 2 (PSTPIP2), a positive membrane curvature inducer, also can be bound by NS5A to remodel intracellular membranes (Chao et al., 2012).

HCV is considered to alter the local lipid composition to further modulate DMVs, resulting from the strong dependence on PI4KIIIα and PI4P. The subcellular localization of PI4KIIIα is altered via the interaction with NS5A and NS5B, leading to the distribution change of PI4P from Golgi membranes and the inner leaflet of the plasma membrane to the cytoplasm (Bianco et al., 2012, Reiss et al., 2011). The alternant distribution of PI4P modulates the lipid composition of DMVs by nonvesicular cholesterol transportation, associating with the four-phosphate adaptor protein 2 (FAPP2) and OSBP (Khan et al., 2014, Wang et al., 2014). In addition, VAPA and VAPB are also involved in this process through recruiting with NS5A. OSBP binds with VAPA and VAPB via the FFAT motif to further facilitate cholesterol transportation and RNA replication (Wang et al., 2014). Cell autophagy is another pathway to form DMVs, resulting from the morphologically similarity between autophagosomes and DMVs. It has been identified that autophagosomes act as platforms for HCV RNA synthesis and inhibit innate immune antiviral response to further promote RNA replication (Fig1.10) (Ke and Chen, 2011, Sir et al., 2012).

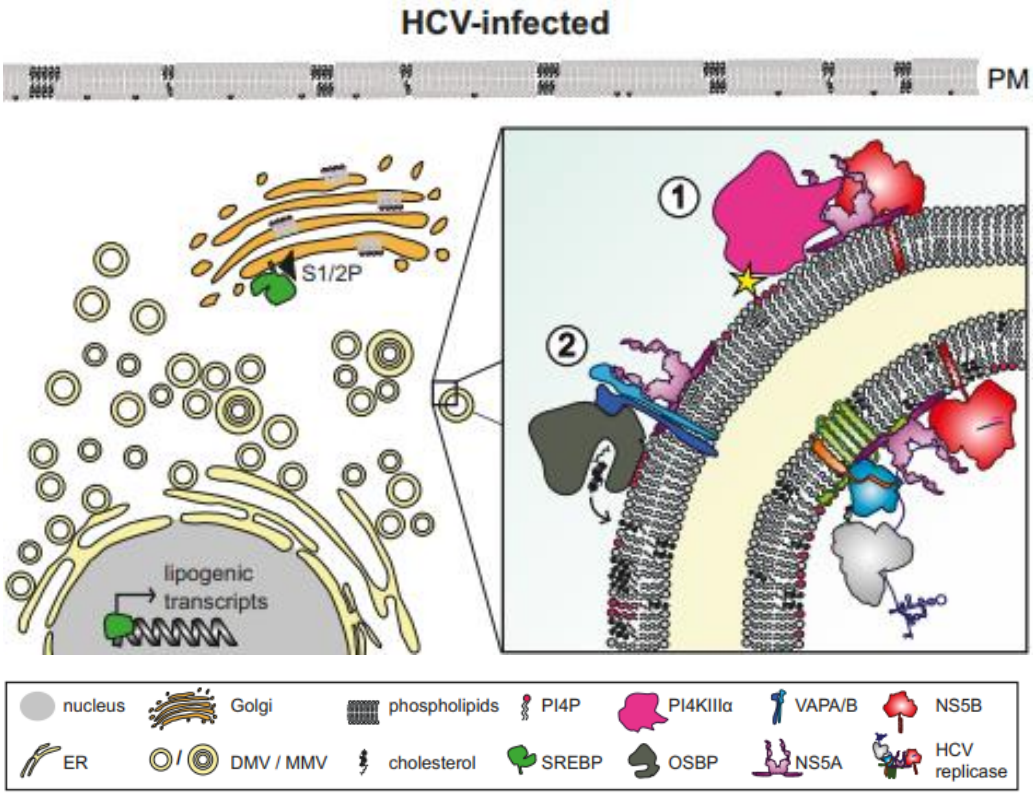

Fig 1.10 Model of HCV-interacted host cell proteins and lipids in the process of MV formation.

The subcellular localization of PI4KIIIα is altered via the interaction with NS5A and NS5B, leading to the distribution change of PI4P from Golgi membranes and the inner leaflet of the plasma membrane to the cytoplasm. OSBP recruitment by PI4P binds to VAPA and VAPB to further facilitate cholesterol transportation and RNA replication (Paul et al., 2014).

1.4.4 HCV Particle Production

The currently identified process of HCV particle production and release indicates three steps: viral assembly on the surface of LDs, envelopment of viral particles at the ER and egress via the VLDL secretory pathway (Herker and Ott, 2011, Popescu and Dubuisson, 2010).

1.4.4.1 Viral assembly

HCV assembly occurs at assembly sites associated with ER-derived membranes near Rc and requires the involvement of LDs. Core protein has been demonstrated to accumulate on the surface of LDs in HCV infection (Miyanari et al., 2007). Mutations in the signal peptide peptidase cleavage site and D2 domain of the core are both reported to abrogate viral assembly (Boulant et al., 2007, Miyanari et al., 2007, Targett-Adams et al., 2008b), indicating the core recruitment at the LD. DGAT1, an enzyme required for LD biogenesis, has been reported to be involved in this process to facilitate the LD/core localization through binding with Core (Herker et al., 2010). The localization of Core to LDs also requires the MAPK-regulated cytosolic phospholipase A2 (Menzel et al., 2012). The core recruitment at the LD surface is essential for the LDs target for the other viral protein and cellular factors, facilitating the transportation of the newly replicated RNA genomes and glycoproteins to the assembly site (Fig1.11) (Barba et al., 1997, Lindenbach, 2013, Miyanari et al., 2007).

NS5A is also regarded as an LD localization protein and is responsible for transforming the newly replicated RNA genome to the core protein, which is located on the LDs surface (Boson et al., 2017, Zayas et al., 2016). DGAT1 and TIP47 have been reported to be involved in the process. DGAT1 is responsible for enhancing the interaction between NS5A and Core and assists them in moving to the surface of LDs (Camus et al., 2013), while TIP47 can bind with NS5A and further facilities the formation of MVs (Vogt et al., 2013).

This role indicates that NS5A is an essential viral protein as a transition to link viral replication and assembly. In addition to the core protein, newly replicated RNA, glycoproteins E1 and E2 are also critical components to form the LVPs in the viral

assembly process. The recruitment of glycoproteins to core protein requires the NS2-P7 and NS3/4A complex (Jirasko et al., 2010, Phan et al., 2009, Popescu et al., 2011). NS2 and p7 can interact with E1E2, Core, NS3/4a and NS5A and guide them into assembly sites, allowing the correct assembly of LVPs (Boson et al., 2011, Denolly et al., 2017, Jirasko et al., 2008, Ma et al., 2011, Popescu et al., 2011, Stapleford and Lindenbach, 2011). The main function of P7 in this process is as an auxiliary for NS2 and plays an essential role in the later stage of viral envelopment (Bacon et al., 2011, Denolly et al., 2017, Gentzsch et al., 2013). NS3/4A linker region and helicase domain is the essential region to interact with NS2, while the role in assembly might not be dependent on helicase activity (Kohlway et al., 2014b, Phan et al., 2009). Additionally, the homotypic self-interactions of the NS4A two transmembrane domains (TMDs) have also been reported to be involved in LVPs production (Kohlway et al., 2014a). NS4B and NS5B were also observed to affect HCV assembly (Gouklani et al., 2012, Jones et al., 2009, Paul et al., 2011), but the mechanism is still unclear.

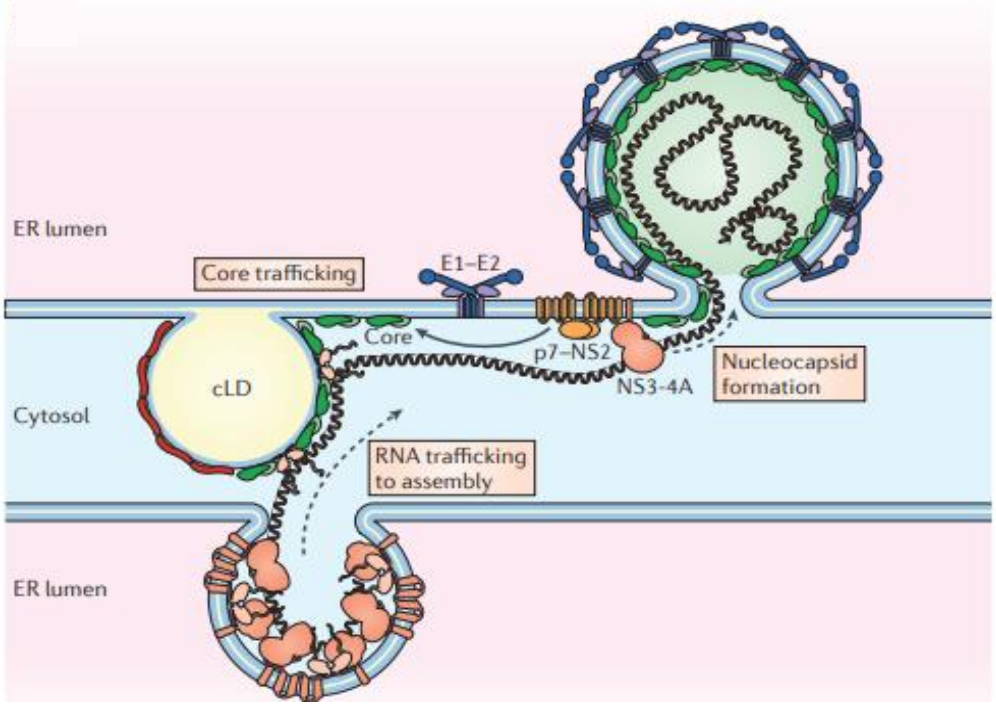

Fig 1.11 The model of HCV assembly.

HCV assembly occurs on the localisation of Core protein with LDs, and nascent viral RNA is transported by NS5A from replication sites towards to viral assembly site. Several host factors are involved, such as DGAT1, A2 and TIP47. The interaction of p7–NS2 with NS3-4A guides viral glycoproteins E1 and E2, core protein, to the viral assembly site to form the HCV viral particles (Lindenbach and Rice, 2013).

1.4.4.2 Viral budding, maturation and release

Viral budding and fission mainly rely on the endosomal sorting complex required for the transport (ESCRT) pathway, of which has regarded as the main evasion route for enveloped viruses (Votteler and Sundquist, 2013, Welsch et al., 2007). Several studies have identified that HCV particle release is also dependent on components (ESCRT-III and VPS4) of the ESCRT pathway (Ariumi et al., 2011, Corless et al., 2010, Tamai et al., 2012). In addition, ubiquitinated NS2 has been reported to be involved in the

assessment of the ESCRT pathway through interaction with hepatocyte growth factor–regulated tyrosine kinase substrate (HRS) using its ubiquitination interacting motif (UIM) (Barouch-Bentov et al., 2016). Moreover, the endocytic recycling compartment ERC is also modulated by ESCRT to further facilitate HCV particle release (Corless et al., 2010, Tamai et al., 2012).

The newly produced HCV particles are transported to the Golgi based on a conventional secretory pathway, where glycoproteins E1E2 undergo a complex post-translationally modification (Vieyres et al., 2014). Modified glycoproteins E1E2 are a component of large disulphide-linked complexes. This construct is natively folded and plays a critical role in the acid resistance of LVPs (Tscherne et al., 2006, Vieyres et al., 2010). In addition, the rearrangement of this structure appears to induce the low pH-mediated fusion of LVPs (Fig1.12) (Krey et al., 2005).

HCV particles were also reported to interact with serum lipoproteins (Apo A1, B, C1, and E) during the secretory pathway. Newly produced HCV particles were found to have an intermediate buoyant density during release, which is similar to VLDL particles (Gastaminza et al., 2008, Gastaminza et al., 2006). HCV particle production also requires microsomal triglyceride transfer protein (MTP) mediating the transportation of triacylglycerol into nascent ER lumen and lipid loading of ApoB (Gastaminza et al., 2008, Huang et al., 2007). Several studies have indicated that HCV production is dependent on ApoB and ApoE (Bartenschlager et al., 2011, Da Costa et al., 2012, Long et al., 2011). Notably, based on the observation of HCV particle formation in most cells, they are unable to produce authentic VLDL particles. In addition, nascent HCV particles were found to incorporate with ApoE during the secretory pathway (Coller et al., 2012). These studies suggested that HCV production may also depend on ApoE-containing microsome-associated LDs (maLDs).

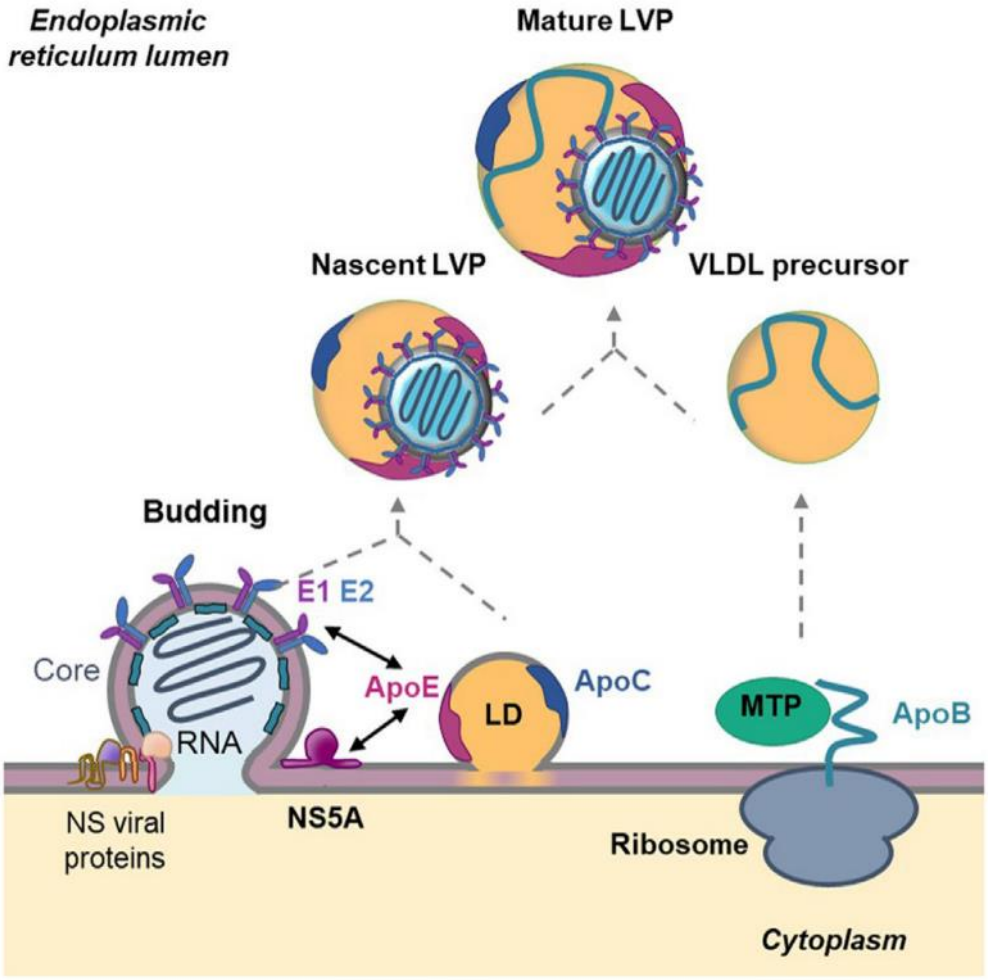

Fig 1.12 the model of HCV particle egress.

Core proteins form the nucleocapsid for HCV particles, which are enveloped by ER-derived membranes embedded with glycoproteins E1 and E2. The formation of nascent LDs requires the involvement of ApoE through interacting with NS proteins and glycoproteins E1 and E2. In addition, ApoB associates with the production of VLDL precursors through modulation by MTP. The newly produced HCV particles and low-density lipoprotein form the mature LVPs (Wrensch et al., 2018).

1.5 Cyclophilin A

1.5.1 Overview of Cyclophilin A

Cyclophilin A (CypA) belongs to the Cyp family which has peptidyl-prolyl isomerase

(PPIase) activity (Fig 1.13). Cyps catalyze the isomerization of peptide bonds preceding prolines to interconvert these proline residues between cis and trans isomers. In addition, CypA is also considered to facilitate other proteins folding and assembly (Davis et al., 2010, Stamnes et al., 1992). Cyps are highly conserved in evolution and widely exist in all prokaryotes and eukaryotes, indicating 60 reported Cyps in plants, fungi, animals, and bacteria. There are 17 human Cyps that are structurally distinct but highly conserved in the PPIase domain (Davis et al., 2010, Kallen et al., 1991). They have different subcellular localization, including cytoplasm (CypA), ER (CypB) and mitochondria (CypD) (Hoffmann and Schiene-Fischer, 2014, Kumari et al., 2013). Other Cyps are produced from cells and regarded as intercellular mediators (Nigro et al., 2013, Sherry et al., 1992, Spik et al., 1991, Suzuki et al., 2006).

The most abundant and best characterized member is CypA, having a proportion of about 0.1–0.6% in total cytosolic proteins (Dornan et al., 2003, Wang and Heitman, 2005). CypA was firstly identified from the Cyp family and initially purified from bovine thymocytes, which could bind to the immunosuppressive drug cyclosporin A (CsA) in lymphoid cells (Handschumacher et al., 1984). The CypA-CsA complex can bind to calcineurin and then abrogate T-cell activation by inhibiting the calcineurin-dependent dephosphorylation of the nuclear factor of activated T-cells (NFAT) (Borel et al., 1994, Clipstone and Crabtree, 1992, Liu et al., 1991). Additionally, some non-immunosuppressive CsA derivative and cyclophilin inhibitors (CypI) have been generated to interact with Cyps in a calcineurin-independent manner, allowing inhibitors activity in the loss of immunosuppression (Ahmed-Belkacem et al., 2016, Colpitts et al., 2020, Goto et al., 2006, Hopkins et al., 2010, Ma et al., 2006, Mackman et al., 2018). Among them, SCY-635 and alisporivir have demonstrated clinical efficacy in HCV infection (Sweeney et al., 2014).

CypA is considered to be a modulator of innate immune signalling pathways. CypA mediates the ubiquitination of RIG-I by E3 ligase TRIM25 and further modulates RIG-I activity (Liu et al., 2017). CypA has also been reported to interact with the nuclear factor kappa B (NF-κB) p65 subunit and then facilitate the stability and nuclear translocation of P65 (Sun et al., 2014). Furthermore, the autophosphorylation of PKR is regulated by CypA via interaction (Daito et al., 2014).

CypA has been found to play the roles in replication in many RNA viruses, such as HIV-1 (Liao et al., 2021), coronaviruses (CoVs) (de Wilde et al., 2018), HCV, dengue virus and other flaviviruses (Gallardo-Flores and Colpitts, 2021). Increasing evidence displays the role of CypA in modulating virus replication through binding with viral proteins, assisting the virus in evading innate immunity. However, the molecular mechanisms are still unclear. Much research reported the broad-spectrum antiviral activity of CypI, indicating that Cyps show promise as the targets for antiviral therapy.

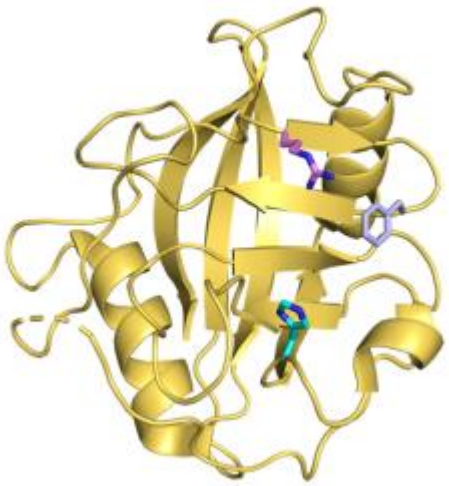

Fig 1.13 The structure of CypA (PDB: 4IPZ).

PPI active site residues R55 is in pink, F60 is in violet, and H126 is in cyan (Gallardo-Flores and Colpitts, 2021).

1.5.2 Cyclophilin A and HCV Infection

The function of CypA is confirmed in HCV due to the inhibitor CsA. Before the virus was identified as HCV, the intravenous administration of CsA had been reported to improve hepatocyte ultrastructural changes in two experimentally infected chimpanzees (Teraoka et al., 1988). Hence, CsA was speculated to inhibit the replication of non-A, non-B type 1 hepatitis (predecessor of HCV) (Feinstone et al., 1975). In 2003, CsA was finally identified to abrogate HCV RNA replication in a genotype 1b replicon system (Watashi et al., 2003). The expression of viral proteins NS5A and NS5B was also found to decrease, indicating the potential therapeutic role of CsA in HCV (Nakagawa et al., 2004). Importantly, the blocking role of CsA in HCV replication was independent of its immunosuppressive function (Watashi et al., 2003). The same inhibition was also found in genotype 2a, albeit with less effectiveness (Ishii et al., 2006). Based on the effective disruption, CsA was used in HCV therapy combined with the IFN treatment regimen in the lack of efficient treatment. The combination of CsA and IFN achieved sustained virological response, which showed improved therapy outcomes with fewer side effects (Inoue et al., 2003, Inoue and Yoshiba, 2005).

The inhibited activity of CsA further suggests the role of Cyps in HCV replication. The loss of CypA, CypB and CypC in Huh7 cells suppressed the HCV replication in genotype 1b, while CypA showed the most effective inhibition among them (Nakagawa et al., 2005). However, in MH-14 cells, the silencing of CypB has a more potent disruption of HCV replication in genotype 1b than the lack of CypA (Watashi et al., 2005). Notably, compared with the CypB and CypC, only CypA in Huh7.5 cells was essential for the replication of genotype 1a, genotype 1b and genotype 2a (Yang et al., 2008). Consistently, the silencing of CypA, but not CypB expression in Huh7-Lunet or

Huh7.5 cells, has been demonstrated to inhibit HCV replication of genotype 2a HCV. In addition, the re-expression of CypA in the silenced cells resulted in the recovery of HCV replication (Kaul et al., 2009). The peptidyl-prolyl isomerase activity of CypA is also identified to be responsible for HCV replication through the mutagenesis analysis of CypA (Chatterji et al., 2009, Kaul et al., 2009). Considering the important role of CypA in HCV replication and the abundant expression level (at least 10-fold higher than other Cyps), CypA became the essential factor in HCV infections.

Although CsA was utilized to treat HCV infection, the antiviral mechanism of CsA against HCV still needs to be investigated. Mutagenic analysis in genotype 1b has demonstrated that NS5A and NS5B affected the susceptibility of HCV replication to CsA. Moreover, CsA showed different resistance to the mutants in NS5A and NS5B, suggesting different mechanisms of CsA against HCV through NS5A, NS5B or NS5A/NS5B complex (Fernandes et al., 2007). This study indicated a potential interaction between Cyps and NS5A or NS5B.

The interaction between CypA and NS5A has been mapped to domain II and domain III. CypA is suspected of inducing protein conformational changes of NS5A through binding with naturally disordered domain II and domain III. PPIase active sites of CypA and CypB have been identified to directly interact with domain II, and some similar studies also confirmed the interaction with the CypA isomerase pocket (Chatterji et al., 2010, Foster et al., 2011, Hanoulle et al., 2009a). Notably, domain II of NS5A contains a proline-rich region, which is regarded as the putative substrate for CypA PPIase activity and responsible for CypA binding and isomerisation (Coelmont et al., 2010, Grisé et al., 2012). The potential target of PPIase activity of CypA in NS5A domain II might not be restricted to a particular proline. Multiple prolines are likely to be involved in the interaction (Hanoulle et al., 2009a). PPIase activity is required for HCV

replication, which can be blocked by CsA and other CypI. The mutation of active sites (R55A, F60A, and H126Q) of CypA reduced 99% PPIase activity on a peptide substrate, whereas these mutations have no effect on CsA-binding and calcineurin inhibition (Zydowsky et al., 1992). Some mutants selected by CsA treatment in a proline-rich region of domain II, especially the NS5A D316E/Y317N double mutant, showed resistance to CsA in different HCV genotypes (Yang et al., 2010).

CypA-NS5A interaction may influence HCV RNA replication in several different ways. First, the interaction affects the function of RNA binding of NS5A. The binding of CypA PPIase active sites with a proline-rich region in NS5A Domain II improved RNA binding capacity and enhanced RNA replication efficiency (Foster et al., 2011, Nag et al., 2012). CypA is considered to share the binding sites in NS5A domain II with NS5B, leading to the formation of CypA/NS5A/NS5B complex to modulate RNA replication (Liu et al., 2009, Ngure et al., 2016). In addition, CypA might also associate with the formation of the NS5A-mediated viral replicase complexes (RC). CsA and some CypI have been shown to inhibit RC formation but did not affect the integrity of already established RC. In addition, the silence of CypA or CsA treatment disrupted RC formation, and the re-expression of CypA recovered this function (Chatterji et al., 2015, Colpitts et al., 2020). Furthermore, CypA is considered to be responsible for RC formation through the binding with NS5A (Madan et al., 2014). Collectively, these findings suggest the critical role of CypA in HCV replication, binding to NS5A Domain II to rearrange its structure and regulate the formation of NS5A and interaction partners mediated RC.

Some studies have also identified the role of CypA in the HCV particle assembly. CypA also interacts with NS5A domain III, which has been demonstrated to play an essential role in virus particle assembly and production (Verdegem et al., 2011). CypI-treated replicon harbouring or HCV-infected cells resulted in the alteration of morphology of

lipid droplets, enhancing their size and reducing their amount. In addition, the CypI treatment interfered with cellular lipid and protein trafficking in the VLDL pathway (Anderson et al., 2011). The association with lipid droplets and very low-density lipoprotein (VLDL) both pointed out the role of CypA in HCV assembly and production.

CypA is also reported to be involved in double-stranded RNA (dsRNA)-activated protein kinase PKR-dependent antiviral pathway during HCV infection. CypA can modulate the activity of PKR through CypA-PKR interaction. Furthermore, CypI or CsA treatment in HCV-infected cells led to the reduction of phosphorylated PKR and downstream factor eIF2a, affecting the PKR-mediated protein translation (Daito et al., 2014). Similarly, studies also confirmed the inhibition of phosphorylated PKR and further revealed the role of PKR in HCV evasion of the innate immune response by reducing ISG translation (Bobardt et al., 2014). Furthermore, CsA and CypI have been reported to enhance the expression of IFN-β and ISGs in a PKR and downstream interferon regulatory factor-1 (IRF1) -dependent manner (Colpitts et al., 2020). More mechanism of PKR in the HCV life cycle is described in 1.5.

1.6 dsRNA-activated protein kinase (PKR)

1.6.1 Overview of PKR

dsRNA-dependent protein kinase (PKR) is a serine-threonine kinase that was first cloned and identified as an antiviral protein (551 amino acids) induced by IFN in 1990 (Meurs et al., 1990). It is also known as Protein kinase RNA-activated; double-stranded RNA-domain kinase (Hugon et al., 2009). PKR is regarded as a host IFN-stimulated gene. PKR promoter contains an IFN-stimulated response element (ISRE) as a transcriptional motif to respond to type I IFN. PKR has not been found in plants, fungi, protists and invertebrates, whereas it is widely and constitutively expressed in

vertebrate cells (Taniuchi et al., 2016). PKR acts as both a sensor of virus infection by binding to viral dsRNA resulting in activation of the kinase, and an effector via downstream consequences such as inhibition of protein translation and induction of apoptosis (Cesaro and Michiels, 2021).

PKR is comprised of two functionally distinct domains: an N-terminal double-stranded RNA binding domain (RBD) and a C-terminal catalytic kinase domain which are connected by a flexible linker (Fig 1.14A). The RBD (1-170aa) contains two tandem repeats (approximately 65 aa residues each) of a conserved dsRNA binding motif (dsRBM1 and dsRBM2), separated by a 23 aa linker (Feng et al., 1992). Both dsRBMs exhibit high-affinity interaction with dsRNA, suggesting that dsRNA first bind with dsRBM1 of PKR and subsequently stable bind with dsRBM2 (Dabo and Meurs, 2012). Although both motifs are indispensable for dsRNA binding, dsRBM1 is more important than dsRBM2 using the mutagenesis analysis (Green and Mathews, 1992, McCormack et al., 1994, Schmedt et al., 1995). The structure of dsRBMs in the N-terminus of PKR has been identified using NMR (Fig1.14B) (Nanduri et al., 1998). Both dsRBMs are basic, helical domains with an αββββα topology conformation. The 23aa linker displays a completely random coil conformation, which might be responsible for the flexibility of dsRBMs to facilitate the binding to dsRNA (Nanduri et al., 2000) (Fig1.14B). Furthermore, dsRBM1 has been identified to modulate the interaction between PKR and other proteins (Hitti et al., 2004). dsRBM2 of PKR interacts with the kinase domain in C- terminus to modulate the enzyme activity (Nanduri et al., 2000).

The catalytic domain of PKR is divided into 11 conserved subdomains. The crystal structure of the C-terminal of PKR shows that the smaller β-sheet N-terminal lobe and the larger α-helical C-terminal lobe form a typical protein kinase fold, regulating the formation of dimerisation (Dzananovic et al., 2018) (Fig 1.14C). The surface of the C-

terminal lobe of the kinase domain (subdomains V–VII) contains a unique α-helix which can be specifically recognized by its best-characterized substrate eIF2α, being descriptive of eIF2α kinase region (Dar et al., 2005) (Fig 1.14A). The length and sequence of this region are various in other members of the eIF2α kinase family, including general control nonderepressible kinase 2 (GCN2), PKR-like Endoplasmic Reticulum Kinase (PERK) and Heme-Regulated eIF2 alpha kinase (HRI) (Chang et al., 1992, Wek, 1994).

PKR is activated via the interaction with dsRNA, resulting in a number of conformational changes (Dey et al., 2005). Based on biochemical and genetic analyses, homodimerisation is likely to be the essential alteration. This homodimerisation result in a series of PKR autophosphorylation at multiple serine and threonine sites, including Ser242, Thr255, Thr258, Ser83, Thr88, Thr89, Thr90, Thr446 and Thr451 (Taylor et al., 2001). Especially Thr446 and Thr451, which can be constitutively phosphorylated during PKR activation, facilitating the stability of PKR dimer and enhancing its catalytic activity (Hugon et al., 2009, Watanabe et al., 2018). PKR modulates cell function as a pattern recognition receptor due to the activation by dsRNA. In addition to IFN and dsRNA, PKR can also be activated by multiple factors, including heat shock proteins, growth factors, heparin, cytokines, tumour necrosis factor-alpha (TNF), interleukin 1 (IL-1), LPS, Toll-interleukin 1 receptor domain-containing adaptor protein (TIRAP) and Toll-like receptor 4 (TLR4) (Goh et al., 2000, Horng et al., 2001, Li et al., 2006, Yeung et al., 1996). Some cellular stressors and insults also can induce PKR activity response, such as calcium, reactive oxygen species, irradiation, mechanical stress, and endoplasmic reticulum stress caused by tunicamycin, arsenite, thapsigargin or hydrogen peroxide (Garcia et al., 2007, Gil and Esteban, 2000, Hugon et al., 2017, Watanabe et al., 2018).

Activated PKR has numerous and various functions. eIF2α is phosphorylated and activated on Ser51, leading to the inhibition of the initial translation and reduction of general protein synthesis (Hoang et al., 2018). The decrease in protein synthesis results in the reduction of viral replication and even induces apoptosis (Garcia et al., 2007). This role of PKR in apoptosis can also occur in an eIF2α phosphorylation independent manner, associating with FADD/caspase-8/caspase-3 and caspase-9 APAF pathways (Gil et al., 2002, von Roretz and Gallouzi, 2010).

PKR also regulates various cell-signalling pathways, including MAPK, Signal transducer and activator of transcription 1 (STAT1), STAT3, NF-κB pathways, IRF1 or IRF3, and activating transcription factors (Bonnet et al., 2000, Guerra et al., 2006, Kirchhoff et al., 1995, Takada et al., 2007, Wong et al., 1997, Zhang and Samuel, 2008). PKR-deficient mouse embryonic fibroblasts showed a decreased response to IRF-1 and NF-κB, indicating PKR is involved in the modulation of these signalling pathways (Kumar et al., 1997). PKR has been reported to interact with IκB (Inhibitor of NF-κB) and degrade its activity to promote NF-κB activation (Kumar et al., 1994, Zamanian-Daryoush et al., 2000). In addition, NF-κB activation is independent of the catalytic activity of PKR (Bonnet et al., 2006, Bonnet et al., 2000). PKR also associates with the TNF receptor-associated factor (TRAF) to mediate the activation of NF-κB (Gil et al., 2004). Furthermore, PKR induces IFNβ by NF-κB and IRF1 (Kumar et al., 1997) and facilities IFN response by stabilizing IFN-β mRNA (Schulz et al., 2010).

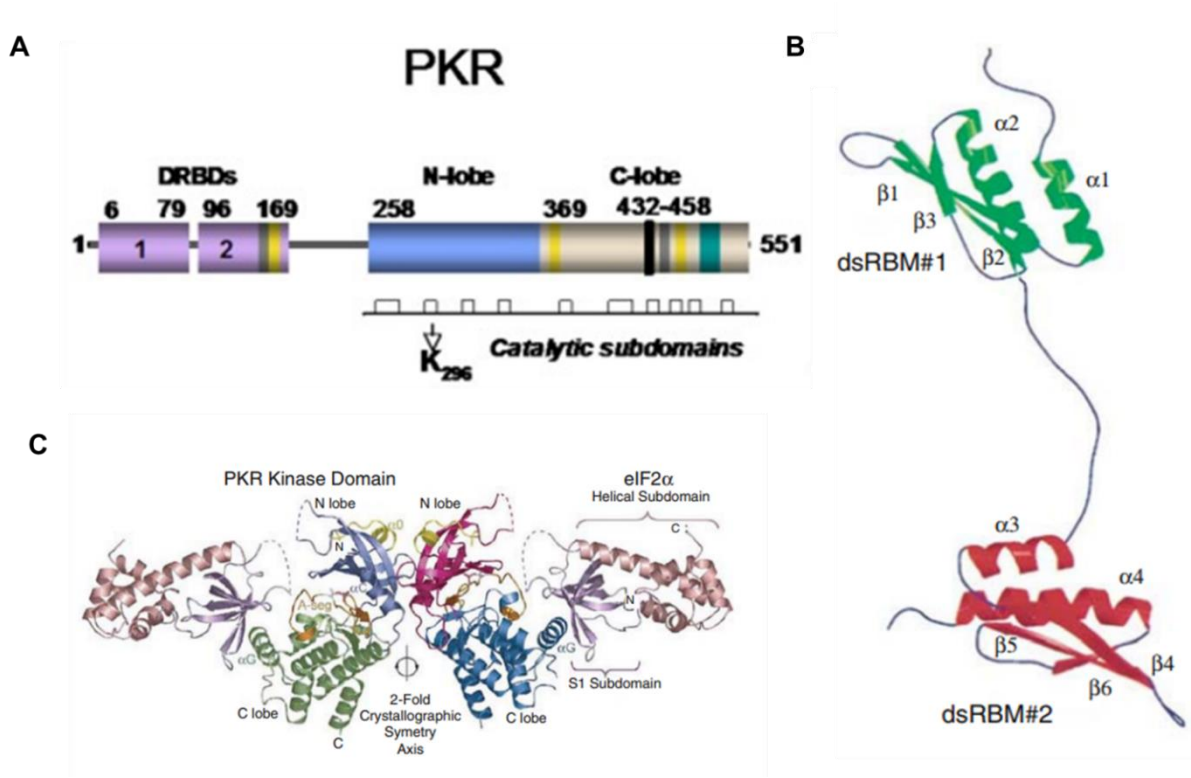

Fig 1.14 Structural analysis of PKR.

A. Basic structure of PKR. PKR consist of an N-terminal double-stranded RNA binding domain (RBD) and a C-terminal catalytic kinase domain. eIF2α binding site (487-500aa) is labelled in green (Dabo and Meurs, 2012). B. The crystal structure of the dRBDs of human PKR. dRBD1 and dRBD2 both with an αββββα fold separated by a flexible linker. C. The crystal structure of catalytic kinase domain dimerisation with the complex of eIF2α (Sadler and Williams, 2007).

1.6.2 PKR and HCV infection

Many viruses have developed mechanisms to evade the inhibition of innate antiviral immune response by suppressing PKR activity. HCV, as one of them, antagonises IFN via the interaction with PKR through many viral elements and proteins, including IRES, Core, E2, and NS5A.

NS5A has been reported to interact with PKR through the Interferon sensitive determinant region (ISDR) in domain II (237–276aa), which associates with the

sensitivity or resistance of patients to IFN (Enomoto et al., 1996) (Fig 1.15). In addition, NS5A can directly bind the catalytic kinase domain of PKR and then induces IFN resistance (Gale Jr et al., 1998, Gale Jr et al., 1997). Sequentially, NS5A also was demonstrated to inhibit PKR activity and eIF2α phosphorylation in the combinate infection with a vaccinia virus (He et al., 2001). The mechanism for the inhibition of NS5A to PKR is still not clear in HCV-infected cells, whereas it might associate with IRES. IRES is located at 5' UTR and contains four stem-loop domains, numbered I to IV. The loops II, III and IV all contribute to the initiation of translation. Of note, loop II also participates in RNA replication, whereas loop III and IV are exclusively for translation. NS5A has a higher affinity for loop III and IV compared with loop II, leading to the modulation of loop II for PKR activity and eIF2α-mediated inhibition of the translation of the cellular mRNAs. Since the different affinity of NS5A and PKR in adjacent IRES loops, their interaction is accumulated in IRES and results in the inhibition of PKR (Dabo and Meurs, 2012).

PKR is also considered to be a binding partner with core protein. A study has identified the interaction in the N-terminus of PKR and the first 58 aa of core protein (Yan et al., 2007). Additionally, the mutagenesis analysis in the catalytic kinase domain of PKR indicated the role of core protein in enhancing cell cycle deregulation, resulting in the loss of the phosphorylation of PKR in sites Thr451 and the hindrance of PKR activation (Alisi et al., 2005). Notably, the silencing of PKR increases the expression of core protein, while the overexpression of PKR significantly reduces HCV core expression in full-length HCV cell lines (Tokumoto et al., 2007). Moreover, PKR and core proteins are both targeted to the insulin pathway through the suppressor of cytokine signalling 3 (SOCS3), providing a potential interaction mechanism. In addition, HCV E2 contains

a PKR-eIF2α phosphorylation homology domain (PePHD) which also inhibits the dsRNA ability and activation of PKR (Taylor et al., 1999).

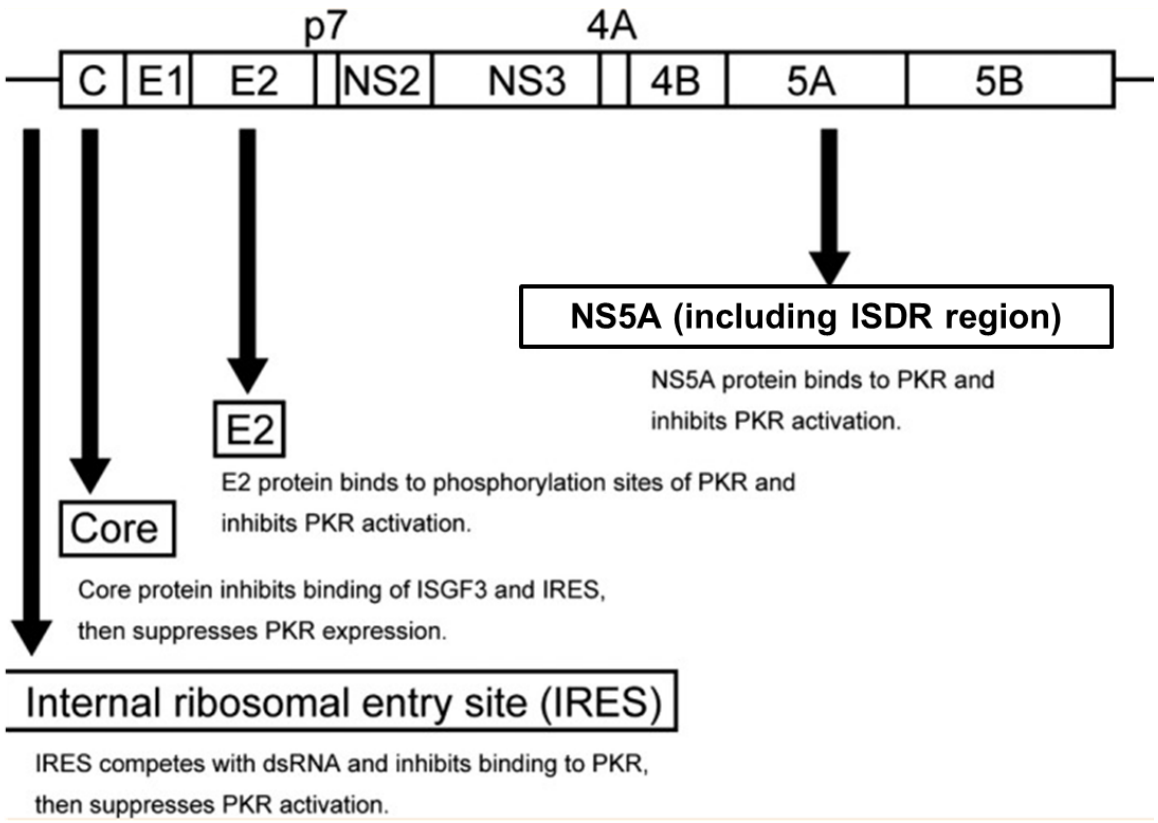

Fig 1.15 The role of viral proteins in HCV to suppress PKR activity.

NS5A contains an ISDR which can bind to PKR to facilitate the evasion of HCV to the IFN pathway. The PePHD of the E2 protein also inhibits PKR activity to bind with dsRNA (Watanabe et al., 2018).

1.7 Aims and objective

HCV infection is one of the leading causes of acute and chronic hepatitis, which may lead to chronic liver diseases such as liver cirrhosis and HCC. More than 58 million people are infected with HCV worldwide and nearly 300,000 death every year from this viral infection (Organization, 2021). Although most chronic hepatitis C was solved by current therapy combinations of DAAs in HCV different genotypes, the side effects

and drug resistance of the patients are still the major challenge for treatment. To date, the high resistance rates are more likely due to the contribution of genotype 3 (Dore et al., 2015, Lawitz et al., 2013, Nelson et al., 2015).

The non-structural 5A protein (NS5A) of HCV plays a critical role in both virus genome replication and the assembly of infectious virus particles. NS5A is a target for potent and highly efficacious direct acting antivirals used extensively for HCV treatment. NS5A comprises 3 domains. DI is most highly conserved and structured region in NS5A compared with DII and DIII. The mutants in NS5A DI (Y93H/N) induces the resistance of DAA (Lawitz et al., 2015).

This study aimed to further explore the mechanisms by which NS5A interacts with host factors in genome replication and viral assembly, aiming to identify potential DAA targets. In addition, I also plan to reveal the resistance mechanism of genotype 3 (DBN3a) through comparing the consensus residues of NS5A DI in genotype 2a (JFH1). To test this, mutagenic studies of NS5A DI was performed within these two genotypes, both in sub-genomic replicon and infectious virus. The mutants with phenotypes were further analysed by high resolution confocal microscopy (Airyscan) and a series of host factor silenced cell lines. Furthermore, the interaction between NS5A DI with potential associated host factors which affected viral replication and assembly were demonstrated by *in vivo* co-immunoprecipitation (Co-IP) assay and *in vitro* pulldown assay. The downstream host factors which showed the effect on modulating this interaction also be identified. This observation may have implications for the undefined mechanism for NS5A acts as the DAAs target and the novel treatment role in host factor inhibitors.

Chapter 2: Materials and Methods

2.1. General materials

2.1.1 Bacterial strains

Escherichia coli (*E. coli*) DH5α: Genotype F- Φ80lacZΔM15 Δ (lacZYA-argF) U169 recA1 endA1 hsdR17 (rk-, mk-) phoA supE44 λ- thi-1 gyrA96 relA1 were used for molecular cloning.

BL21 (DE3) pLysS: Genotype F- ompT gal dcm lon hsdSB (rB- mB-) λ (DE3) pLysS (cmR) were used for protein expression.

2.1.2 Mammalian cell culture

Huh7 (human hepatocellular carcinoma) (Nakabayashi et al., 1982) cells and Huh-7.5 (a derivative of Huh7 from which a stable subgenomic replicon was 'cured' by IFN treatment and which exhibit a defect in RIG-I) (Blight et al., 2002) were used for electroporation and infection. HEK-293T (human embryonic kidney 293T) cells were used for transfections.

Cells were cultured in Dulbecco's Modified Eagles Medium (DMEM; Sigma) supplemented with 10 % foetal bovine serum (FBS), 100 IU penicillin/ml, 100 µg/ml streptomycin and 1 % non-essential amino acids (Lonza) in a humidified incubator at 37°C, 5 % CO2.

2.1.3 Plasmid and virus constructs

All the DNA constructs are listed in Appendix Tables 9.1 and 9.2. Sub-genomic replicons with a luciferase reporter (mSGR-luc-JFH1) and infectious virus constructs of JFH1 (mJFH-1) were described previously (Hughes et al., 2009). NS5A mutations were constructed using Q5 Site-Directed Mutagenesis Kit (New England BioLabs; E0554S) and cloned into either mSGR-luc-JFH-1 or mJFH-1 via the *BamHI/AfeI*

restriction sites.

The pCMV10-NS3-5B (JFH-1) was constructed by Douglas Ross-Thriepland (University of Leeds) (Ross-Thriepland et al., 2013), and the NS5A domain I fragment with mutations was cloned into this wild-type (WT) vector by cloning the *NsiI-RsrII* fragment containing the mutations from the corresponding mJFH-1 constructs.

Sub-genomic replicons with a luciferase reporter (SGR-luc-DBN3a) (Ward et al., 2020) were described previously. NS5A mutations were constructed into SGR-luc-DBN3a using overlap PCR via *SpeI/BamHI* restriction sites.

NS5A domain I (amino acids 35 to 215/35 to 249) with mutations was PCR amplified and then cloned into pET-28a-Sumo vector using *BamHI/XhoI* restriction sites to construct pET-28a-Sumo-NS5A DI and mutants.

PKR was amplified from Huh7 RNA and cloned into pcDNA3.1 vector using BamHI/XhoI restriction sites to construct pcDNA3.1-PKR.

Lentivirus constructs for silencing CypA, CypB, PKR, RIG-I and IRF1 were obtained from Prof. Greg Towers (UCL) (Colpitts et al., 2020). EGFP-RIG-I plasmid was obtained from Prof. Andrew Macdonald (University of Leeds).

GST-CypA and GST-CypA-H126Q were provided by Prof. Philippe A Gallay of The Scripps Research Institute, San Diego (Chatterji et al., 2010).

2.1.4 Oligonucleotide primers

DNA oligonucleotides were ordered from Integrated DNA Technologies and resuspended in nuclease-free water to 100 μM and stored at -20°C. All primers used are listed in Appendix Table 9.3-9.5.

2.1.5 Antibodies and inhibitors

Rabbit anti-Core (polyclonal serum R4210) was obtained from John McLauchlan (Center for Virus Research, Glasgow), and mouse-anti E2 (AP33) was obtained from Arvind Patel (Center for Virus Research, Glasgow). The following antibodies were also used: sheep-anti NS5A (in-house polyclonal antiserum) (Macdonald et al., 2003), Rabbit anti-CypA (Enzo; BML-SA296-0100), rabbit anti-CypB (Abcam;ab16045), mouse-anti β-Actin (Sigma Aldrich; A1978), rabbit anti-PKR (Abcam; ab32035), rabbit anti-phospho-PKR T446 (Abcam;ab32036), rabbit anti- Rig-I (D14G6) (Cell signaling; 3743), mouse-anti His (BIO-RAD; MCA1396GA), sheep anti-GST (in-house), mouse-anti p65 (F-6) (Santa Cruz; sc-8008), mouse anti-dsRNA J2 (Scicons; 10010200), rabbit anti-eIF2α (Cell Signaling; 9722S), rabbit anti-phospho eIF2α (Cell Signaling; 9721S) and rabbit anti-IRF1 (Cell Signaling; 8478S).

Secondary IRDye 680 and 800 labelled antibodies were obtained from LI-COR, AlexaFluor-conjugated 488, 594 and 647 antibodies and BODIPY (558/568)-C12 dye was obtained from ThermoFisher Scientific.

CsA (Sigma-Aldrich; 30024) were resuspended in dimethyl sulfoxide (DMSO, Sigma-Aldrich) as 20 mM stocks. The PKR inhibitor C16 was obtained from Sigma-Aldrich (I9785).

2.1.6 Chromatography columns and resins

The following resins and beads are used: HisTrap FF column (Cytiva; 17531901), Glutathione Sepharose 4B (GST) resin (Cytiva;17075601), protein G beads (Invitrogen; 1004D), Dynabead His-Tag beads (ThermoFisher Scientific; 10103D).

2.2 Basic techniques of molecular biology

2.2.1 Manipulation of nucleic acid

2.2.1.1 Preparation of plasmid DNA from bacteria

The transformation was performed by incubating 50 µL competent bacteria (DH5α) with plasmid DNA or ligation products on ice for 30 minutes. Subsequently, adding 1 ml lysogeny broth (LB) without antibiotics to the mixture, followed by incubation at 37 °C for 40 min. Afterwards, transformed bacteria were evenly spread onto agar plates with antibiotics (100 µg/ml ampicillin or 50 µg/ml kanamycin) and incubated at 30 °C or 37 °C overnight. The next day, single colonies were picked from agar plates into LB medium containing the same antibiotic, and cultures were grown at 180 rpm, 30 °C or 37 °C overnight. Bacterial broths were pelleted at 4000 x g, 10 min at room temperature (RT), removing the supernatants and then processing the purification from bacterial pellet to DNA using the miniprep kit (New England BioLabs) or maxiprep kit (Thermo Scientific).

2.2.1.2 Site-directed (Quikchange) mutagenesis

The Q5 Site-Directed Mutagenesis Kit (New England BioLabs) was used to construct mSGR-Luc-JFH1 mutations. The exponential amplification of 25 µL PCR reactions is shown in the following table.

	25 µL RXN	Final concentration
Q5 Hot start High-Fidelity 2X Master Mix	12.5 µL	1X
10 µM Forward Primer	1.25 µL	0.5 µM
10 µM Reverse Primer	1.25 µL	0.5 µM
Template DNA (25ng/ µl)	1 µL	25 ng
Nuclease-free water	9.0 µL	

PCR reactions were cycled under the following conditions:

Reaction Step	Temperature	Time
Initial Denaturation	98 °C	30 seconds
25 cycles	98 °C	10 seconds
	50-72 °C	30 seconds
	72 °C	30 seconds/kb (6 minutes for HCV replicons)
Final Extension	72 °C	2 minutes

PCR products were then performed with KLD enzyme mix, a multi-enzyme mix containing kinase, ligase and DpnI for efficient phosphorylation, ligation of PCR products and removal of input template. Afterwards, the transformation was performed with competent DH5α cells. After selecting the single colonies, extracted DNA was then sent for sequencing with relevant primers.

2.2.1.3 Overlap extension polymerase chain reaction (PCR)

SGR-Luc-DBN3a Forward primer: GGTGGCTTTTAAGATCATGGG and SGR-Luc-DBN3a Reverse primer TTAGAGAACTGAGCAATGCGGTA were used to clone two overlap fragments with NS5A DI mutant primers (Appendix Table 9.4), respectively. Subsequently, these two fragments acted as the template to amplify the long extension fragments then were then cloned into SGR-luc-DBN3a via *SpeI/BamHI* restriction sites.

2.2.1.4 PCR

Plasmids pCDNA3.1-PKR and pET-28a-sumo-NS5A DI (35-215aa/35-249aa) were constructed using PCR. The exponential amplification of 50 µL PCR reactions is shown in the following table.

Component	50 µL reaction	Final concentration
Nuclease-free water	To 50 µL	
5 X GC Buffer	10 µL	1X
10 mM dNTPs	1 µL	200µM
10µM Forward Primer	2.5 µL	0.5 µM
10µM Reverse Primer	2.5 µL	0.5 µM
Template DNA	variable	< 250 ng
DMSO	1.5 µL	3%
Phusion DNA Polymerase	0.5 µL	1.0 units/50 µL PCR

PCR reactions were cycled under the following conditions: 98°C 30 s, 98°C 5-10 s, 45-72°C10-30 s, 72°C 15-30 s per kb, 72°C 10min.

2.2.1.5 Endonuclease digestion of DNA

1 µL Restriction Endonucleases (New England Biolab) were mixed with 15 µg of DNA in a total 50 µL reaction at 37 °C for 3-4 h. Digested DNA fragments were separated by agarose gel electrophoresis and extracted from the gel using the commercial DNA gel extraction kit (New England BioLabs).

2.2.1.6 DNA agarose gel electrophoresis

1% (w/v) DNA agarose gels were dissolved by 1x TAE buffer (40 mM Tris, 20 mM Acetate and 1 mM EDTA) followed by heating until the agarose completely melted and supplemented with SYBR® safe DNA gel Stain (Invitrogen) 1:20,000. After adding 6X

DNA loading buffer into DNA samples, they were loaded into the well of the DNA gel with the Hyper ladder I marker (Bioline). The gel was electrophoresed the gel in 1x TAE buffer at 180 V for 60 min. DNA was visualised by ultraviolet illumination using a Gene Genius bio-imaging system (Syngene).

2.2.1.7 DNA Ligation

After extracting both DNA insert and vector from DNA gel, T4 ligase (New England BioLabs) was mixed with them at the ratio of 1:3 in a total of 10 µL reaction and then incubated at 16 °C overnight. The ligation product was transformed into competent DH5α.

2.2.1.8 DNA sequencing and sequence analysis

All DNA constructs were sequenced using relevant primers by Genewiz Company. DNA sequences were aligned and analysed by DNA Dynamo Sequence Analysis Software.

2.2.1.9 Phenol: Chloroform purification of DNA

DNA which was prepared to use for *in vitro* transcription were purified from solutions contaminated with proteins by adding an equal volume of phenol: chloroform: isoamyl alcohol (25:24:1), followed by vortexing for 1 min and then centrifuged at 13,000 rpm for 5 min at 4 °C. Upper Aqueous phase layer was gently transferred to a fresh tube. An equal volume of chloroform was mixed and centrifuged at 13,000 rpm at 4°C. The upper aqueous phase was then mixed with 1 volume of isopropanol and 0.1 volume 3 M ammonium acetate (pH 5.2), followed by incubation at -20 °C for 2 h and pelleted at 13,000 rpm for 20 min. The pelleted DNA was washed once with 70% ethanol, air-dried for 5 min and then resuspended in 20 µL Diethyl pyrocarbonate (DEPC)-water. The Nanodrop spectrophotometer (Thermo Scientific) was used to quantify the

concentration of DNA by measuring absorbance at 260 and 280 nm. The ratio of absorbance at 260 nm to 280 nm (260/280) is the standard to assess the purity of DNA.

2.2.1.10 *In vitro* transcription of RNA

The DNA template constructs (e.g. mSGR-Luc-JFH1/mJFH1/SGR-Luc-DBN3a/DBN3a) (5-8 µg) prepared for *in vitro* transcription were linearised by 10 U restriction enzyme Xbal in a 50 µL reaction at 37°C overnight. To remove the single-stranded DNA, Mung Bean Nuclease (New England BioLabs) was used to process the linearised samples at 30°C for 40 min. Linearised DNA was then purified as described in section 2.2.1.9.

1µg of linearised DNA as the template was used for *in vitro* transcription which was processed using the T7 RiboMax Express kit (Promega). After operating a similar procedure to DNA purification, RNA pellets were washed in 1 ml 70% ethanol and finally resuspended in 20 µL DEPC water.

The Nanodrop spectrophotometer (Thermo Scientific) was also used to quantify the concentration of RNA, but only by measuring absorbance at 260 nm. Purified RNA was also analysed by RNA agarose gel electrophoresis.

2.2.1.11 RNA agarose gel electrophoresis

Preparation of RNA agarose gels was performed following the same recipe by mixing 1% (w/v) agarose with 30 ml MOPS (3-(N-morpholino) propanesulphonic acid) buffer (40 mM MOPS, 10 mM sodium acetate, 1 mM EDTA) and microwaved at 340 W for 2 min until it dissolved completely. After the temperature dropped to about 60°C, 6.5% (v/v) of formaldehyde and SYBR® safe DNA gel Stain (Invitrogen) (1:20,000) were added and allowed to set in the gel cast. 1 µg of RNA samples mixed with RNA loading

buffer (47.5% Formamide, 9 mM EDTA, and 0.0125% SDS, Xylene Cyanol, and Bromophenol Blue (w/v)) were heated at 65°C for 10 min before loading into gels, which was electrophoresed at 70 V for 1 h.

2.2.2 Mammalian tissue culture techniques

2.2.2.1 RNA Electroporation

Huh7 / Huh7.5 cells or host factor silenced cell lines were washed twice in ice-cold PBS. Electroporation was conducted by resuspending $1x10^7$ cells in ice-cold PBS containing 2-10 µg of RNA at 950 µF and 270 V. Cells were resuspended in complete media and then seeded separately into 96-well plates at $3x10^4$ cells / well, and 6-well plates at $3x10^5$ cells / well.

2.2.2.2 Transfection of DNA

Huh7 /Huh7.5 cells were washed with PBS and incubated with 1 ml Opti-MEM (Gibco) at 37 °C before the transfection medium was added. 2 µL of lipofectamine 2000 (Thermo Fisher Scientific) was diluted in 200 µL Opti-MEM and incubated at RT for 5 min. Meanwhile, 2000 ng of PCMV-10-NS3-5B-mutants DNA and were mixed with 200 ul Opti-MEM and incubated at RT for 5 min. The transfection reagent and RNA were mixed and incubated under RT for 20 min before adding onto the monolayer in a drop-wise manner. After 6 h, the transfection medium was removed and replaced with fresh complete DMEM. Typically at 48 hours post-transfection (hpt), cells were washed twice in PBS and lysed in Glasgow Lysis Buffer (GLB, 10 mM PIPES, pH 7.2, 120 mM KCl, 30 mM NaCl, 5 mM MgCl2, 1% Triton X-100, 10% Glycerol).

2.2.2.3 Lentivirus production and construction of stable knockout cell lines.

HEK293T cells in 10 cm dishes were transfected with 1 µg packaging plasmid p8.91,

1 µg envelope plasmid pMDG encoding VSV-G protein and 1.5 µg transfer plasmid pHIV-SIREN encoding shRNA or lenti-CRISPRv2 encoding sgRNA to CypA, CypB, PKR and RIG-I as described (Colpitts et al., 2020). Lentivirus supernatants were collected at 48 h and filtered through a 0.45 µm syringe. Huh7.5 cells were seeded into 6 well plates at a density of 2.5 x 10^5 cells/well and transduced with 1 ml/well lentivirus and 8 µg/ml polybrene for 24 h. Transduced cells were selected using 2.5 µg/ml puromycin at 72 h post-transduction. Loss of target protein expression was confirmed by western blot.

2.2.3 Protein technology

2.2.3.1 SDS-PAGE and Western blot

Transfected or electroporated cells were washed twice with 1 ml PBS, and total lysates were prepared by adding 1 x GLB with protease and phosphatase inhibitors and scraping the wells with pipette tips. After incubating it on ice for 30 min, cell debris was removed by centrifuging at top speed for 10mins at 4 °C and protein concentration was determined using the Pierce BCA Protein Assay kit (Thermo Scientific).

Cell lysates were mixed with an equal volume of 5 x reducing loading buffer (1M Tris-Hcl, pH=6.8; 10% SDS; 10% β-mercaptoethanol; 40% glycerol; bromophenol-blue) and then boiled for 5 min at 95°C. An equal amount of each sample and protein marker (11-245kDa; New England BioLabs) were fractionated using 10-12% polyacrylamide gel at 130 V for 1.5 h. The running buffer used here was 1x diluted from 10x stock containing 576 g glycine, 121.2 g Tris base and 20% SDS.

For the purified proteins, one of the duplicate gels was used for Coomassie blue staining by immersing in Coomassie blue for 30 min, and then in the destaining solution (10% acetic acid; 10% methanol) for 1 h.

Samples on the other duplicate gel were transferred to polyvinylidene fluoride microporous membranes (PVDF) at 15A, 500mA for 1 h in transfer buffer (25 mM Tris, 192 mM Glycine, 20% (v/v) methanol). The membrane was then blocked with 50% (v/v) Odyssey blocking buffer (LI-COR) diluted in 1X Tris-buffered saline with Tween-20 (TBS-T) (50 mM Tris-HCl pH 7.4, 150 mM NaCl, 0.1% Tween-20) for 1 h at RT. Membranes were probed with primary antibodies (1:1000 dilution) at 4°C overnight and stained with IRDye labelled anti-mouse (700 nm) and anti-rabbit (800 nm) secondary antibodies for 1 h at RT. Membranes were imaged on the LI-COR Odyssey Sa Imager.

2.2.3.1 Purification of NS5A domain I (35-215aa/35-249aa)

Plasmids were freshly transformed into *Escherichia coli* BL21 (DE3) pLysS and grown at 37 °C until OD_{600} values reached 0.6-0.8. Protein expression was induced by 100 µM isopropyl β-D-1-thiogalactopyranoside (IPTG) at 18 °C for at least 6 h. Cells were recovered by centrifugation at 8000 x g for 15 min and resuspended in 50 ml binding buffer (100 mM Tris pH 8.2, 200 mM NaCl, 20 mM imidazole) supplemented with 40 µL DNase, 40 µL RNaseA, 2 mg/ml Lysozyme and protease inhibitors (Roche) per 1 L of pelleted culture. After incubation on ice for 30 min, samples were sonicated at an amplitude of 10 microns for 12 pulses of 20 sec separated by 20 sec on ice. After centrifugation at 4000 x g for 1 h at 4 °C twice, supernatants were filtered through a 0.45 µm syringe filter. Samples were transferred to a 1 ml HisTrap FF column (Cytiva; 17531901) equilibrated with binding buffer and the column was washed three times using 5 column volumes of binding buffer. The samples were eluted with the binding buffer containing 250 mM imidazole and dialyzed against 20 mM Tris-HCl, pH 8.2, 150 mM NaCl and 10% (v/v) glycerol.

2.2.3.2 Purification of GST-CypA and GST-CypA-H126Q

Plasmids were transformed into *E. coli* BL21 (DE3) pLysS and induced for expression at 18 °C for 6 h as described above. Cells were recovered by centrifugation and resuspended in 10 mL GST-CypA lysis buffer (50mM Tris-HCl, pH 8.0, 100mM NaCl, 10% glycerol) containing 40 µL DNase, 40 µL RNaseA, 2 mg/ml Lysozyme and protease inhibitors (Roche) per 1L of pelleted culture. Cell suspensions were incubated on ice for 30 min and lysed by sonication. After centrifuging at 4000 x g for 1 h at 4 °C twice, the supernatant was filtered through a 0.45 µm filter. GST-CypA and GST-CypA-H126Q protein were then transferred to glutathione Sepharose 4B resin (GE Healthcare) following the manufacturer's instructions. After three washes with PBS and twice with lysis buffer, the resin was eluted with elution buffer (50 mM Tris-HCl, 10 mM reduced glutathione, pH 8.0) and the eluates were dialyzed in the dialysis buffer (50 mM Tris-HCl, pH 7.5, 100 mM NaCl, 5 mM $MgCl_2$, 10% glycerol, 0.5% NP-40). Purified proteins were aliquoted and stored at -80 °C until use.

2.3 Subgenomic replicon assays

2.3.1 Luciferase assay

After 4, 24, 48, 72 and 96 hours post-electroporation (hpe), cells were harvested by lysing with 30 µl or 200 µl passive lysis buffer (PLB; Promega) and incubated for 15 min at RT and stored at -80°C until used. The analysis was carried out using the luciferase assay reagent (Promega) and a FluoStar Optima luminometer to measure the levels of luciferase expression. The data was recorded as relative light units (RLU).

2.3.2 Drug efficacy assay

Huh7.5 or Huh7 cells were electroporated and seeded as described above to check replication levels in 96-well plates by luciferase activity. The serially diluted cyclosporin A (CsA), Daclatasvir (DCV) and Sofosbuvir (SOF) were prepared to use at 4 hpe. (The concentration of dilution is shown in the table below). Following the removal of the medium by washing in PBS twice, the cells were harvested at 48 hpe by using 30 µL PLB. Luciferase activity was determined as described in 3.2.11. Data were modelled using the model of log (agonist) vs response model and EC50 was calculated through GraphPad Prism.

DAAs	**The concentration of dilution**										
CsA	100µM	20µM	4µM	800nM	160nM	32nM	6.4nM	1.28nM	256pM	50pM	10pM
DCV	10nM	1nM	100pM	10pM	1pM	100fM	10fM	1fM	0.1fM		
SOF	100µM	10µM	1µM	100nM	10nM	1nM	100pM	10 pM	1pM		

2.3.3 GST pulldown assay

20µL GST beads were transferred into 1.5mL Eppendorf tubes. After washing the beads twice with 400 µL binding buffer (100mM Tris, 0.5 M NaCl, 1% Triton X100), 5 µg GST (diluted with washing buffer) protein was added into beads and incubated at 4°C for 2 h. The beads were then washed with binding buffer for 5 mins and centrifugation at 500 rcf for 5 mins at 4°C were performed to remove non-specific binding. After discarding the binding buffer, 400 µL washing buffer with 3% BSA was added into beads to block overnight. Afterwards, 1.5 µg His-sumo tagged NS5A (35-215aa) or NS5A (35-249aa) proteins which were diluted with washing buffer, was added into washed beads and incubated at 4°C for 2 h. After washes using binding buffer, the bound material was eluted with 20 µL SDS sample buffer and heated for 10 min at 95°C. These samples were analyzed using western blot by anti-GST and anti-

His antibodies.

2.3.4 Immunofluorescence analyses

Cells were seeded onto 16mm glass coverslips in 12 well plates, fixed, permeabilised and blocked as described above. Cells were probed with sheep anti-NS5A (1:2000), and mouse anti-P65 (1:500) in PBS/3% BSA at RT. for 2 h. After three washes, cells were incubated with Alexa Fluor-488 or -647 conjugated secondary antibodies (1:500 in PBS/3% BSA) at RT. in the dark for 1 h. Cells were mounted onto glass slides with Prolong Gold antifade reagent (Invitrogen) containing 4',6'-diamidino-2-phenylindole dihydrochloride (DAPI) and sealed with nail varnish. Confocal images were acquired using a Zeiss LSM880 upright microscope with Airyscan. Post-acquisition analysis of images was performed using Fiji ImageJ (v1.49) software (Schindelin et al., 2012).

2.3.5 Mean fluorescence intensity analysis

The mean fluorescence intensity (MFI) of the cells was measured employing laser excitation with the P65 channel. The proportion of MFI in the nucleus to MFI in all cells was calculated to show the rate of P65 translocation to the nucleus.

2.3.6 Colocalisation analysis

Overlap coefficients were analysed by Just-Another Co-localisation Plugin (JACop) in Fiji software from 5 cells derived from two independent experiments. Data were exported to GraphPad Prism and analysed using two-tailed Student's t-tests.

2.4 JFH1 full virus assays

2.4.1 Electroporation of full virus mutants

Huh7.5 cells were washed twice using ice-cold PBS and then were diluted to $1X10^7$ cells/ml. 10 µg of mutants were electroporated into $4X10^6$ cells using 4mm

electroporation cuvette (Geneflow) at 950 μF and 270 V. Afterward, electroporated cells were suspended using 10ml medium and then seeded into T75cm^2 flasks. After 72h incubator, the supernatants as extracellular viruses were collected and stored at 4°C. Meanwhile, the cells were washed using 10 ml PBS and then scraped in 1 ml PBS, putting them into -80°C after 5 freeze-thaw cycles.

2.4.2 IncuCyte S3 analysis

Following immunofluorescence staining for NS5A, plates were detected using an IncuCyte S3 (Essen BioScience). Viral titres were obtained by analysing the total number of virus-positive cells per well for each dilution. As this method measures the absolute number of infected cells rather than the number of foci of infected cells, the titres are represented as infectious units per mL (IU/mL).

2.4.3 qRT-PCR

Total cellular RNA was harvested by lysis in TRIzol (Invitrogen) and extracted using chloroform. cDNA was synthesised from 1 ug RNA by reverse transcription using LunaScript RT SuperMix Kit (NEB; E3010). qRT-PCRs were performed using Luna Universal qPCR Master Mix (NEB; M3003) with SYBR Green. Amplification was performed using the following primers:

JFH-1 Forward: 5'-TCTGCGGAACCGGTGAGTA-3'

JFH-1 Reverse: 5'-TCAGGCAGTACCACAAGGC-3'.

2.4.4 Titration of Virus

Huh7.5 cells were seeded into 96-well plates (3000 cells/well) and incubated at 37°C overnight. The following day, the freeze-thaw intracellular virus was centrifuged at 16000 rpm for 5 min and the pellets were removed. Intracellular and extracellular virus

samples were serially diluted two-fold and added to Huh7.5 cells. At 48 h, cells were fixed in 4% (w/v) paraformaldehyde (PFA) for 30 min and washed twice with PBS. Cells were permeabilised with 0.25% Triton X-100 (Sigma-Aldrich) in PBS for 8 min and blocked with 3% BSA diluted in PBS. Cells were probed with primary antibodies (sheep anti-NS5A 1:2000) in PBS/3% BSA at 37°C for 1 h. Cells were washed five times in PBS and incubated with Alexa Fluor-594 donkey anti-sheep (1:750) in PBS/3% BSA at RT for 1 h. Plates were analysed using IncuCyte S3 software.

2.4.5 Immunofluorescence analyses

Cells were seeded onto 16mm glass coverslips in 12-well plates, fixed, permeabilised and blocked as described above. Cells were probed with sheep anti-NS5A (1:2000), rabbit anti-Core (1:500) or mouse anti-dsRNA J2 (1:200) in PBS/3% BSA at RT for 2 h. After three washes, cells were incubated with Alexa Fluor-488 or -647 conjugated secondary antibodies (1:500 in PBS/3% BSA) at RT in the dark for 1 h. Lipid droplets were stained with BODIPY (558/568)-C12 dye (1:1000). Cells were mounted onto glass slides with Prolong Gold antifade reagent (Invitrogen) containing 4',6'-diamidino-2-phenylindole dihydrochloride (DAPI) and sealed with nail varnish. Confocal images were acquired using a Zeiss LSM880 upright microscope with Airyscan. Post-acquisition analysis of images was performed using Fiji ImageJ (v1.49) software (Schindelin et al., 2012).

2.4.6 Quantification of LD size and distribution

LD and DAPI channels were visualised using Fiji software and merged. LD size and distribution were analysed using the Analyse Particles module of Fiji. Data were analysed using GraphPad Prism and compared using two-tailed Student's t-tests.

2.4.7 Co-localisation analysis

Overlap coefficients were analysed by Just-Another Co-localisation Plugin (JACop) in Fiji software from 10 cells derived from three independent experiments. Data were exported to GraphPad Prism and analysed using two-tailed Student's t-tests.

2.4.8 Co-immunoprecipitation (Co-IP) assay

Cells were seeded into 6-well plates and lysed at 72 hpe using IP buffer (25 mM Tris-HCl pH 7.4, 150 mM NaCl, 1% NP-40, 1 mM EDTA; 5% glycerol) containing protease inhibitors for 1 h on ice. Lysates were centrifuged (13,000 × g for 5 min at 4°C) and supernatants were precleared with 10 µL protein G beads (Invitrogen; 1004D) at 4°C for 1 h. Cell lysates were then incubated with anti-PKR or anti-phospho-PKR antibodies at 4°C overnight prior to the addition of 20 µL protein G beads for 2 h at 4°C. After extensive washing, the immunoprecipitated proteins were heat denatured at 95°C for 5 min, separated by SDS-PAGE and analysed by western blot.

2.4.9 His pulldown assay

His-SUMO tagged NS5A DI (5 µg) was diluted using 1x binding & wash buffer (BWB: 50 mM sodium phosphate pH 8.0, 300 mM NaCl, 0.02% Tween-20) and added to 20 µL Dynabead His-Tag beads (ThermoFisher Scientific; 10103D). After incubation on a roller at 4°C for 1 h, the beads were washed five times with BWB at 4°C. Lysates from pcDNA3.1-PKR transfected HEK293 cells were diluted with 1x pulldown buffer (3.25 mM Sodium-phosphate pH 7.4, 70 mM NaCl, 0.02% Tween-20) and added to the His-Tag beads at 4°C for 2 h. Beads were washed five times with BWB at 4°C, heat denatured at 95°C for 5 min, separated by SDS-PAGE and analysed by western blot.

2.5 Statistical analysis

Statistical analysis was performed using unpaired two-tailed Student's t-tests on GraphPad Prism version 9.30. **** ($P<0.0001$), *** ($P<0.001$) , ** ($P<0.01$) and * ($P<0.1$) indicate significant difference from wild type ($n>=3$). Data in histograms were displayed as the means ± S.E.

Chapter 3: Mutagenic analysis of the role of NS5A domain I in HCV genome replication: comparison of genotypes 2 and 3

3.1 Introduction

HCV genome replication is a poorly understood process, particularly regarding the roles of both virus proteins and host cell factors. The replication complex (RC) consisting of non-structural proteins NS3-NS5B is the central element of the genome replication process. It is required to catalyse the synthesis of nascent RNA and is associated with host cell factors to form the membranous web (MW) by rearranging the intracellular membranes, including the ER, Golgi complex, mitochondria, endosomes and peroxisomes (Den Boon and Ahlquist, 2010, Diaz et al., 2010, Miller et al., 2003, Paul et al., 2013). Subsequently, HCV replication occurs in these organelles in the cytosol.

Since NS5A was reported to regulate the response for host cell interferon (IFN), it has been a well-studied protein in HCV research. NS5A was initially found to concentrate in the cytoplasm and the perinuclear membrane, including the ER and the Golgi apparatus (Ide et al., 1996, Polyak et al., 1999). This conclusion can be supported by numerous findings. Firstly, the interaction between NS5A and Apolipoprotein A1 (ApoA1) and their colocalisation was investigated in the Golgi apparatus (Shi et al., 2002). Moreover, NS5A modulated HCV RNA replication by interacting with other NS proteins and various cellular factors, including vesicle-associated membrane protein-associated proteins A and B (VAP-A, VAP-B), cyclophilin A (CypA) and phosphatidylinositol-4-kinase IIIα (PI4KIIIα) (Berger et al., 2009, Gao et al., 2004, Goonawardane et al., 2017, Ngure et al., 2016). There is strong evidence that NS5A is involved in HCV replication by playing some critical roles in modulating RC of HCV.

NS5A is a multifunctional proline-rich phosphoprotein, which is comprised of four distinct regions: an amino-terminal 31 amino acid amphipathic alpha helix, domain I

(residues 28–213), domain II (residues 250–342), and domain III (residues 356–447) (Fig 3.1A). The three structural domains are separated by low complexity sequences (LCS-I and LCS-II) (Fridell et al., 2011, He et al., 2006). Unlike domains II and III which are intrinsically disordered, domain I is highly structured and coordinates a zinc atom which facilitates the formation of NS5A dimer and a disulphide bond at the C terminus. Some reports revealed that the two existing dimeric conformations (1ZH1 and 3FQM) possibly represent different functional states (Lambert et al., 2014, Love et al., 2009, Tellinghuisen et al., 2005). In particular, the disulphide bond between Cys142 and Cys190 is only present in one of the dimer conformations (Tellinghuisen et al., 2005), which is likely to further underlie the function of NS5A domain I in HCV replication.

By aligning the sequences among different genotypes, NS5A domain I shows high sequence homology compared to domain II and III (Acton et al., 1996, Kapoor et al., 2011, Kapoor et al., 2013, Smith et al., 2014). The results suggest that domain I has functions that are common to all genotypes, while domain II and III possibly play specific roles in individual genotypes. Moreover, the characteristic of high conservation provides the foundation to study similar functions of NS5A among the different genotypes. Based on the previous research of NS5A of HCV genotype 2a (JFH1), a panel of NS5A domain I mutants can be extrapolated to genotype 3 research. To achieve this I utilised DBN3a-derived SGR containing unique restriction sites at either side of NS5A domain I previously generated by our lab (Ward et al., 2020). Importantly, the DBN3a SGR replicates as efficiently as JFH1 SGR, providing comparability of NS5A function between JFH1 and DBN3.

Previously, a study in our lab demonstrated that the two residues within the genotype 2a NS5A domain I (V67 and P145) play critical roles in HCV assembly, challenging the

dogma that NS5A domain I exclusively participated in genome replication (Yin et al., 2018). In this study, I aim to investigate more residues proximal to V67 and P145 that share the same phenotype as candidates to regulate the assembly of HCV genotype 2a. In addition, a panel of mutants of genotype 2a were performed in genotype 3 SGR to further investigate the roles of genotype 3 NS5A domain I in HCV replication. Meanwhile, more candidate residues in HCV genotype 3 NS5A domain I can be chosen to become potential sites which possibly associate with new DAAs.

3.2 Results

3.2.1 Generating a panel of alanine substitutions in NS5A domain I

In the previous work, two residues V67 and P145 of NS5A domain I were mutated to alanine by site-directed mutagenesis. The phenotype showed a partial defect in HCV replication but was indispensable in HCV assembly (Yin et al., 2018). To determine if this phenotype was unique or representative of a group of residues sharing this function, I sought to identify additional residues which displayed the same phenotype as V67A and P145A. To achieve this goal, I identified a panel of fifteen surface-exposed and highly conserved residues proximal to V67 and P145, shown in Fig 3.1B and 3.1C, and highlighted on the monomeric structures of genotype 1b NS5A DI (PDB 1ZH1 and 3FQM) (Love et al., 2009, Tellinghuisen et al., 2005). To determine whether these residues were conserved between the 7 genotypes of HCV I aligned the NS5A domain I sequence from consensus isolates of each genotype. From these analyses the residues: I52, G70, S71, M72, P102, Y106, W111, P141, C142, Q143, P147, E148, F149, C190 and E191 were finally selected as targets for mutations due to high conservation among the 7 genotypes of HCV and absolute conservation between HCV genotype 1b and 2a (Fig. 3.1D). These residues were targeted for alanine scanning

mutagenesis and subsequent profiling in the context of the mSGR-luc-JFH-1.

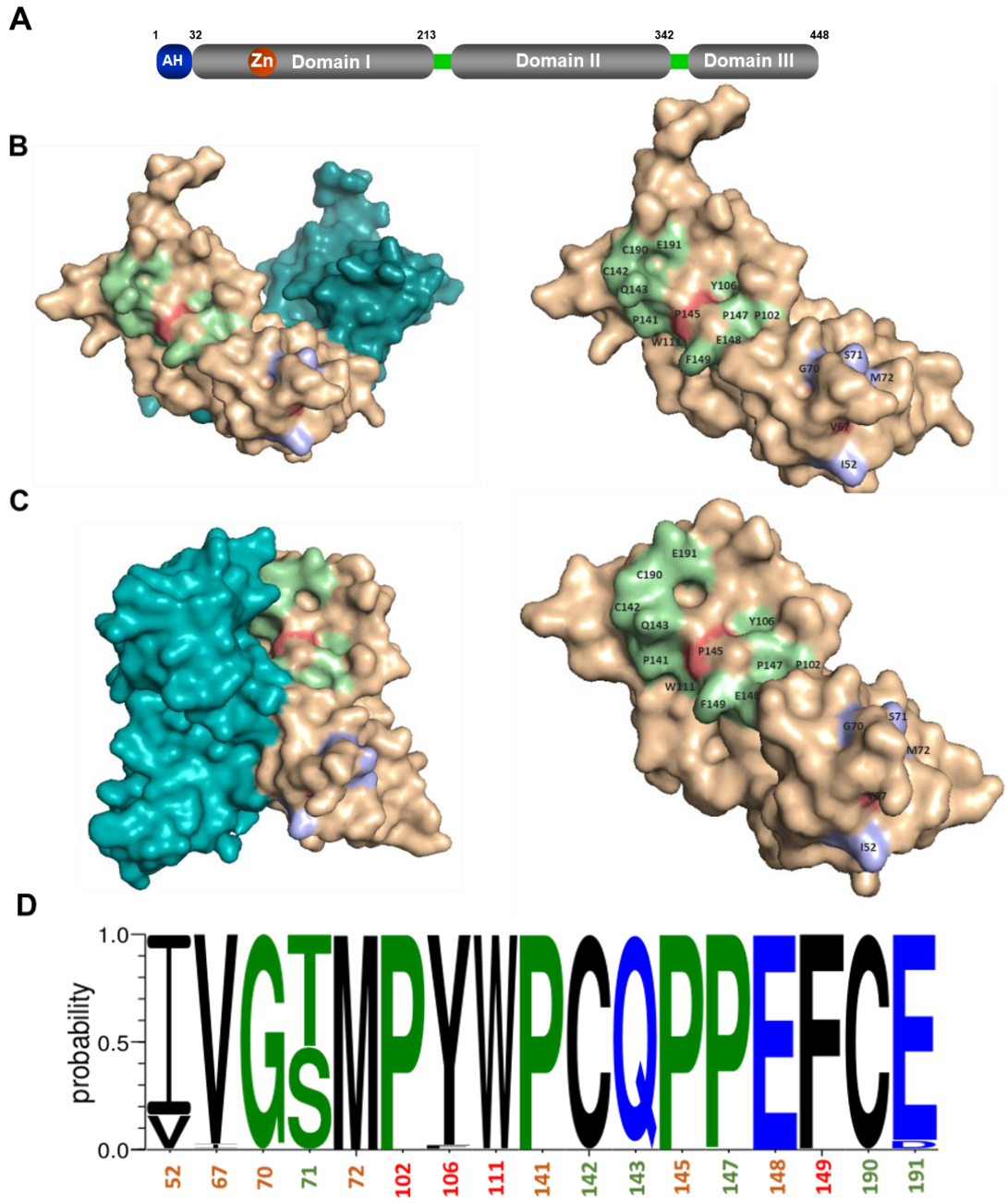

Fig 3.1. Location of mutated residues in DI.

(A) Structure of NS5A illustrating the three domains. AH: amphipathic helix (blue), LCS: low complexity sequence (green). **(B, C)** Conserved and surface exposed residues proximal to V67 (blue) and P145 (green) are displayed in the two NS5A DI (genotype 1b) structures 1ZH1 **(B)** and 3FQM **(C)**. Dimeric forms are shown on the left, with the monomers on the right. **(D)** The alignment of 15 residues in NS5A domain I. The residues were aligned and analyzed among 7 HCV genotypes (673 sequences from HCV database) by Sequence Logo.

3.2.2 Site-directed mutagenesis of NS5A domain I identified 7 residues partially require for genome replication

To evaluate the phenotype of mutations of these residues, the 15 mutants were cloned into mSGR-luc-JFH1, an SGR with a luciferase reporter gene and unique restriction sites engineered at either side of the NS5A coding sequence for facilitate cloning(Hughes et al., 2009, Targett-Adams and McLauchlan, 2005). The final mutant SGRs were verified by sequencing. After linearisation of the replication plasmid DNA and *in vitro* transcription, the RNA transcripts were electroporated into Huh7 cells, with wild-type (WT) mSGR-luc-JFH1, V67A, P145A and a lethal NS5B mutation GND as positive and negative controls, respectively. Luciferase activity was measured at 4, 24, 48 and 72 h post-electroporation (hpe). The absolute luciferase values were shown in Fig 3.2A, and the luciferase values at 24, 48 and 72 hpe were normalised to the 4 hpe signal to control for transfection differences (Fig 3.2B).

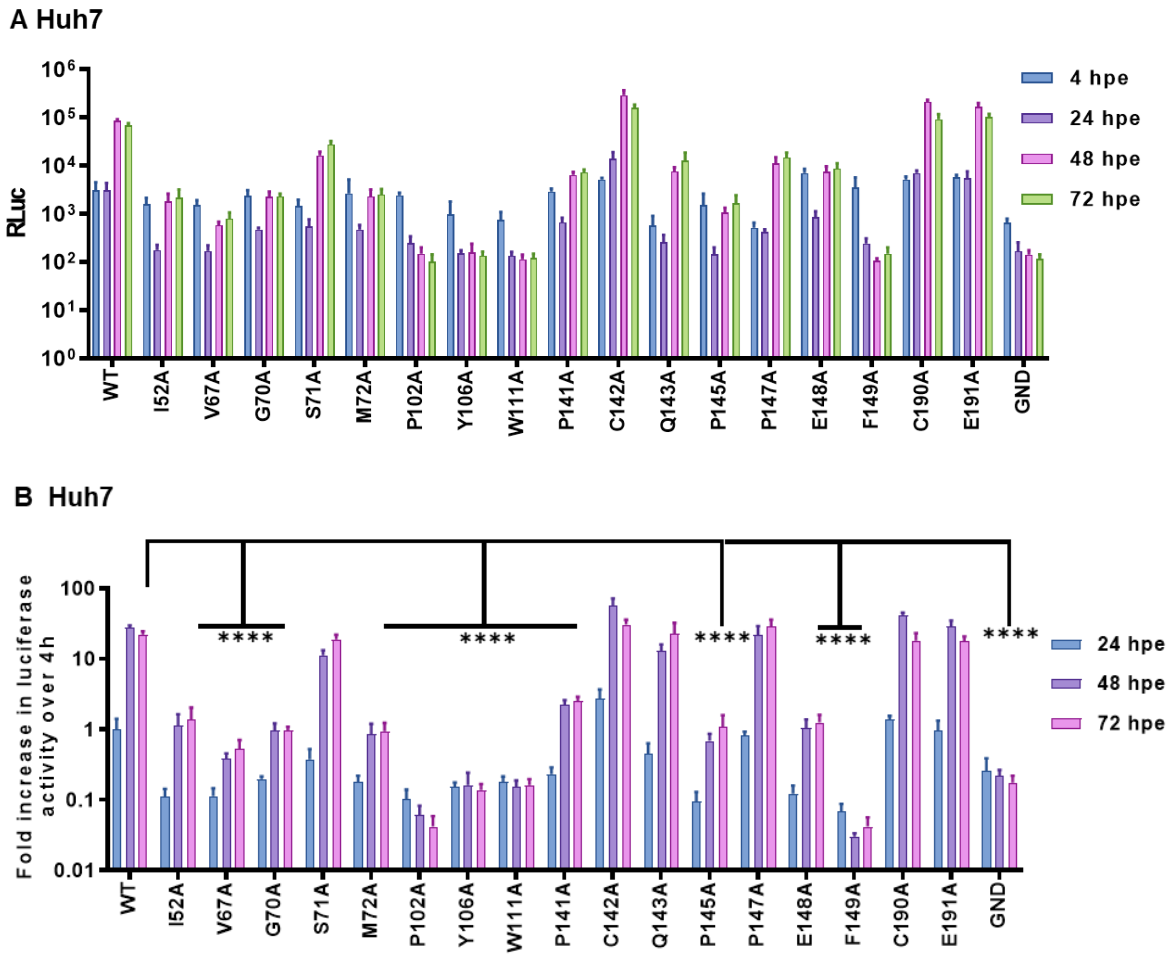

Fig 3.2. Genome replication phenotypes of NS5A domain I mutants in Huh7 cells.

Following the *in vitro* transcriptions of mSGR-luc-JFH1 containing the indicated mutations, electroporation was performed with Huh7 **(A)**. Luciferase activity was measured at 4, 24, 48 and 72 hpe and the data were normalised with respect to 4 hpe **(B).**

As previously observed (Yin et al., 2018), V67A and P145A showed very low levels of replication compared to WT, luciferase values declined between 4-24 hpe and only recovered to input levels by 72 hpe. As expected, GND failed to replicate and luciferase values rapidly declined by 24 hpe and did not recover.

The mutants P102A, Y106A, W111A and F149A were indistinguishable from GND, demonstrating that these residues were absolutely required for HCV genome replication. In contrast, the remaining 11 mutants were able to replicate. S71A, Q143A

and P147A exhibited a modest but non-significant defect, C142A, C190A and E191A even replicated more efficiently than WT, whereas I52A, G70A, M72A, P141A and E148A replicated to a level significantly lower than WT (Fig. 3.2 A&B).

Previously it was shown that although V67A and P145A exhibited a significant decrease in replication in Huh7 cells, this phenotype was not apparent in Huh7.5 cells. This was postulated to be due to the increased permissivity of Huh7.5 cells for HCV replication, resulting from the defect in RIG-I signalling and the innate immune responses in Huh7.5 cells (Blight et al., 2002). Replication of the panel of I mutants was therefore also evaluated in Huh7.5 cells. As previously demonstrated V67A and P145A were able to replicate much more efficiently in Huh7.5 cells, whereas GND was replication defective (Fig 3.3A). P102A, Y106A, W111A and F149A, which were unable to replicate in Huh7 also exhibited an absolute defect in Huh7.5. However, I52A, G70A, M72A, P141A and E148A were able to replicate more efficiently in Huh7.5 compared to Huh7. Lastly, S71A, C142A, Q143A, P147A, C190A and E191A which did not exhibit a replication defect in Huh7 cells, also replicated to WT level in Huh7.5 cells (Fig. 3.3 A and B). It is likely that the RIG-I deletion in Huh7.5 attenuated the innate response to early replication events, allowing mutants with a partial defect to replicate with high efficiency.

These data indicated that I52A, G70A, M72A, P141A and E148A exhibited the same phenotype as V67A and P145A: namely a significant replication defect in Huh7 cells and a partial restoration of this defect in Huh7.5 cells.

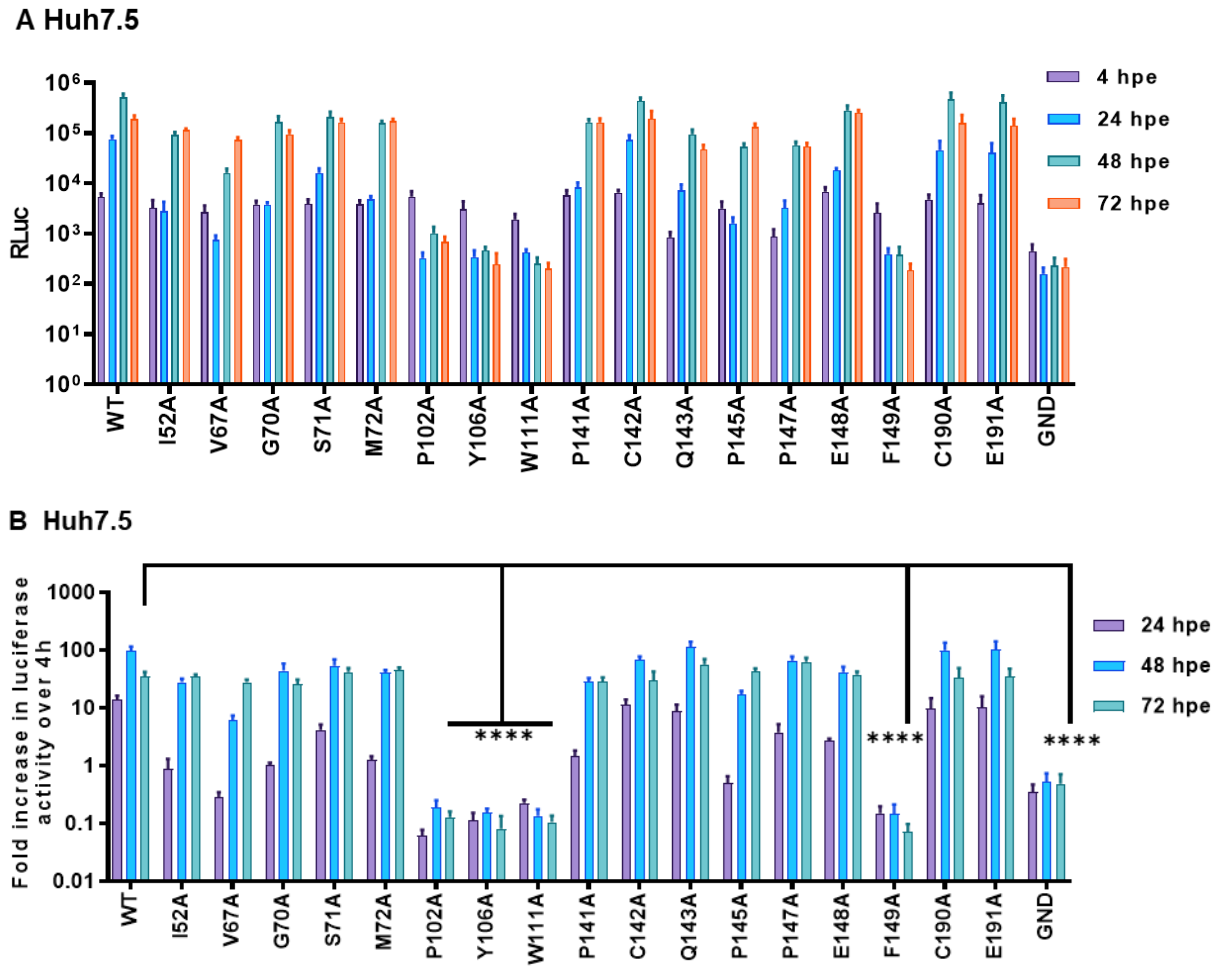

Fig 3.3. Genome replication phenotypes of NS5A domain I mutants in Huh7.5 cells.

The mSGR-luc-JFH1 containing the indicated mutations were electroporated into Huh7.5 cells **(A)**. Luciferase activity was measured at 4, 24, 48 and 72 hpe and the data were normalised with respect to 4 hpe **(B)**.

3.2.3 Defective mutations do not disrupt polyprotein processing

To demonstrate whether the lethal phenotypes resulted from a loss or disruption of a specific function of NS5A, disruption of polyprotein translation or proteolytic processing, the 15 mutants were cloned into an expression construct in which the NS3-5B polyprotein was under the control of a human cytomegalovirus (CMV) promoter (pCMV-10-NS3-5B), thus allowing replication-independent expression of replicase

proteins. These plasmids were transfected into Huh7 and Huh7.5 cells and cells were lysed at 48 hours post transfection (hpt), separated by SDS-PAGE and analysed for protein expression by western blot using an in house antibody raised against NS5A.

Posttranslational modification of NS5A results in a basally phosphorylated 56KDa species and a hyper-phosphorylated 58kDa species, both of which are believed to play an essential role in the HCV life cycle (Ross-Thriepland et al., 2013, Ross-Thriepland and Harris, 2015). These two forms are therefore considered to affect the normal expression of NS5A. The expression of 14 mutants in NS5A DI comparable to WT, specifically the four lethal mutants and five partially defective phenotype. This indicated that the lethal replication phenotype for these mutants was caused by loss or disruption of a specific function of NS5A rather than global effects on NS5A translation and polyprotein cleavage (Fig 3.4). Of note, E191A only has a basal-phosphorylated form which exhibited lower levels of expression than other mutants, it was considered that this might be due to the mutation lowering the stability of the NS5A protein. The lack of hyper-phosphorylation of E191A was showed to have no effect on the genome replication, which still needed to be explored in further work.

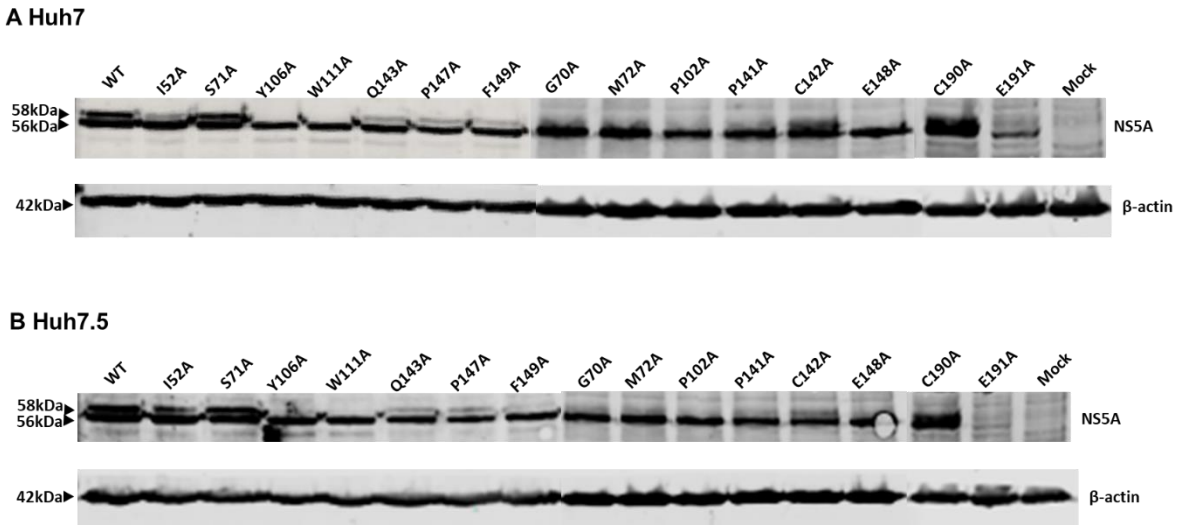

Fig 3.4. Expression of NS5A from pCMV10-NS3-5B expression vector in Huh7 and 7.5 cells.

The pCMV-NS3-NS5B plasmid harboring the mutations were transfected into Huh7 **(A)** and Huh7.5 cells **(B)**. Cell lysates were harvested in GLB at 48hpt, followed by analysis using SDS-PAGE and western blot with anti-NS5A (sheep) and anti-actin (mouse).

3.2.4 The replication sensitivity of partially defective mutants in JFH1 to cyclophilin A (CypA) inhibition

Cyclophilin A (CypA) is a peptidyl-prolyl isomerase (PPIase) identified as a critical host factor for HCV infection. Disruption of its PPIase activity through chemical inhibitors such as cyclosporine A (CsA) has been shown to be deleterious to HCV replication. Previous work from our lab demonstrated that the C-terminus of NS5A domain II is a key determinant of HCV replication dependent on CypA (Ross-Thriepland et al., 2013). Given that the function of CypA in virus genome replication remains undefined, and domain I is also proline rich, I sought to investigate whether the phenotype of these partially defective mutants results from the loss of CypA dependence and interaction. To demonstrate this, we firstly investigated whether these SGR mutants altered the

sensitivity of HCV genome replication to CsA. SGR-luc-JFH1 WT, I52A, V67A, G70A, M72A, P141A, P145A, E148A and D316E (CsA-resistance mutant in NS5A domain II) (Yang et al., 2010) were electroporated into Huh7.5 cells and CsA efficacy assay was performed at 4 hpe, Daclatasvir (DCV-NS5A inhibitor) and Sofosbuvir (SOF-NS5B inhibitor) were used as controls. Replication was monitored by observing luciferase activity at 48 hpe. Replication data demonstrated that seven mutants (I52A, V67A, G70A, M72A, P141A, P145A and E148A) were more sensitive to CsA treatment than WT, with a decrease in the half maximal effective concentration (EC_{50}) by 16%-79% (Fig 3.5A). The CsA efficacy assay from three biological repeats show that the EC_{50} values of partially defective mutants were significantly reduced compared to WT (Fig 3.5B). These results indicated that domain I may have potential association with CypA. To control for global effects of the mutants on DAA sensitivity, cells were treated with DCV (Fig. 3.5 C) or SOF (Fig.3.5 D). The EC_{50} results showed that all the mutants shared a similar sensitivity to DCV and SOF compared with WT, whereas V67A and P145A exhibited a particularly lower level of EC_{50} for DCV and SOF treatment.

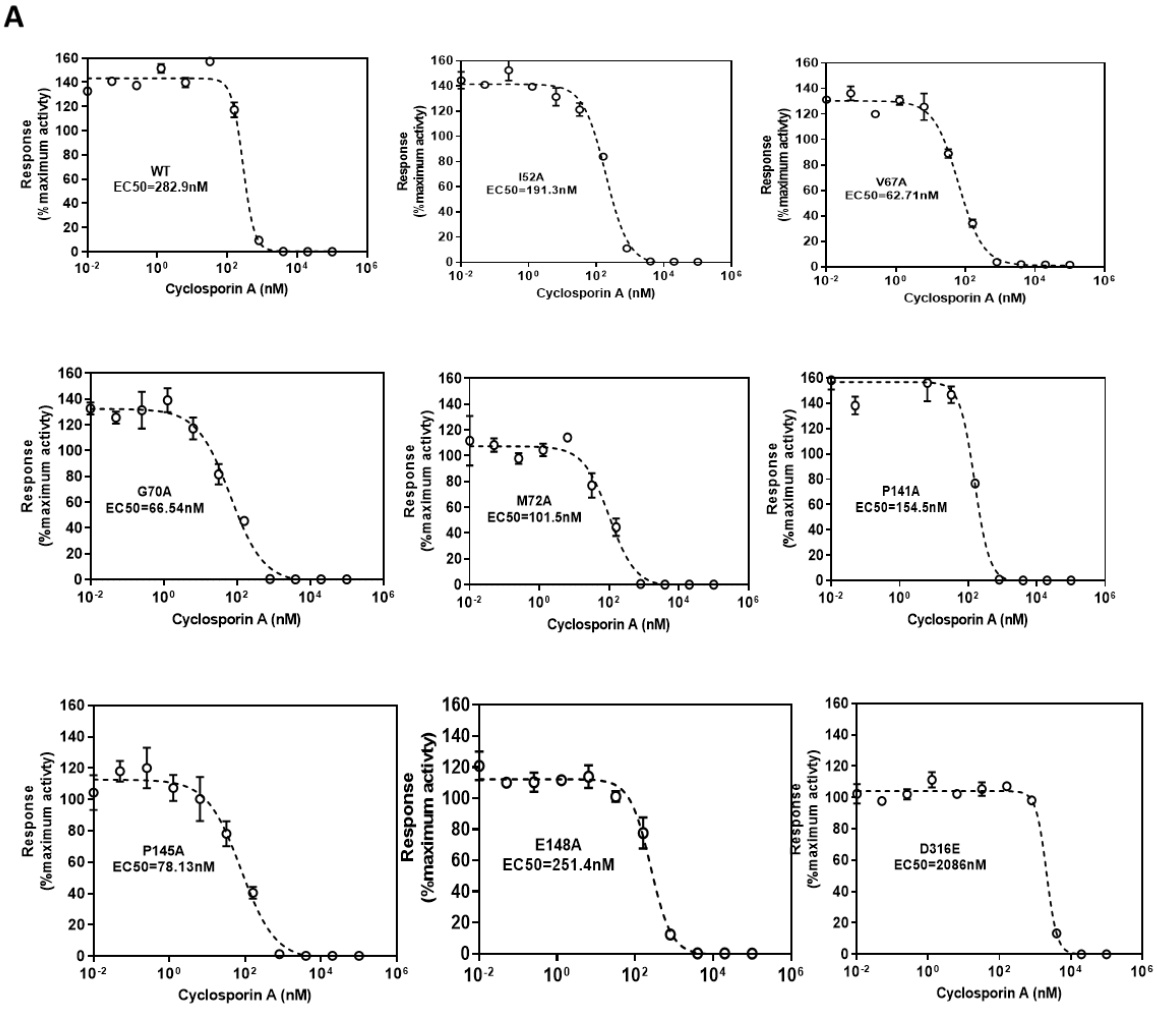
A
WT
EC50=282.9nM
I52A
EC50=191.3nM
V67A
EC50=62.71nM
G70A
EC50=66.54nM
M72A
EC50=101.5nM
P141A
EC50=154.5nM
P145A
EC50=78.13nM
E148A
EC50=251.4nM
D316E
EC50=2086nM
Response (%maximum activity)
Cyclosporin A (nM)

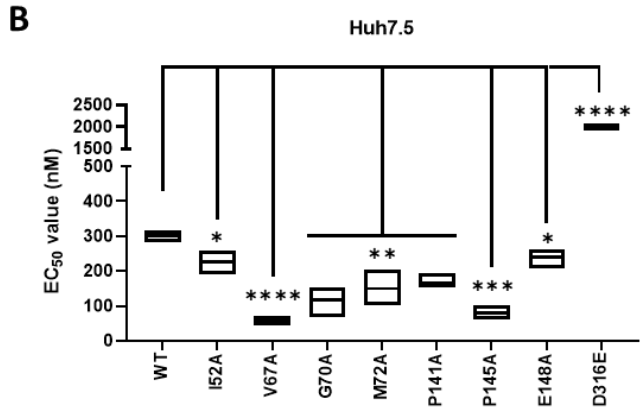
B
Huh7.5
EC50 value (nM)
WT
I52A
V67A
G70A
M72A
P141A
P145A
E148A
D316E

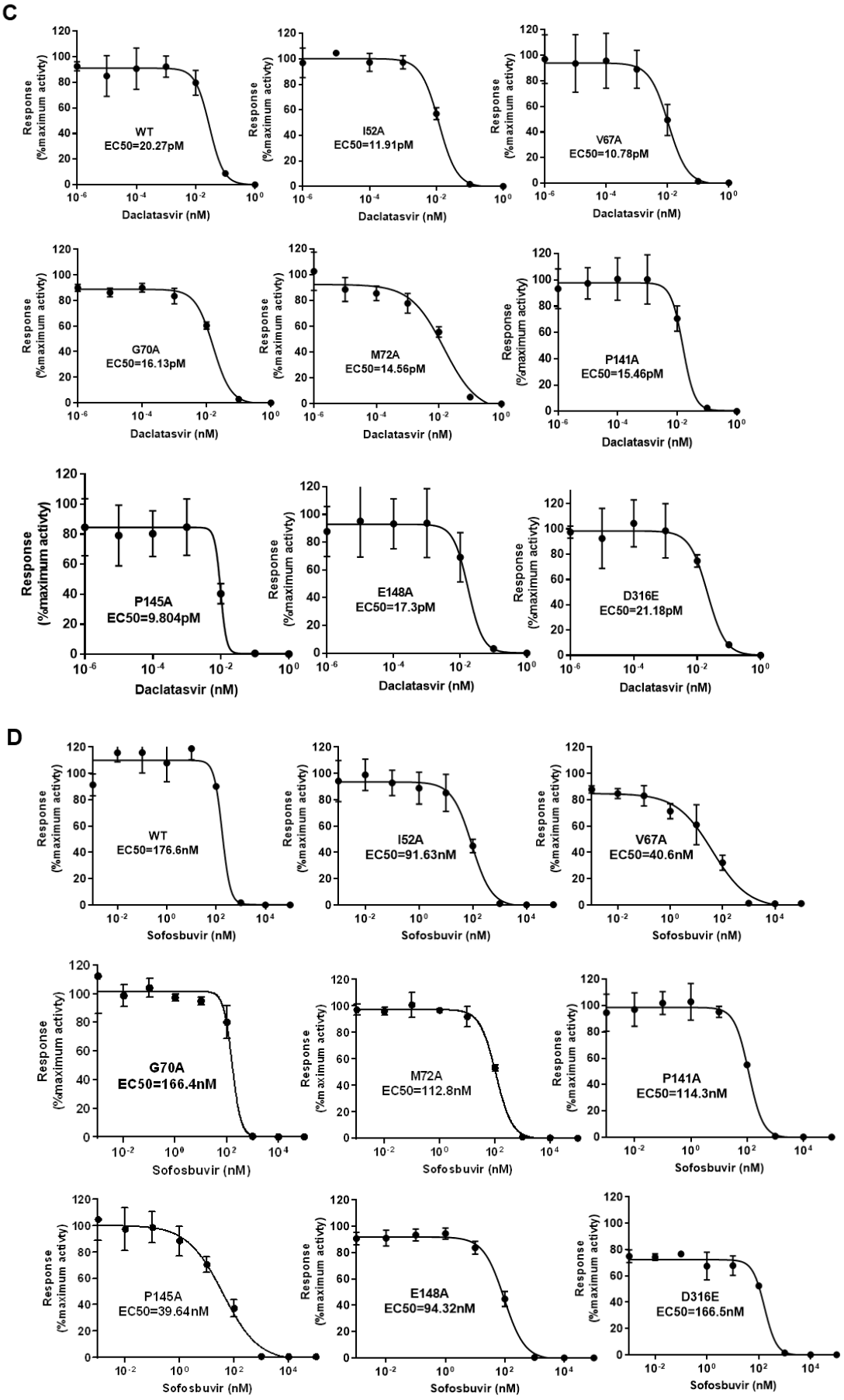
C
WT
EC50=20.27pM
I52A
EC50=11.91pM
V67A
EC50=10.78pM
G70A
EC50=16.13pM
M72A
EC50=14.56pM
P141A
EC50=15.46pM
P145A
EC50=9.804pM
E148A
EC50=17.3pM
D316E
EC50=21.18pM
Response (%maximum activty)
Daclatasvir (nM)
D
WT
EC50=176.6nM
I52A
EC50=91.63nM
V67A
EC50=40.6nM
G70A
EC50=166.4nM
M72A
EC50=112.8nM
P141A
EC50=114.3nM
P145A
EC50=39.64nM
E148A
EC50=94.32nM
D316E
EC50=166.5nM
Sofosbuvir (nM)

Fig 3.5. The effect of NS5A domain I mutations on CsA treatment.

(A) Huh7.5 cells were electroporated with mSGR-luc-JFHI RNA which contains domain I mutations, seeded into 96-well plates and treated with serial dilutions of CSA. The results of luciferase activity were normalised to the DMSO control and the data processed using the EC_{50} model of GraphPad 9.3.0. **(B)** Quantification of EC_{50} for CsA treatment. DCV **(C)** and SOF **(D)** were also diluted serially and used as controls. The cells were harvested at 48 hpe and the luciferase assay were carried out. The results of luciferase activity were normalised to the DMSO control and the data processed using the EC_{50} model of GraphPad 9.3.0.

To investigate the relevant efficiency between CypA and NS5A/5B inhibitor, the EC_{50} values were normalised by scatterplot. The correlation between CsA and DCV displayed similar pattern to that between CsA and SOF (Fig 3.6 A&B). For DCV and SOF treatment, the mutations which showed high sensitivity to one inhibitor were also sensitive to the other (Fig 3.6 C). We also detected the correlation between replication and mutant sensitivity to inhibitors as we considered that the impaired replication of mutations may render them more sensitive to the inhibitor. However, the graph demonstrates that there was no absolute correlation between the replication and efficiency of inhibitor (Fig 3.6 D, E&F).

These results suggested that the mutants of NS5A DI increased the sensitivity of viral replication to CsA treatment. I hypothesised that the tight interaction between NS5A and CypA was disrupted by NS5A DI mutants, resulting in the reduction of CypA which contributed to viral replication. Therefore, the low dosage of CsA treatment (low EC_{50}) inhibited HCV replication in these mutants compared to WT. Notably, the increased CsA sensitivity was not completely due to replication and the correlation between CsA and the two known DAAs showed similar pattern. It might indicate the potential threptic function of CsA as a DAA in HCV replication.

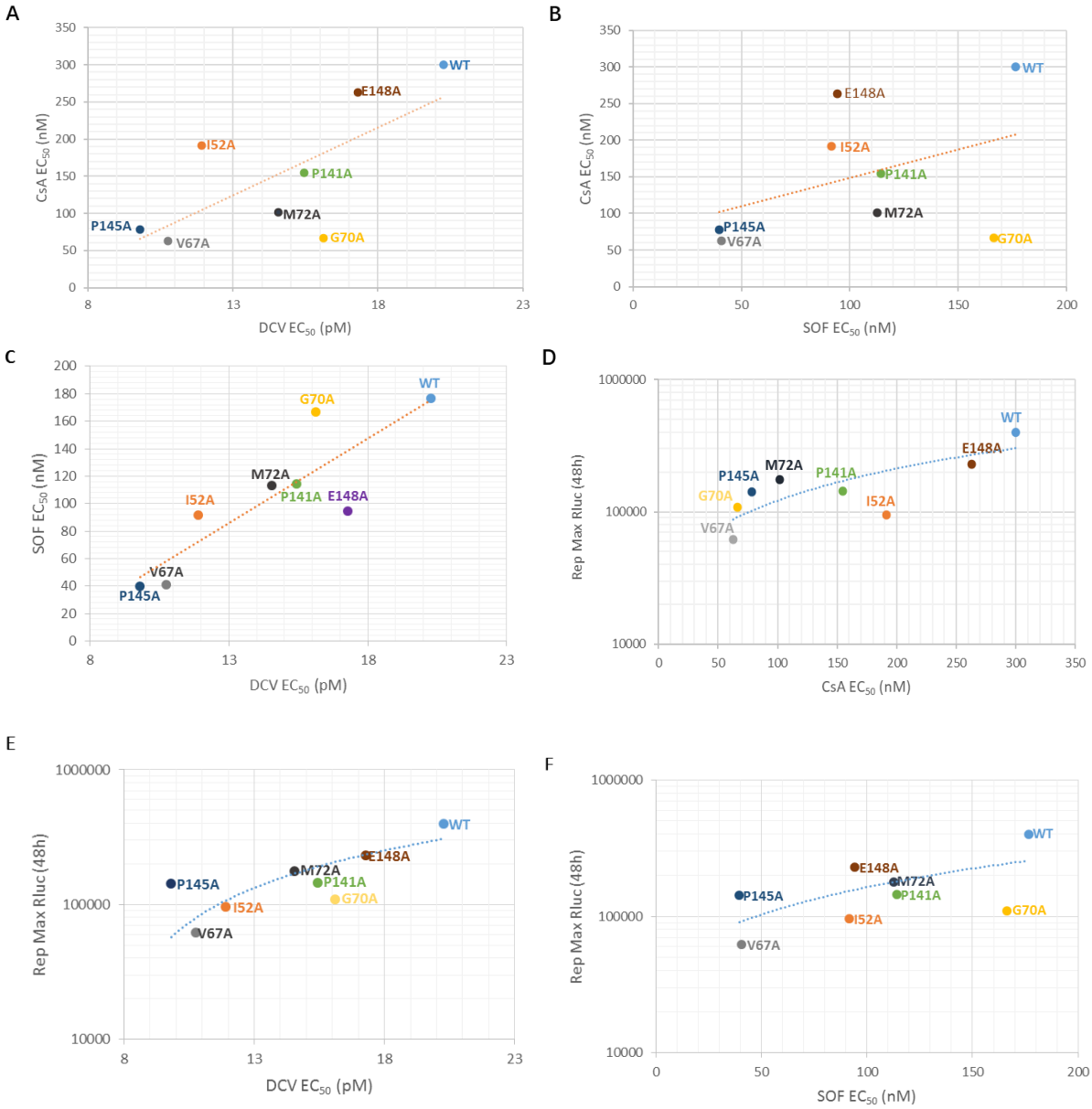

Fig3.6. Correlation between the replication efficiency of partially defective mutants and EC_{50} of inhibitor treatments.

(A) The correlation of EC_{50} between CsA and DCV. **(B)** The correlation of EC_{50} between CsA and SOF. **(C)** The correlation of EC_{50} between DCV and SOF. The correlation between replication of mutations and CsA **(D)**, DCV **(E)** and SOF **(F)** are displayed.

3.2.5 Extrapolation of the partially defective phenotype from genotype 2a to genotype 3a

Compared to other genotypes of HCV, the infection with genotype 3 is associated with a higher incidence of steatosis and hepatocellular carcinoma, as well as a more rapid fibrosis progression (Nkontchou et al., 2011). Despite the combination of DAAs inhibited chronic HCV infection efficiently, this serious condition of genotype 3 infection results in lower response rates to DAAs treatment, leading to lower cure rates (Chan et al., 2017).

The current recommended combination of DAAs treatment of Genotype 3 is using the NS5A inhibitor DCV and VEL with the NS5B polymerase inhibitor SOF (Liver, 2017). Moreover, based on previous experience of therapy, glecaprevir/pibrentasvir and SOF/VEL/voxilaprevir were also considered to be effective DAA treatments against genotype 3 by the European Association for the Study of the Liver (Liver, 2018). Notably, the triple combination of SOF/VEL/voxilaprevir achieved 99% SVR rate after 8 weeks for treatment-naive, treatment-experienced and cirrhosis patients (Jacobson et al., 2017).

The RASs in viral sequences are the major obstacle to direct-acting antiviral agents (DAAs) treatment. The Y93H substitution in NS5A was the most prevalent in genotype 3 treatment with DAAs, resulting in lower SVR rates, especially for cirrhosis patients (Leroy et al., 2016, Nelson et al., 2015). The *in vitro* analysis using S52 ΔN gt3a replicon model against DAA treatment demonstrated that A30K (8.9%) and Y93H (12.3%) were the most common substitutions, and paired RASs (A30K + L31M and A30K + Y93H) were demonstrated to contain high resistance to daclatasvir, velpatasvir, elbasvir, and pibrentasvir (Smith et al., 2019). Y93H, L31M or A/Q30K were also found

in Genotype 1a and 1b with NS5A inhibitor DAAs treatment (Malandris et al., 2021). In addition, pibrentasvir treatment analysis using a genotype 2 HCV replicon system revealed that NS5A F28S/M31I showed significantly higher replication ability than WT while the combined mutants were sensitive to the treatment of HCV NS3/4A inhibitor, NS5B inhibitor, IFN-α, and ribavirin (Suda et al., 2019). Moreover, NS5A Y93H substitutions in genotype 2a enhanced infectious virus production and was sensitive to the NS3 protease inhibitor simeprevir using infectious JFH1-based recombinant HCV (Nitta et al., 2016).

Based on the common role of these RASs among different genotypes, the substitutions in genotype 2a which showed sensitivity to CsA can be broadened to genotype 3a to further control HCV infection. Moreover, the research into genotype 3 sub-genomic replicon system is undoubtedly a significant study for both viral genome replication and DAA resistance. Previously, several genotype 3 SGR constructs were generated, but their use were limited by the defect in replication and the restriction on the detecting methods (Saeed et al., 2013, Saeed et al., 2012, Witteveldt et al., 2016). Our lab recently developed an SGR from the DBN3a infectious clone (Ramirez et al., 2016) which contains a low CpG/UpA-luciferase reporter. This DBN3a -Luc-SGR showed approximately 100-fold increase in luciferase values which was as efficient as mSGR-Luc-JFH1, thereby circumventing the low efficiency in replication of HCV genotype 3 SGR (Ward et al., 2020).

To further understand the mode of action of DAAs that target NS5A domain I of HCV genotype 3 and the difference between genotype 2 and 3, the mutations mirroring those made in JFH1 (V52A, V67A, G70A, M72A, P141A, P145A and E148A) were cloned into the DBN3a -Luc-SGR containing a luciferase reporter gene. DBN3a -Luc-SGR WT and NS5B mutant GNN were electroporated into Huh7 cells with these seven

mutants as positive and negative replication controls respectively. At 4, 24, 48, 72 and 96hpe, the cell lysates were harvested and replication was analysed via luciferase assay. The absolute luciferase values were shown in Fig 3.7A, and the data at 24, 48 ,72 and 96 hpe in Fig 3.7B was normalised to the 4 hpe signal.

According to the results in Fig 3.2A & B, I52A, V67A, G70A, M72A, P141A, P145A and E148A in mSGR-Luc-JFH1 all showed partial defect in replication compared to WT. Additionally, all of them showed gradual recovery in replication at 72h. In SGR-Luc-DBN3a, most mutants (I52A, V67A, G70A, M72A, P145A and E148A) showed the same phenotype as that in JFH1, indicating the partially defective phenotype in DBN3a genome replication. However, P141A exhibited a WT level replication in SGR-Luc-DBN3a, which was a completely different phenotype from itself in JFH1 (Figure 3.7 A&B).

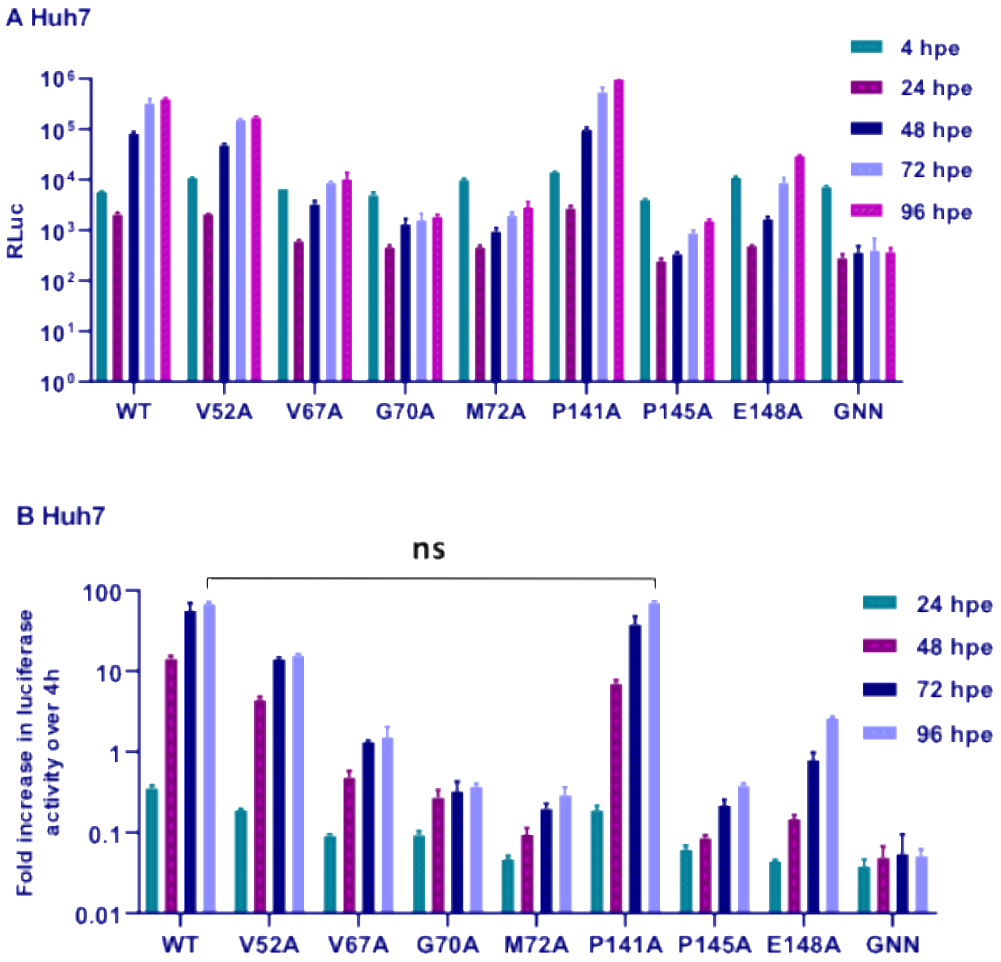

Fig 3.7. Genome replication phenotypes of SGR-Luc-DBN3a NS5A domain I mutants in Huh7 cells.

In vitro transcribed SGR-Luc-DBN3a RNAs were electroporated into Huh7 cells. Luciferase assay was performed at 4, 24, 48, 72 and 96hpe **(A)** and was further normalised to 4hpe **(B).** SGR-Luc-DBN3a WT and GNN were used as a positive and negative control.

In common with the restored phenotype of the mSGR-Luc-JFH1 mutants in Huh7.5 cells (Fig 3.3A & B), the replication capacity of all partially defective mutants in SGR-Luc-DBN3a were also detected in Huh7.5 cells. As shown in Fig 3.8A and 3.8B, the replication of V52A, V67A, G70A, M72A and E148A showed a significant recovery in Huh7.5 cells even though the replication peak was detected at 96hpe. However, two mutants maintained their phenotypes in both cell lines. P141A still showed a WT level

replication in Huh7.5 cells, while P145 showed a large attenuation of replication in both cell lines. The increasing luciferase values over 24-96hpe displayed that P145A still maintained higher replication capacity than GNN.

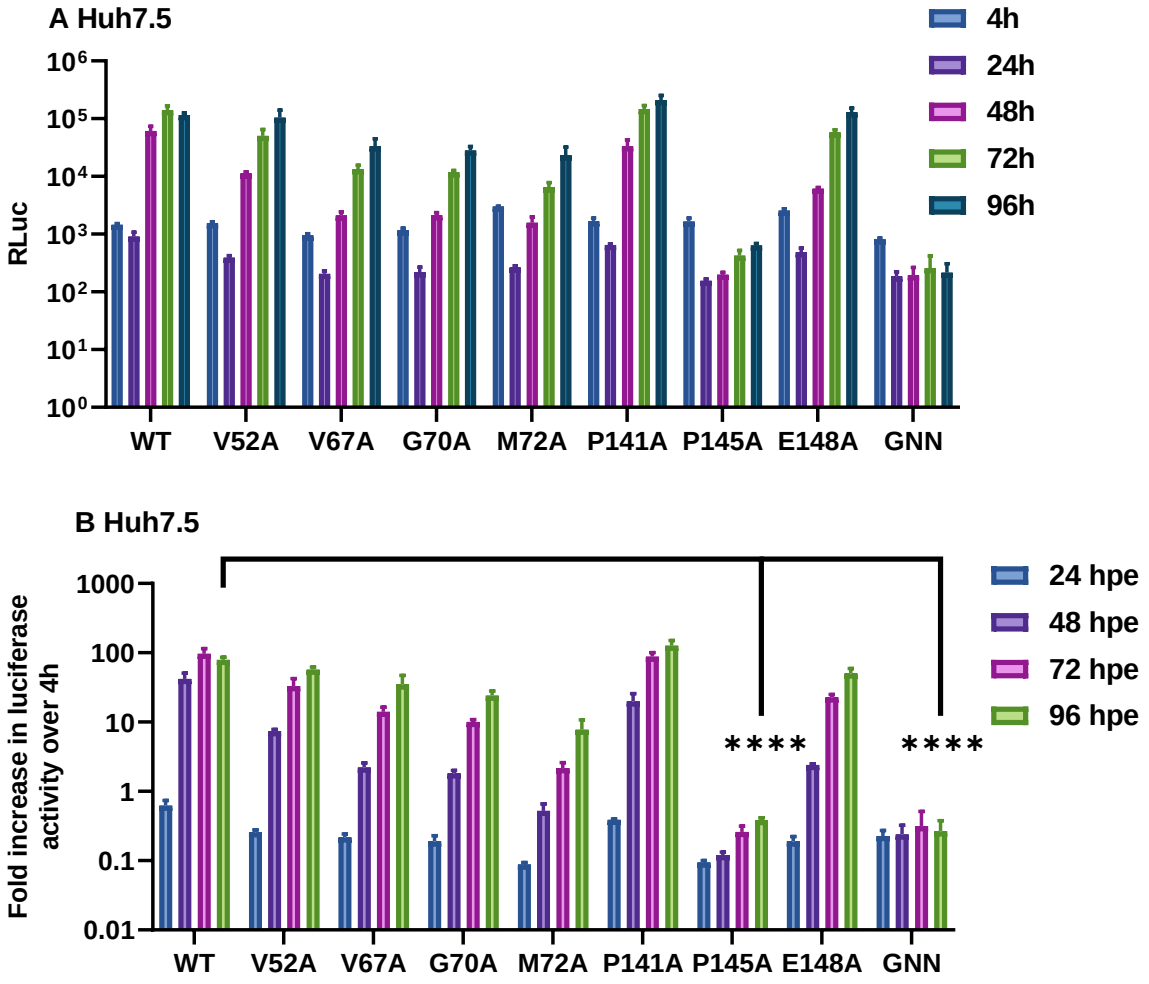

Fig 3.8. Genome replication phenotypes of SGR-Luc-DBN3a NS5A domain I mutants in Huh7.5 cells.

In vitro transcribed SGR-Luc-DBN3a RNAs were electroporated into Huh7.5 cells. Luciferase assay was performed at 4, 24, 48, 72 and 96hpe **(A)** and was further normalized to 4hpe **(B)**. SGR-Luc-DBN3a WT and GNN were used as a positive and negative control.

Together, we confirmed that V52A, V67A, G70A, M72A and E148A exhibited the same phenotype as that in JFH1: the replication was partially defective in Huh7 and was remarkably restored in Huh7.5, indicating that these residues were likely to play a

parallel role in two different genotypes. Notably, the phenotype of P141A and P145A showed a striking contrast which may reveal the difference between genotype 2 and 3.

3.2.6 The replication sensitivity of partially defective mutants in DBN3a to cyclophilin A (CypA) inhibition

Based on the sensitivity to CsA treatment of JFH1 SGR mutations, the mutations in DBN3a NS5A DI were considered to also have the ability to modulate the sensitivity of replication to CsA treatment. To demonstrate this, the panel of SGR-Luc-DBN3a mutants was screened for CsA sensitivity.

SGR-Luc-DBN3a, V52A, V67A, G70A, M72A, P141A and E148A were electroporated into Huh7.5 cells and CsA was added to cells after 4 hpe. Luciferase activity at 72 hpe revealed that all seven mutants were more sensitive to CsA treatment than WT, particularly for G70A and M72A (Fig 3.9A). The CsA efficacy assay from three biological repeats showed that the EC_{50} values of partially defective mutants in DBN3a were significantly reduced compared to WT (Fig 3.9B). These results suggested the potential association between DBN3a NS5A DI and CypA, thereby providing a reference for finding putative binding sites of CypA.

We considered that the sensitivity to CsA treatment might be affected by the impaired replication of mutations. To test this, the association between replication and mutants sensitivity to inhibitors was presented as a curve. Interestingly, the graph in Figure 3.9 C demonstrated that the sensitivity indeed had some correlations to replication for some poorly replicating mutants like V67A, G70A and M72A. For V52A, P141A and E148A which showed WT levels of replication in Huh7.5 did not correspond to the

associated curve. We considered that the replication of those poorly replicating mutants was more vulnerable to CsA treatment.

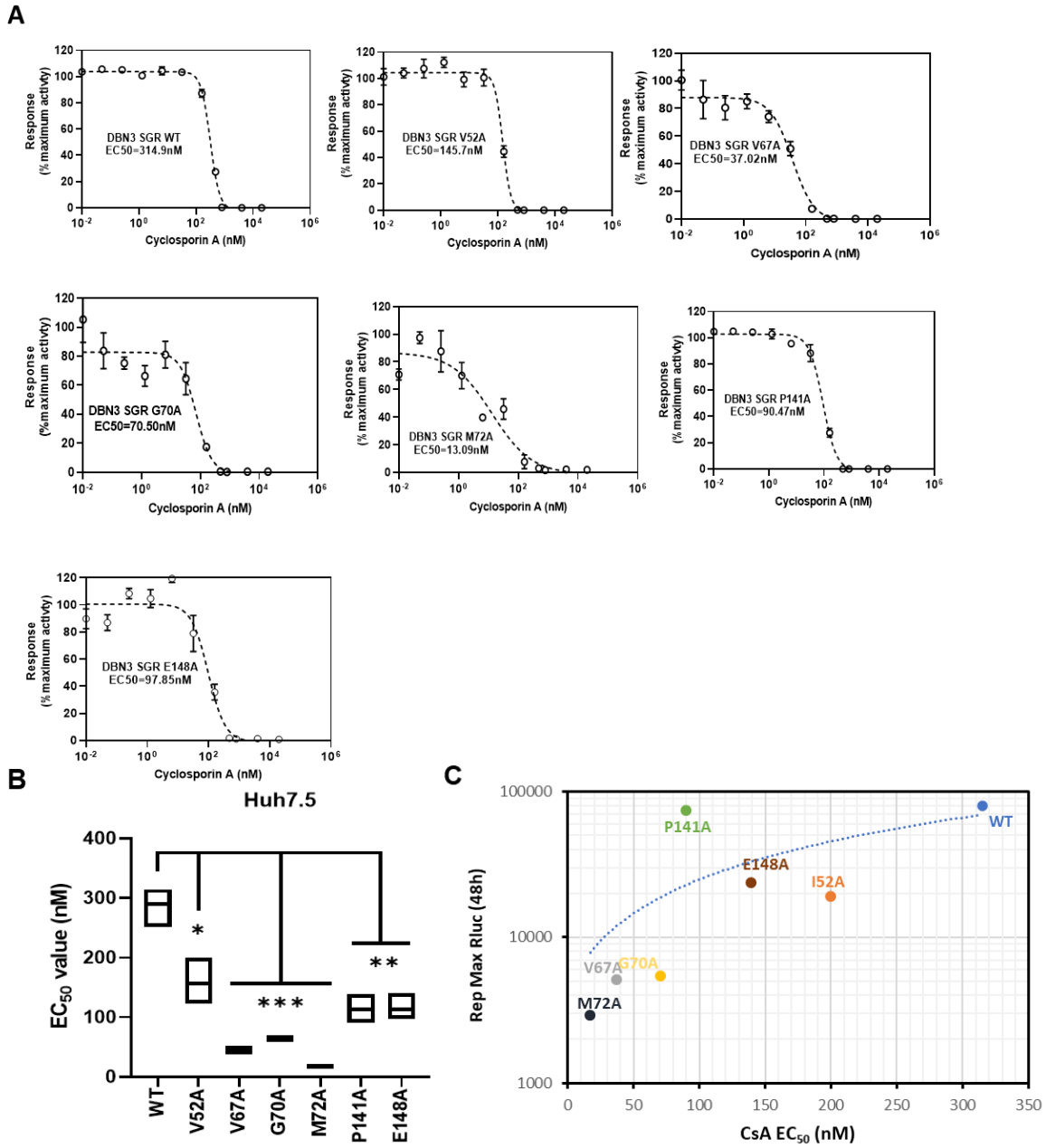

Fig 3.9. The effect of SGR-Luc-DBN3a NS5A domain I mutations on CsA treatment.

Huh7.5 cells were electroporated with SGR-Luc-DBN3a mutants RNA and then seeded into 96-well plates. The cells were treated with serial dilutions of CSA at 4hpe. **(A)** The cells were harvested at 72 hpe and the luciferase assay were carried out. The results of luciferase activity were normalized to the DMSO control and the data processed using the EC_{50} model of GraphPad 9.3.0 **(B)** Quantification of EC_{50} for CsA treatment. **(C)** Correlation of replication efficiency and CsA EC_{50} of SGR-Luc-DBN3a mutants.

3.3 Discussion

The present study identified five residues (I52, G70, M72, P141 and E148) in NS5A domain I of JFH1 played the essential role in HCV genome replication. The alanine substitution of these residues showed partial defect in genome replication which displayed the same phenotype as V67A and P145A. They were selected due to their surface exposure, conservation and proximity to V67 and P145. Although the phenotype we found was significant, the mechanism of NS5A DI in HCV genome replication still required further investigation.

The interaction between CypA and NS5A DII and DIII has been demonstrated (Chatterji et al., 2010, Foster et al., 2011, Hanoulle et al., 2009a). NS5A DI was also involved in replication, while the binding mechanism with CypA is still unclear. As shown in Fig 3.5, the mutations of NS5A DI exhibited different sensitivity to CsA treatment compared to WT, suggesting that NS5A DI may associate with CypA. The conclusion still needs to be investigated by alternative assays such as pulldown assay and siRNA or CRISPR/Cas9 knockdown assay.

Furthermore, previous work revealed an essential role of CypA in enhancing RIG-I-mediated antiviral immune responses by controlling the ubiquitination of RIG-I and MAVS (Liu et al., 2017). Whilst the present study of the interaction between CypA and RIG-I showed that CypA was involved in RIG-I detection of HCV, CypA inhibitor was more potent in Huh7 cells. The enhanced replication capacity in Huh7.5 compared to Huh7 can be partially attributed to a defect in RIG-I and concomitant block to an innate immune response to cytoplasmic dsRNA. This is reminiscent of the phenotype of NS5A domain I mutations whose defects were not seen in Huh7.5. Therefore, it could be that these residues were involved in counteracting RIG-I/CypA. To our knowledge,

CypA plays a critical role in HCV replication, and this hypothesis contributes to exploring the novel mechanism of CypA to facilitate genome replication through inhibiting the antiviral pathway.

Interestingly, I found one mutant E191A which disrupted the expression of NS5A protein, but did not affect viral replication. NS5A belongs to the viral replication complex which is essential to HCV replication. As the mechanism of NS5A's involvement in HCV replication has still not been fully determined yet, these results may shed light into an understudied area. E191 is located at the C-terminus of NS5A domain I, which has a disulphide bond required to maintain the dimerisation of NS5A (Tellinghuisen et al., 2005). E191A may disrupt the disulphide bond which connects the sidechains of the conserved Cys 142 and Cys 190, resulting in the disruption of NS5A dimeric conformation, followed by several changes of interaction between NS5A and NS5B or host factor. Alternatively, I suspected E191A may disrupt the binding site on NS5A for the anti-NS5A antibody used. The mechanism by which E191 exhibited high level of replication still needs to be explored further.

New compounds DAAs were developed in 2011, which directly target the HCV NS3 protease, NS5B polymerase, and NS5A. Although these represent a major advancement in the treatment of HCV and has achieved a sustained virological response exceeding 90% in most genotypes, HCV genotype 3a is less responsive to these drugs and the cure rates for genotype 3 infection have lagged behind the other genotypes (Chan et al., 2017, Geddawy et al., 2017). HCV genotype 3a sub-genomic replicon (SGR-Luc-DBN3a), with a low CpG/UpA-luciferase reporter, replicated as efficient as JFH-1 SGR, which can be used to explore the resistance of genotype 3 to DAA (Ward et al., 2020). To achieve that, the mutations were cloned into DBN3a from JFH1, further investigating whether these mutations also displayed the same

phenotypes in genotype 3a. Interestingly, despite SGR-luc-DBN3a being reported to replicate as efficiently as JFH1 SGR, the replication level still needed 72hpe or even 96hpe to reach the peak. In addition, the replication of all mutants which showed a partially defective phenotype in Huh7 cells were recovered but still failed to reach WT level in Huh7.5 cells. This suggested that the conserved residues in NS5A DI had deeper effect on genome replication in DBN3a than JFH1. In particular, P141A and P145A exhibited the different phenotypes between the two genotypes, indicating that they played the different roles in genotype 2 and 3. It is worth noticing that despite the high conservation of NS5A domain I among HCV all genotypes, the consensus residues might provide different functions.

Lastly, since the potential association between CypA and JFH1 NS5A DI was shown by CsA treatment assay, I suspected that the mutants DBN3 NS5A DI would also displayed similar sensitivity to CsA treatment. As expected, the drug efficacy assay observed that the sensitivity of DBN3 NS5A DI to inhibitors was also modulated by partially defective mutants (Fig 3.9), suggesting that they had same function to CypA as the JFH1 NS5A DI. However, the mechanism and distinctiveness of exact interaction need further analysis.

Chapter 4: The interaction between CypA and NS5A domain I in HCV JFH1 inhibits the NF-κB pathway to promote viral replication but not assembly

4.1 Introduction

Cyclophilin A (CypA) is one of the best characterised members of the Cyclophilin (Cyp) family of immunophilins which is ubiquitously expressed in both prokaryotic and eukaryotic cells. CypA is one of the most abundant proteins in the cytoplasm (0.1–0.4% of total protein content) (Harding et al., 1986, Ryffel et al., 1991). It contributes to a broad range of cellular functions, including T-cell activation, cell signalling, transcriptional regulation, and protein folding and trafficking (Naoumov, 2014, Nigro et al., 2013).

CypA possesses peptidyl-prolyl cis-trans activity (PPIase), which was first characterised in mammals as a target of an immunosuppressive drug cyclosporin A (CsA), preventing the proinflammatory cytokine production (Hanes, 2015, Thapar, 2015). CypA inhibitors (CypIs) were initially reported in 2003 to reduce HCV replication (Watashi et al., 2003). CsA was demonstrated to be effective against HCV replication directly in a cell culture–based replicon system, which was independent of the interferon (IFN) signal transduction pathway (Nakagawa et al., 2004, Watashi et al., 2003). CsA was demonstrated to inhibit replication of the JFH1 replicon, whereas the efficiency was slightly less than genotype 1b (Ishii et al., 2006). In addition, PPIase motif of CypA was shown to play an essential role in HCV infection (Chatterji et al., 2009, Kaul et al., 2009). At present, non-structural proteins of HCV, such as NS5B, NS5A, and NS2 have all been proposed to have potential interactions with CypA (Robida et al., 2007, Watashi et al., 2005).

In particular, a CsA-sensitive interaction between NS5A and CyPA can be demonstrated *in vitro* (Chatterji et al., 2010, Fernandes et al., 2010, Hanoulle et al., 2009a). Interaction between NS5A domain II and CypA is crucial for HCV replication

(Ross-Thriepland et al., 2013), and the RNA-binding properties of NS5A were increased due to the binding of CypA (Foster et al., 2011). These findings further suggested the possibility for CypIs to be the anti-HCV drug candidates preclinically and clinically. Although NS5A DI was revealed to be involved in the modulation of HCV replication (Love et al., 2009, Tellinghuisen et al., 2005) , the association between CypA and NS5A DI was poorly understood.

CypA is also considered to regulate the PKR-dependent antiviral immunity pathway during HCV infection. CsA and other CypIs treatments in HCV-infected cells resulted in the reduction of activated or phosphorylated PKR and the downstream factor eIF2α (Daito et al., 2014). Additionally, they increased the expression of IFN-β, ISGs and the downstream factor IRF1 (Colpitts et al., 2020). Intracellular CypA also modulated the accumulation and activation of NF-κB in cancer, indicating that CypA might be an important regulator to activate the NF-κB pathway (Sun et al., 2011). Moreover, CypA interacted with the NF-kB subunit p65 and enhanced its nuclear translocation (Sun et al., 2014). However, limited report focused on the association between CypA and NF-kB in HCV replication. The detailed mechanism of CypA regulate antiviral factors to promote HCV replication needs further investigation.

In this study, we first identified the interaction between CypA and JFH1 NS5A DI. Five mutants in JFH1 NS5A DI showed partially reduced replication due to the loss of interaction with CypA. The interaction between CypA and NS5A DI inhibited NF-κB pathway to further promote HCV replication in Huh7.5 cells, while the interaction was not essential for HCV assembly. However, although DBN3a NS5A DI were more sensitive to CsA treatment, it was not involved in the binding with CypA to modulate the DBN3a replication. The complete dependence on CypA for DBN3a replication further revealed the different response between JFH1 and DBN3a to DAAs.

4.2 Results

4.2.1. The replication of partially defective mutants in JFH1 NS5A DI are more dependent on CypA compared to WT.

To further understand the effect of CypA in NS5A DI mutants replication, we constructed CypA silenced cell lines in Huh7 and Huh7.5 cells using stably expressing specific shRNA (Fig 4.1A). To avoid the effect of puromycin screening for cells, a non-targeting guide RNA silenced cell lines (Huh7 shCTRL and Huh7.5 shCTRL) were also constructed to be a positive control. NS5A DI mutants which showed partial defect in replication were electroporated into these four cells lines as described above, the luciferase values at 24, 48 and 72 hpe were normalised to the 4 hpe signal to control for transfection differences. Surprisingly, neither WT nor partially defected mutants replicated in Huh7 CypA silenced cell lines (Fig 4.1B). However, in Huh7.5 CypA silenced cell lines, even though the replication of WT gradually recovered over time, partially defective mutants did not display restoration and were indistinguishable with GND (Fig 4.1C). Previous research has shown that CypA was critical for HCV replication in Huh7 cells, but not in Huh7.5 cells (Colpitts et al., 2020), which was consistent with the WT data (Fig 4.1B and 4.1C). As shown in Fig 4.1D and 4.1E, the replication of all partially defective mutants were consistent with the results in Huh7 and Huh7.5 cells (Fig 3.2B and 3.3B), further indicating the new phenotypes in CypA silenced cell lines were due to the lack of replicative ability rather than the puromycin treatment. The replication disruption in the absence of CypA demonstrated that, partially defective mutants were more dependent on CypA in both Huh7 and Huh7.5 cells compared to WT. NS5A DI in JFH1 might be involved in the interaction with CypA to promote HCV replication.

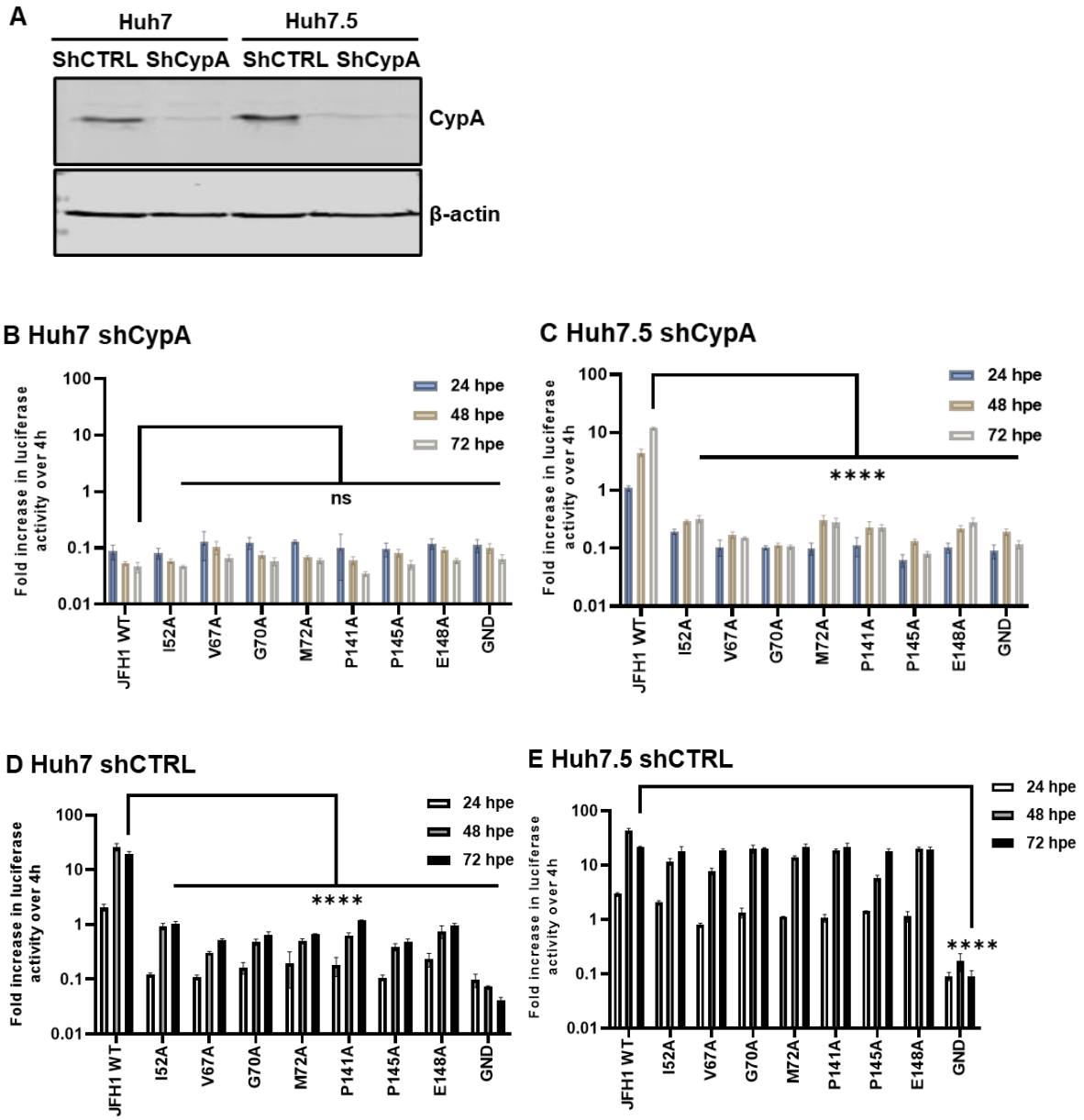

Fig4.1. Virus replication phenotypes of JFH1 in the absence of CypA.

(A) CypA expression was detected in CypA silenced and shCTRL Huh7 and Huh7.5 cells by western blot. *In vitro* transcribed mSGR-Luc-JFH1 RNAs containing the indicated mutations were electroporated into **(B)** Huh7 CypA silenced cell line, **(C)** Huh7.5 CypA silenced cell line, **(D)** Huh7 control cell line and **(E)** Huh7.5 control cell line. Luciferase activity was measured at 4, 24, 48 and 72 hpe and the data were normalised with respect to 4 hpe.

4.2.2 CypB does not contribute to the modulation of genome replication in JFH1

Since the PPIase activity of CypB also can be disrupted through CsA, we then investigated whether CypB is involved in modulating HCV replication through NS5A domain I. To test this, Huh7 and Huh7.5 CypB silenced cell lines were generated using stably expressing specific shRNA. The Huh7 shCTRL and Huh7.5 shCTRL cell lines were used as a positive control (Fig 4.2A). The JFH1 NS5A DI mutants were also electroporated into these two cell lines to evaluate the viral genome replication. Unlike CypA, the replication in the absence of CypB slightly affected WT replication at 48hpe but the replication was consistently increased to the normal level at 72hpe in Huh7 CypB silenced cell lines. Notably, the lack of CypB can also affect the replication of partially defective mutants, which showed a completely disruption of replication in the Huh7 cells (Fig 4.2B). However, as shown in Fig 4.2C, the replication of both WT and partially defective mutants in the Huh7.5 CypB silenced cell lines were recovered to the normal level as in huh7.5 cells (Fig 3.3B) and Huh7.5 shCTRL cell line (Fig 4.1E). This confirmed that the replication of neither JFH1 WT nor the indicated mutants were dependent on CypB in Huh7.5 cells. The replication of JFH1 WT in the absence of CypA and CypB was consistent with previous finding (Kaul et al., 2009).

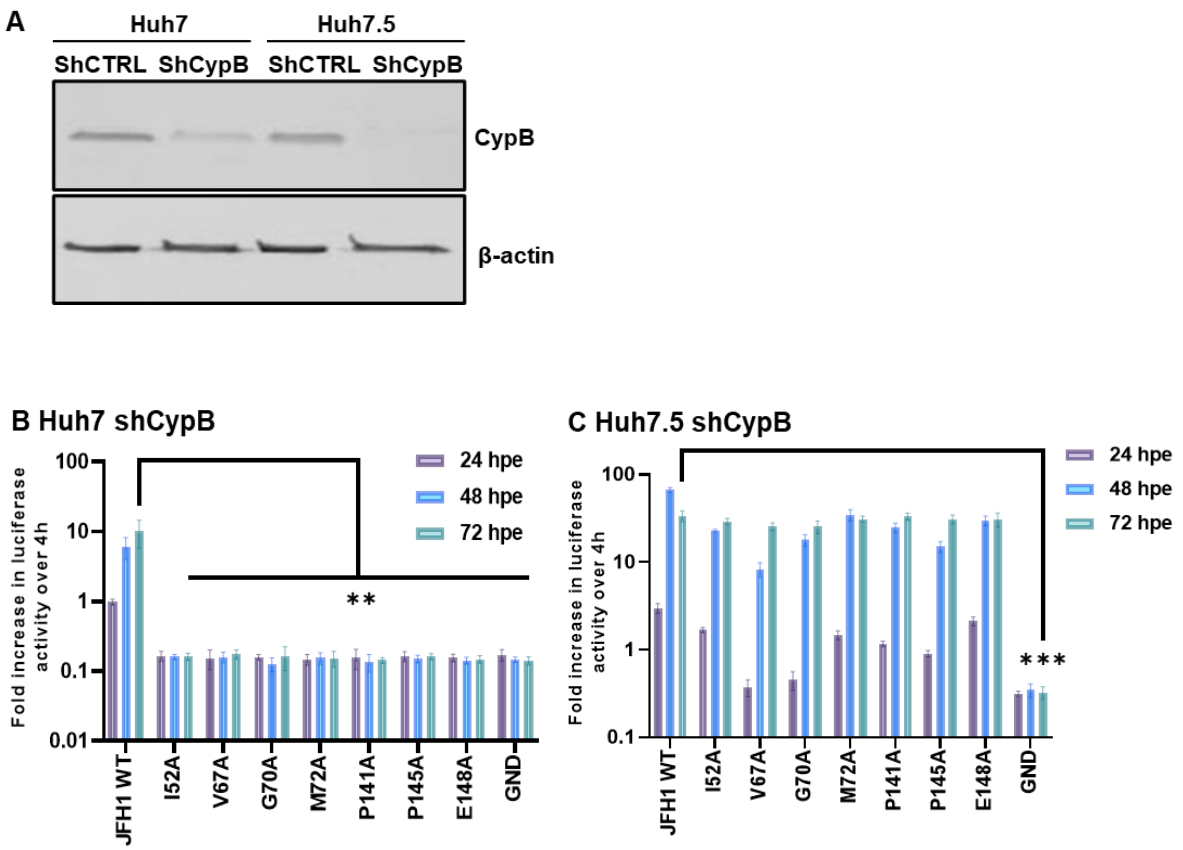

Fig 4.2 Virus replication phenotypes of JFH1 in the loss of CypB.

(A) CypB expression was detected in CypB silenced and shCTRL Huh7 and Huh7.5 cells by western blotting. *In vitro* transcribed mSGR-luc-JFH1 RNAs containing the indicated mutations were electroporated into **(B)** Huh7 CypB silenced and **(C)** Huh7.5 CypB silenced cell lines. Luciferase activity was measured at 4, 24, 48 and 72 hpe and the data were normalised with respect to 4 hpe.

Concordantly, JFH1 WT only disrupted the replication ability in huh7 CypA silenced cell line, while it maintained the WT level replication in both other cell lines (Fig 4.3 A and 4.3 C). However, the replication of I52A (the representative of partially defective mutants) in JFH1 was disrupted in Huh7 CypA, CypB silenced cell lines and Huh7.5 CypA silenced cell lines but only recovered in Huh7.5 CypB silenced cell lines (Fig 4.3 B and 4.3 D).

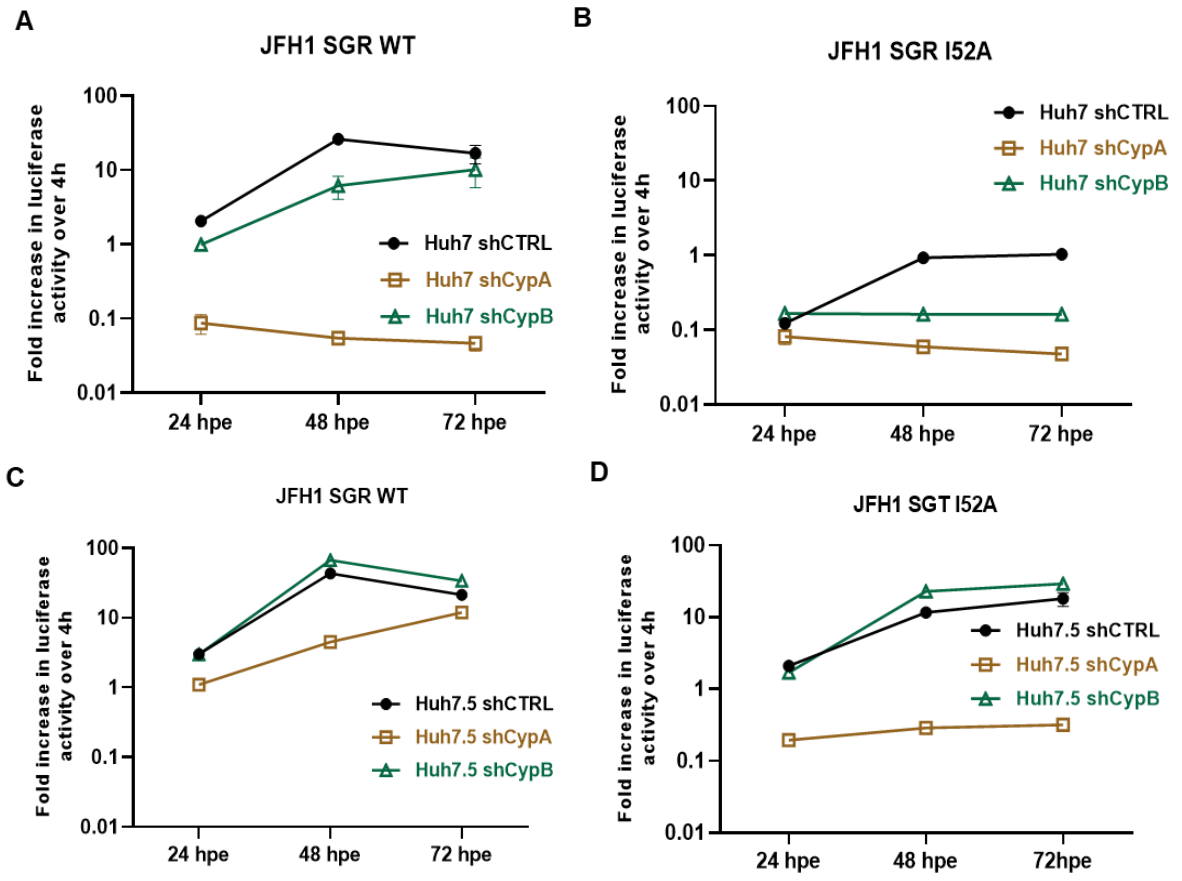

Fig 4.3 Comparisons of the replication of JFH1 WT and I52A in all cell lines.

The replication comparisons of **(A)** JFH1 WT and **(B)** I52A measured at 24, 48 and 72 hpe which were normalised to 4 hpe in Huh7 silenced cell lines. The replication comparisons of **(C)** JFH1 WT and **(D)** I52A measured at 24, 48 and 72 hpe which were normalised to 4 hpe in Huh7.5 silenced cell lines.

4.2.3 CypA interacts with NS5A DI WT but not partially defective mutants

Since the partially defective mutants of NS5A DI in JFH1 were more sensitive to CsA than WT (Fig 3.5), I hypothesised that NS5A domain I of JFH1 can interact with CypA to enhance the replication of HCV. To test this, GST-CypA and His-tagged NS5A DI were constructed and expressed in E.coli. The purified proteins were used in a GST-pulldown assay and the presence of NS5A DI was detected by western blotting. The GST protein and GST-CypA-H126Q protein (PPIase negative mutant of CypA) were

used as negative controls. As shown in Fig 4.4A, the expressions of purified NS5A domain I (35-215aa, 35-249aa) can be detected by SDS-PAGE and Western blot using NS5A antibody. As expected, CypA was indeed able to interact with NS5A DI and the interaction was not detected in negative controls (Fig 4.4B). To further confirm the interaction, we also constructed the His-tagged NS5A DI+LCSI domain (35-249aa), which was reported to enhance the binding between NS5A DI with host factors (Chong et al., 2016). Following assessing to the GST-pulldown experiment, the same interaction was observed in CypA and NS5A DI (Fig 4.4C).

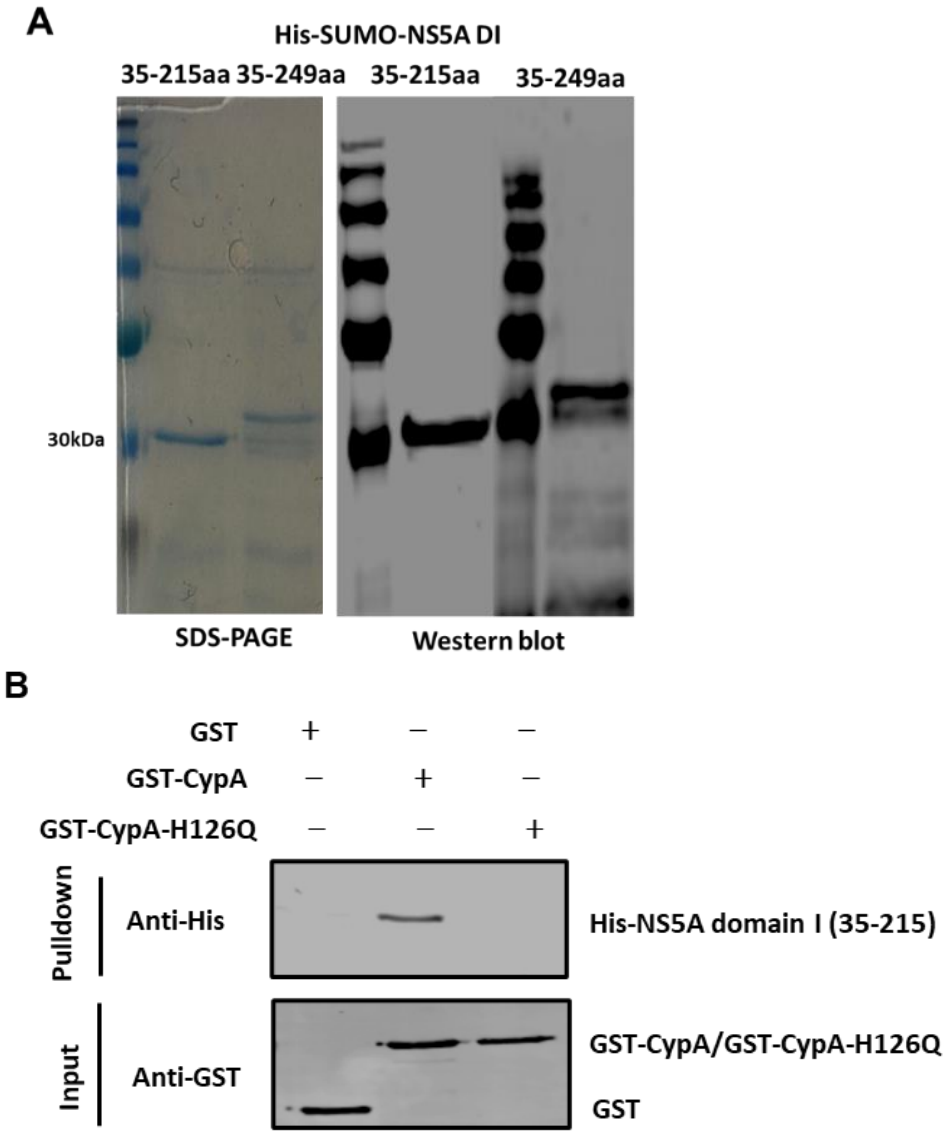

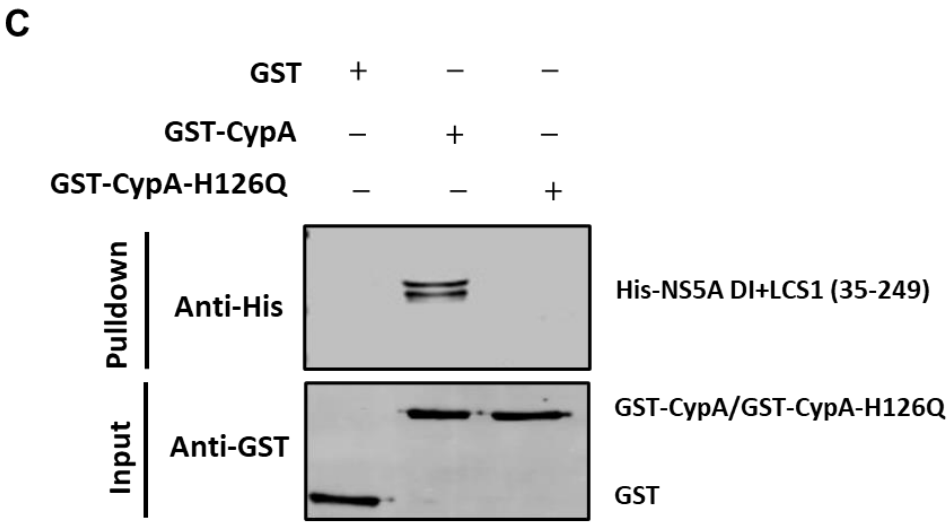

Fig 4.4 The interaction between CypA and JFH1 NS5A DI.

(A) The expressions of purified His tagged JFH1 NS5A DI (35-215aa) and NS5A DI + LCS I domain (35-249aa) were detected by SDS-PAGE and Western blot using sheep anti-NS5A. GST protein, GST tagged CypA and CypA-H126Q were purified and bound to GST resin as a bait to precipitate **(B)** purified His tagged JFH1 NS5A DI (35-215aa) and **(C)** purified His tagged JFH1 NS5A DI + LCS I domain (35-249aa) which were expressed in *E. coli.* Pulldowns were analysed by western blotting for His (top), and inputs verified by western blotting for the GST (bottom).

To further confirm whether the interaction between NS5A DI and CypA was associated with its PPIase activity, 5 uM, 2uM, 1uM and 0 uM of CsA were used to inhibit the CypA activity during the binding process. GST-CypA alone (mock) was used as a positive control. As shown in Fig 4.5A, only 0 uM CsA (DMSO alone) treated CypA and GST-CypA (mock) were able to precipitate NS5A DI, while 5,2 and 1 uM CsA completely disrupted this interaction. The same results were observed in NS5A+LCSI domain (35-249aa) proteins (Fig 4.5 B), indicating that the interaction between CypA and JFH1 NS5A DI was dependent on PPIase activity of CypA.

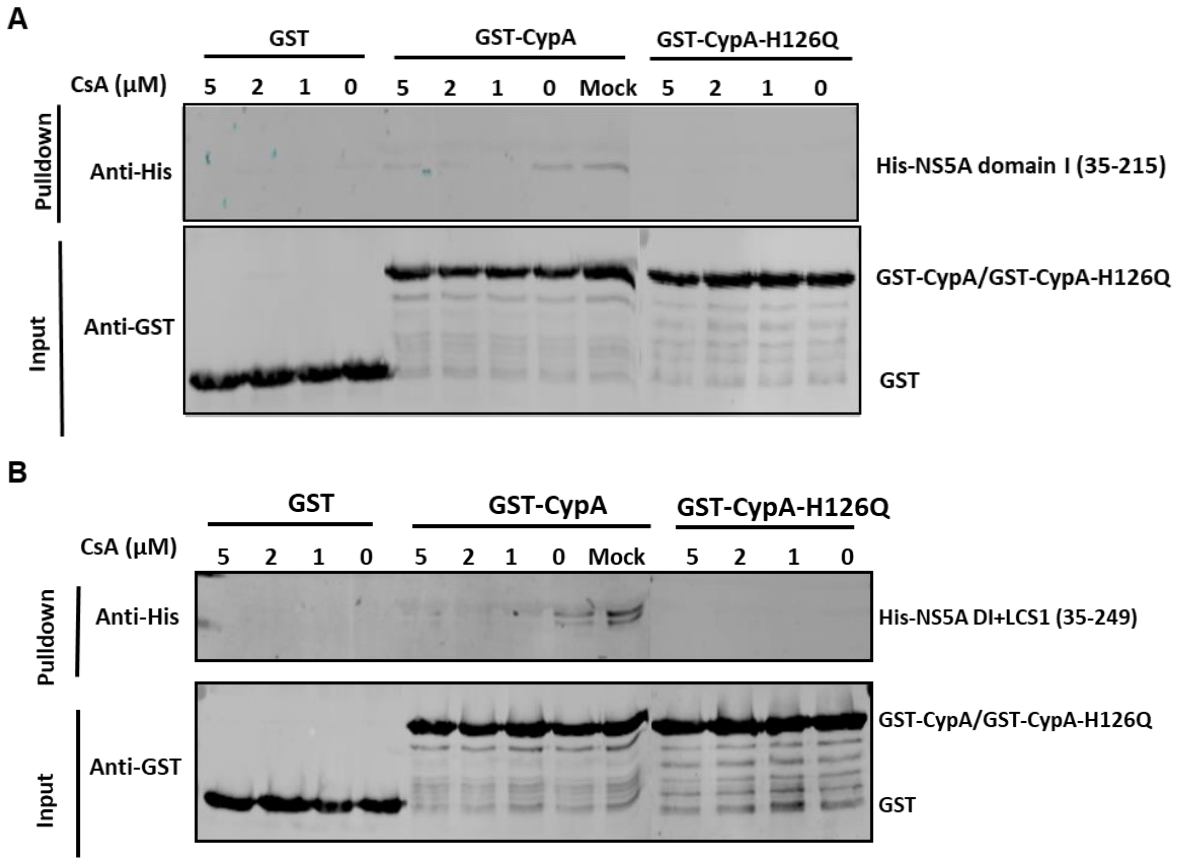

Fig 4.5 The JFH1 NS5A DI-CypA interaction was dependent on PPIase activity of CypA.

Different concentration of CsA (5, 2, 1 and 0 μM) was added into GST resin for 10min before binding **(A)** purified JFH1 NS5A DI (35-215aa) or **(B)** purified JFH1 NS5A DI+LCSI domain (35-245aa). GST-CypA (Mock-no DMSO treatment) was used to be a positive control. The resin was treated with SDS buffer and then were analysed by western blot using anti-His (top) and anti-GST antibody (bottom).

To shed light on whether partially defective mutants in JFH1 NS5A DI also interacted with CypA, I52A was cloned into PET-28a-His sumo vector as a representative of these mutants to be expressed and purified as described. The expression of purified His-SUMO-NS5A DI I52A (35-215aa) can be detected by SDS-PAGE and Western blot using NS5A antibody. His-SUMO-NS5A DI WT (35-215aa) was used as positive

control (Fig 4.6A). 1 uM CsA treatment was used as a negative control to inhibit the PPIase activity of CypA. Following assessing to the GST-pulldown experiment, the precipitation was detected using western blotting. As shown in Fig 4.6B, I52A was incapable of interacting with CypA, suggesting that the loss of replication capacity of I52A due to the deficiency of interaction with CypA.

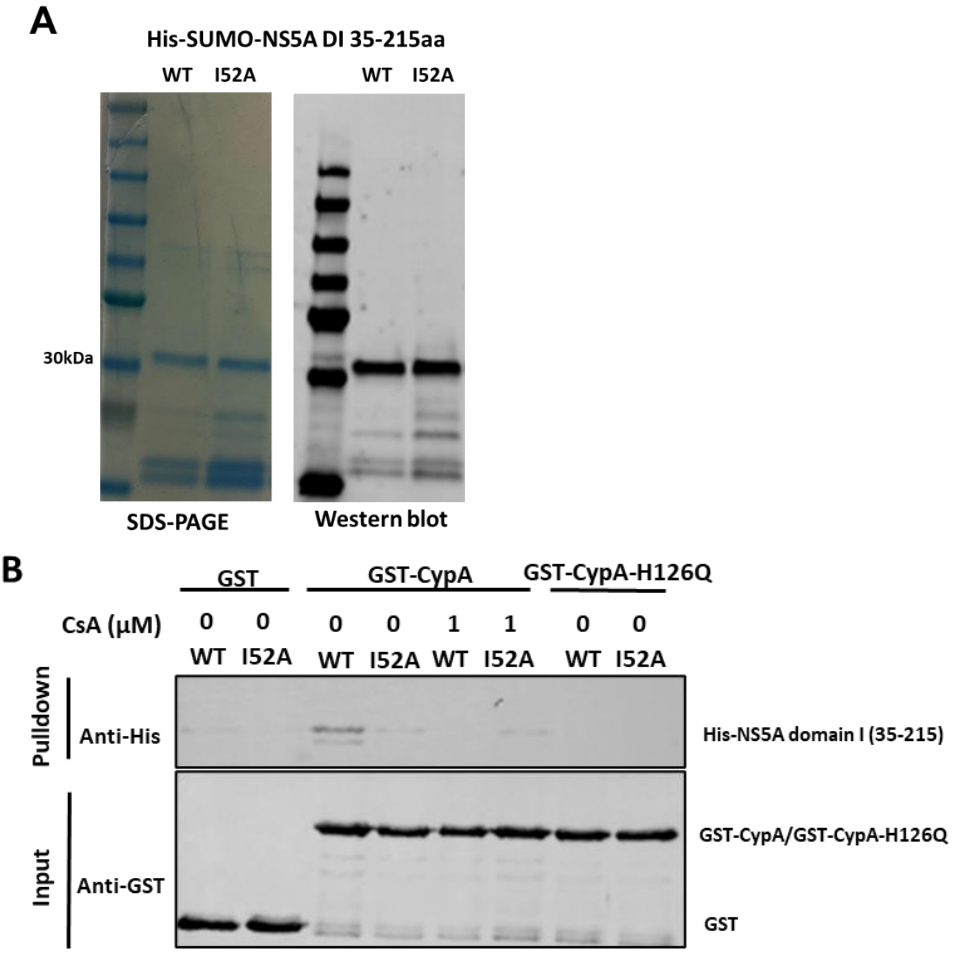

Fig 4.6 CypA interact with JFH1 NS5A DI but not partially defective mutants.

(A) the expressions of purified His-SUMO-NS5A DI WT and I52A (35-215aa) were detected by SDS-PAGE and Western bolt using sheep anti-NS5A. **(B)** Purified GST, GST tagged CypA and CypA-H126Q were bound to GST resin as a bait to precipitate purified His tagged JFH1 NS5A DI (35-215aa) and I52A. 1 μM CsA treatment as a negative control. The resin was treated with SDS buffer and then were analysed by western blot using anti-His (top) and anti-GST antibody (bottom).

These results concluded that NS5A DI indeed interacted with CypA and the interaction was associated with PPIase activity of CypA. Furthermore, the interaction can be disrupted by partially defective mutants in NS5A DI, resulting in the completely reduction of replication in the loss of CypA.

4.2.4 PKR and RIG-I have no effect on the modulation of I52A replication through CypA.

PKR expression shown to be reduced in Huh7.5 cells compared with Huh7 cells (Colpitts et al., 2020), so western blotting analysis of different cell lines was performed. As shown in Fig 4.7A, although the CypA and CypB silenced cell lines did not affect the expression of PKR, Huh7 silenced cell lines exhibited higher PKR expression compared to Huh7.5 silenced cell lines. These results suggested that PKR is likely to be involved in HCV replication. PKR inhibits RNA translation during viral infection and enhances antiviral activity induced by IFN (Pham et al., 2016). Different from other viruses, the replication of HCV decreased when PKR was blocked, and the PKR inhibitor C16 increased IFN-β promoter induction (Arnaud et al., 2010). In addition, NS5A interacts with the protein kinase catalytic domain of PKR, which promotes HCV to evade IFN (Gale Jr et al., 1997). To evaluate the essential factors which affected the HCV replication through NS5A domain I, following the electroporation of WT, I52A and GND into Huh7 and Huh7.5 cells, 1 μM CsA and C16 was treated at 4hpe. The luciferase values were measured at 48hpe. As expected, the replication of WT exhibited a slight decrease at 1 μM C16 treatment in both cell lines, this result was consistent with the previous finding (Arnaud et al., 2010). However, C16 rescued the failure of WT replication with CsA treatment in both cell lines, more significantly in Huh7.5 cells. In contrast to WT, the replication of I52A increased in both cells with C16 treatment. Crucially, silencing CypA and PKR resulted in the more significant recovery

of I52A replication in Huh7.5 cells than in Huh7 cells (Fig 4.7B and 4.7C). Thus, these results confirmed that once the structure of NS5A domain I was disturbed by mutants or HCV replication was disrupted by CsA, PKR was released to activate and induce IFN to inhibit HCV replication.

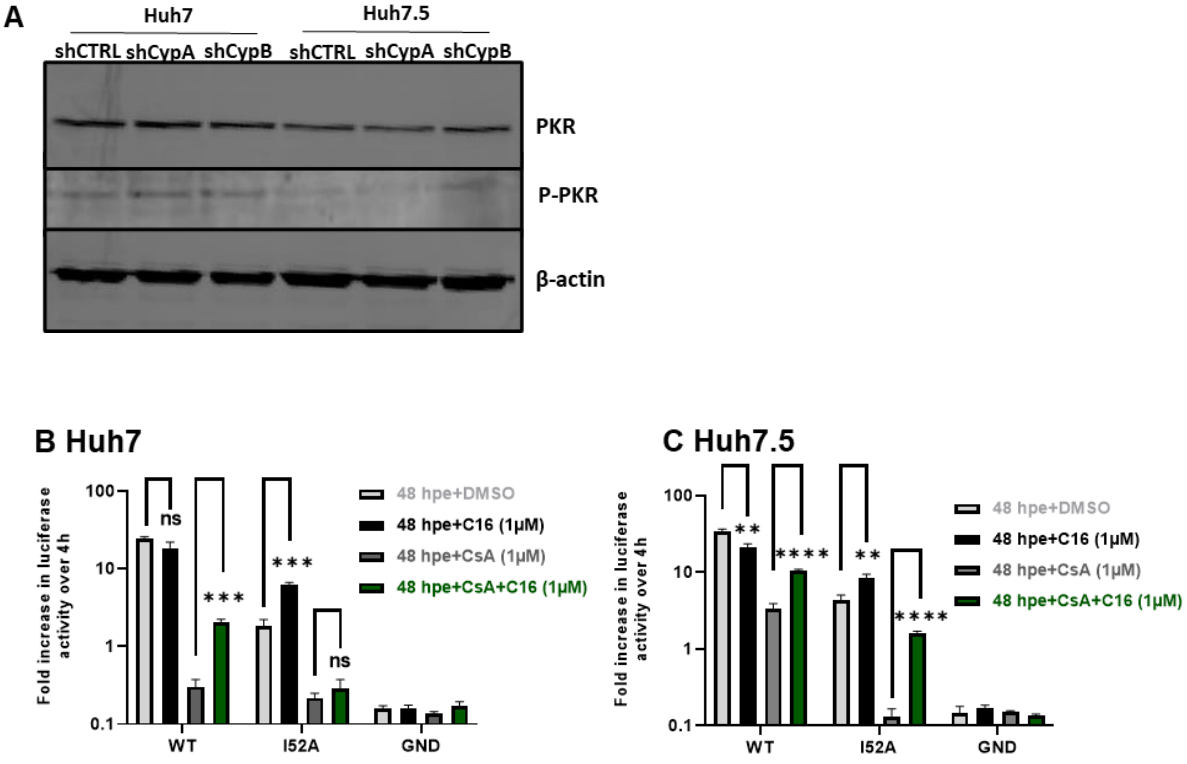

Fig 4.7 PKR inhibitor rescued the attenuated replication ability of WT and I52A resulted from CsA treatment.

(A) Cell lysates were harvested and analysed by western blotting with PKR and phospho-PKR antibodies. mSGR-Luc-JFH1 WT and I52A were electroporated into **(B)** Huh7 and **(C)** Huh7.5 cells, and cells were treated with 1 μM CsA or C16 at 4hpe. Luciferase activity was measured at 48 hpe and the data were normalised with respect to 4 hpe.

Next, I sought to evaluate the role of PKR in HCV replication through interacting with CypA or CypB. We electroporated WT and I52A into Huh7 and Huh7.5 CypA or CypB silenced cell lines. C16 was added after 4hpe. The luciferase data displayed that C16 failed to increase the replication of WT either in Huh7 or Huh7.5 CypA silenced cell lines (Fig 4.8A and 4.8B). However, the replication of I52A in Huh7.5 CypA silenced cell lines showed a slight recovery in the inhibition of PKR (Fig 4.8B). Moreover, C16 had a more significant effect on I52A replication in CypB silenced cell lines (Fig 4.8C and 4.8D).

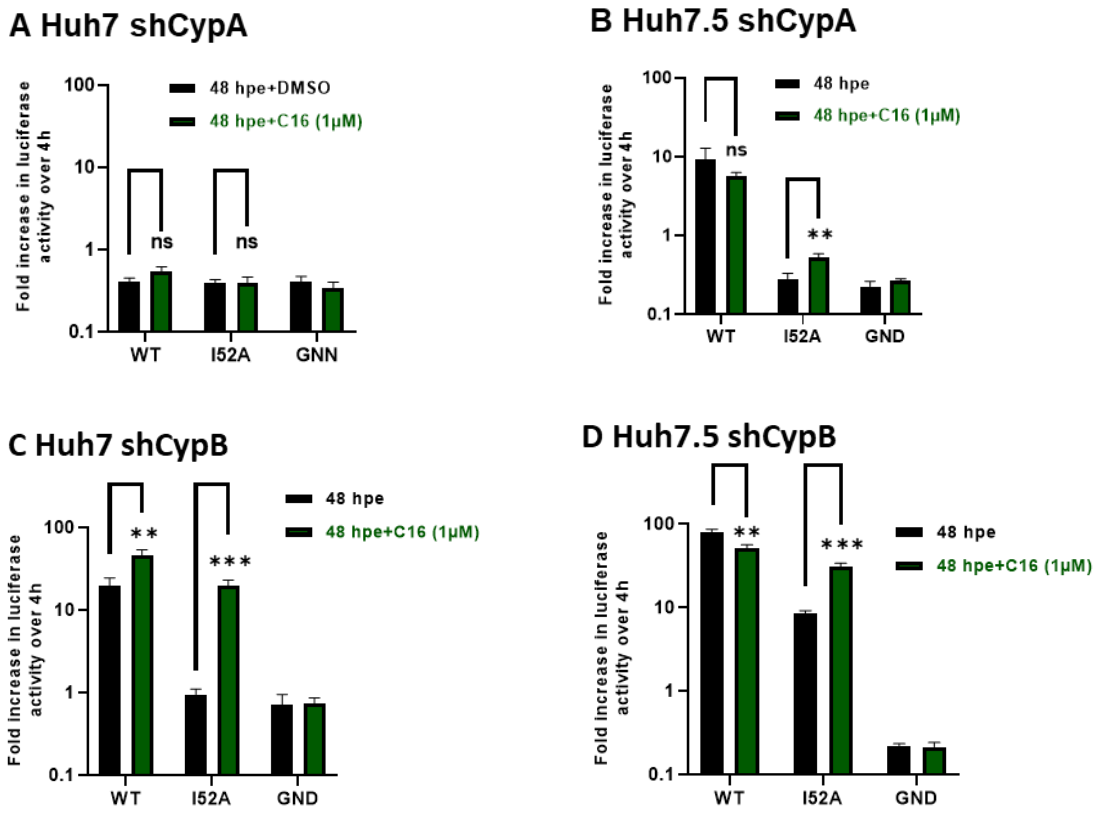

Fig 4.8 PKR modulated JFH1 replication via CypB but not CypA.

mSGR-Luc-JFH1 WT and I52A were electroporated into **(A)** Huh7 CypA silenced cell line, **(B)** Huh7.5 CypA silenced cell line, **(C)** Huh7 CypB silenced cell line and **(D)** Huh7.5 CypB silenced cell line. 1μM C16 was treated with cells at 4hpe. Luciferase activity was measured at 48 hpe and the data were normalised with respect to 4 hpe.

In addition, PKR silenced cell lines were also constructed in Huh7 and Huh7.5 cells (Fig 4.9A), and then treated with CsA or C16 at 4hpe. The loss of PKR in both cells did not affect the phenotype of WT and I52A at the treatment of CsA (Fig 4.9B and 4.9C). To avoid the re-expression of remained PKR during the HCV genome replication, C16 was also added to the cells to inhibit the PKR production. C16 treatment did not had much effect to rescue the replication of WT and I52A with CsA treatment in Huh7 PKR silenced cell lines (Fig 4.9B), whereas, C16 was able to significant restore the replication of WT and I52A with CsA treatment in Huh7.5 PKR silenced cell lines (Fig 4.9C). The reduction of WT replication and recovery of I52A replication with C16 treatment was consistent with the data showed in Fig 4.7. This might indicate a potential HCV evasion mechanism for the PKR-induced antiviral pathway. I hypothesised that HCV can bind and exploit PKR as a proviral factor to enhance viral replication, therefore the loss of PKR would result in the decrease of HCV replication (Fig 4.9C). However, mutations (such as mutants in NS5A DI) which disrupts the interaction between HCV and PKR might restore PKR as an antiviral factor to inhibit HCV replication. Therefore, the absence of PKR induced the increase of replication in I52A.

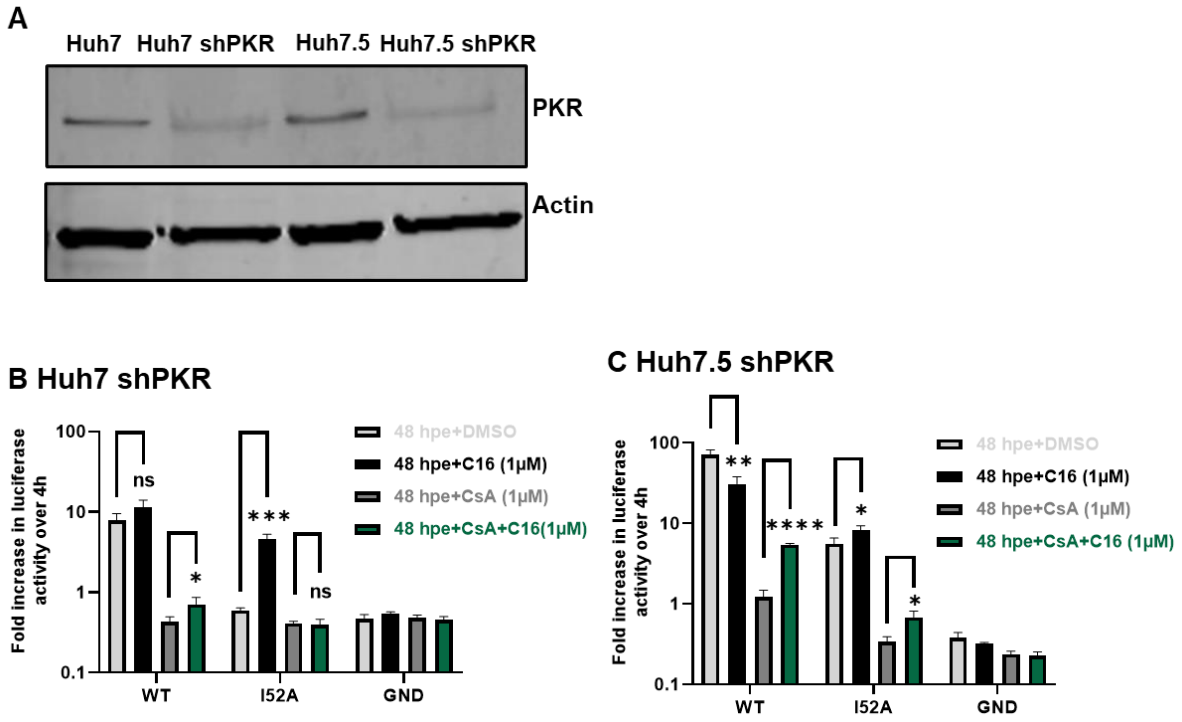

Fig. 4.9 PKR had no effect on replication phenotype of JFH1 inhibited by CsA.

(A) PKR expression was detected in silenced Huh7 and Huh7.5 cells by western blot. *In vitro* transcribed mSGR-Luc-JFH1 WT and I52A RNAs were electroporated into **(B)** Huh7 PKR silenced and **(C)** Huh7.5 PKR silenced cell lines. Cells were treated with 1 μM CsA or C16 at 4 hpe. Luciferase activity was measured at 48 hpe and the data were normalised with respect to 4 hpe.

Collectively, C16 treatment did not recover I52A replication in the absence of CypA, indicating that CypA was absolutely essential for HCV replication through NS5A domain I. However, C16 treatment efficiently enhanced I52A replication in the absence of CypB, confirming that CypB but not CypA inhibited the activity of PKR to promote I52A replication.

Since JFH1 showed different replication ability in the absence of CypA in Huh7 and Huh7.5 cells (RIG-I deficient cells), I considered that RIG-I was also involved in the replication modulation. To further understand whether RIG-I participated into CypA-

modulated HCV replication in Huh7 cells, RIG-I silenced cell line was generated in Huh7 cells using CRISPR/Cas9 (Fig 4.10A). WT, I52A and GND were electroporated into this cell line and CsA or C16 treatment was introduced to cells at 4hpe, the luciferase values were measured at 48hpe. Surprisingly, the absence of RIG-I did not affect the replication of WT and I52A (Fig 4.10B), which showed the same phenotypes as the Huh7 cells (Fig 3.2). Furthermore, WT and I52A showed lethal phenotypes to CsA treatment in the Huh7 RIG-I silenced cell line (Fig 4.10B). Additionally, EGFP-RIG-I was also transfected into Huh7.5 cells to overexpress RIG-I (Fig 4.10C). Similarly, the transfection of RIG-I had no effect on phenotypes and CsA potency (Fig 4.10D). These results indicated that RIG-I was not involved in modulating HCV replication inhibited by CsA, which were consistent with the previous report (Binder et al., 2007). Notably, the C16 treatment also can rescue the failure of I52A replication in Huh7.5 RIG-I silenced cell line, which is consistent with the data in Fig 4.7C. The same pattern of C16 treatment results of WT or I52A in 4.7, 4.9 and 4.10 further demonstrated the proviral role of PKR in HCV replication. When HCV replication was affected by NS5A DI mutants, the antiviral role of PKR can be restored.

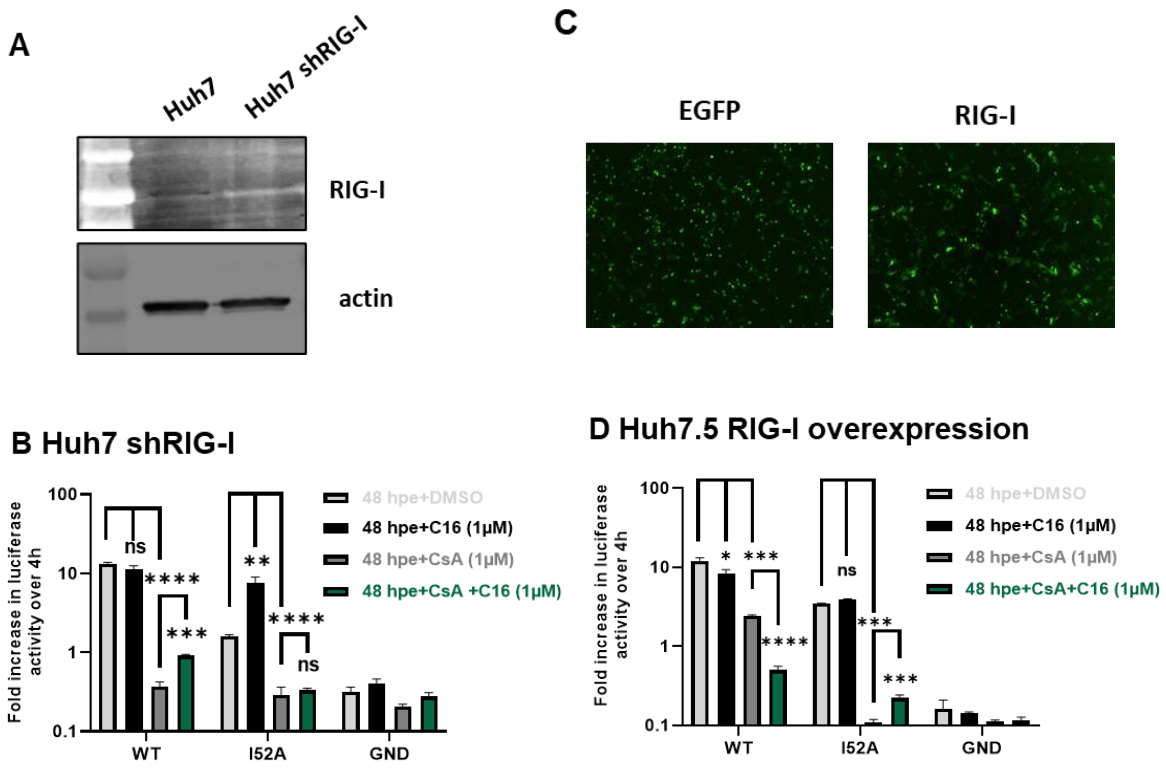

Fig 4.10 RIG-I did not affect the replication of JFH1 WT and I52A in the treatment of CsA.

(A) RIG-I expression was detected in silenced Huh7 cells by western blot. **(B)** *In vitro* transcribed mSGR-Luc-JFH1 WT and I52A RNAs were electroporated into Huh7 RIG-I silenced cell line. Cells were treated with 1 μM CsA or C16 at 4hpe. Luciferase activity was measured at 48 hpe. **(C)** RIG-I was overexpressed through transfecting EGFP-RIG-I plasmid into Huh7.5 cells. **(D)** *In vitro* transcribed mSGR-Luc-JFH1 WT and I52A RNAs were electroporated into Huh7.5 cells which overexpressed with RIG-I. Cells were treated with 1μM CsA or C16 at 4hpe. Luciferase activity was measured at 48 hpe and the data were normalised with respect to 4 hpe.

4.2.5 The binding of CypA and NS5A DI inhibits activation of NF-κB to promote HCV replication

It has been reported that the nuclear accumulation and activation of NF-κB is tightly associated with intracellular CypA (Sun et al., 2014). Translocation of the p65 subunit

from the cytoplasm to the nucleus indicates the activation of NF-κB. To understand whether NF-κB modulated HCV genome replication through the interaction between CypA and JFH1 NS5A DI, we analysed electroporated cells with WT and I52A in Huh7.5 and Huh7.5 CypA silenced cell lines by immunofluorescence with an antibody specific to p65 (Fig4.11 A-D). As expected, treatment with the NF-κB activator TNFα resulted in efficient nuclear translocation of p65, whereas no such translocation was observed in mock-infected cells in both cell lines (Fig 4.11B and 4.11D). GND was also considered to be a negative control and showed no translocations as mock. Notably, in Huh7.5 shCTRL cell line, HCV did not induce the P65 translation, while I52A completely activate NF-κB which comparable to TNF-α treated cells (Fig 4.11A). However, both WT and I52A induced NF-κB activation in Huh7.5 CypA silenced cell line (Fig 4.11C). In addition, the quantification results for mean fluorescence intensity of P65 in nucleus showed that the high percentage of fluorescence intensity were detected for I52A in both cell lines, while the WT only showed high fluorescence intensity in Huh7.5 CypA silenced cell line (Fig 4.11E). Although NS5A cannot be detected due to the disruption of replication in I52A under CypA downregulation (Fig 11C), all cells in I52A can be detected with the same P65 translocation as TNF- α treated cells (Fig 11D). The percentage of nuclear fluorescence that co-localised with P65 also displayed the same trend (Fig 4.11F).

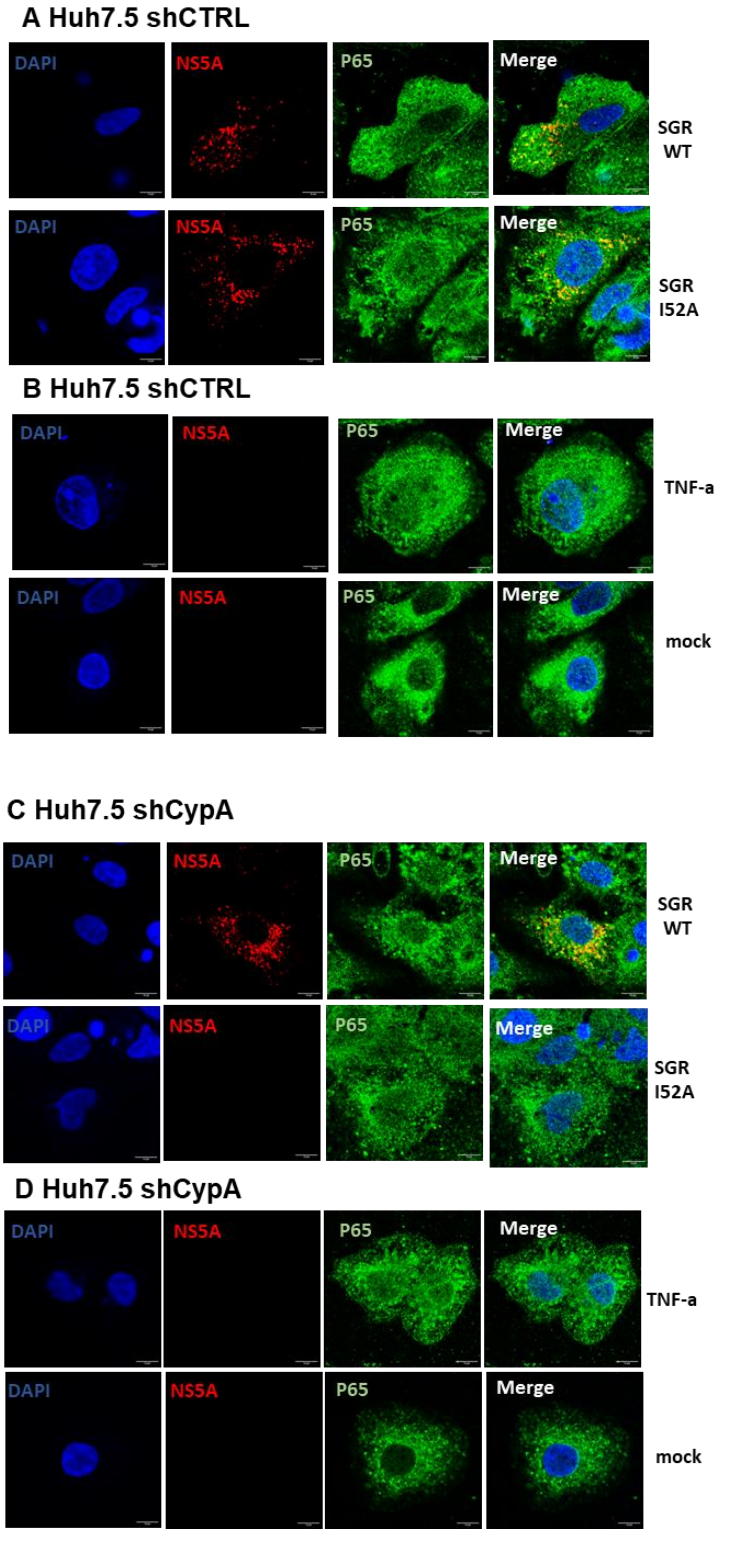
A Huh7.5 shCTRL
DAPI
NS5A
P65
Merge
SGR WT
SGR I52A
B Huh7.5 shCTRL
TNF-a
mock
C Huh7.5 shCypA
D Huh7.5 shCypA

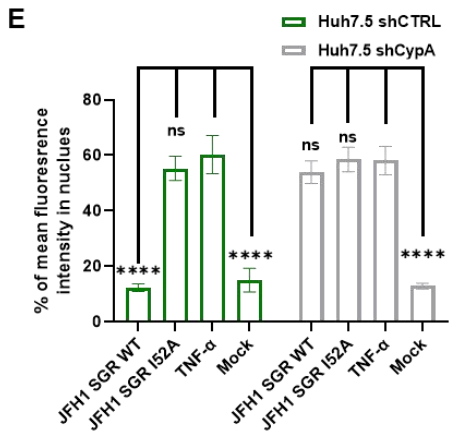
E
Huh7.5 shCTRL
Huh7.5 shCypA
% of mean fluoresrence intensity in nuclues
ns
****
JFH1 SGR WT
JFH1 SGR I52A
TNF-α
Mock

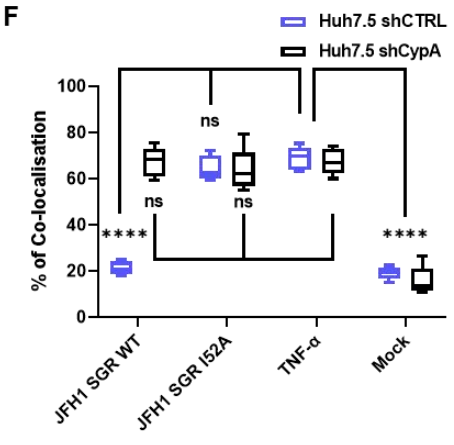
F
Huh7.5 shCTRL
Huh7.5 shCypA
% of Co-localisation
ns
****
JFH1 SGR WT
JFH1 SGR I52A
TNF-α
Mock

Fig 4.11 The interaction between CypA and NS5A DI modulated NF-κB pathway in HCV genome replication.

(A) Huh7.5 control cell line and **(C)** Huh7.5 CypA silenced cell line were electroporated with mSGR-luc-JFH1 WT and I52A RNAs. At 72 hpe, cells were fixed and stained with mouse anti-P65 (green), sheep anti-NS5A (red) and DAPI**. (B and D)** As a positive control to activate the NF-κB pathway uninfected Huh7.5 cells were treated with TNF-α for 24h. Mock: uninfected Huh7.5 cells. **(E)** The quantification of P65 mean fluorescence intensity (MFI) proportion in nucleus to MFI of whole Huh7.5 control cell line (green) and whole Huh7.5 CypA silenced cell line (grey) were calculated using Fiji. **(F)** Quantification of the percentage of DAPI colocalised with P65 in Huh7.5 control cell line (blue) and Huh7.5 CypA silenced cell line (black). Co-localisation was analysed in 5 cells using Fiji.

Together, the inhibition of NF-κB activation can only be detected in Huh7.5 shCTRL cells, indicating that the interaction between CypA and NS5A DI was able to inhibit NF-κB activation. In contrast, the loss of the interaction completely induced NF-κB activation, which resulted in the defective phenotype of replication in the absence of CypA.

4.2.6 HCV assembly is absolutely dependent on CypA but not CypB

We next evaluated the role of CypA in HCV assembly and production. WT and I52A in mJFH1 infectious virus were electroporated in Huh7.5 cells, and the extracellular virus as applied to Huh7.5 shCTRL, CypA and CypB silenced cell lines. Both WT and I52A were able to produce virus in Huh7.5 shCTRL cell lines, while neither WT nor I52A produced virus in the absence of CypA (Fig 4.12A). Interestingly, although virus production of WT and I52A were reduced in the absence of CypB, the virus titre were significantly higher than GND. This suggest that CypA, but not CypB affected the HCV assembly and production. We also evaluated the virus titre in Huh7.5 cells which was

infected with the extracellular virus harvested from electroporated Huh7.5 CypA and CypB silenced cell lines. As shown in Fig 4.12B and 4.12C, CypA absolutely disrupt the virus production, however, the productions of WT and I52A were not affected in the absence of CypB. These results were consistent with the virus production in Fig 4.12A.

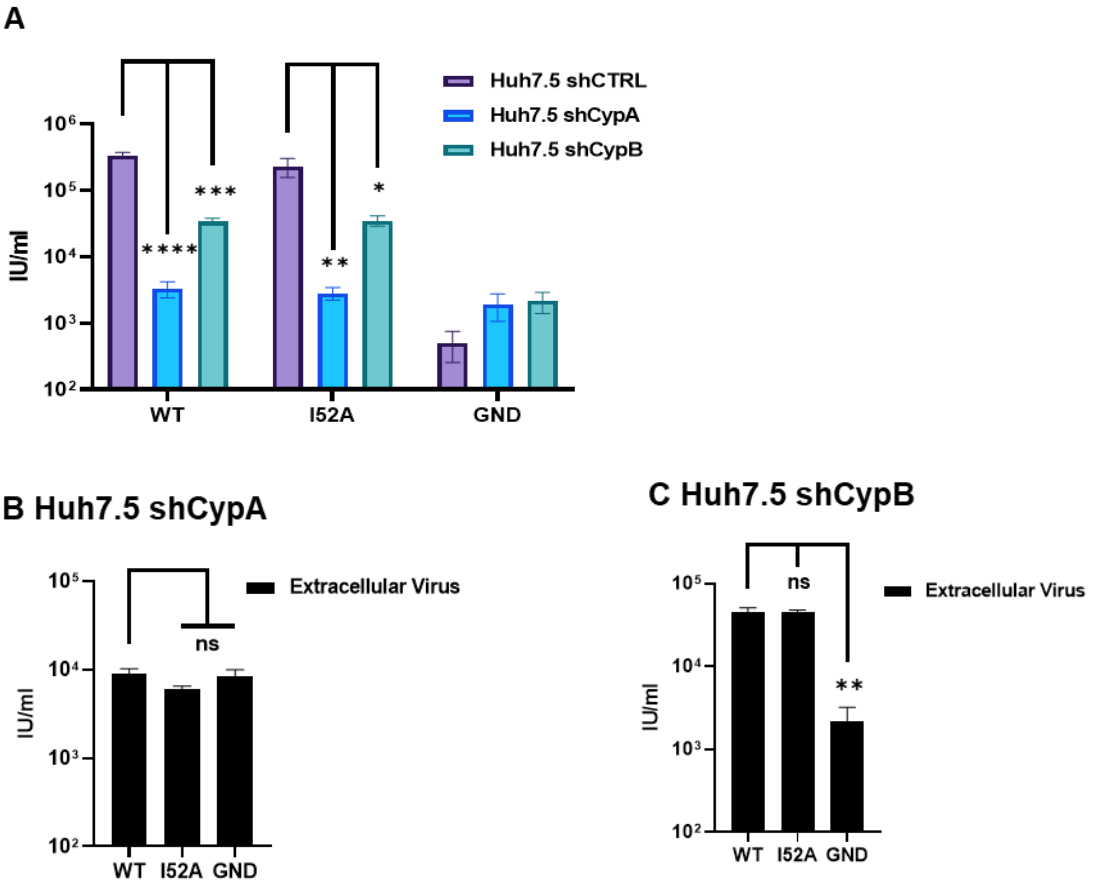

Fig 4.12 JFH1 virus assembly phenotype in different Huh7.5 silenced cell lines.

(A) Huh7.5 cells were electroporated with mJFH1 WT and I52A RNAs as described, together with an NS5B GND mutant as negative control. Extracellular virus harvested at 72 hpe was titrated in Huh7.5 control, Huh7.5 CypA silenced and CypB silenced cell lines and quantified using the IncuCyte S3. **(B)** Huh7.5 CypA silenced and **(C)** CypB silenced cell line were electroporated with mJFH1 WT and I52A RNAs as described. Extracellular virus were harvested at 72 hpe and was titrated in Huh7.5 control cell line and quantified using the IncuCyte S3.

To further understand the effect of the interaction between NS5A DI and CypA in HCV assembly, we also evaluated the NF-κB activation in mJFH1 WT and I52A electroporated Huh7.5 shCTRL and CypA silenced cell lines. Surprisingly, the P65 translocation was not detected in both WT and I52A in Huh7.5 shCTRL cell line (Fig 4.13A). However, in Huh7.5 CypA silenced cell line, only I52A can activate NF-κB. WT was unable to induce P65 translocation to nucleus even though WT cannot produce virus in the lack of CypA (Fig 4.13B). The quantification of the mean fluorescence intensity in nucleus of P65 and the percentage of nucleus fluorescence that co-localised with P65 also observed the same results (Fig 4.13C and 4.13D).

These analysis revealed that CypA but not CypB was absolutely required in the HCV assembly. Additionally, the interaction between CypA and NS5A DI did not involve in the HCV production. However, the loss of both CypA and NS5A DI completely activated NF-κB pathway.

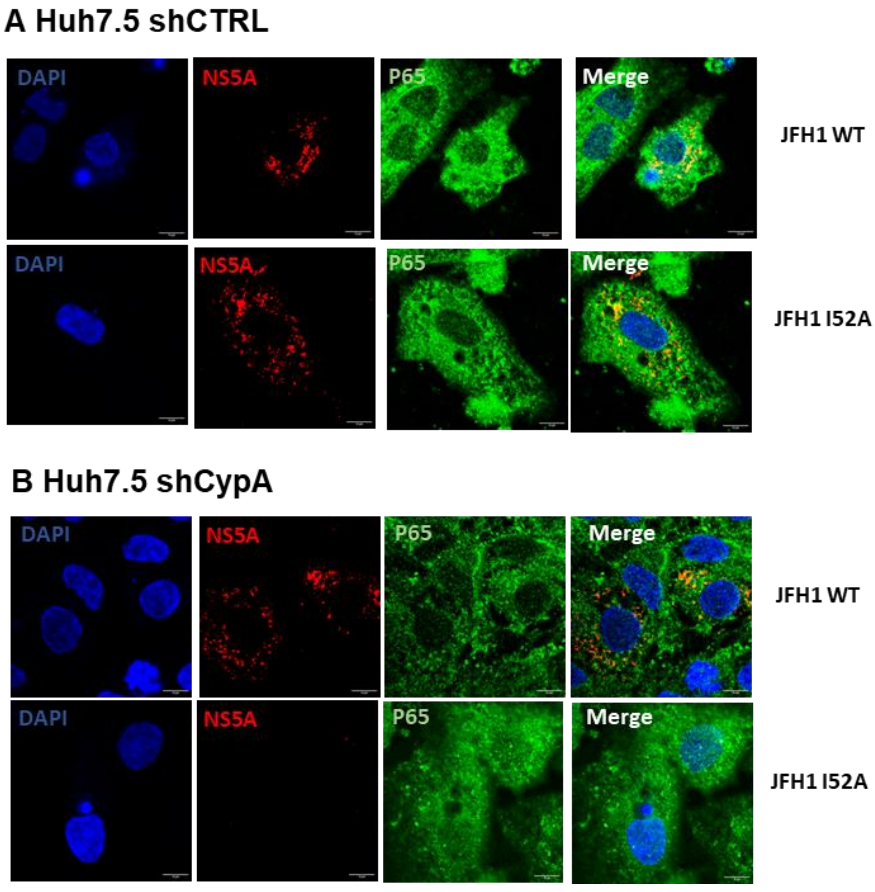

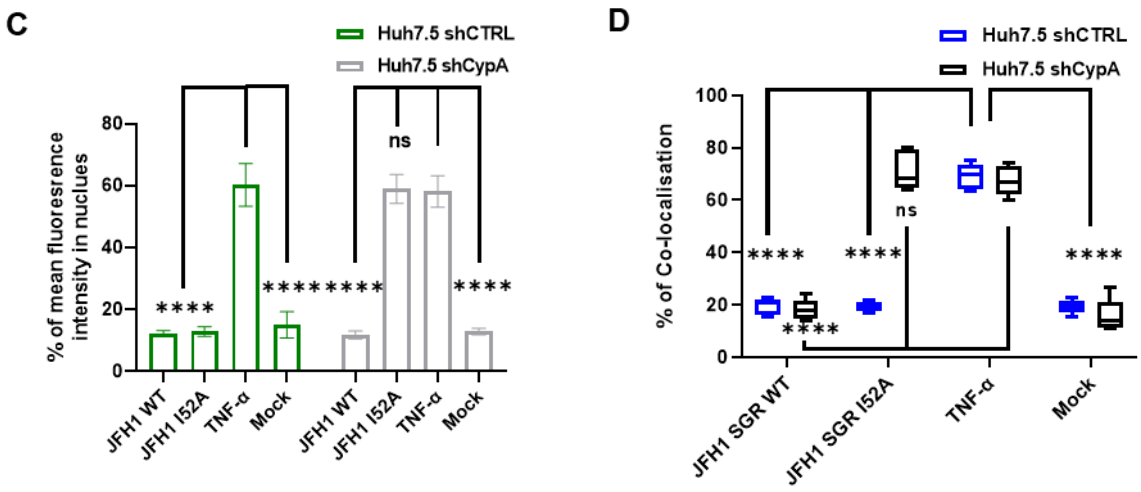

Fig 4.13 NF-κB activation was not affected by the interaction of CypA and NS5A DI during HCV assembly.

(A) Huh7.5 control cell line and **(B)** Huh7.5 CypA silenced cell line were electroporated with mJFH1 WT and I52A RNAs. At 72 hpe, cells were fixed and stained with mouse anti-P65 (green), sheep anti-NS5A (red) and DAPI. As a positive control to activate the NF-κB pathway uninfected Huh7.5 cells were treated with TNF-α for 24h. Mock: uninfected Huh7.5 cells **(Fig 4.12 B and D). (C)** The quantification of P65 mean fluorescence intensity (MFI) proportion in nucleus to MFI of whole Huh7.5 control cell line (green) and whole Huh7.5 CypA silenced cell line (grey) were calculated using Fiji. **(D)** Quantification of the percentage of DAPI colocalized with P65 in Huh7.5 control cell line (blue) and Huh7.5 CypA silenced cell line (black). Co-localisation was analyzed in 5 cells using Fiji.

4.2.7 The replication of SGR-Luc-DBN3a is absolutely dependent on CypA.

To further analyse the replication phenotypes in DBN3a replicon, the same experiments were performed in Huh7 and Huh7.5 CypA silenced cell lines with DBN3a NS5A DI mutants. Intriguingly, silencing of CypA absolutely disrupted the replication of both DBN3a DI WT and mutants, which were indistinguishable with GNN (Fig 4.14A and 4.14B). This suggested that DBN3a replication was absolutely dependent on CypA, whereas the requirement of NS5A DI in DBN3a replication cannot be confirmed.

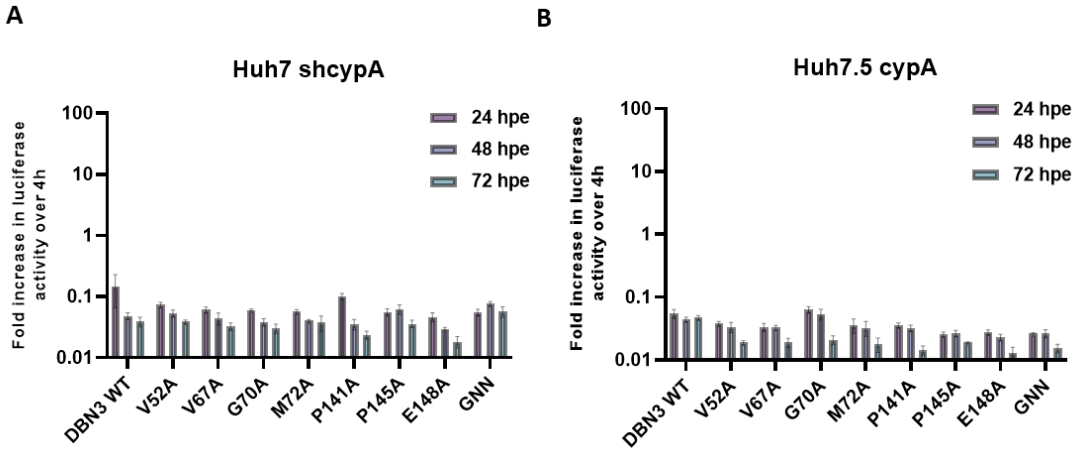

Fig 4.14 Virus replication phenotypes of DBN3a in the absence of CypA.

In vitro transcribed SGR-Luc-DBN3a RNAs containing the indicated mutations were electroporated into **(A)** Huh7 CypA silenced and **(B)** Huh7.5 CypA silenced cell lines. Luciferase activity was measured at 4, 24, 48 and 72 hpe and the data were normalised with respect to 4 hpe.

These mutants in DBN3a NS5A DI were also electroporated into CypB silenced cell lines. As shown in Fig 4.15A and 4.15B, WT and mutants can replicate at WT level in the absence of CypB in both cell lines, which is comparable to the replication in normal Huh7 and Huh7.5 cell lines (Fig 3.7 and Fig 3.8). This suggested that DBN3a replication was independent on CypB and was not associated with NS5A DI.

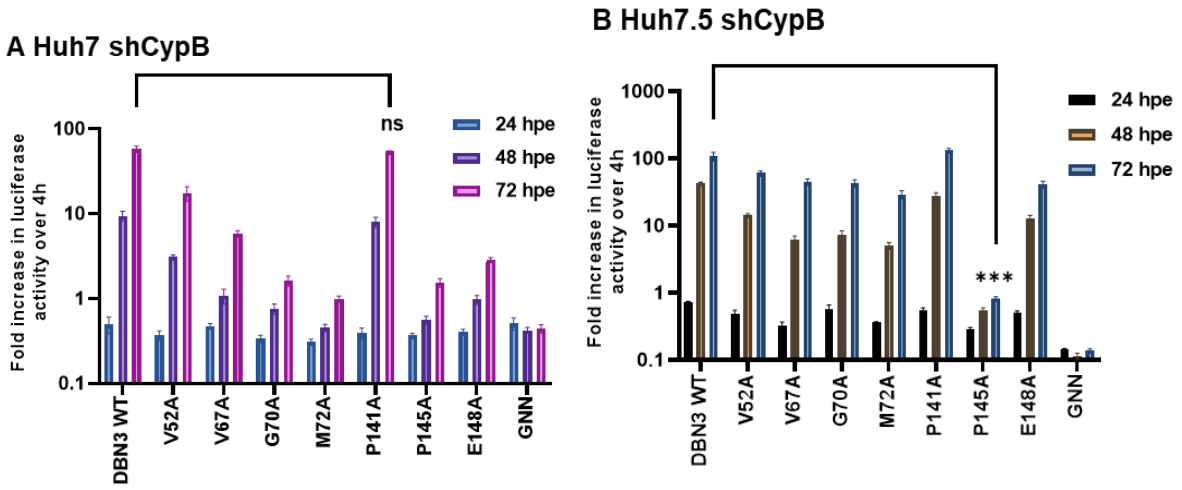

Fig 4.15 Virus replication phenotypes of DBN3 in the loss of CypB.

In vitro transcribed SGR-Luc-DBN3a RNAs containing the indicated mutations were electroporated into **(A)** Huh7 CypB silenced and **(B)** Huh7.5 CypB silenced cell lines. Luciferase activity was measured at 4, 24, 48 and 72 hpe and the data were normalised with respect to 4 hpe.

To assessed whether the new phenotypes in these cell lines could be due to the puromycin treatment rather than a lack of replicative ability, we electroporated these observed mutants of DBN3a into Huh7 and Huh7.5 shCTRL cell lines (Fig 4.16A and 4.16B), which is a non-targeting guide RNA silenced cell lines constructed in the same manner as those silencing CypA. As expected, the phenotype was consistent with the results in Huh7 and Huh7.5 cells (Fig 3.7 and 3.8).

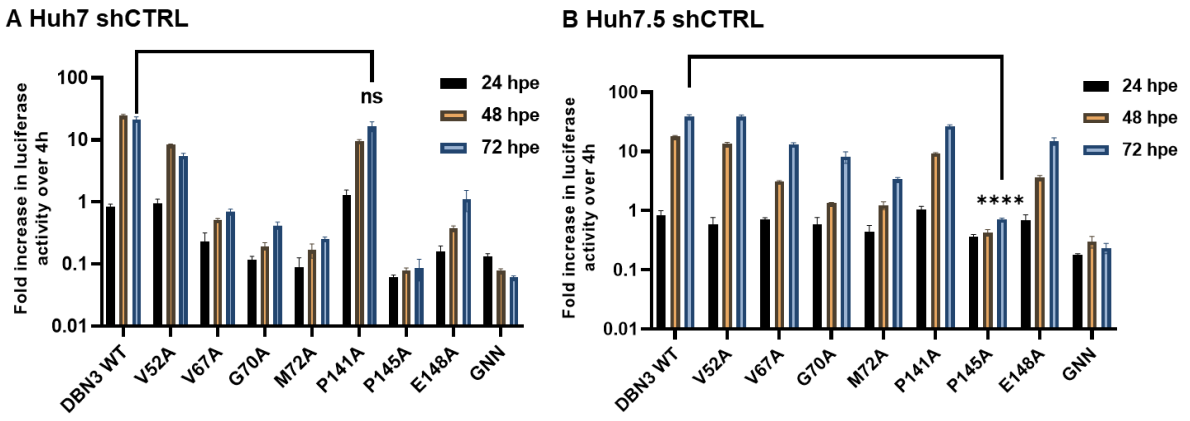

Fig 4.16 DBN3 genome replication in Huh7 and Huh7.5 control cell lines.

In vitro transcribed SGR-Luc-DBN3a RNAs containing the indicated mutations were electroporated into **(A)** Huh7 control cell line and **(B)** Huh7.5 control cell line. Luciferase activity was measured at 4, 24, 48 and 72 hpe and the data were normalised with respect to 4 hpe.

4.3 Discussion

This study further demonstrated the replication mechanism for partially defective mutants in JFH1 NS5A DI (I52A, G70A, M72A, P141A and E148A), and identified the novel interaction between JFH1 NS5A DI and CypA. Furthermore, the interaction tightly regulated the translocation of NF-kB subunit P65 in the nucleus, indicating that the activation of NF-kB was also involved in modulating JFH1 replication through NS5A DI and CypA (Fig 4.17).

CypA has been demonstrated to interact with NS5A to enhance HCV replication (Watashi et al., 2003). However, previous research only focused on this interaction in NS5A DII (Foster et al., 2011, Ross-Thriepland et al., 2013). As an important part of NS5A, NS5A DI was also considered to participate in HCV replication. Therefore, I hypothesised that NS5A DI may also be associated with CypA. The partially defective mutants were more sensitive with the treatment of CsA compared to WT, which further

supported the hypothesis (Fig 3.5). The replication results of JFH1 WT and partially defective mutants in Huh7 and Huh7.5 CypA silenced cell lines were intriguing: attenuated replication ability of JFH1 WT caused by the loss of CypA was recovered in Huh7.5 (RIG-I deficient cells), while the partially defective mutants showed consistent disruption of replication (Fig 4.1). This suggested that the deficiency of some IFN pathways induced by RIG-I might completely allow JFH1 replication without CypA preservation. However, the replication of partially defective mutants was absolutely dependent on CypA, even in Huh7.5 cells. Moreover, the interaction between NS5A DI and CypA was validated using pulldown assay (Fig 4.4). Combining all results, CypA was hypothesised to interact with NS5A DI to facilitate the HCV evasion of antiviral pathway.

We also found out the PKR was not the target of CypA through binding to NS5A DI. This conclusion is contradictory to the previous studies which indicated that CypA modulated the PKR pathway (Colpitts et al., 2020, Daito et al., 2014). Despite the fact that many evidence of Cyp inhibitor they used showed that CypA modulated the PKR-mediated antiviral pathway, CypB should not be ignored as it also contains PPIase activity which can be inhibited by Cyp inhibitors. Although the effect of the loss of CypB on HCV genome replication was less potent, it was shown to play a role in inhibiting PKR (Fig 4.8). The mechanism of the Cyp family antagonising the antiviral pathway to enhance JFH1 replication through NS5A DI is complicated, may be associated with the interaction between CypA and CypB (Fig 4.17).

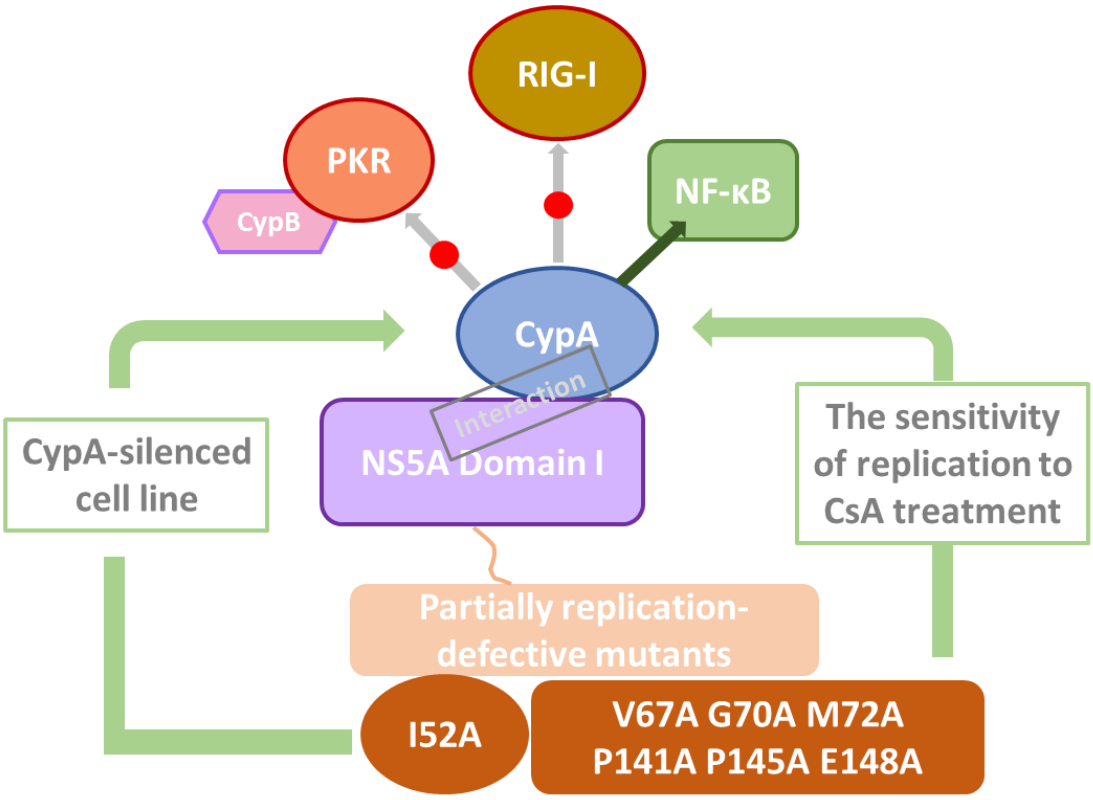

Fig 4.17 The mechanism for the regulation of CypA in HCV genome replication through NS5A DI.

Five mutants (I52A, G70A, M72A, P141A and E148A) in JFH1 NS5A DI showed partially reduced replication due to the loss of interaction with CypA. The interaction between CypA and NS5A DI inhibited NF-κB pathway to further promote HCV replication. PKR and RIG-I did not affect the CypA-modulated HCV genome replication. CypB might be involved in the inhibition of PKR activation.

The interaction between CypA and JFH1 NS5A DI was critical for inhibiting the NF-kB pathway, the prevention cannot be maintained once the interaction was disrupted (Fig 4.11). CypA might complete protect NS5A from NF-kB activation through the interaction with NS5A DI (Fig 4.18A), while the I52A mutant in NS5A DI resulted in the exposure of NS5A and further activated NF-kB to suppress the HCV genome replication (Fig 4.18B). Although NF-kB was activated in the absence of CypA (Fig 4.18C and 4.18D), WT and I52A showed completely different phenotypes in HCV

replication. WT may maintain the replication ability through other intracellular factors to antagonise the activation of NF-kB pathway (Fig 4.18C). However, the partially defective replication of I52A was presumably due to the loss of the protection of other intracellular factors from NF-kB activation (Fig 4.18D). Interestingly, the interaction between CypA and NS5A DI had no effect on JFH1 viral assembly. The lack of both CypA and NS5A DI resulted in the NF-kB activation, indicating viral assembly of JFH1 may require the separate mechanism of CypA or NS5A DI. These results suggested that the interaction between CypA and NS5A DI was only responsible for HCV replication but not viral assembly. To date, limited reports showed the association between CypA and NF-kB in the field of HCV. The modulation for CypA to NF-kB pathway only displayed in cancer (Sun et al., 2014, Sun et al., 2011). This study was the first to reveal that CypA as a regulator to bind with viral protein of HCV to prevent NF-kB pathway.

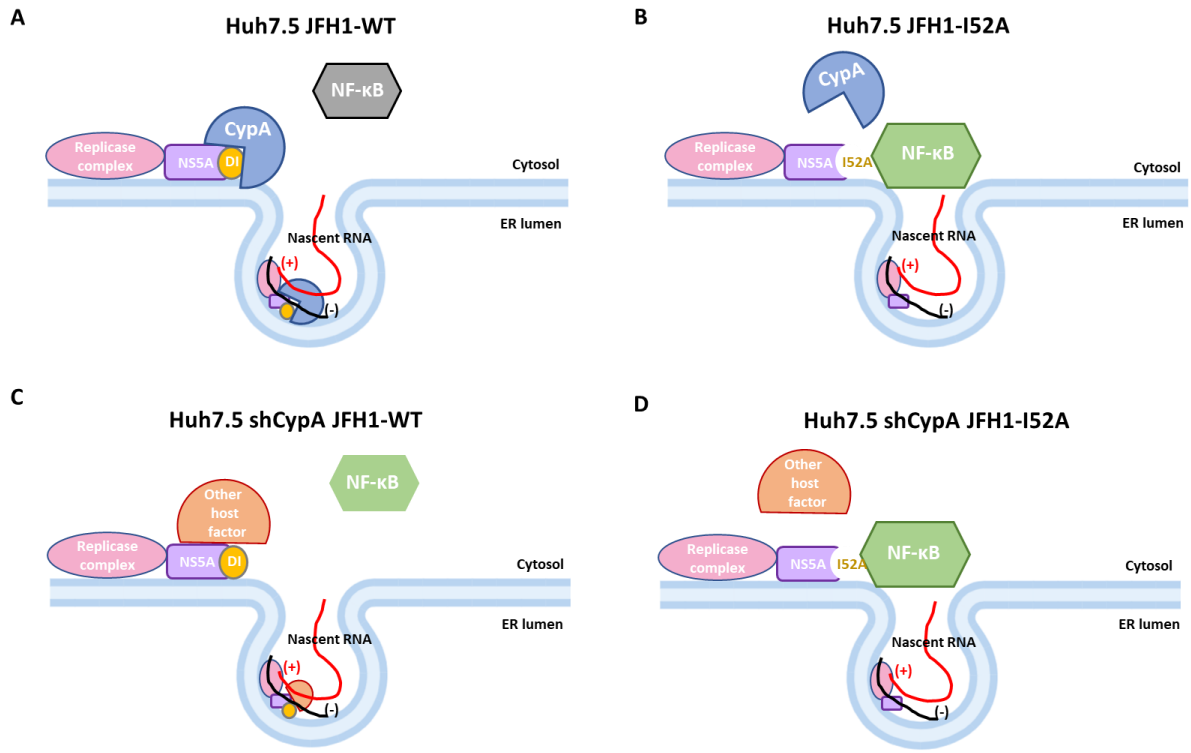

Fig 4.18 working model for the proposed roles of interaction between CypA and NS5A to antagonise NF-kB activity.

The replication of DBN3a showed more dependency on CypA compared to JFH1, and exhibited the same dependence in the deficiency of antiviral pathway (Table 4.1).

JFH1 SGR	Huh7	Huh7.5	Huh7 shCypA	Huh7.5 shCypA	Huh7 shCypB	Huh7.5 shCypB
Partial defect	+	++	-	-	-	+
WT phenotype	++	++	-	++	+	+

DBN3 SGR	Huh7	Huh7.5	Huh7 shCypA	Huh7.5 shCypA	Huh7 shCypB	Huh7.5 shCypB
Partial defect	+	++	-	-	+	++
WT phenotype	++	++	-	-	++	++

Table 4.1 The summary of the phenotype of JFH1 and DBN3a in different silenced cell lines.

"- " absolute disruption of replication ."+"partially defective disruption of replication. "++" WT level replication.

These results were surprising, as DBN3a was considered less responsive and highly resistant to some direct-acting antivirals (DAAs) treatments (Andriulli et al., 2008, Kanwal et al., 2014), whereas the replication showed high sensitivity to CsA treatment (Fig 3.9) and strong dependency on CypA (Fig 4.14). CsA was added to the standard-of-care interferon (IFN) treatment regimen due to the effective treatment for HCV genotype 1b and 2a. These results might suggest that CsA as a novel DAA to treatment DBN3a, while the detailed mechanism needs to be further investigated.

In conclusion, this chapter revealed the novel interaction between JFH1 NS5A DI and CypA. Additionally, this interaction was shown to play an essential role in modulating the NF-kB pathway during genome replication of JFH1. The mechanism of CypA enhancing HCV replication was further explored. Moreover, the different effects of

CypA in DBN3a and JFH1 mutants also showed the diverse functions of NS5A DI in replication of HCV different genotypes.

Chapter 5: Mutagenic analysis of the role of NS5A domain I in HCV assembly

5.1 Introduction

The process of HCV assembly and release is still not very clear. However, an increasing number of reports demonstrated that the release process of viral particles is associated with liver lipid metabolism which are critical for HCV assembly, budding and secretion (Denolly et al., 2019, Targett-Adams et al., 2010).

The current studies of HCV particle production suggested that assembly occurs on the surface of LDs, and was then produced via the secretory pathway associated with the very low density lipoprotein (VLDL) following the envelopment at the ER (Counihan et al., 2011, Herker and Ott, 2011, Popescu and Dubuisson, 2010). The infectious virion is a lipoviroparticle with a lipid composition which always exhibited lower buoyant densities with the higher infectious rate (Bartenschlager et al., 2011). Furthermore, viral structural and nonstructural proteins, as well as several host factors participate in the assembly of infectious HCV particles. Additionally, the assembly of virions occurs at assembly sites proximal to lipid droplets (LDs), which are the storage sites for neutral lipids in cells where core proteins can be accumulated (Miyanari et al., 2007). The accumulation and association between core protein and LDs are required for the formation of infectious virus particles, as the inhibition of their interaction results in assembly disruption (Boulant et al., 2008, Targett-Adams et al., 2008b).

It has been also demonstrated that HCV RNA and replication complex (including NS proteins) are recruited by the core protein to LD-associated membranes, further suggesting that LDs provides a platform to permit the virion formation (Miyanari et al., 2007). Moreover, Core and NS5A protein have been demonstrated to play a critical role in the assembly process. The interaction between the serine residues of NS5A and the core protein prompted their recruitment to LDs (Masaki et al., 2008). Therefore,

based on the results above and the role of NS5A in HCV replication, NS5A has been identified as an essential protein which plays a role in the transition between viral replication and assembly.

Of the three domains of NS5A in HCV life cycle, the effect of NS5A on HCV assembly comes largely from the determinants of domain III. Firstly, the phosphorylation of a C-terminal serine residue in domain III by casein kinase IIα is vital for virion formation, because this modification is more likely to regulate the interaction between Core and NS5A protein (Tellinghuisen et al., 2008a). Additionally, the interaction between NS5A and Core was disrupted when the residues close to the C-terminus were mutated (Appel et al., 2008). Also, it has been reported that domain III encodes determinants which appear to interact with the p7-NS2 complex to regulate the early stage of assembly through protein-protein interaction (Jirasko et al., 2010, Ma et al., 2011, Popescu et al., 2011). It is noteworthy that, the inherent theory that domain I was only essential for RNA replication was challenged in 2018, suggesting NS5A domain I also has a critical role in HCV assembly and release (Yin et al., 2018). Two mutations V67A and P145A in NS5A DI showed partial defect in replication and absolute abrogation of assembly.

As mentioned in chapter 1, the highly conserved NS5A domain I is preceded by a membrane-anchoring amphipathic α-helix and is divided into an N-terminal subdomain IA and a C-terminal subdomain IB due to its specific 3-dimensional structure. The characteristic structures of subdomain IA is a 3-stranded anti-parallel β-sheet (B1-B3) which is proximal to an α-helix. To distinguish this α-helix from the N-terminal membrane-anchoring amphipathic α-helix (H1), it was therefore called H2. These feature elements create a structural scaffold for the zinc coordination site, including 4 absolutely conserved cysteine residues Cys 39, Cys 57, Cys 59, and Cys 80, which

were shown to be indispensable for RNA replication (Tellinghuisen et al., 2004). Subdomain IB is a novel fold that contains 2 anti-parallel β-sheets (B4-B7 and B8-B9) adjacent to several extensive random coil structures. Interestingly, like core protein, NS5A domain I also had a disulfide bond located at the C-terminus of subdomain IB, connecting conserved cysteine residues Cys 142 and Cys 190 (Fig. 4.2). Since the disulfide bond which is maintained by Cys 142 and Cys 190 has been proved dispensable for RNA replication, more research would focus on the role of this structure for viral assembly and release.

During the process of virion production, a number of cellular NS5A-interacting partners have been revealed to play roles in LD functions and viral assembly. Firstly, the interaction between NS5A and apolipoprotein E (ApoE) is required for viral assembly, which can be disrupted by mutating two residues in NS5A domain I, resulting in the attenuated recruitment of other NS proteins to surface of LDs (Benga et al., 2010, Evans et al., 2004). In addition, Annexin A2, a cellular membrane sorting protein, interacts with NS5A domain III to facilitate viral assembly (Backes et al., 2010). Another host factor implicated in HCV assembly is diacylglycerol acyltransferase-1 (DGAT1), an enzyme essential for LD biogenesis. It guides the Core and NS5A proteins trafficking from ER membrane to LDs by enhancing the interaction between core and NS5A. Meanwhile, DGAT1 has also been shown to enhance the recruitment of NS5A to LDs and transport of NS5A and genome RNA to the assembly sites (Camus et al., 2013, Herker et al., 2010). Also, tail interacting protein of 47 kDa (TIP47) has been reported to have the same role as DGAT1 in the assembly sites. A new role of TIP47 revealed that combining LD membranes into the membranous web via interacting with NS5A (Ploen et al., 2013, Vogt et al., 2013).

As described above, HCV particles assemble by budding into the ER. At the early stage, the interaction between Core and NS5A protein is critical for the association with LDs, which transports the genome RNA form the replication sites to assembly sites (Appel et al., 2008, Masaki et al., 2008, Miyanari et al., 2007). Virus particles presumably complete the budding process dependent on the ESCRT pathway and are released from cells by secretory pathway.

In this study, I aim to find out more residues proximal to V67 and P145 of NS5A DI to validate the assembly phenotype. Additionally, alterations in the morphology and distribution of lipid droplets in these phenotype mutants were also detected, revealing the role of NS5A DI mutants in modulating the morphology of LDs. Furthermore, more residues in JFH1 NS5A DI were observed to further demonstrate the mechanism of NS5A DI in virus assembly.

5.2 Results

5.2.1 The role of domain I in virus production

To further demonstrate whether the eleven residues that were dispensable for genome replication played a role in virus assembly and release, alanine substitution of all of these residues were generated in the full-length mJFH-1 infectious clone (Hughes et al., 2009). The assembly phenotype of these mutants was evaluated in Huh7.5 cells as in our hands they more efficiently supported virus genome replication (Fig 3.3). To this end, Huh7.5 cells were electroporated as described previously. The mutant virus titres were analyzed using supernatants harvested from electroporated cells at 72h by immunofluorescence assay. As a positive and negative control, WT and the NS5B GND mutant were analysed using the same methods. As shown in Fig 5.1, nine of

these mutants produced similar levels of released infectious virus to WT, however two of the mutants (C142A and E191A) exhibited a significant defect in virus production.

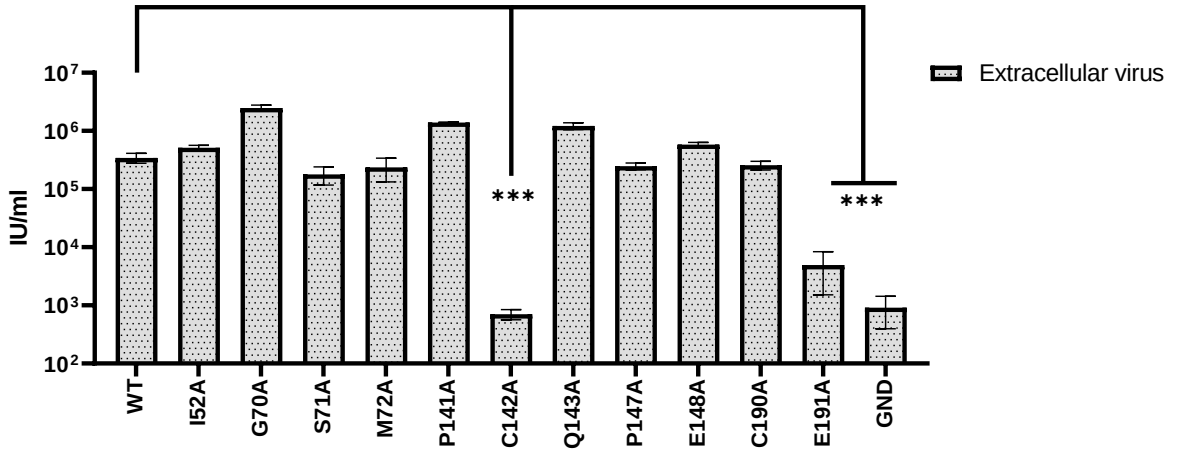

Fig5.1 Virus assembly phenotypes in Huh7.5 cells.

Huh7.5 cells were electroporated with mJFH-1 WT and the DI mutant RNAs as indicated, together with an NS5B GND mutant as negative control. Extracellular virus harvested at 72 hpe was titrated in Huh7.5 cells and quantified using the IncuCyte S3.

These results were surprising, all mutants which showed partially defective phenotype in SGR turned out to show different results in full virus, exhibiting high titre comparable to WT (Fig 5.1). However, C142A and E191A which exhibited high levels of replication in SGR were shown to disrupt the capacity of JFH1 full virus production (Fig 3.3), suggesting they were required for assembly of infectious HCV particles (Fig 5.1).

Therefore, the further investigations were focused on these two mutants. Interestingly, C142 was shown to be connected to C190 by a disulphide bond in the ‘open’ dimer conformation (1ZH1), but not the ‘closed’ dimer (3FQM) of NS5A DI (Fig 5.2). Previous mutagenesis had shown that this disulphide bond is not required for genome replication (Tellinghuisen et al., 2004), consistent with our replication data (Fig 3.2 and 3.3). As C190 is positioned between C142 and E191 on the NS5A DI surface (Fig 5.2),

I included C190A as a control in the detailed analysis of the C142A and E191A phenotypes, as described henceforth.

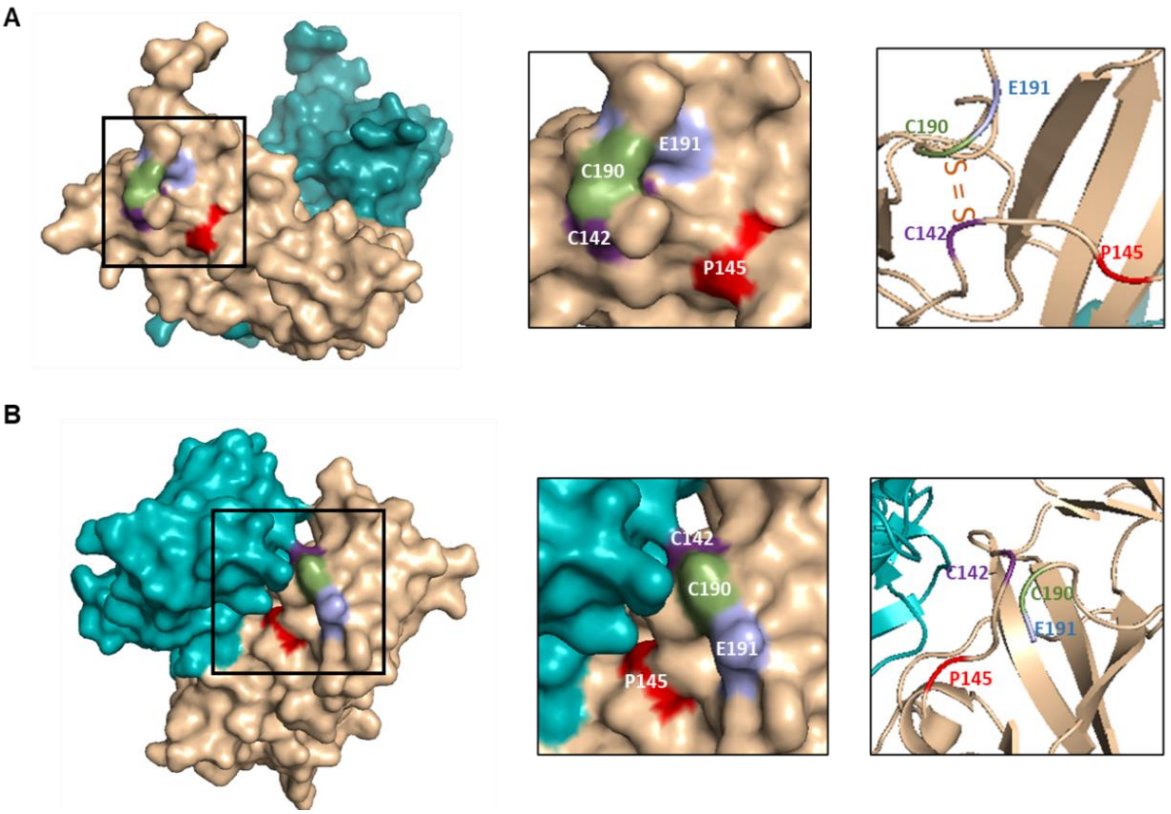

Fig 5.2 Location of mutated residues in DI.

The three surface exposed residues C142A, C190A and E191A proximal to P145 are displayed in two NS5A DI (genotype 1b) structures 1ZH1 **(A)** and 3FQM **(B)**. Images on the right are zoomed into the boxed region shown in both space fill and ribbon format. Note that the disulphide bond formed by C142A and C190A was only observed in 1ZH1.

Virus genome replication was first confirmed for the mutant infectious clones C142A, C190A and E191A both directly by qPT-PCR (Fig 5.3 A), and indirectly by quantifying NS5A positive cells using an IncuCyte S3 cell imager (Stewart et al., 2015) (Fig 5.3 B). Reassuringly, replication of all three mutants was indistinguishable from WT, mirroring the SGR data. Western blot analysis confirmed that NS5A and the structural proteins Core and E2 were expressed at equivalent levels to WT (Fig 5.3 C).

To assess both virus assembly and release I proceeded to determine intracellular and extracellular virus titres (Fig 5.3 D). This analysis revealed that C142 was absolutely required for virus assembly with levels of both intracellular and extracellular virus indistinguishable from the negative control (NS5B GND). In contrast C190A had no effect on WT levels of infectivity, and E191A exhibited an intermediate phenotype with an approximately 2-log reduction compared to WT.

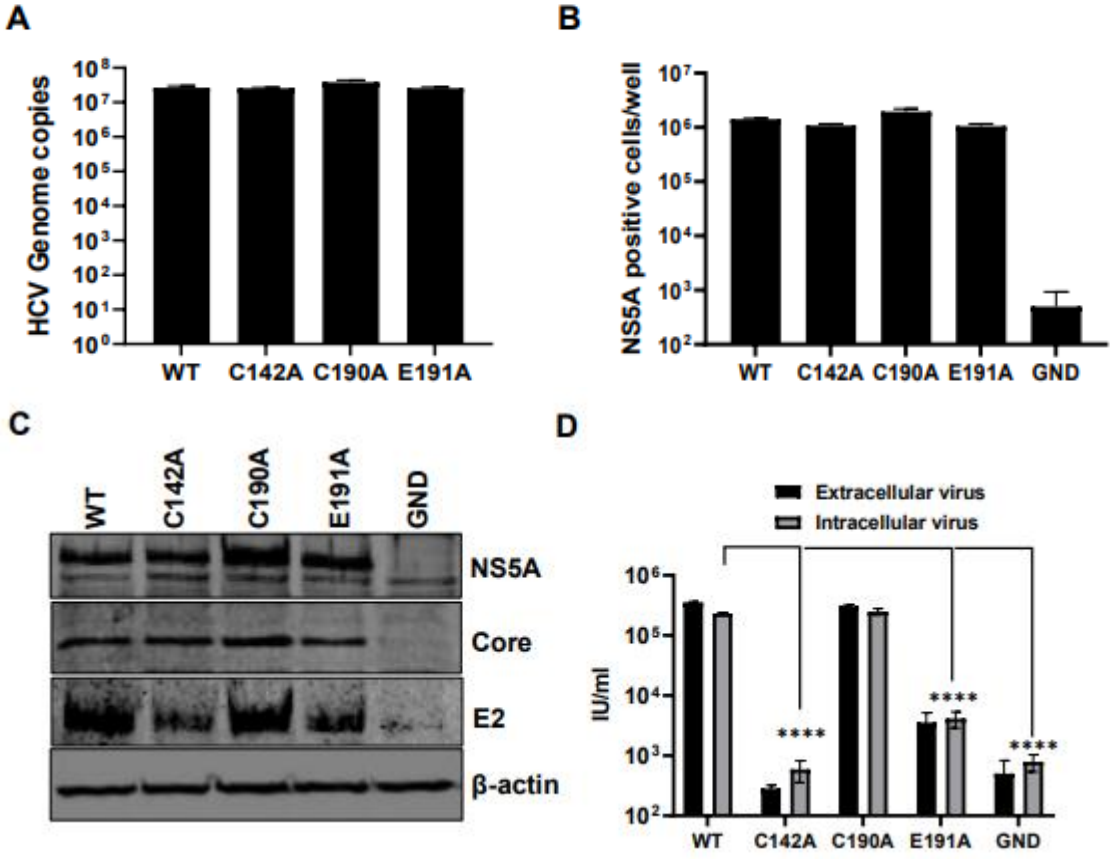

Fig 5.3 Virus assembly phenotypes in Huh7.5 cells.

Huh7.5 cells were electroporated with mJFH-1 WT and DI mutant C142A, C190A and E191A RNAs, together with an NS5B GND mutant as negative control. Virus genome replication was analysed directly by quantification of genome copies in cell lysates using qRT-PCR **(A),** and indirectly by enumerating NS5A positive cells at 72 hpe using the IncuCyte S3 **(B)**. **(C)** Cell lysates were collected at 72 hpe and analysed by western blotting with the indicated antibodies. **(D)** Extra- and intracellular virus harvested at 830 72 hpe were titrated in Huh7.5 cells and quantified using the IncuCyte S3.

I conclude that C142 and E191 play a role in virus assembly, and the fact that C190 is dispensable further suggests that the disulphide bond observed in the 'open' structure of DI is not required for the function of NS5A during genome replication or assembly. As mutants that disrupted virus particle assembly, E191A was different from C142A, exhibiting a partial defect in HCV assembly (Fig 5.3 D). Our previous western blot results suggested that E191A disrupted the structure of NS5A (Fig 3.3). Therefore, I considered that the partial defect in HCV viral titre of the E191A mutant was in part due to the rapid turnover of NS5A.

5.2.2 NS5A DI mutants alter the morphology and distribution of lipid droplets.

To better characterise the role of C142 and E191 on infectious virus production, I used high resolution confocal microscopy (Airyscan) to observe the co-localisation between viral proteins and cellular factors. Key organelles during virus assembly are lipid droplets (LDs), to which both Core (Barba et al., 1997) and NS5A (Shi et al., 2002) are recruited. Since the phenotype of disulphide bond mutants in NS5A were consistent with Core protein (Kushima et al., 2010), I sought to determine the alternation of LD in different phenotype. The disruption of LDs either pharmacologically or genetically (Peyrou et al., 2013) inhibits virus assembly. Previously research in our group showed that in cells infected with the P145A mutant virus, LDs were more abundant and smaller in size compared to WT infected cells (Yin et al., 2018). Following electroporation of three mutants RNA into Huh7.5 cells, the co-localisation between NS5A, Core proteins and LD were demonstrated at 72 hpe using immuno-fluorescence assay. As shown in Fig 5.4, this phenotype was recapitulated for both C142A and E191A: I first observed the most obvious difference was that the size of LDs of C142A and E191A, which were sharply reduced compared to WT and C190A.

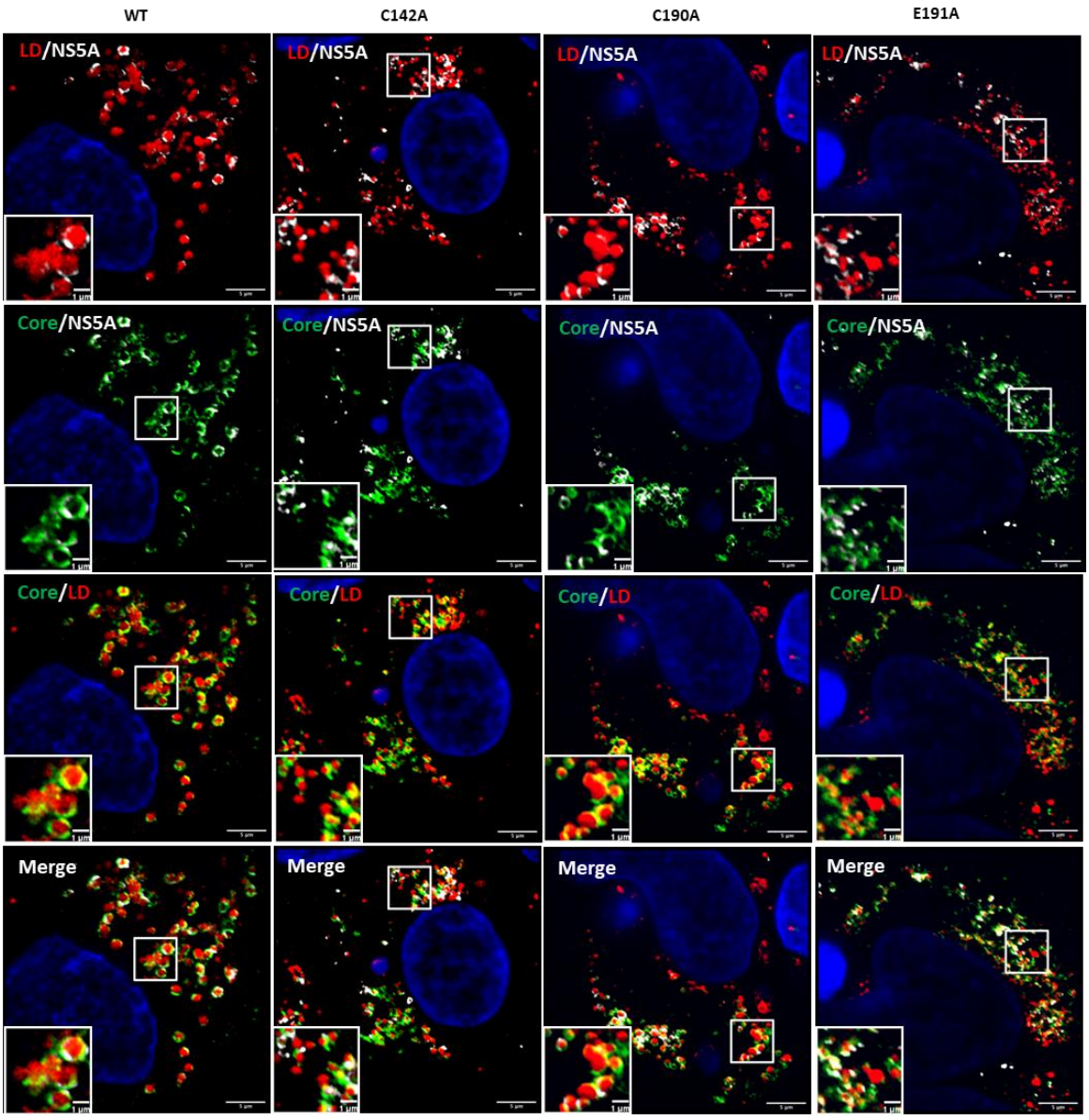

Fig 5.4. Co-localisation between NS5A, Core and LD.

Huh7.5 cells were electroporated with mJFH-1 WT and DI mutant C142A, C190A and E191A RNAs and seeded on to coverslips. At 72 hpe cells were stained with sheep anti-NS5A (white), rabbit anti-Core (green), BODIPY 558/568-C12 (red) and DAPI. Co-localisation was observed using Airyscan microscopy. Representative images are presented. Scale bars are 5 μm and 1 μm (insets).

Moreover, the quantification of LD sizes of different mutants further verified this conclusion: cells infected with WT and C190A exhibited an average of 100 LD with a cross-sectional area of approximately 1.0 μm^2, whereas C142A and E191A

displayed >200 LD with a significantly smaller area (0.2 μm^2), similar to mock-infected cells (Fig 5.5 A).

The differences in both LD size and quantity were consistent with the assembly defective phenotypes of C142A and E191A. I then hypothesized that the difference of productivity between C142A and E191A due to the correlation between viral proteins and LD. To extend this analysis the quantification of the colocalisation of Core and NS5A with LDs were performed. As shown in Fig 5.5 B, the percentage of NS5A co-localising with LDs was significantly decreased for C142A and E191A compared to WT. However, the inverse value (percentage of LD colocalised with NS5A was comparable for all mutants and WT, consistent with the suggestion that the interaction of NS5A with LD was disrupted by C142A and E191A mutations. Similar results were observed for the interaction of LD with Core (Fig 5.5C). Finally, I quantified the colocalisation of Core and NS5A and observed a reduction for C142A and E191A (Fig 5.5D). This reduction was less pronounced for E191A, consistent with the less marked phenotype of this mutant.

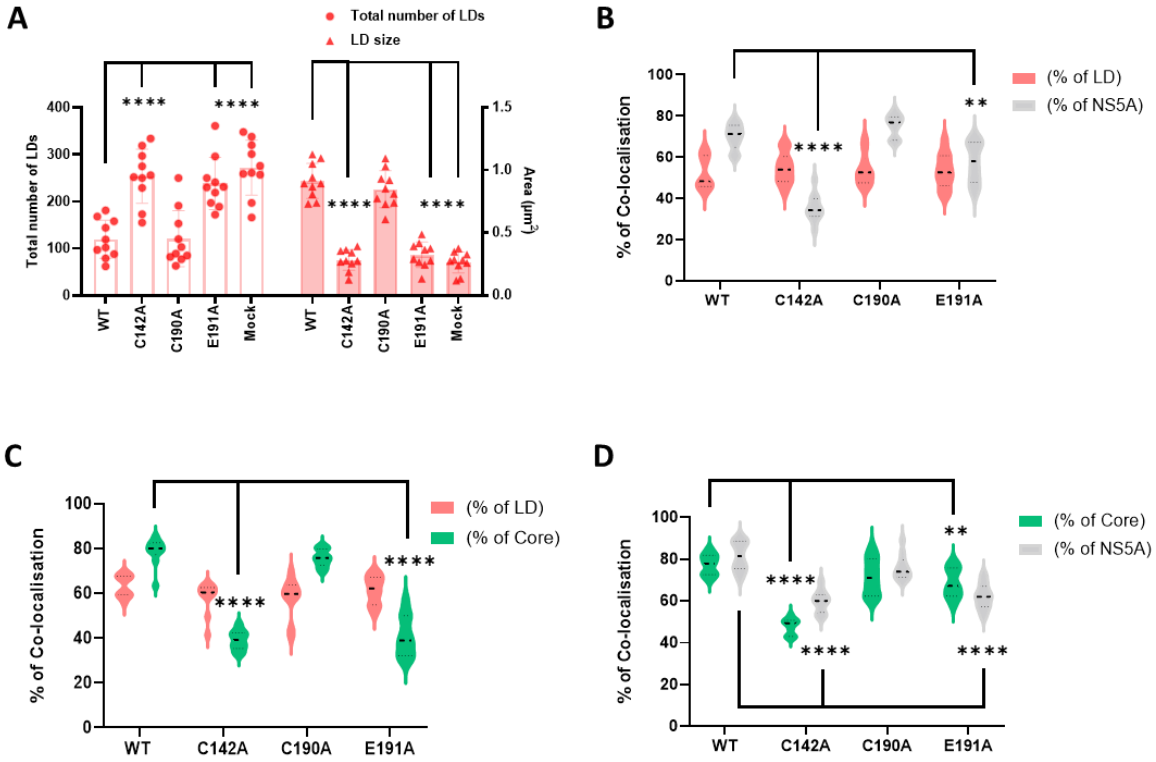

Fig 5.5 Quantification of LD size and co-localisation with NS5A and Core.

(A) LD numbers and size in cells from Fig 5.4 were calculated using Analyze Particles module of Fiji. Mock: uninfected Huh7.5 cells. **(B)** Quantification of the percentage of LD colocalized with NS5A (red), and NS5A colocalized with LD (grey). **(C)** Quantification of the percentage of LDs colocalized with Core (red), and Core colocalized with LD (green). **(D)** Quantification of the percentage of Core colocalized with NS5A (green), and NS5A colocalized with Core (grey). Co-localisation was analyzed in 10 cells for each construct using Fiji. Significant differences from WT denoted by ** (P<0.01) and**** (P<0.0001).

To also assess the distribution of LDs, I quantified their distance from the nucleus. As shown in the representative images in Fig. 5.6A, and quantified in Fig 5.6B, LDs in C142A and E191A infected cells were significantly closer to the nucleus than WT or C190A, although still more dispersed than mock infected cells.

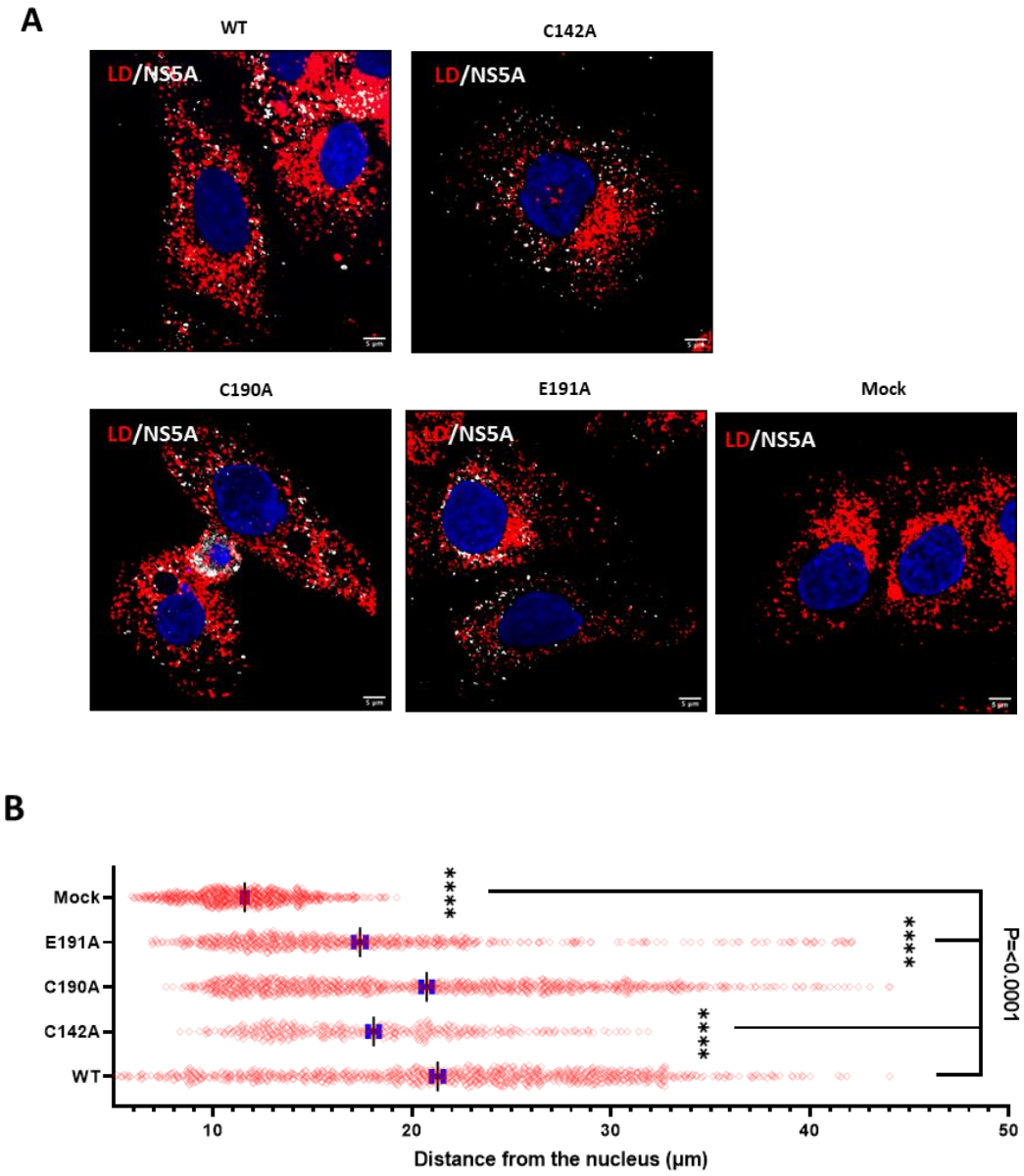

Fig 5.6. Analysis of LD distribution.

(A) Cells were stained at 72 hpe with sheep anti NS5A (white), BODIPY 558/568-C12 (red) and DAPI. **(B)** Distances of LDs from the nuclear membrane were evaluated using the Analyze Particles module of Fiji. Significant differences from WT denoted by **** (P<0.0001).

Together, these data are consistent with the proposition that NS5A DI is involved in the targeting of NS5A to LDs and functions to perturb LD morphology and distribution to promote virus assembly.

5.3 Discussion

This study builds on our group previously published work (Yin et al., 2018) and provides further evidence that DI of NS5A plays a key role in HCV assembly. However, the analysis revealed that only a limited number of residues are involved in this role as only two residues (C142 and E191) share the previously identified function exhibited by V67 and P145. In particular I observed that although a significant patch of highly conserved residues is present on the surface of the NS5A DI monomer in proximity to P145, this is dispensable for virus assembly. This is consistent with NS5A mediating a switch from virus replication to assembly, presumably by interacting with a different subset of cellular and/or viral factors. The nature of the switch remains obscure although phosphorylation of the serine cluster in the low complexity sequence linking DI and DII has been proposed. As C142 and E191 are close to the C-terminus of DI it is conceivable that they are regulated by phosphorylation. It has been hypothesised that the two dimeric forms – open (1ZH1) and closed (3FQM) represent the two conformations of NS5A with different functions. In this regard it is interesting to speculate that in the closed dimer C142 is partially occluded within the dimer interface (Fig 5.2B) and more likely for the open form to function in virus assembly

The next implication is the phenotype of E191A, which showed partial defect in virus assembly. E191 was selected due to its location at the C terminus of NS5A domain I and immediately after the conserved disulphide-forming C190, so I wondered whether it might also participate in maintaining the stability of the disulphide bond. The alanine substitution of E191 still retained some virus productivity even though the virus titration was significantly different from WT, which was the same as C142A (Fig 5.3D). The colocalisation between NS5A and Core or LDs explained why E191A produced a lower virus titre (Fig 5.5B and 5.5D). Compared to C142A which showed that the

colocalisations between viral proteins and LDs were dramatically reduced, the percentage of NS5A colocalised with LDs and Core colocalised with NS5A in E191A were higher than that in C142A. The Core-NS5A colocalisation indicated that role of NS5A in viral assembly through interacting with Core, which transports the RNA genome and recruits the replication complex to the LD (Miyanari et al., 2007, Shavinskaya et al., 2007). The increased colocalisation in E191A indicated that the Core protein delivered more RNA genome and NS5A to LDs, and such increased recruitment drove the slight recovery in production compared to C142. Interestingly, this study found the NS5A protein of E191A cannot be normally expressed as WT in replication-independent way (Fig 3.4). Combined with the colocalisation results, the Core protein in E191A might play some roles in mutant virus assembly when the expression and function of NS5A DI was disrupted via E191A.

A role for DI in virus assembly is consistent with the observation that treatment of infected cells with an NS5A DAA (ledipasvir) inhibited virus assembly within 2 h. In contrast, inhibition of genome replication was not observed until >12 h, most likely due to the inability of NS5A DAAs to inhibit pre-existing replication complexes (McGivern et al., 2014). Given that NS5A DAAs target DI, the implication of this data are that DI plays a role in assembly, as well as genome replication.

These data show that for WT and C190A that efficiently assemble into infectious virus particles, the number of LDs per-cell is lower in comparison to mock infected cells (Fig 5.5). This was concomitant with an increase in the size of LDs, suggesting that virus infection coalesces LDs into larger entities that support the process of virus assembly. LDs were also distributed throughout the cytoplasm compared to the restricted perinuclear distribution observed in mock infected cells (Fig 5.6). These changes were not apparent for assembly defective mutants for which, the colocalisation of NS5A and

Core with LDs, and the NS5A:Core colocalisation were all reduced. Together, these data are consistent with the hypothesis that NS5A DI regulates the recruitment of both NS5A and Core to LDs, and modulates LD morphology and distribution to facilitate virus assembly.

In conclusion, this study demonstrated two NS5A DI mutants (C142A and E191A) displayed the same assembly phenotype with V67A and P145A. These two mutants had the same function as V/P mutants which modulated the morphology and distribution of lipid droplets. The detailed mechanism of this phenotype still needs further investigations.

Chapter 6: NS5A domain I antagonises PKR to facilitate the assembly of infectious hepatitis C virus particles

6.1 Introduction

Double-stranded RNA (dsRNA)-dependent protein kinase (PKR) is a serine-threonine kinase that was first identified as an antiviral protein induced by IFN in 1990 (Meurs et al., 1990). PKR acts as both a sensor of virus infection by binding to viral dsRNA resulting in activation of the kinase, and also an effector via downstream consequences such as inhibition of protein translation and induction of apoptosis (Cesaro and Michiels, 2021).

The replication and production of HCV were also modulated by PKR. However, the effect of PKR on the HCV lifecycle is controversial: PKR activation resulted in higher efficiency of HCV replication and production, virus titre was reduced following the loss of PKR (Arnaud et al., 2010). Paradoxically HCV has been reported to recruit and activate PKR to trigger induction of interferon stimulated genes (ISGs) (Arnaud et al., 2011, Arnaud et al., 2010). NS5A and NS5B interact with PKR and block its activation: NS5A interacts with PKR via a region in DII termed the interferon-sensitivity determining region (ISDR), the sequence of which correlates with the sensitivity of virus isolates to IFN treatment (Gale Jr et al., 1998). NS5B interacts with PKR via its RNA polymerase motif to activate PKR which results in decreased major histocompatibility complex I (MHC-I) expression (Gale Jr et al., 1997). These interactions further contribute to the evasion of antiviral pathway for HCV.

PKR has been shown to be activated by the dsRNA generated during virus replication (Ehrenfeld and Hunt, 1971). PKR consists of two dsRNA binding domains (dsRBD) at the N-terminus, and a C-terminal kinase catalytic domain (Feng et al., 1992). The dsRBD has the ability to recognise a stretch of >33 base pair dsRNA and results in the auto-phosphorylation of PKR to induce its enzymatical activation (Cole, 2007).

Activated PKR has a number of downstream effects: the best characterised is the phosphorylation of the α subunit of eukaryotic initiation factor 2 (eIF2α) at Ser51 (Meurs et al., 1992). This blocks mRNA translation by preventing recycling of eIF2 to the initiation complex (Sudhakar et al., 2000). PKR also activates the transcription factor NF-κB independently of PKR catalytic activity (Bonnet et al., 2006, Bonnet et al., 2000). PKR activation leads to the dissociation of the inhibitor IκB from the p50/p65 NF-κB complex, which then enters the nucleus and activates transcription (Kumar et al., 1994, Zamanian-Daryoush et al., 2000). IFN regulatory factor 1 (IRF1) is also activated by PKR, and is blocked by binding of the NS5A ISDR to PKR (Pflugheber et al., 2002).

In this study, I aim to further explore the mechanism of NS5A domain I in viral assembly. This research observed that PKR participated in the HCV assembly through NS5A DI and the downstream factor IRF1 was also involved in this modulation.

6.2 Results

6.2.1 PKR silencing or inhibition recovers the virus assembly phenotype of C142A and E191A

It was recently shown that CypA is critical for HCV genome replication in Huh7 cells but not Huh7.5 cells (Colpitts et al., 2020). Further analysis led to the conclusion that NS5A interacts with CypA to evade PKR-dependent antiviral responses. The differential sensitivity of HCV to CypA in Huh7 compared to Huh7.5 cells was reminiscent of our initial observation that P145A fails to undergo genome replication in Huh7 cells, but is only modestly impaired in Huh7.5 cells (Yin et al., 2018) (Fig 3.2 and 3.3). This led us to assess whether either CypA and/or PKR play a role in virus assembly and whether the NS5A DI mutants studied thus far can shed light on such

mechanisms. To test this, CypA or PKR silenced cell lines were constructed and then were electroporated with mSGR-luc-JFH-1 or mJFH1 WT. The SGR WT luciferase value was measured at 48hpe and the supernatant of mJFH1-WT was collected at 72hpe to evaluated the titration in Huh7.5 cells. Consistent with previous studies, I first confirmed that silencing of CypA or PKR in Huh7.5 cells had no effect on genome replication (Fig 6.1A). I did however, note that the production of infectious virus was unaffected by PKR silencing but reduced by ~100-fold in CypA shRNA cells (Fig. 6.1B).

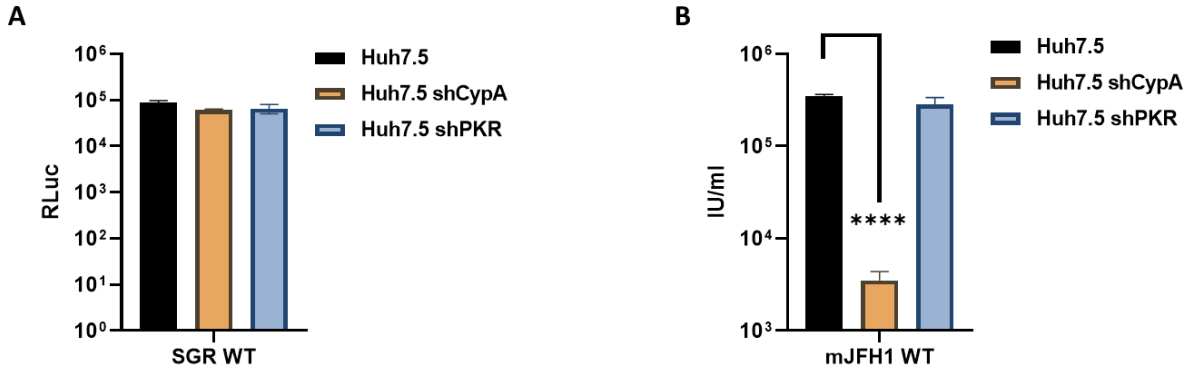

Fig 6.1. Genome replication and virus assembly phenotypes in Huh7.5 silenced for CypA or PKR.

(A) In vitro transcripts of mSGR-Luc-JFH-1 WT were electroporated into Huh7.5, Huh7.5 CypA or PKR silenced cell lines. Luciferase activity was measured at 72hpe. **(B)** *In vitro* transcripts of mJFH-1 WT were electroporated into Huh7.5, Huh7.5 CypA or PKR silenced cell lines. Extracellular infectious virus was titrated at 72 hpe.

I proceeded to analyse the genome replication and assembly of the three DI mutants in PKR silenced Huh7.5 cells (Fig6.2A). The virus replication activity was evaluated by (1) quantifying NS5A positive cells using IncuCyte S3 (2) detecting the virus genome copy using qRT-PCR (3) evaluating viral protein expression by western blot at 72 hpe (Fig 6.2B-D). As expected, genome replication (Fig 6.2B) and viral protein production

(Fig 6.2C, D) were unaffected by the lack of PKR. Indeed, overall levels of genome replication as measured by qRT-PCR modestly increased compared to Huh7.5 cells (compare Fig 6.2B to Fig 5.3A). A surprising picture emerged when we analysed the assembly and release of the mutants: production of infectious virus by C142A and E191A was restored to the same level as WT and C190A in PKR silenced Huh7.5 cells (Fig 6.2E). To further confirm that this was due to the lack of PKR, as opposed to an off-target effect of the sgRNA, Huh7.5 cells were treated with the small molecule PKR inhibitor C16 at 24 hpe. Reassuringly, pharmacological inhibition of PKR function also restored the production of infectious virus by C142A and E191A (Fig 6.2F).

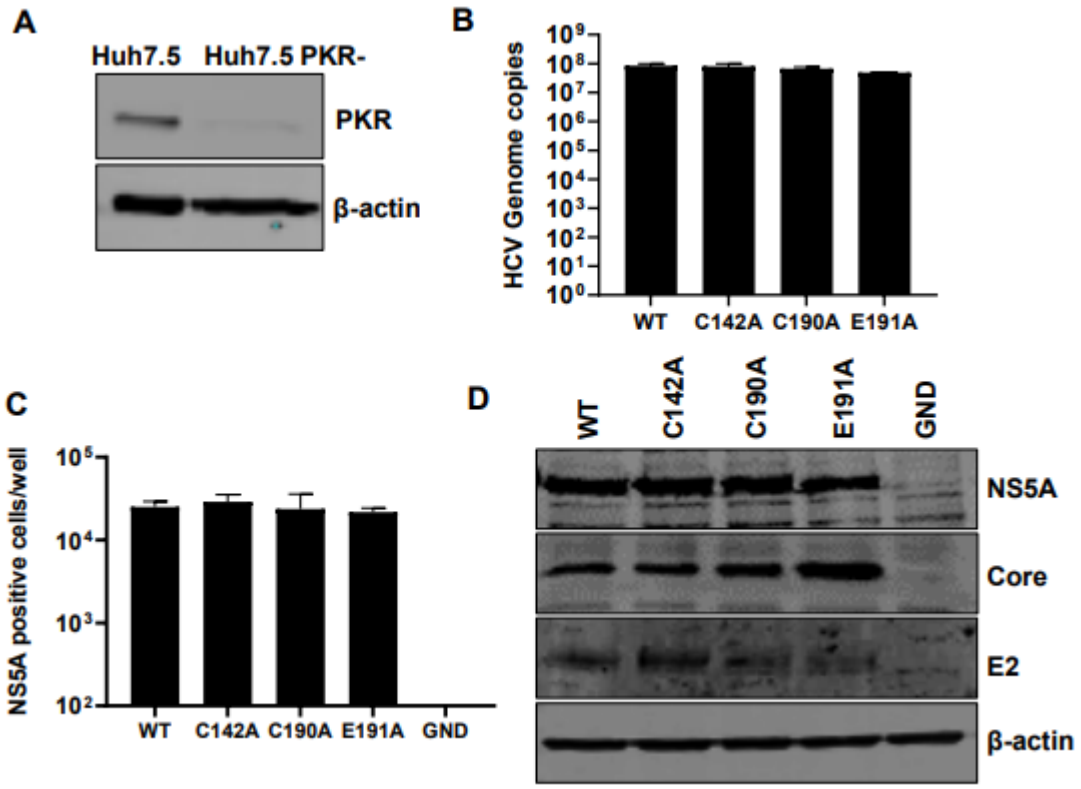

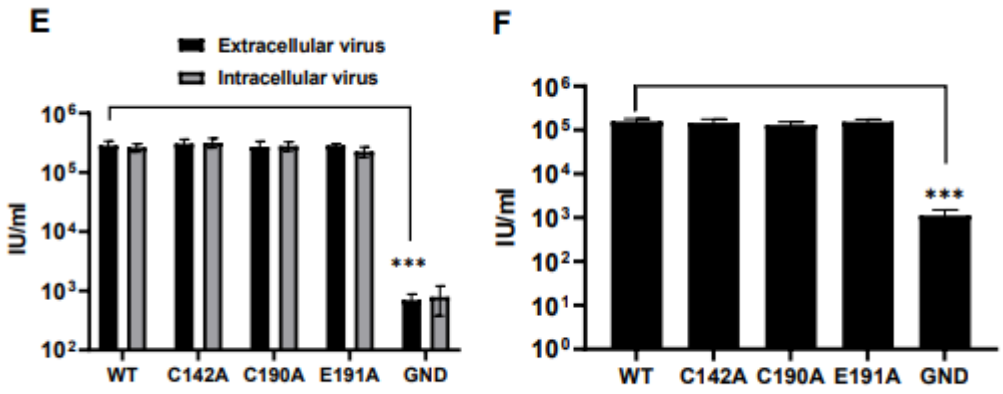

Fig 6.2. Virus assembly in PKR-silenced Huh7.5 cells.

(A) PKR expression was detected in silenced Huh7.5 cells by western blot. Huh7.5 cells were electroporated with mJFH-1 WT and DI mutant C142A, C190A and E191A RNAs, together with an NS5B GND mutant as negative control. Virus genome replication was analysed directly by quantification of genome copies in cell lysates using qRT-PCR **(B)**, and indirectly by enumerating NS5A positive cells at 72 hpe using the IncuCyte S3 **(C)**. **(D)** Cell lysates were collected at 72 hpe and analysed by western blotting with the indicated antibodies. **(E)** Extra- and intracellular virus harvested at 72 hpe were titrated in Huh7.5 cells and quantified using the IncuCyte S3. **(F)** Electroporated cells were treated with the PKR inhibitor C16 from 24 hpe, extracellular virus was harvested at 72 hpe and titrated as described in **(E)**.

The conclusion from these data is that, the replication of WT and these mutants were not affected by the lack of PKR. Furthermore, the assembly phenotype of C142A and E191A were rescued by the absence of PKR. These two residues were absolutely required for virus assembly in Huh7.5 cells presumably by disrupting NS5A DI to allow PKR to block HCV assembly. These data are consistent with a role for PKR in blocking virus assembly and point to a role of NS5A DI in antagonising this previously undefined function of PKR.

6.2.2 PKR silencing restores the LD phenotype of the assembly mutants.

I next sought to determine whether the restoration of infectious virus production by PKR silencing was associated with concomitant changes in LD morphology, distribution and the association with NS5A and Core. Therefore, the confocal analysis were repeated as described in Figs 5.4-5.6 in PKR silenced cells. As previously described, WT and three mutants were electroporated into Huh7.5 PKR silenced cell line. The cells were fixed at 72hpe and the fluorescence of NS5A, Core protein and LD were detected by IF assay. The confocal images in Fig 6.3 displayed the same size of LD in C142A and C190A as WT.

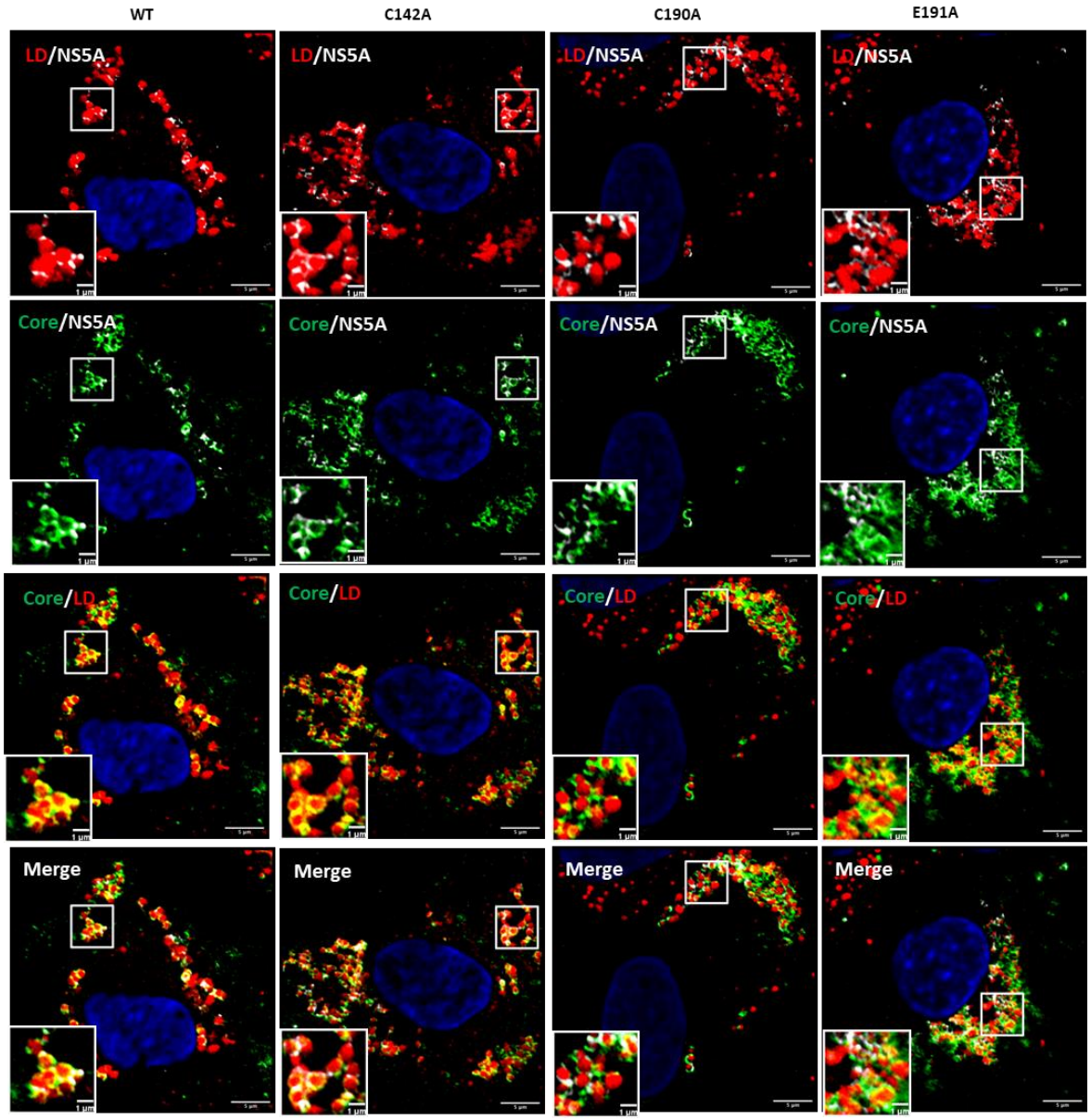

Fig 6.3. Co-localisation between NS5A, Core and LD in PKR-silenced Huh7.5 cells.

Huh7.5 cells silenced for PKR expression were electroporated with mJFH-1 WT and DI mutant C142A, C190A and E191A RNAs and seeded on to coverslips. Cells were stained at 72 hpe with sheep anti-NS5A (white), rabbit anti-Core (green), BODIPY 558/568-C12 (red) and DAPI. Co-localisation was observed using Airyscan microscopy. Representative images are shown. Scale bars are 5 μm and 1 μm (insets).

As shown in the quantification in Fig 6.4, no differences between WT and the three mutants with regard to LD number and size were observed (Fig 6.4A), although it

should be noted that overall the size of LDs in infected cells was slightly reduced (Fig 5.5A). Co-localisation analysis also revealed that, unlike in Huh7.5 cells, no differences were observed between WT or the three mutants in terms of their co-localisation between NS5A and LD (Fig 6.4B), Core and LD (Fig 6.4C) or NS5A and Core (Fig 6.4D).

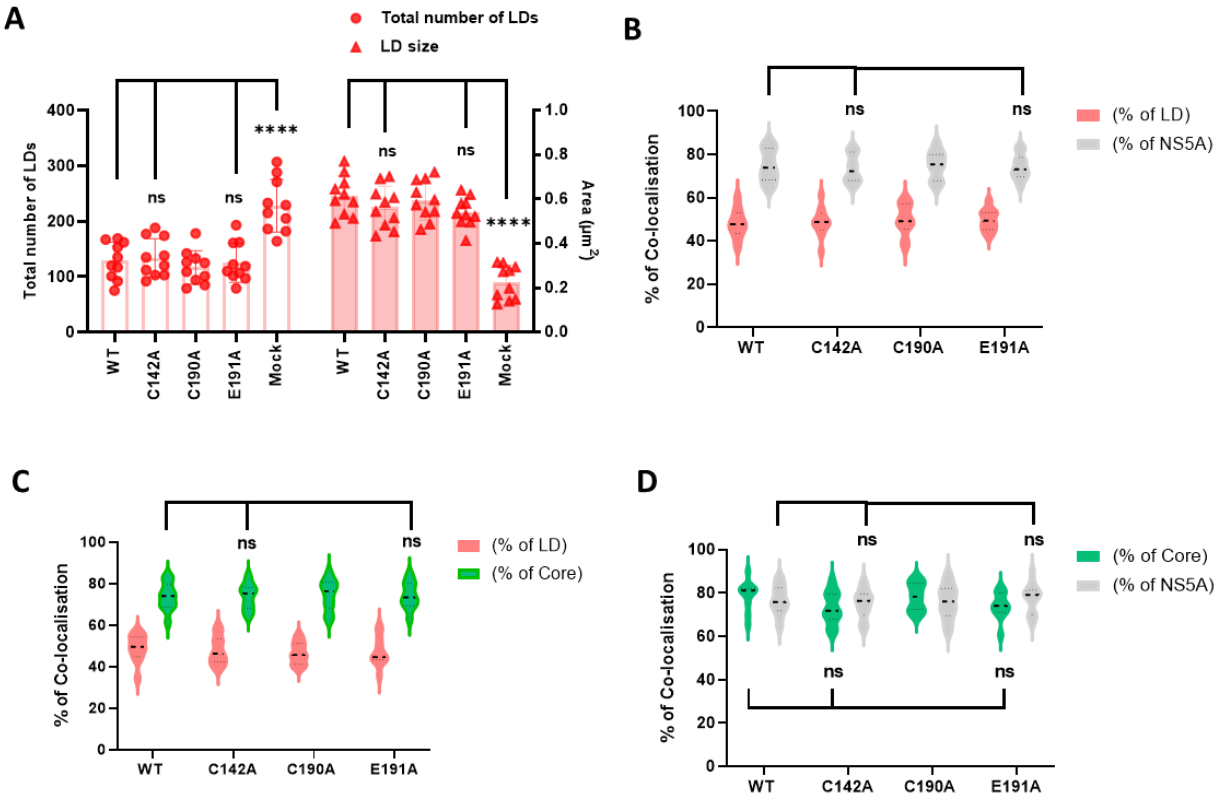

Fig 6.4. Quantification of LD size and co-localisation with NS5A and Core in PKR-silenced Huh7.5 cells.

(A) LD numbers and size from Fig 8 were calculated using Analyze Particles module of Fiji. Mock: uninfected Huh7.5 cells. **(B)** Quantification of percentage of LDs colocalizing with NS5A (red), and NS5A colocalized with LD (grey). **(C)** Quantification of the percentage of LD colocalized with Core (red), and Core colocalized with LD (green). **(D)** Quantification of the percentage of Core colocalized with NS5A (green), and NS5A colocalized with Core (grey). Co-localisation was analysed in 10 cells for each construct using Fiji. Significant differences from WT denoted by ns (P>0.05) and **** (P<0.0001).

The complete restoration of the colocalization suggested that the loss of PKR dramatically enhanced the targeting of NS5A and Core protein to LDs. Moreover, the colocalisation of Core and NS5A also increased to WT level, indicating that PKR not only altered the colocalisation between viral proteins and organelle LD, but also modulated the recruitment of Core and NS5A in the assembly process.

Lastly, I assessed the distribution of LDs by quantifying their distance from the nucleus. As shown in the representative images in Fig. 6.5 A, and quantified in Fig 6.5 B, the distribution of LDs in PKR silenced cells was comparable to that observed in Huh7.5 cells: in C142A and E191A infected cells LDs were significantly closer to the nucleus than WT and C190A, although still more dispersed than mock infected cells.

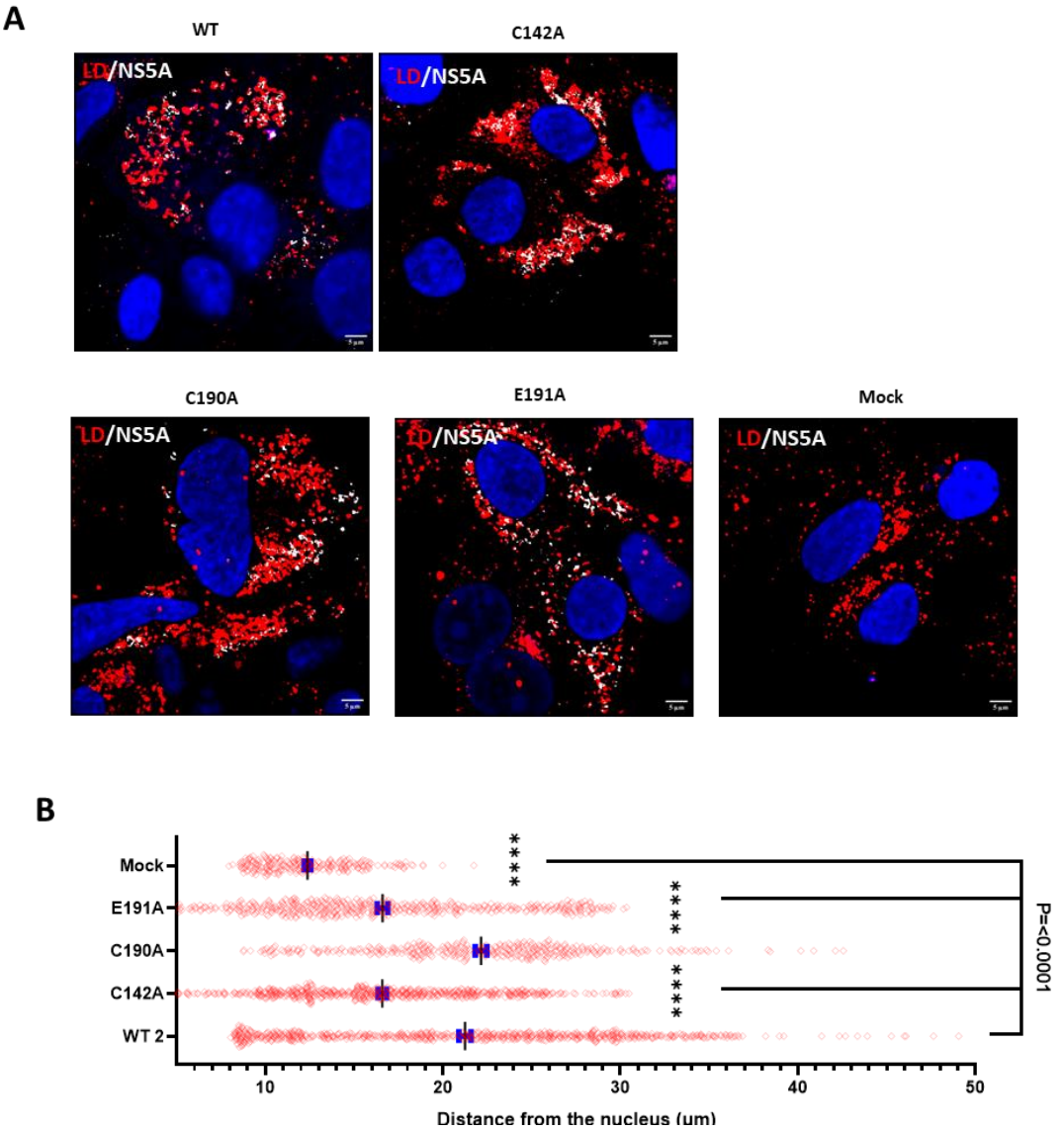

Fig 6.5. Analysis of LD distribution in PKR-silenced Huh7.5 cells.

(A) Cells were stained at 72 hpe with sheep anti-NS5A (white), BODIPY 558/568-C12 (red) and DAPI. **(B)** Distance of LDs from the nucleus was evaluated using the Analyze Particles module of Fiji. Significant differences from WT denoted by **** (P<0.0001).

The results were interesting because PKR can partially disrupt LD characteristics in NS5A DI phenotype mutants. Thus, I propose that in these analysis, the loss of PKR restores the colocalisation ability between viral proteins and LDs. It is worth noticing that the closer LD distance to nucleus of C142A and E191A was unaffected but LD

size was recovered to WT level in the absence of PKR. These data are consistent with the suggestion that PKR functions to disrupt virus assembly by blocking the HCV-mediated perturbations of LD morphology. Furthermore, NS5A DI antagonises this function of PKR through the surface exposed residues C142 and E191.

6.2.3 Assembly defective mutants C142A and E191A exhibit reduced dsRNA abundance.

I next sought to understand the differences between WT and the NS5A DI assembly-defective mutants with regard to PKR activation. PKR is activated by binding to dsRNA via two N-terminal RNA-binding domains (dsRBD) (Cole, 2007, Garcia et al., 2006). This leads to dimerisation of PKR, autophosphorylation and activation of the C-terminal kinase domain. dsRNA is generated as a replication intermediate and co-localises with NS5A, Core and LDs (Targett-Adams et al., 2008a). Furthermore, the HCV genome contains many structured RNA elements with extensive double-stranded regions (Mauger et al., 2015). Although genome replication is likely protected from PKR as it occurs within the membranous web (Paul and Bartenschlager, 2015), nascent genomes must be transported through the cytoplasm to sites of assembly and during this process may be detected by PKR. I therefore assessed the co-localisation between dsRNA, NS5A and LDs in Huh7.5 cells using a well-characterised dsRNA-specific antibody, J2 (Targett-Adams et al., 2008a). As expected, in WT infected cells, we observed co-localisation of dsRNA with both NS5A and LDs (Fig 6.6).

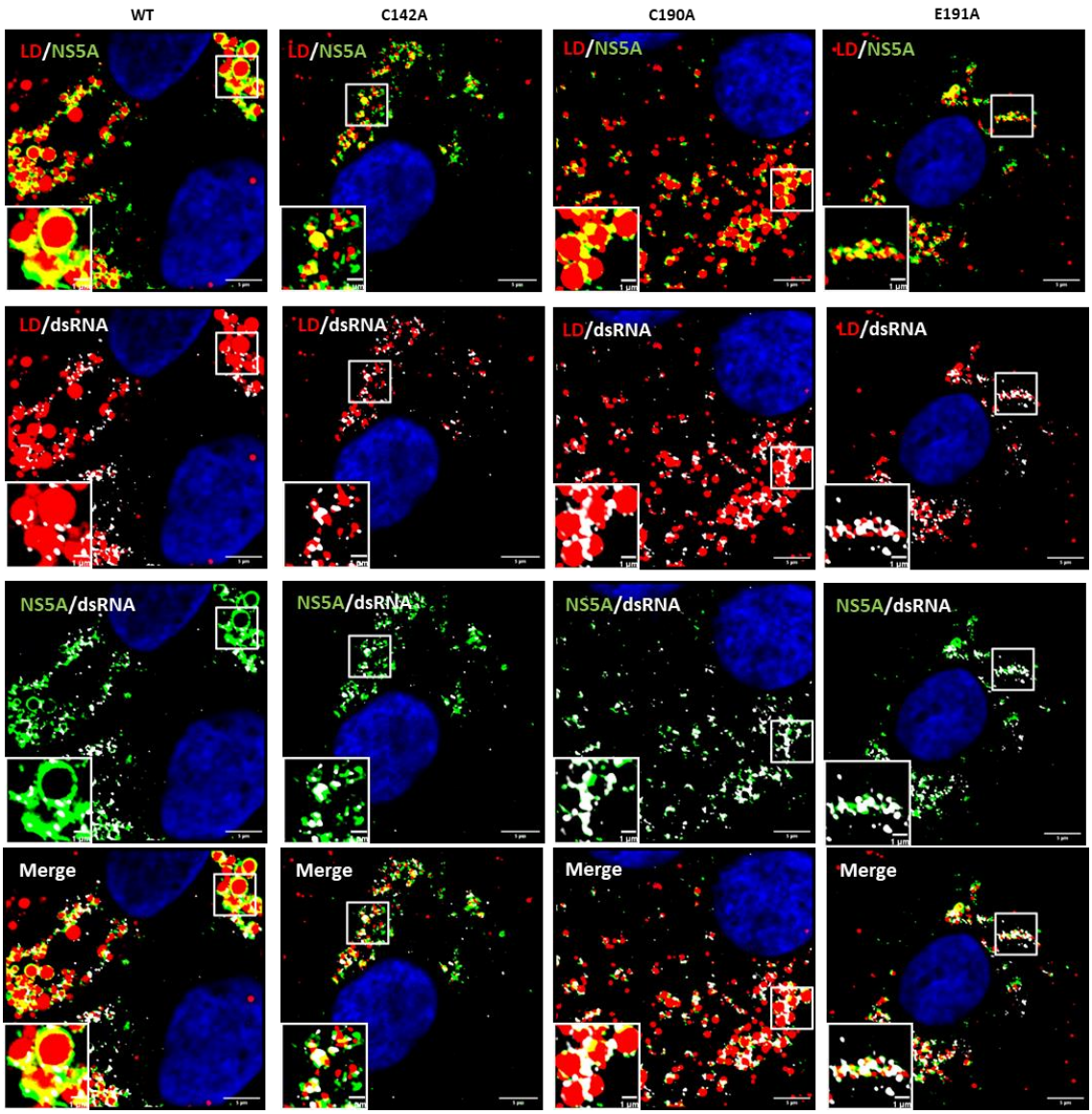

Fig 6.6. Co-localisation of NS5A, dsRNA and LD.

Huh7.5 cells were electroporated with mJFH-1 WT and DI mutant C142A, C190A and E191A RNAs and seeded on to coverslips. At 72 hpe cells were stained with sheep anti-NS5A (green), mouse anti-dsRNA J2 (white), BODIPY 558/568-C12 (red) and DAPI. Co-localisation was observed using Airyscan microscopy. Representative images are shown. Scale bars are 5 μm and 1 μm (insets).

This colocalisation was also quantified in cells infected with the three mutants and surprisingly, revealed no significant differences in the co-localisation of NS5A and dsRNA (Fig 6.7A) or LD and dsRNA (Fig 6.7B). However, the number of dsRNA foci

in C142A and E191A were reduced compared to WT and C190A (Fig 6.7C-D). WT and C190A infected cells exhibited 200-300 dsRNA punctae whereas C142A and E191A infected cells had between 100-200 punctae. Given that the overall levels of HCV genomes in all of these cells were equivalent (Fig 5.3A and 6.2B), this suggests that the majority of dsRNA foci actually represent nascent genomes, rather than replicative intermediates. However, the reason for the decrease of dsRNA on the surface of LDs needed further confirmation. To test this, the total dsRNA fluorescence of each mutant was measured by Fiji. As shown in Fig 6.7 E, both WT and mutants displayed the same mean fluorescence intensity. This result suggested that the decrease of dsRNA on the surface of LDs might result from the aggregation of dsRNA rather than direct RNA degradation.

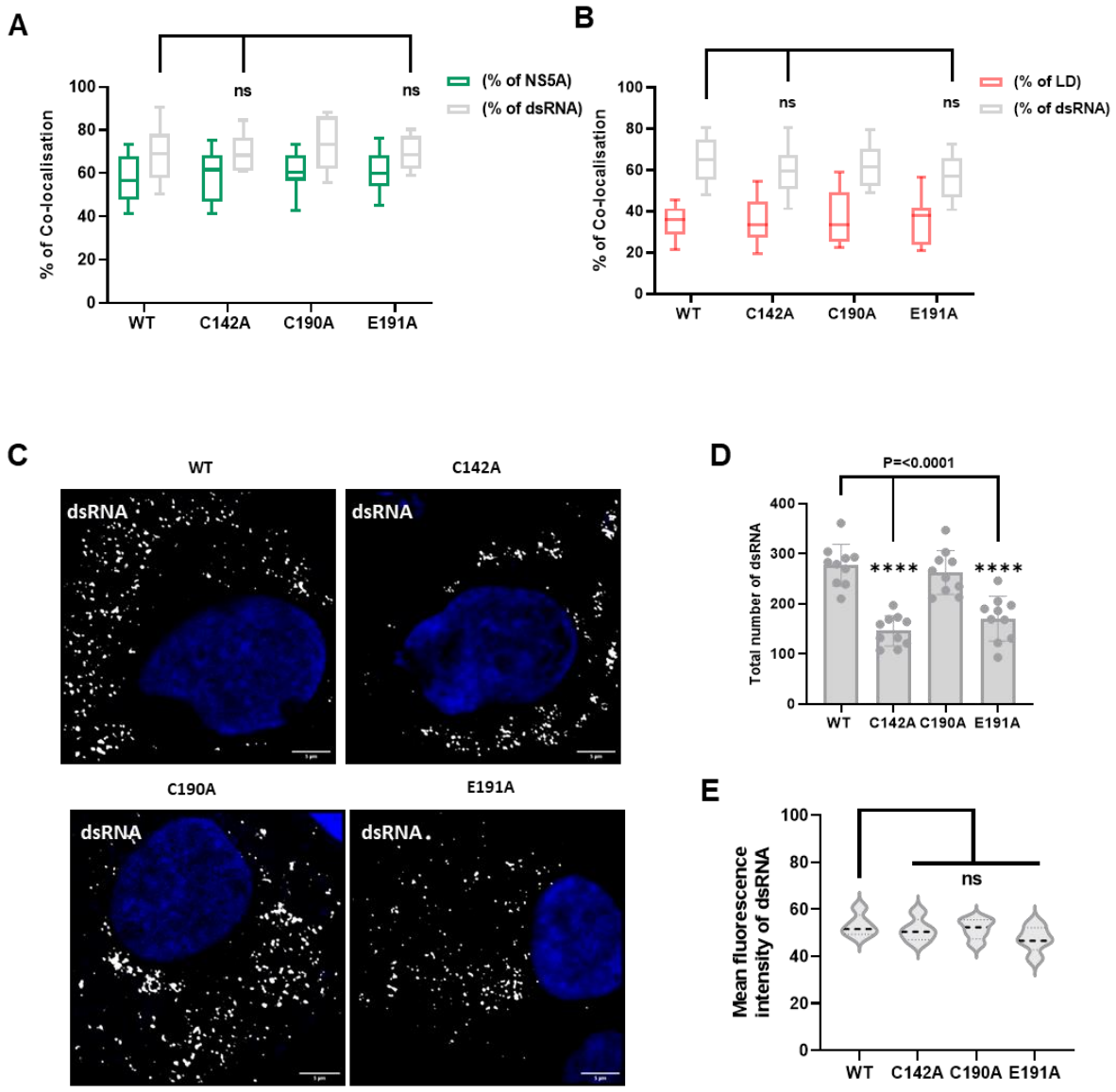

Fig 6.7. Quantification of dsRNA punctae and co-localisation with NS5A and LD.

(A) Quantification of the percentage of NS5A colocalized with dsRNA (green), and dsRNA colocalized with NS5A (grey). **(B)** Quantification of the percentage of LD colocalized with dsRNA (red), and dsRNA colocalized with LD (grey). Co-localisation was analyzed in 10 cells from Fig 11 using Fiji. **(C)** Representative images of Huh7.5 cells electroporated with mJFH-1 WT and DI mutants C142A, C190A and E191, seeded onto coverslips and stained at 72 hpe with mouse anti-dsRNA J2 (white) and DAPI. Scale bars are 5 μm. **(D)** Numbers of dsRNA punctae of each sample from (C) were calculated using the Analyze Particles module of Fiji. **(E)** Mean fluoresence intensity of dsRNA of each sample from (C) were calculated using Fiji.

For the two assembly defective mutants, C142A and E191A, we propose that our results showed the failure of NS5A to block PKR binding to dsRNA elements in nascent genomes, resulting in PKR activation, dsRNA aggregation and stimulation of an antiviral response.

6.2.4 NS5A DI interacts with PKR.

NS5A has been previously demonstrated to directly interact with PKR via a region in D2 termed the interferon sensitivity determining region (ISDR) (Gale Jr et al., 1997). These studies were performed with NS5A from genotype 1b and showed exquisite sensitivity to the amino acid sequence of the ISDR. The homology in this region between genotype 1b and JFH-1 (genotype 2a) is low (44% identity) so it is unlikely that the ISDR in JFH-1 binds to PKR, although this has not been formally proven. I considered that the ability of NS5A DI to block PKR could be explained by a direct interaction between the two proteins, dependent on C142 and E191. To test this I immunoprecipitated PKR from Huh7.5 cells electroporated with either WT or the three mutants and investigated the presence of NS5A in the immunoprecipitates by western blotting. As shown in Fig 6.8A, only WT and C190A NS5A co-precipitated with PKR, whereas C142A and E191A NS5A did not. We also investigated whether NS5A was able to bind to activated PKR by performing immunoprecipitations with an antibody to phosphorylated PKR (P-PKR). Although overall levels of P-PKR were low, this analysis clearly showed that (as for the total PKR) only WT and C190A NS5A co-precipitated with P-PKR (Fig 6.8B).

To further validate the interaction between NS5A DI and PKR, His-SUMO tagged NS5A DI (WT and mutants) were expressed in E.coli, purified and used as bait to precipitate PKR which was overexpressed in HEK293T cells. Confirming the co-

immunoprecipitation data, only WT and C190A DI, but not C142A and E191A, were able to precipitate PKR from the cell lysate (Fig 6.8C), confirming that DI is indeed able to bind to PKR. These data are consistent with the hypothesis that NS5A DI binds directly to PKR to prevent it activating downstream pathways that would lead to an antiviral response against virus assembly. I therefore turned my attention to identifying the downstream PKR effector(s) responsible.

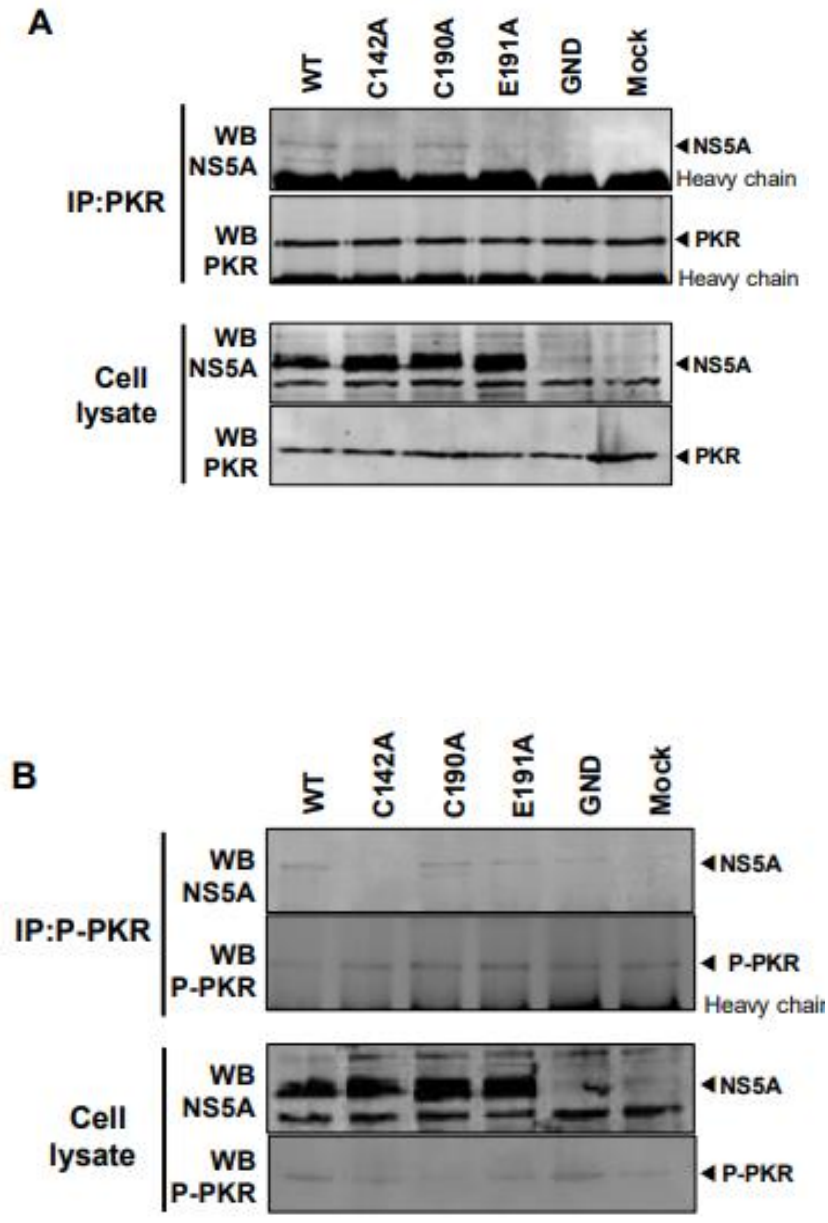

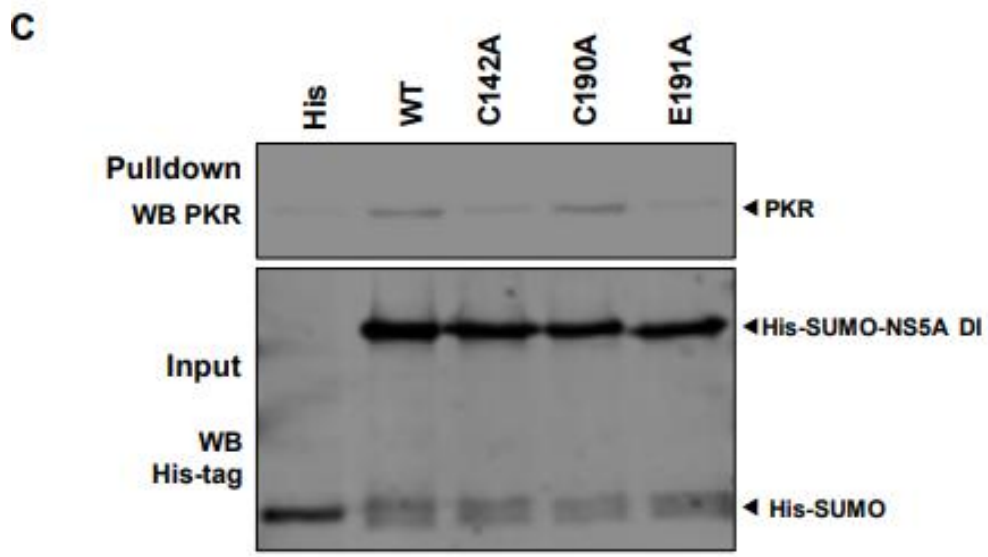

Fig 6.8. Protein-protein interaction analysis of NS5A and PKR.

(A, B) Huh7.5 cells electroporated with mJFH-1 WT and DI mutants C142A, C190A and E191 were lysed and immunoprecipated with anti PKR antibody **(A)** or anti phospho-PKR antibody **(B)**. Immunoprecipitates (top) and lysates (bottom) were analysed by western blot with the indicated antibodies. **(C)** His-SUMO tagged NS5A DI and mutants were purified and bound to Dynabead His-Tag beads as a bait to precipitate PKR protein which was overexpressed in HEK293T cells. Pulldowns were analysed by western blotting for PKR (top), and inputs verified by western blotting for the His-tag (bottom).

6.2.5 A role for the PKR effector IRF1 in blocking HCV assembly.

A well characterised downstream effector of PKR is the phosphorylation of eIF2α at Ser51 to block protein synthesis. PKR also activates NFκB independently of its catalytic activity (Bonnet et al., 2006, Bonnet et al., 2000), as well as interferon regulatory factor 1 (IRF1). Although the mechanism by which PKR activates IRF1 is uncharacterised, unlike NFκB activation it is dependent on PKR catalytic activity (Kirchhoff et al., 1995).

Western blotting of infected cell lysates with antibodies to either Ser51-phosphorylated eIF2α or total eIF2α revealed no differences between WT and the three mutants (Fig 6.9). I therefore concluded that eIF2α phosphorylation by PKR is not implicated in the downstream effects on HCV assembly.

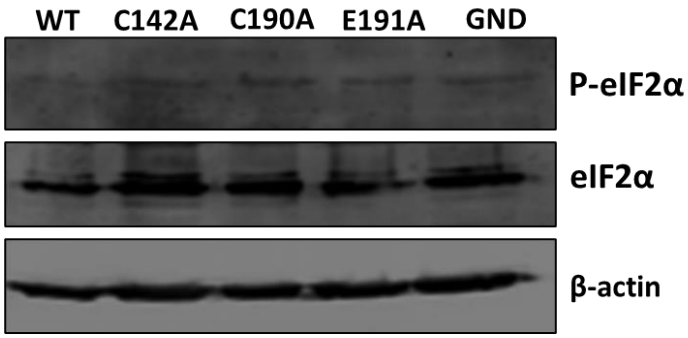

Fig 6.9. Expression of eIF2α and phospho-eIF2α.

Huh7.5 cells were electroporated with mJFH-1 WT and DI mutant C142A, C190A and E191A RNAs, together with an NS5B GND mutant as negative control. Cells were harvested at 72 hpe and lysed with GLB. eIF2α and phospho-eIF2α was analysed by western blotting.

Activation of NF-κB results in translocation of the p65 subunit from the cytoplasm to the nucleus. As shown in Fig 4.11, the interaction between CypA and NS5A DI antagonise the activation of NF-κB to promote HCV genome replication. To test whether this downstream effector NF-κB was also responsible for the PKR effect on virus assembly we analysed infected cells by immunofluorescence with an antibody specific to p65 (Fig 6.10). As expected, treatment with the NFκB activator TNFα resulted in efficient nuclear translocation of p65, however as shown in the representative images in Fig 6.10 no such translocation was observed for either mock-infected or HCV-infected cells (WT or mutants). This suggested that activation of NFκB by PKR is not required for its effect on virus assembly, consistent with a requirement of PKR catalytic activity for the virus assembly block (Fig 6.2F).

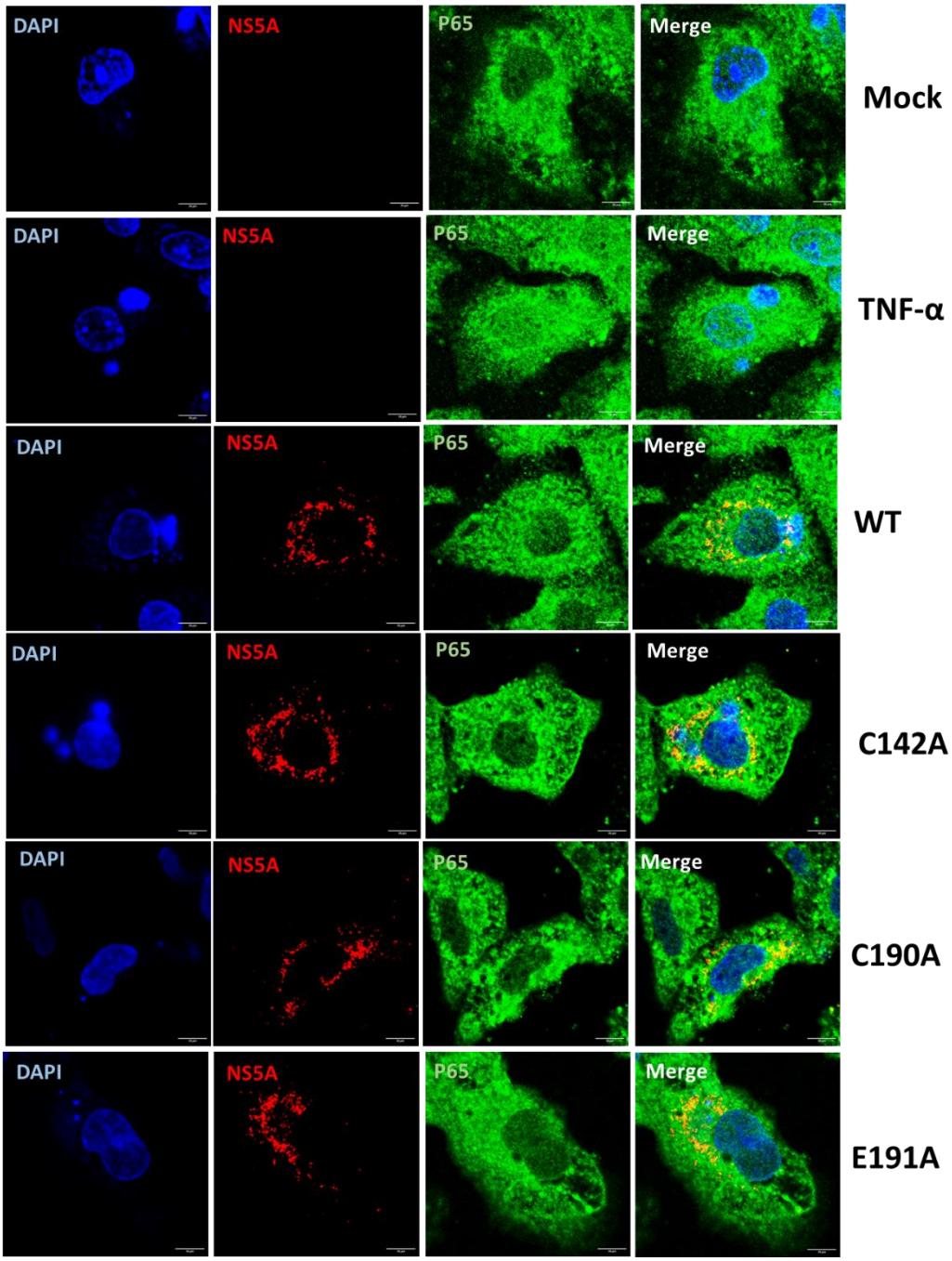

Fig 6.10. NF-κB activation in Huh7.5 cells infected with mJFH-1 or DI mutants.

Huh7.5 cells were electroporated with mJFH-1 WT and DI mutants C142A, C190A and E191A RNAs. At 72 hpe, cells were fixed and stained with mouse anti-P65 (green), sheep anti-NS5A (red) and DAPI. As a positive control to activate the NF-κB pathway uninfected Huh7.5 cells were treated with TNF-α for 24h. Mock: uninfected Huh7.5 cells.

Finally, I focused on IRF1 which drives expression of antiviral interferon-stimulated genes (ISGs) (Taniguchi et al., 2001). IRF1 has been previously demonstrated to negatively regulate HCV genome replication (Kanazawa et al., 2004), and the silencing of either IRF1 itself, or its effector targets PSMB9, APOL1 and MX1 enhanced HCV genome replication (Yamane et al., 2019). The effects of IRF1 on HCV assembly have not been evaluated. To test this, IRF1 was silenced in Huh7.5 cells using CRISPR/Cas9 (Fig 6.11A), and these cells were electroporated with WT or the mutant HCV RNAs. As was observed for PKR silenced cells, genome replication (Fig 6.11B) and viral protein production (Fig 6.11C, D) was unaffected by IRF1 silencing. Reassuringly, when I analysed the assembly and release of the mutants, the production of infectious virus by C142A and E191A were restored to the same levels as WT and C190A in IRF1-silenced Huh7.5 cells (Fig 6.11E). These data confirmed that the ability of PKR to inhibit the assembly of HCV is mediated by its activation of the downstream effector IRF1.

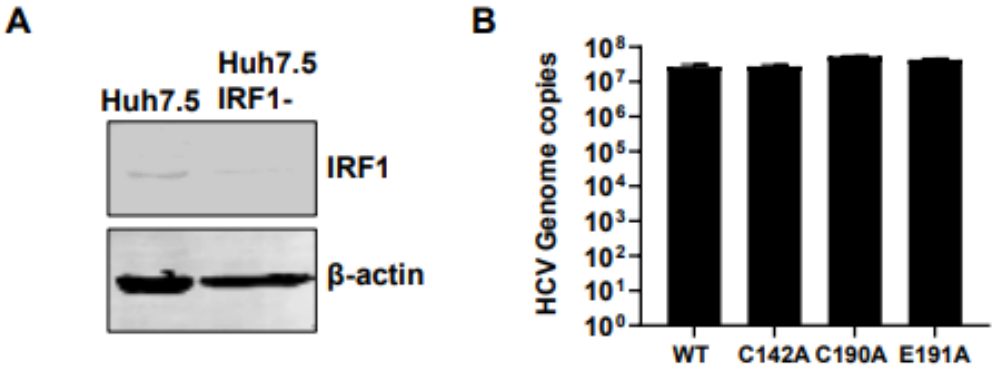

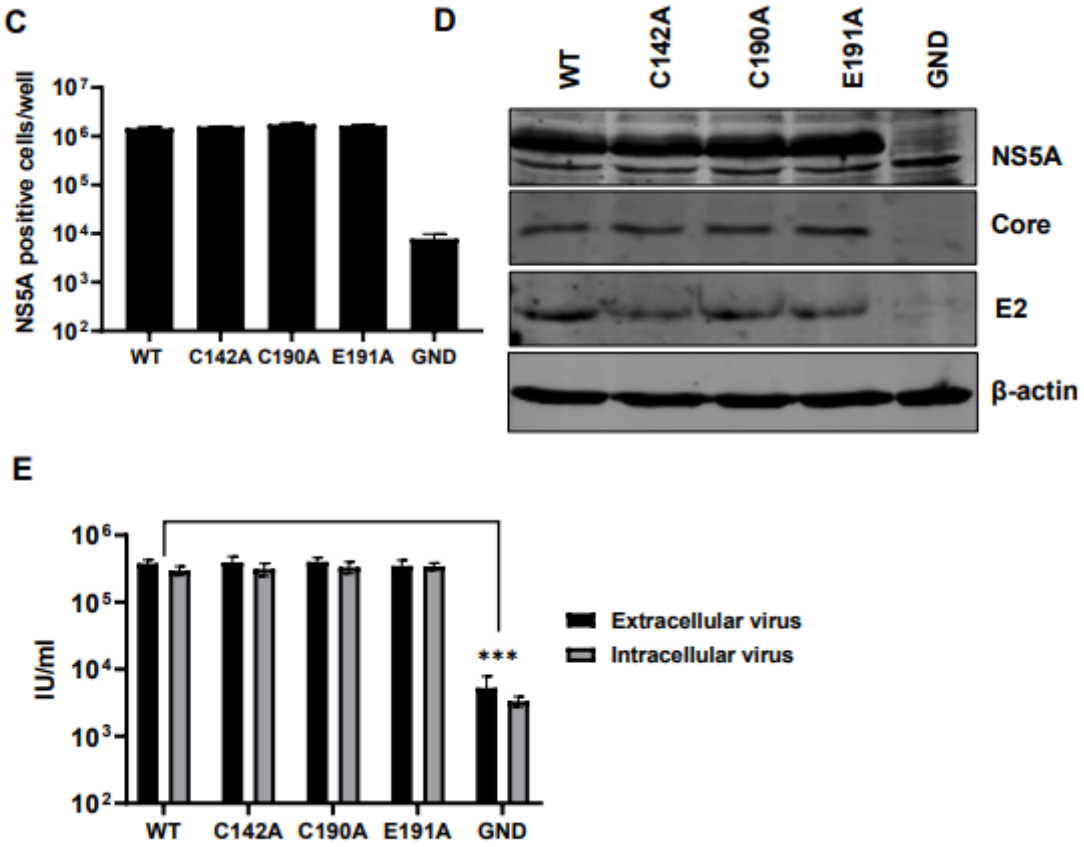

Fig 6.11 Virus assembly in IRF1-silenced Huh7.5 cells.

(A) IRF1 expression was detected in silenced Huh7.5 cells by western blotting. Huh7.5 cells were electroporated with mJFH-1 WT and DI mutant C142A, C190A and E191A RNAs, together with an NS5B GND mutant as negative control. Virus genome replication was analysed detected directly by quantification of genome copies in cell lysates using qRT-PCR **(B),** and indirectly by enumerating NS5A positive cells at 72 hpe using the IncuCyte S3 **(C). (D)** Cell lysates were collected at 72 hpe and then analysed by western blot with the indicated antibodies. **(E).** Extra- and intracellular virus harvested at 72 hpe were titrated onto Huh7.5 cells and quantified using the IncuCyte S3.

6.3 Discussion

This study demonstrated the mechanism behind the NS5A DI assembly phenotype. Antiviral activity of PKR was inhibited by HCV NS5A DI and mediated by IRF1. The novel function of NS5A DI was revealed: preventing antiviral factors to promote HCV assembly.

The silencing of PKR restored the phenotype of the two assembly defective mutants provides clues to the mechanism of action of DI in regulating assembly. NS5A binds viral RNA (Foster et al., 2010) and the open form (Tellinghuisen et al., 2005) presents a basic surface in the groove between the monomers that is a possible RNA binding motif (Fig 3.1B). An attractive hypothesis is therefore that NS5A is involved in transporting nascent genomic RNA from sites of replication to sites of assembly (Lee et al., 2019, Lindenbach and Rice, 2013). In this scenario, the LD is a waystation on the route and at that point NS5A could deliver the RNA to the Core protein, rather like a baton in a relay race. One potential consequence of this is that the RNA would be transiently exposed in the cytosol, permitting detection by innate cytosolic sensors such as PKR. PKR is activated by binding to short (30 bp) dsRNA elements but can activated by imperfect dsRNA or single stranded RNA (Mayo et al., 2016). In this regard, the HCV 5' IRES has been shown to be both a potent activator (Shimoike et al., 2009) and inhibitor (Toroney et al., 2010) of PKR. We postulate that DI interferes with the binding of PKR to nascent genomes, possibly by direct binding to PKR (Fig 6.8), preventing PKR activation and the induction of downstream antiviral pathways. Our study is the first detailed analysis showing that NS5A DI blocked PKR to evade antiviral pathway and facilitate HCV assembly (Fig 6.12).

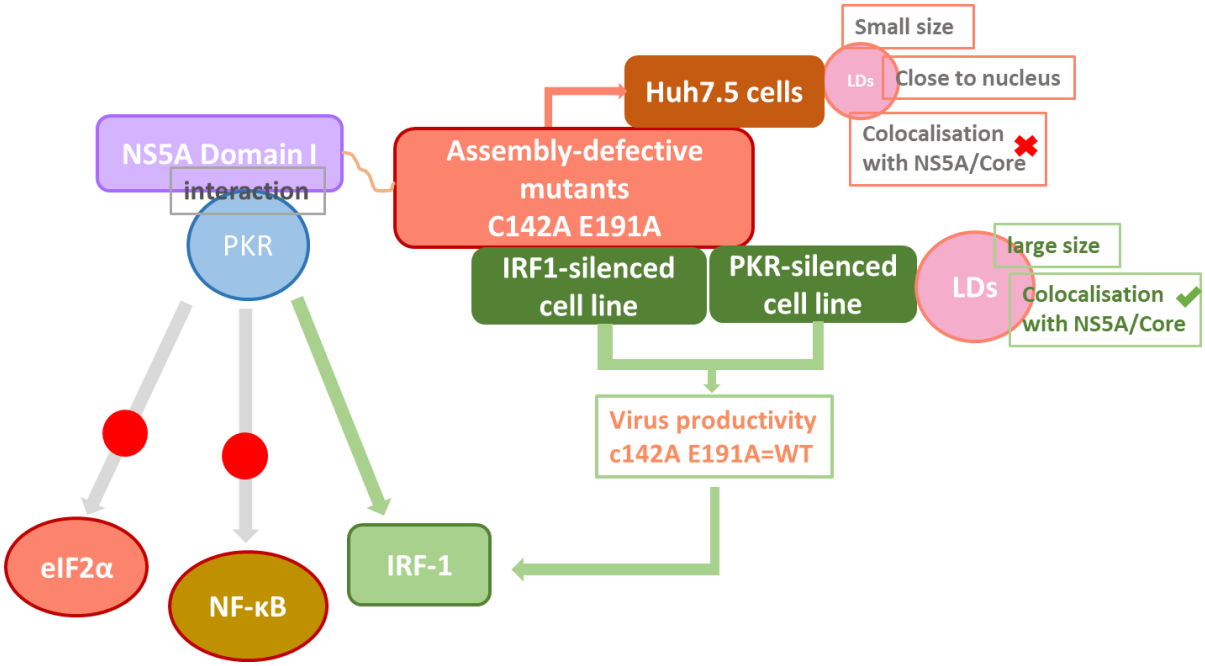

Fig 6.12 The mechanism for PKR to regulate HCV viral assembly through IRF1.

Two residues (C142 and E191) were disrupted the production of infectious virus particles. LD formation and the co-localisation between Core, NS5A and LDs were disrupted in cells infected with these two mutants. Silencing of either PKR or the downstream factor IRF1 restored the production of infectious virus, LD size and co-localisation with Core and NS5A for these two mutants. NS5A DI functions to allow HCV to evade inhibition of virus assembly by PKR and IRF1 and uncovers a hitherto unidentified function of PKR to inhibit virus assembly.

PKR silencing also restored the LD phenotype (Figs 6.3 and 6.4), suggesting that activated PKR functions to block virus assembly through regulating LD mophology. The only factor that did not recover in C142A and E191A when PKR was depleted was the LD distance to the nucleus (Fig 6.5). The LDs became larger and were transported away from the nucleus during HCV infection (Yin et al., 2018). However, LDs were still distributed around the nucleus even though the phenotype of C142A and E191A disappeared. The results were intriguing as PKR can partially disrupt LD characters in NS5A DI phenotype mutants. Interestingly, PERK, which has the same function as PKR in RNA translation, is an important sensor to regulate ER stress and can be

activated by unfolded protein response (UPR) (Fels and Koumenis, 2006, Harding et al., 2000). Given the proposed role of LD formation can also regulate ER stress (Zhang and Zhang, 2012), I hypothesised PKR also can modulate ER stress during HCV infection through regulating LD formation. The active spliced XBP1 (XBP1s) reflecting the ER stress showed slight decrease in C142A and E191A in Huh7.5 cells but was increased to WT level in Huh7.5 PKR silenced cell line (Fig 6.12). This result suggested that PKR attenuated the ER stress in C142A and E191A presumably due to the modulation of LD formation, thereby indicating that PKR can further regulate LD even if it fails to affect the LD distribution.

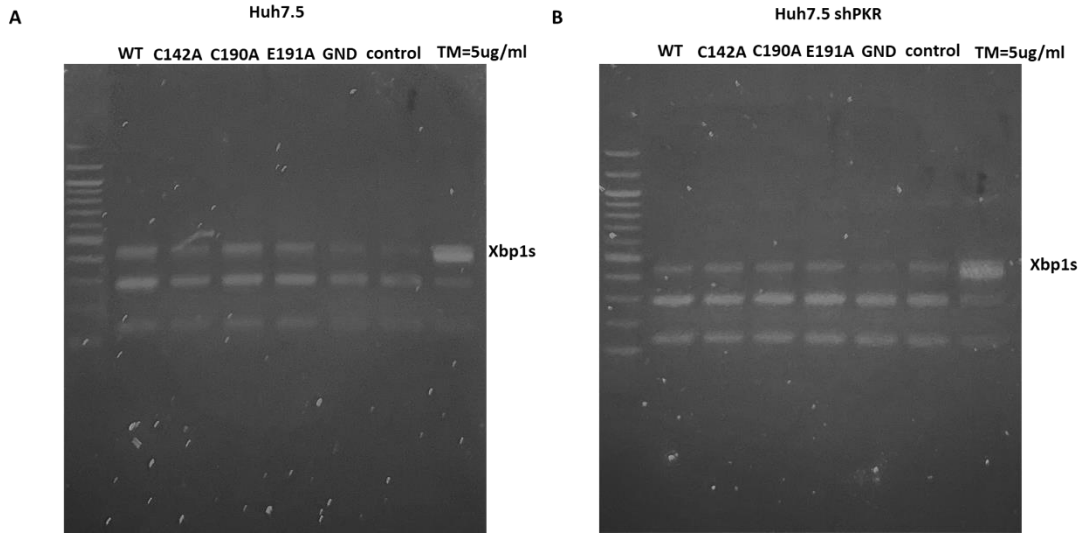

Fig 6.13 ER stress was restored for C142A and E191A in the loss of PKR.

In vitro transcripts of mJFH-1 and related mutants were electroporated into Huh7.5 cells **(A)** and Huh7.5 PKR silenced cell line **(B)**. Total RNAs in cells harvested using Trizol at 72hpe were reverse transcribed to cDNA and then amplified using Xbp1 primers. PCR products were analysed by gel electrophoresis. Tunicamycin was used as a positive control to induce the ER stress.

The data suggest that neither eIF2α phosphorylation, nor activation of NFκB, are involved in the block to virus assembly (Fig 6.9 and 6.10), although these analyses

were performed at 72 hpe and we cannot rule out transient effects at earlier times. PKR also activates IRF1, the silencing of which also restores the function of the virus assembly mutants. The implication of this observation is that one or more proteins whose expression is IRF1-dependent function to block virus assembly. In this regard a recent study (Yamane et al., 2019) identified a number of IRF1 regulated genes (PSMB9, ApoL1 and MX1), which when silenced enhanced HCV replication approximately 3-fold. Overexpression of PSMB9 (a component of the proteosome) led to a 10-fold increase in HCV virus production, but a specific effect on virus assembly for ApoL1 and MX1 was not investigated. Whilst these factors may play a role, it is unlikely that they explain the 1000-fold reduction in virus production exhibited by C142A, which is completely restored by either PKR or IRF1 silencing. Of note ApoL1 (apolipoprotein L1) is an LD associated protein and, whilst other apolipoproteins have been implicated in HCV assembly (eg ApoE), the role of ApoL1 has not been investigated (Hueging et al., 2015). The recruitment of ApoL1 to LDs is regulated by DGAT-1 (Chun et al., 2022), which is required for HCV assembly and recruits both NS5A and Core to LDs (Camus et al., 2013, Herker et al., 2010). ApoL1 may therefore be an antiviral effector induced by PKR that acts on LD morphology to block virus assembly.

In conclusion, NS5A DI can evade PKR activated antiviral pathways through blocking its activation to promote the HCV assembly and production. This study contributed to the understanding of how PKR modulates the LD formation and further demonstrates that downstream factor IRF1 participates in the regulation of HCV assembly. This study thoroughly investigated the mechanism of the role of NS5A DI and PKR in virus assembly.

Chapter 7: Conclusions and future perspectives

This study is based on a previous study which showed that residues V67 and P145 in non-structural protein 5A (NS5A) domain I (DI) played an essential role in viral assembly but were dispensable for RNA replication (Yin et al., 2018). This research, for the first time, revealed the novel function of NS5A DI in assembly, whereas the mechanism was still unclear. Therefore, this study aims to observe the broad-spectrum of this novel function in NS5A DI and explore the mechanism for this specific phenotype which were partially defective in replication and completely abrogative in assembly.

The surface-exposed residues proximal to V67 and P145 screened by Pymol showed three replication phenotypes after alanine mutagenesis analysis. I52, G70 and M72 proximal to V67, or P141 and E148 proximal to P145 exhibited the same phenotype as V67/P145, which showed reduced replication in Huh7 cells and were restored to wildtype (WT) levels in Huh7.5. S71 proximal to V67, or C142, Q143, P147, C190 and E191 proximal to P145 were dispensable for genome replication in either Huh7 or Huh7.5 cells. P102, Y106, W111 and F149 proximal to P145 were absolutely required for genome replication in both Huh7 and Huh7.5 cell lines, so these four residues were excluded from assembly phenotype analysis. Interestingly, the mutagenesis analysis of these replication-defective residues in genotype 3 (DBN3) showed some different phenotypes. NS5A DI was highly conserved in all HCV genotypes, these residues showed different phenotypes with JFH1 and might be a breakthrough for overcoming the DAAs resistance in DBN3.

The mutagenesis analysis in JFH1 full-length virus demonstrated two residues (C142 and E191) displayed the same assembly phenotype as V67/P145A in Huh7.5 cells. Interestingly, all residues (I52, G70, M72, P141 and E148) showed the same replication phenotype as V67/P145A, whereas they maintained the full viral production

ability in Huh7.5 cells. These different phenotypes indicated the role of NS5A in HCV replication and assembly. NS5A has a role in transporting nascent RNA from sites of replication to assembly sites via lipid droplets (LDs) within the cytoplasm (Boson et al., 2017, Zayas et al., 2016). The colocalisation analysis showed C142A and E191A altered the morphology of LDs and disrupted the colocalisation with the core or LDs. These results further identified the role of NS5A DI in RNA transportation to the surface on LDs between HCV replication and assembly. The interaction between NS5A DI with other NS proteins associated with replicase complex and host factors required for viral assembly can be further investigated.

Therefore, the mechanism and the involvement of host factors for HCV replication and assembly were important to investigate. This study demonstrated the interaction between Cyclophilin A (CypA) and NS5A DI through *in vitro* pull-down assay and this interaction relied on peptidylprolyl isomerase (PPIase) activity of CypA. The NS5A DI partially defective mutants and CypA silenced cells were also exploited to observe the CypA involvement in NS5A DI-associated HCV replication. In addition, the interaction between CypA and NS5A DI also modulated the NF-kB pathway during the viral replication but not viral production. The CypA binding sites in HCV has been reported in NS5A DII and DIII (Chatterji et al., 2010, Foster et al., 2011, Hanoulle et al., 2009a). This study initially revealed that CypA also interacted with NS5A DI to regulate HCV replication and to inhibit the activity of NF-kB pathway to further promote HCV evasion from antiviral pathway. Cyclosporin A (CsA) acts as a potentially antiviral reagent for HCV treatment (Inoue et al., 2003, Inoue and Yoshiba, 2005), the therapy mechanism still needs to be further investigate. To date, the resistance to the DAA is still a severe challenge for HCV therapy, more mechanistic analysis of CsA function need to be confirmed. NS5A DI has also been identified to be the putative target for one class of

DAAs, this study explored the potential action model of CsA treatment and provide the reference to other compounds. However, NS5A DI in DBN3 did not exhibit association with CypA in this study, resulting from the absolute dependence on CypA in full-length DBN3. The detailed interaction sites with CypA in DBN3 still need to be further explored.

In contrast, double-stranded RNA (dsRNA)-activated protein kinase (PKR) interacted with NS5A DI to modulate HCV assembly but not replication. All mutants maintained the replication capacity in PKR silenced cells further demonstrating that PKR had no effect on RNA replication via NS5A DI. The interaction between PKR and NS5A DI has been identified to modulate HCV assembly via downstream interferon regulatory factor-1 (IRF1). HCV exploited several proteins including NS5A to inhibit PKR activity and further escape the antiviral function of innate immune pathway. However, the mechanism is still not fully understood. This study further revealed the role of NS5A DI in blocking PKR activity to facilitate HCV assembly, indicating the potential therapeutic function of PKR inhibitor. The role of PKR inhibitor such as C16 in HCV therapy can be further investigated. In addition, the downstream factors of IRF1 also worth studying. Various factors downstream of IRF1 have been demonstrated to be affected due to the loss of IRF1, such as PSMB9, ApoL1 and MX1. The silence or overexpression of these downstream factors can be further utilised to demonstrate whether they are also involved in modulating HCV assembly. PKR has been reported to target NS5A DII Interferon sensitive determinant region (ISDR) (Enomoto et al., 1996). The co-function between NS5A DI and DII in HCV assembly still needs to be further demonstrated.

PKR was also identified to affect the amount of double-stranded RNA (dsRNA) during viral assembly. PKR can be activated by dsRNA and the Core protein of HCV, further

inducing antiviral response (Dey et al., 2005). DsRNA is generated as a replication intermediate is transported from replication sites to assembly sites by NS5A and co-localises with NS5A, Core and LDs (Targett-Adams et al., 2008b). This study firstly indicated that PKR had a role in degrading dsRNA through interacting with NS5A in assembly-defective mutants. More HCV evasion mechanism can be further identified through Core, E2, NS5A (different domain) and NS5B.

The mutant C142A in NS5A DI has been observed to completely abrogate HCV assembly. This result is interesting because C142 and C190 form the disulphide bond in NS5A DI, which has been demonstrated to be dispensable for HCV replication and only exists in the NS5A DI opened conformation 1ZH1 but not closed conformation 3FQM (Tellinghuisen et al., 2005). This study further identified the role of disulphide bond in assembly, suggesting the crystal structure 1ZH1 might be involved in HCV assembly. Notably, C190 had no effect on HCV assembly even though it formed a disulphide bond bond with C142. However, the mechanism behind these residues require further exploration. It has been hypothesised that C142 played more important role in disulphide bond formation and might bind to other residues or C142A in the other dimer to construct a newly disulphide bond to maintain viral assembly. Notably, the two disulphide bond residues in the Core protein (C128 and C184) showed the same replication and assembly phenotypes (Kushima et al., 2010), suggesting the co-function of Core and NS5A protein in HCV assembly. The connection of disulphide bond residues in these two viral proteins might affect the Core/NS5A interaction and the colocalisation of core and NS5A on the surface of LDs. Interestingly, the disulphide bond mutant C128A in the core protein had no effect on modulating morphology of LDs, whereas the mutant C142A in NS5A DI altered the LD distribution, size and

colocalisation. This result indicated the structure stability of NS5A is more important to the colocalisation and LD morphology than core protein.

The mutant E191A in NS5A DI also affected HCV assembly but was not as essential as C142A. Notably, E191A cannot completely express NS5A in the replication-independent expression system of replicase proteins. Based on the location of E191A which is proximal to disulphide bond, this result further suggests that disulphide bond was dispensable for RNA replication but played essential role in viral assembly. Furthermore, the NS5A antibody I used to detect NS5A expression targets NS5A DIII. The disrupted expression of NS5A in E191A might indicate the binding between NS5A DI and DIII during HCV assembly. DIII is considered dispensable for HCV replication but is absolutely required for HCV assembly. It needs to be further investigated whether the role of NS5A DI in viral assembly requires the involvement of NS5A DIII.

The location of all residues was referenced from the NS5A DI crystal structure in genotype 1b. However, the structural homology of NS5A DI between genotype 1b and genotype 2a (JFH1) is still unclear. Although the structure of JFH1 NS5A DI can be predicted using alphafold, it is important to understand the actual NS5A DI structure and provide the reference to further research on JFH1 genome replication and viral assembly. The purified NS5A DI (35-215) (35-249) and mutants are the best samples to use for the research of protein structures.

The host factors mechanism of this novel role of NS5A DI in replication and assembly has been identified in this study. The NS5A DI/Core interaction modulated the activity of NF-kB pathway to facilitate HCV RNA replication. Additionally, NS5A DI interacted with PKR and modulated its downstream factor IRF1 to block PKR activity, which further promoted HCV assembly. However, the correlation with other NS5A domains

or other viral proteins and the mechanism in different phenotypes (especially DBN3) need more experiments to demonstrate.

In this study, we confirmed the novel role of NS5A DI in HCV genome replication and viral particles assembly. The interaction between CypA and NS5A DI inhibited NF-κB pathway to further promote HCV replication, whereas the interaction was not involved in modulating HCV viral assembly. One possible explanation of these replication results is that NS5A DI interacts with CypA which is considered to protect NS5A/replicase complex from NF-kB-mediated inhibition of HCV genome replication. After RNA replication, nascent RNA is transported from sites of replication to sites of assembly which is guided by NS5A. NS5A DI is involved in the evasion of antiviral pathway during viral assembly through interacting with PKR and blocking PKR activity. Another potential mechanism of this process is that NS5A DI protect nascent RNA from transiently exposure in the cytosol, avoiding detection by PKR and other cytosolic sensors (Fig 7.1).

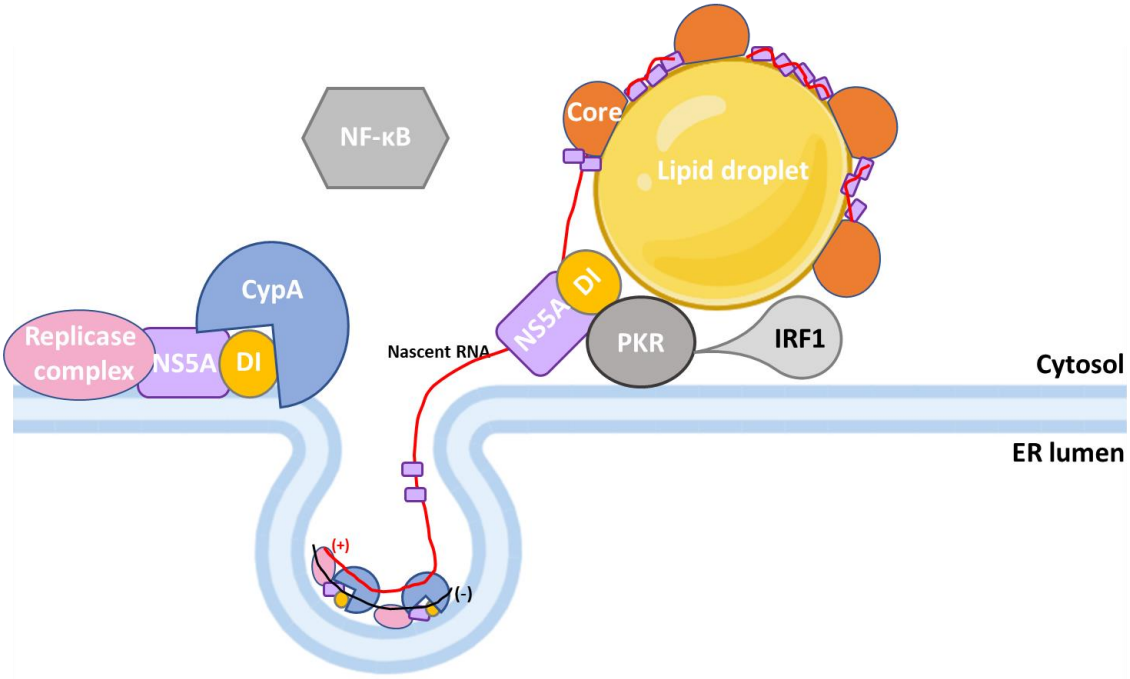

Fig 7.1 Working mechanism for the proposed roles of NS5A DI in virus genome replication and assembly.

Chapter 8 References

ACTON, S., RIGOTTI, A., LANDSCHULZ, K. T., XU, S., HOBBS, H. H. & KRIEGER, M. 1996. Identification of scavenger receptor SR-BI as a high density lipoprotein receptor. *Science,* 271**,** 518-520.

ADAMS, R. L., PIRAKITIKULR, N. & PYLE, A. M. 2017. Functional RNA structures throughout the Hepatitis C Virus genome. *Current opinion in virology,* 24**,** 79-86.

AHMED-BELKACEM, A., COLLIANDRE, L., AHNOU, N., NEVERS, Q., GELIN, M., BESSIN, Y., BRILLET, R., CALA, O., DOUGUET, D. & BOURGUET, W. 2016. Fragment-based discovery of a new family of non-peptidic small-molecule cyclophilin inhibitors with potent antiviral activities. *Nature communications,* 7**,** 1-11.

AIZAWA, Y., SEKI, N., NAGANO, T. & ABE, H. 2015. Chronic hepatitis C virus infection and lipoprotein metabolism. *World Journal of Gastroenterology: WJG,* 21**,** 10299.

ALISI, A., MELE, R., SPAZIANI, A., TAVOLARO, S., PALESCANDOLO, E. & BALSANO, C. 2005. Thr 446 phosphorylation of PKR by HCV core protein deregulates G2/M phase in HCC cells. *Journal of cellular physiology,* 205**,** 25-31.

ALTER, M. J. 2007. Epidemiology of hepatitis C virus infection. *World journal of gastroenterology: WJG,* 13**,** 2436.

AMAKO, Y., SARKESHIK, A., HOTTA, H., YATES III, J. & SIDDIQUI, A. 2009. Role of oxysterol binding protein in hepatitis C virus infection. *Journal of virology,* 83**,** 9237-9246.

ANDERSON, L. J., LIN, K., COMPTON, T. & WIEDMANN, B. 2011. Inhibition of cyclophilins alters lipid trafficking and blocks hepatitis C virus secretion. *Virology journal,* 8**,** 1-13.

ANDRE, P., KOMURIAN-PRADEL, F., DEFORGES, S., PERRET, M., BERLAND, J., SODOYER, M., POL, S., BRECHOT, C., PARANHOS-BACCALA, G. & LOTTEAU, V. 2002. Characterization of low-and very-low-density hepatitis C virus RNA-containing particles. *Journal of virology,* 76**,** 6919-6928.

ANDRIULLI, A., MANGIA, A., IACOBELLIS, A., IPPOLITO, A., LEANDRO, G. & ZEUZEM, S. 2008. Metaâ€analysis: the outcome of antiâ€viral therapy in HCV genotype 2 and genotype 3 infected patients with chronic hepatitis. *Alimentary pharmacology & therapeutics,* 28**,** 397-404.

ANSALDI, F., ORSI, A., STICCHI, L., BRUZZONE, B. & ICARDI, G. 2014. Hepatitis C virus in the new era: perspectives in epidemiology, prevention, diagnostics and predictors of response to therapy. *World journal of gastroenterology: WJG,* 20**,** 9633.

APPEL, N., PIETSCHMANN, T. & BARTENSCHLAGER, R. 2005. Mutational analysis of hepatitis C virus nonstructural protein 5A: potential role of differential phosphorylation in RNA replication and identification of a genetically flexible domain. *Journal of virology,* 79**,** 3187-3194.

APPEL, N., SCHALLER, T., PENIN, F. & BARTENSCHLAGER, R. 2006. From structure to function: new insights into hepatitis C virus RNA replication. *Journal of Biological Chemistry,* 281**,** 9833-9836.

APPEL, N., ZAYAS, M., MILLER, S., KRIJNSE-LOCKER, J., SCHALLER, T., FRIEBE, P., KALLIS, S., ENGEL, U. & BARTENSCHLAGER, R. 2008. Essential role of domain III of nonstructural protein 5A for hepatitis C virus infectious particle assembly. *PLoS pathogens,* 4**,** e1000035.

AQIB, S. M., MUNIR, B. & HUSSAIN, A. 2021. S3416 A Comparison of Sensitivity and Specificity of Transient Elastography ie Fibro Scan With Serum Aminotransferase Levels ie ALT and AST in Chronic HCV-Infected Patients. *Official journal of the American College of Gastroenterology| ACG,* 116**,** S1403.

ARGENTINI, C., GENOVESE, D., DETTORI, S. & RAPICETTA, M. 2009. HCV genetic variability: from quasispecies evolution to genotype classification.

ARIUMI, Y., KUROKI, M., MAKI, M., IKEDA, M., DANSAKO, H., WAKITA, T. & KATO, N. 2011. The ESCRT system is required for hepatitis C virus production. *PloS one,* 6**,** e14517.

ARNAUD, N., DABO, S., AKAZAWA, D., FUKASAWA, M., SHINKAI-OUCHI, F., HUGON, J., WAKITA, T. & MEURS, E. F. 2011. Hepatitis C virus reveals a novel early control in acute immune response. *PLoS pathogens,* 7**,** e1002289.

ARNAUD, N., DABO, S., MAILLARD, P., BUDKOWSKA, A., KALLIAMPAKOU, K. I., MAVROMARA, P., GARCIN, D., HUGON, J., GATIGNOL, A. & AKAZAWA, D. 2010. Hepatitis C virus controls interferon production through PKR activation. *PloS one,* 5**,** e10575.

ASSELAH, T. & MARCELLIN, P. 2012. Direct acting antivirals for the treatment of chronic hepatitis C: one pill a day for tomorrow. *Liver International,* 32**,** 88-102.

BACKES, P., QUINKERT, D., REISS, S., BINDER, M., ZAYAS, M., RESCHER, U., GERKE, V., BARTENSCHLAGER, R. & LOHMANN, V. 2010. Role of annexin A2 in the production of infectious hepatitis C virus particles. *Journal of virology,* 84**,** 5775-5789.

BACON, B. R., GORDON, S. C., LAWITZ, E., MARCELLIN, P., VIERLING, J. M., ZEUZEM, S., POORDAD, F., GOODMAN, Z. D., SINGS, H. L. & BOPARAI, N. 2011. Boceprevir for previously treated chronic HCV genotype 1 infection. *New England Journal of Medicine,* 364**,** 1207-1217.

BAECHLEIN, C., FISCHER, N., GRUNDHOFF, A., ALAWI, M., INDENBIRKEN, D., POSTEL, A., BARON, A. L., OFFINGER, J., BECKER, K. & BEINEKE, A. 2015. Identification of a novel hepacivirus in domestic cattle from Germany. *Journal of virology,* 89**,** 7007-7015.

BANKWITZ, D., STEINMANN, E., BITZEGEIO, J., CIESEK, S., FRIESLAND, M., HERRMANN, E., ZEISEL, M. B., BAUMERT, T. F., KECK, Z.-Y. & FOUNG, S. K. 2010. Hepatitis C virus hypervariable region 1 modulates receptor interactions, conceals the CD81 binding site, and protects conserved neutralizing epitopes. *Journal of virology,* 84**,** 5751-5763.

BARBA, G., HARPER, F., HARADA, T., KOHARA, M., GOULINET, S., MATSUURA, Y., EDER, G., SCHAFF, Z., CHAPMAN, M. & MIYAMURA, T. 1997. Hepatitis C virus core protein shows a cytoplasmic localization and associates to cellular lipid storage droplets. *Proceedings of the National Academy of Sciences,* 94**,** 1200-1205.

BAROUCH-BENTOV, R., NEVEU, G., XIAO, F., BEER, M., BEKERMAN, E., SCHOR, S., CAMPBELL, J., BOONYARATANAKORNKIT, J., LINDENBACH, B. & LU, A. 2016. Hepatitis C virus proteins interact with the endosomal sorting complex required for transport (ESCRT) machinery via ubiquitination to facilitate viral envelopment. *MBio,* 7**,** e01456-16.

BARTENSCHLAGER, R., LOHMANN, V., WILKINSON, T. & KOCH, J. O. 1995. Complex formation between the NS3 serine-type proteinase of the hepatitis C virus and NS4A and its importance for polyprotein maturation. *Journal of virology,* 69**,** 7519-7528.

BARTENSCHLAGER, R., PENIN, F., LOHMANN, V. & ANDRÉ, P. 2011. Assembly of infectious hepatitis C virus particles. *Trends in microbiology,* 19**,** 95-103.

BENGA, W. J., KRIEGER, S. E., DIMITROVA, M., ZEISEL, M. B., PARNOT, M., LUPBERGER, J., HILDT, E., LUO, G., MCLAUCHLAN, J. & BAUMERT, T. F. 2010. Apolipoprotein E interacts with hepatitis C virus nonstructural protein 5A and determines assembly of infectious particles. *Hepatology,* 51**,** 43-53.

BENNETT, J. E., DOLIN, R. & BLASER, M. J. 2019. *Mandell, douglas, and bennett's principles and practice of infectious diseases E-book*, Elsevier Health Sciences.

BERGER, K. L., COOPER, J. D., HEATON, N. S., YOON, R., OAKLAND, T. E., JORDAN, T. X., MATEU, G., GRAKOUI, A. & RANDALL, G. 2009. Roles for endocytic trafficking and phosphatidylinositol 4-kinase III alpha in hepatitis C virus replication. *Proceedings of the National Academy of Sciences,* 106**,** 7577-7582.

BIANCO, A., REGHELLIN, V., DONNICI, L., FENU, S., ALVAREZ, R., BARUFFA, C., PERI, F., PAGANI, M., ABRIGNANI, S. & NEDDERMANN, P. 2012. Metabolism of phosphatidylinositol 4-kinase IIIα-dependent PI4P Is subverted by HCV and is targeted by a 4-anilino quinazoline with antiviral activity. *PLoS pathogens,* 8**,** e1002576.

BINDER, M., KOCHS, G., BARTENSCHLAGER, R. & LOHMANN, V. 2007. Hepatitis C virus escape from the interferon regulatory factor 3 pathway by a passive and active evasion strategy. *Hepatology,* 46**,** 1365-1374.

BLIGHT, K. J., KOLYKHALOV, A. A. & RICE, C. M. 2000. Efficient initiation of HCV RNA replication in cell culture. *Science,* 290**,** 1972-1974.

BLIGHT, K. J., MCKEATING, J. A. & RICE, C. M. 2002. Highly permissive cell lines for subgenomic and genomic hepatitis C virus RNA replication. *Journal of virology,* 76**,** 13001-13014.

BOBARDT, M., CHATTERJI, U., LIM, P., GAWLIK, K. & GALLAY, P. 2014. Both cyclophilin inhibitors and direct-acting antivirals prevent PKR activation in HCV-infected cells. *The open virology journal,* 8**,** 1.

BONNET, M. C., DAURAT, C., OTTONE, C. & MEURS, E. F. 2006. The N-terminus of PKR is responsible for the activation of the NF-κB signaling pathway by interacting with the IKK complex. *Cellular signalling,* 18**,** 1865-1875.

BONNET, M. C., WEIL, R., DAM, E., HOVANESSIAN, A. G. & MEURS, E. F. 2000. PKR stimulates NF-κB irrespective of its kinase function by interacting with the IκB kinase complex. *Molecular and cellular biology,* 20**,** 4532-4542.

BOREL, J. F., FEURER, C., GUBLER, H. & STÄHELIN, H. 1994. Biological effects of cyclosporin A: a new antilymphocytic agent. *Agents and actions,* 43**,** 179-186.

BOSON, B., DENOLLY, S., TURLURE, F., CHAMOT, C., DREUX, M. & COSSET, F.-L. 2017. Daclatasvir prevents hepatitis C virus infectivity by blocking transfer of the viral genome to assembly sites. *Gastroenterology,* 152**,** 895-907. e14.

BOSON, B., GRANIO, O., BARTENSCHLAGER, R. & COSSET, F.-L. 2011. A concerted action of hepatitis C virus p7 and nonstructural protein 2 regulates core localization at the endoplasmic reticulum and virus assembly. *PLoS pathogens,* 7**,** e1002144.

BOULANT, S., DOUGLAS, M. W., MOODY, L., BUDKOWSKA, A., TARGETT‐ADAMS, P. & MCLAUCHLAN, J. 2008. Hepatitis C virus core protein induces lipid droplet redistribution in a microtubule‐ and dynein‐dependent manner. *Traffic,* 9**,** 1268-1282.

BOULANT, S., TARGETT-ADAMS, P. & MCLAUCHLAN, J. 2007. Disrupting the association of hepatitis C virus core protein with lipid droplets correlates with a loss in production of infectious virus. *Journal of general virology,* 88**,** 2204-2213.

BRADLEY, D., MCCAUSTLAND, K., KRAWCZYNSKI, K., SPELBRING, J., HUMPHEY, C. & COOK, E. 1991. Hepatitis C virus: Buoyant density if the factor VIII‐derived isolate in sucrose. *Journal of medical virology,* 34**,** 206-208.

BRADLEY, D. W., MCCAUSTLAND, K. A., COOK, E., SCHABLE, C. A., EBERT, J. W. & MAYNARD, J. E. 1985. Posttransfusion non-A, non-B hepatitis in chimpanzees: physicochemical evidence that the tubule-forming agent is a small, enveloped virus. *Gastroenterology,* 88**,** 773-779.

BRADRICK, S. S., WALTERS, R. W. & GROMEIER, M. 2006. The hepatitis C virus 3â€²-untranslated region or a poly (A) tract promote efficient translation subsequent to the initiation phase. *Nucleic acids research,* 34**,** 1293-1303.

BRASS, V., BERKE, J. M., MONTSERRET, R., BLUM, H. E., PENIN, F. & MORADPOUR, D. 2008. Structural determinants for membrane association and dynamic organization of the hepatitis C virus NS3-4A complex. *Proceedings of the National Academy of Sciences,* 105**,** 14545-14550.

BRASS, V., BIECK, E., MONTSERRET, R., WÖLK, B., HELLINGS, J. A., BLUM, H. E., PENIN, F. & MORADPOUR, D. 2002. An amino-terminal amphipathic α-helix mediates membrane association of the hepatitis C virus nonstructural protein 5A. *Journal of Biological Chemistry,* 277**,** 8130-8139.

BRAZZOLI, M., BIANCHI, A., FILIPPINI, S., WEINER, A., ZHU, Q., PIZZA, M. & CROTTA, S. 2008. CD81 is a central regulator of cellular events required for hepatitis C virus infection of human hepatocytes. *Journal of virology,* 82**,** 8316-8329.

BRESSANELLI, S., TOMEI, L., ROUSSEL, A., INCITTI, I., VITALE, R. L., MATHIEU, M., DE FRANCESCO, R. & REY, F. A. 1999. Crystal structure of the RNA-dependent RNA polymerase of hepatitis C virus. *Proceedings of the National Academy of Sciences,* 96**,** 13034-13039.

BUKH, J. 2016. The history of hepatitis C virus (HCV): Basic research reveals unique features in phylogeny, evolution and the viral life cycle with new perspectives for epidemic control. *Journal of hepatology,* 65**,** S2-S21.

BUKH, J., MILLER, R. H. & PURCELL, R. H. Genetic heterogeneity of hepatitis C virus: quasispecies and genotypes. Seminars in liver disease, 1995. © 1995 by Thieme Medical Publishers, Inc., 41-63.

BUKH, J., PURCELL, R. H. & MILLER, R. H. 1992. Sequence analysis of the 5'noncoding region of hepatitis C virus. *Proceedings of the National Academy of Sciences,* 89**,** 4942-4946.

BUKH, J., PURCELL, R. H. & MILLER, R. H. 1993. At least 12 genotypes of hepatitis C virus predicted by sequence analysis of the putative E1 gene of isolates collected worldwide. *Proceedings of the National Academy of Sciences,* 90**,** 8234-8238.

BUKH, J., PURCELL, R. H. & MILLER, R. H. 1994. Sequence analysis of the core gene of 14 hepatitis C virus genotypes. *Proceedings of the National Academy of Sciences,* 91**,** 8239-8243.

BUNG, C., BOCHKAEVA, Z., TERENIN, I., ZINOVKIN, R., SHATSKY, I. & NIEPMANN, M. 2010. Influence of the hepatitis C virus 3â€²-untranslated region on IRES-dependent and cap-dependent translation initiation. *FEBS letters,* 584**,** 837-842.

BURBELO, P. D., DUBOVI, E. J., SIMMONDS, P., MEDINA, J. L., HENRIQUEZ, J. A., MISHRA, N., WAGNER, J., TOKARZ, R., CULLEN, J. M. & IADAROLA, M. J. 2012. Serology-enabled discovery of genetically diverse hepaciviruses in a new host. *Journal of virology,* 86**,** 6171-6178.

BUSCH, M. 2001. Insights into the epidemiology, natural history and pathogenesis of hepatitis C virus infection from studies of infected donors and blood product recipients. *Transfusion clinique et biologique,* 8**,** 200-206.

CALLENS, N., CICZORA, Y., BARTOSCH, B., VU-DAC, N., COSSET, F. O.-L. C., PAWLOTSKY, J.-M., PENIN, F. O. & DUBUISSON, J. 2005. Basic residues in hypervariable region 1 of hepatitis C virus envelope glycoprotein e2 contribute to virus entry. *Journal of virology,* 79**,** 15331-15341.

CAMUS, G., HERKER, E., MODI, A. A., HAAS, J. T., RAMAGE, H. R., FARESE, R. V. & OTT, M. 2013. Diacylglycerol acyltransferase-1 localizes hepatitis C virus NS5A protein to lipid droplets and enhances NS5A interaction with the viral capsid core. *Journal of Biological Chemistry,* 288**,** 9915-9923.

CARRÈRE-KREMER, S., MONTPELLIER-PALA, C., COCQUEREL, L., WYCHOWSKI, C., PENIN, F. & DUBUISSON, J. 2002. Subcellular localization and topology of the p7 polypeptide of hepatitis C virus. *Journal of virology,* 76**,** 3720-3730.

CARRERE-KREMER, S., MONTPELLIER, C., LORENZO, L., BRULIN, B., COCQUEREL, L., BELOUZARD, S., PENIN, F. & DUBUISSON, J. 2004. Regulation of hepatitis C virus polyprotein processing by signal peptidase involves structural determinants at the p7 sequence junctions. *Journal of Biological Chemistry,* 279**,** 41384-41392.

CATANESE, M. T., URYU, K., KOPP, M., EDWARDS, T. J., ANDRUS, L., RICE, W. J., SILVESTRY, M., KUHN, R. J. & RICE, C. M. 2013. Ultrastructural analysis of hepatitis C virus particles. *Proceedings of the National Academy of Sciences,* 110**,** 9505-9510.

CESARO, T. & MICHIELS, T. 2021. Inhibition of PKR by Viruses. *Frontiers in microbiology,* 12.

CHAN, A., PATEL, K. & NAGGIE, S. 2017. Genotype 3 infection: the last stand of hepatitis C virus. *Drugs,* 77**,** 131-144.

CHAN, P.-L., LE, L.-V., ISHIKAWA, N. & EASTERBROOK, P. 2021. Regional progress towards hepatitis C elimination in the Western Pacific Region, 2015-2020. *Global Health & Medicine,* 3**,** 253-261.

CHANG, H. W., WATSON, J. C. & JACOBS, B. L. 1992. The E3L gene of vaccinia virus encodes an inhibitor of the interferon-induced, double-stranded RNA-dependent protein kinase. *Proceedings of the National Academy of Sciences,* 89**,** 4825-4829.

CHANG, S. C., YEN, J.-H., KANG, H.-Y., JANG, M.-H. & CHANG, M.-F. 1994. Nuclear localization signals in the core protein of hepatitis C virus. *Biochemical and biophysical research communications,* 205**,** 1284-1290.

CHAO, T.-C., SU, W.-C., HUANG, J.-Y., CHEN, Y.-C., JENG, K.-S., WANG, H.-D. & LAI, M. M. 2012. Proline-serine-threonine phosphatase-interacting protein 2 (PSTPIP2), a host membrane-deforming protein, is critical for membranous web formation in hepatitis C virus replication. *Journal of virology,* 86**,** 1739-1749.

CHATTERJI, U., BOBARDT, M., SELVARAJAH, S., YANG, F., TANG, H., SAKAMOTO, N., VUAGNIAUX, G., PARKINSON, T. & GALLAY, P. 2009. The isomerase active site of cyclophilin A is critical for hepatitis C virus replication. *Journal of Biological Chemistry,* 284**,** 16998-17005.

CHATTERJI, U., BOBARDT, M., TAI, A., WOOD, M. & GALLAY, P. A. 2015. Cyclophilin and NS5A inhibitors, but not other anti-hepatitis C virus (HCV) agents, preclude HCV-mediated formation of double-membrane-vesicle viral factories. *Antimicrobial agents and chemotherapy,* 59**,** 2496-2507.

CHATTERJI, U., LIM, P., BOBARDT, M. D., WIELAND, S., CORDEK, D. G., VUAGNIAUX, G., CHISARI, F., CAMERON, C. E., TARGETT-ADAMS, P. & PARKINSON, T. 2010. HCV resistance to cyclosporin A does not correlate with a resistance of the NS5A–cyclophilin A interaction to cyclophilin inhibitors. *Journal of hepatology,* 53**,** 50-56.

CHAYAMA, K., SUZUKI, F., SUZUKI, Y., TOYOTA, J., KARINO, Y., KAWAKAMI, Y., FUJIYAMA, S., ITO, T., ITOH, Y. & TAMURA, E. All-oral dual combination of daclatasvir plus asunaprevir compared with telaprevir plus peginterferon alfa/ribavirin in treatment-naive Japanese patients chronically infected with HCV genotype 1b: results from a phase 3 study. Hepatology, 2014. WILEY-BLACKWELL 111 RIVER ST, HOBOKEN 07030-5774, NJ USA, 1135A-1135A.

CHAYAMA, K., TAKAHASHI, S., TOYOTA, J., KARINO, Y., IKEDA, K., ISHIKAWA, H., WATANABE, H., MCPHEE, F., HUGHES, E. & KUMADA, H. 2012. Dual therapy with the nonstructural protein 5A inhibitor, daclatasvir, and the nonstructural protein 3 protease inhibitor, asunaprevir, in hepatitis C virus genotype 1bâ€"infected null responders. *Hepatology,* 55**,** 742-748.

CHEN, S. L. & MORGAN, T. R. 2006. The natural history of hepatitis C virus (HCV) infection. *International journal of medical sciences,* 3**,** 47.

CHEN, Y.-C., SU, W.-C., HUANG, J.-Y., CHAO, T.-C., JENG, K.-S., MACHIDA, K. & LAI, M. M. 2010. Polo-like kinase 1 is involved in hepatitis C virus replication by hyperphosphorylating NS5A. *Journal of virology,* 84**,** 7983-7993.

CHONG, W. M., HSU, S.-C., KAO, W.-T., LO, C.-W., LEE, K.-Y., SHAO, J.-S., CHEN, Y.-H., CHANG, J., CHEN, S. S.-L. & YU, M.-J. 2016. Phosphoproteomics identified an NS5A phosphorylation site involved in hepatitis C virus replication. *Journal of Biological Chemistry,* 291**,** 3918-3931.

CHOO, Q.-L., KUO, G., WEINER, A. J., OVERBY, L. R., BRADLEY, D. W. & HOUGHTON, M. 1989. Isolation of a cDNA clone derived from a blood-borne non-A, non-B viral hepatitis genome. *Science,* 244**,** 359-362.

CHOU, A.-H., TSAI, H.-F., WU, Y.-Y., HU, C.-Y., HWANG, L.-H., HSU, P.-I. & HSU, P.-N. 2005. Hepatitis C virus core protein modulates TRAIL-mediated apoptosis by enhancing Bid cleavage and activation of mitochondria apoptosis signaling pathway. *The Journal of Immunology,* 174**,** 2160-2166.

CHUN, J., RIELLA, C. V., CHUNG, H., SHAH, S. S., WANG, M., MAGRANER, J. M., RIBAS, G. T., RIBAS, H. T., ZHANG, J.-Y. & ALPER, S. L. 2022. DGAT2 Inhibition Potentiates Lipid Droplet Formation To Reduce Cytotoxicity in APOL1 Kidney Risk Variants. *Journal of the American Society of Nephrology,* 33**,** 889-907.

CLIPSTONE, N. A. & CRABTREE, G. R. 1992. Identification of calcineurin as a key signalling enzyme in T-lymphocyte activation. *Nature,* 357**,** 695-697.

COCQUEREL, L., MEUNIER, J.-C., PILLEZ, A., WYCHOWSKI, C. & DUBUISSON, J. 1998. A retention signal necessary and sufficient for endoplasmic reticulum localization maps to the transmembrane domain of hepatitis C virus glycoprotein E2. *Journal of virology,* 72**,** 2183-2191.

COCQUEREL, L., VOISSET, C. & DUBUISSON, J. 2006. Hepatitis C virus entry: potential receptors and their biological functions. *Journal of General Virology,* 87**,** 1075-1084.

COCQUEREL, L., WYCHOWSKI, C., MINNER, F., PENIN, F. O. & DUBUISSON, J. 2000. Charged residues in the transmembrane domains of hepatitis C virus glycoproteins play a major role in the processing, subcellular localization, and assembly of these envelope proteins. *Journal of virology,* 74**,** 3623-3633.

COELMONT, L., HANOULLE, X., CHATTERJI, U., BERGER, C., SNOECK, J., BOBARDT, M., LIM, P., VLIEGEN, I., PAESHUYSE, J. & VUAGNIAUX, G. 2010. DEB025 (Alisporivir) inhibits hepatitis C virus replication by preventing a cyclophilin A induced cis-trans isomerisation in domain II of NS5A. *PloS one,* 5**,** e13687.

COLE, J. L. 2007. Activation of PKR: an open and shut case? *Trends in biochemical sciences,* 32**,** 57-62.
COLLER, K. E., HEATON, N. S., BERGER, K. L., COOPER, J. D., SAUNDERS, J. L. & RANDALL, G. 2012. Molecular determinants and dynamics of hepatitis C virus secretion. *PLoS pathogens,* 8**,** e1002466.
COLPITTS, C. C., RIDEWOOD, S., SCHNEIDERMAN, B., WARNE, J., TABATA, K., NG, C. F., BARTENSCHLAGER, R., SELWOOD, D. L. & TOWERS, G. J. 2020. Hepatitis C virus exploits cyclophilin A to evade PKR. *Elife,* 9**,** e52237.
CORDEK, D. G., CROOM-PEREZ, T. J., HWANG, J., HARGITTAI, M. R., SUBBA-REDDY, C. V., HAN, Q., LODEIRO, M. F., NING, G., MCCRORY, T. S. & ARNOLD, J. J. 2014. Expanding the proteome of an RNA virus by phosphorylation of an intrinsically disordered viral protein. *Journal of Biological Chemistry,* 289**,** 24397-24416.
CORLESS, L., CRUMP, C. M., GRIFFIN, S. D. & HARRIS, M. 2010. Vps4 and the ESCRT-III complex are required for the release of infectious hepatitis C virus particles. *Journal of General Virology,* 91**,** 362-372.
CORMAN, V. M., GRUNDHOFF, A., BAECHLEIN, C., FISCHER, N., GMYL, A., WOLLNY, R., DEI, D., RITZ, D., BINGER, T. & ADANKWAH, E. 2015. Highly divergent hepaciviruses from African cattle. *Journal of Virology,* 89**,** 5876-5882.
CORNBERG, M., TACKE, F. & KARLSEN, T. H. 2019. Clinical Practice Guidelines of the European Association for the study of the Liverâ€“Advancing methodology but preserving practicability. *Journal of Hepatology,* 70**,** 5-7.
COUNIHAN, N. A., RAWLINSON, S. M. & LINDENBACH, B. D. 2011. Trafficking of hepatitis C virus core protein during virus particle assembly. *PLoS pathogens,* 7**,** e1002302.
COX, A. L., NETSKI, D. M., MOSBRUGER, T., SHERMAN, S. G., STRATHDEE, S., OMPAD, D., VLAHOV, D., CHIEN, D., SHYAMALA, V. & RAY, S. C. 2005. Prospective evaluation of community-acquired acute-phase hepatitis C virus infection. *Clinical Infectious Diseases,* 40**,** 951-958.
DA COSTA, D., TUREK, M., FELMLEE, D. J., GIRARDI, E., PFEFFER, S., LONG, G., BARTENSCHLAGER, R., ZEISEL, M. B. & BAUMERT, T. F. 2012. Reconstitution of the entire hepatitis C virus life cycle in nonhepatic cells. *Journal of virology,* 86**,** 11919-11925.
DABO, S. & MEURS, E. F. 2012. dsRNA-dependent protein kinase PKR and its role in stress, signaling and HCV infection. *Viruses,* 4**,** 2598-2635.
DAITO, T., WATASHI, K., SLUDER, A., OHASHI, H., NAKAJIMA, S., BORROTO-ESODA, K., FUJITA, T. & WAKITA, T. 2014. Cyclophilin inhibitors reduce phosphorylation of RNA-dependent protein kinase to restore expression of IFN-stimulated genes in HCV-infected cells. *Gastroenterology,* 147**,** 463-472.
DAR, A. C., DEVER, T. E. & SICHERI, F. 2005. Higher-order substrate recognition of eIF2α by the RNA-dependent protein kinase PKR. *Cell,* 122**,** 887-900.
DAVIS, G. L. 1999. Hepatitis C virus genotypes and quasispecies. *The American journal of medicine,* 107**,** 21-26.
DAVIS, G. L., BALART, L. A., SCHIFF, E. R., LINDSAY, K., BODENHEIMER JR, H. C., PERRILLO, R. P., CAREY, W., JACOBSON, I. M., PAYNE, J. & DIENSTAG, J. L. 1989. Treatment of chronic hepatitis C with recombinant interferon alfa. *New England journal of medicine,* 321**,** 1501-1506.
DAVIS, T. L., WALKER, J. R., CAMPAGNA-SLATER, V., FINERTY JR, P. J., PARAMANATHAN, R., BERNSTEIN, G., MACKENZIE, F., TEMPEL, W., OUYANG, H. & LEE, W. H. 2010. Structural and biochemical characterization of the human cyclophilin family of peptidyl-prolyl isomerases. *PLoS biology,* 8**,** e1000439.
DE CLERCQ, E. 2013. Dancing with chemical formulae of antivirals: A panoramic view (Part 2). *Biochemical pharmacology,* 86**,** 1397-1410.
DE FRANCESCO, R., URBANI, A., NARDI, M. C., TOMEI, L., STEINKÜHLER, C. & TRAMONTANO, A. 1996. A zinc binding site in viral serine proteinases. *Biochemistry,* 35**,** 13282-13287.
DE WILDE, A. H., PHAM, U., POSTHUMA, C. C. & SNIJDER, E. J. 2018. Cyclophilins and cyclophilin inhibitors in nidovirus replication. *Virology,* 522**,** 46-55.

DEGASPERI, E., AGHEMO, A. & COLOMBO, M. 2015. Daclatasvir for the treatment of chronic hepatitis C. *Expert Opinion on Pharmacotherapy,* 16**,** 2679-2688.

DEINHARDT, F., HOLMES, A., CAPPS, R. & POPPER, H. 1967. Studies on the transmission of human viral hepatitis to marmoset monkeys: I. Transmission of disease, serial passages, and description of liver lesions. *The Journal of experimental medicine,* 125**,** 673-688.

DEN BOON, J. A. & AHLQUIST, P. 2010. Organelle-like membrane compartmentalization of positive-strand RNA virus replication factories. *Annual review of microbiology,* 64**,** 241-256.

DENOLLY, S., GRANIER, C., FONTAINE, N., POZZETTO, B., BOURLET, T., GUÉRIN, M. & COSSET, F.-L. 2019. A serum protein factor mediates maturation and apoB-association of HCV particles in the extracellular milieu. *Journal of hepatology,* 70**,** 626-638.

DENOLLY, S., MIALON, C., BOURLET, T., AMIRACHE, F., PENIN, F., LINDENBACH, B., BOSON, B. & COSSET, F.-L. 2017. The amino-terminus of the hepatitis C virus (HCV) p7 viroporin and its cleavage from glycoprotein E2-p7 precursor determine specific infectivity and secretion levels of HCV particle types. *PLoS pathogens,* 13**,** e1006774.

DEUFFIC‐BURBAN, S., POYNARD, T., SULKOWSKI, M. & WONG, J. 2007. Estimating the future health burden of chronic hepatitis C and human immunodeficiency virus infections in the United States. *Journal of viral hepatitis,* 14**,** 107-115.

DEY, M., CAO, C., DAR, A. C., TAMURA, T., OZATO, K., SICHERI, F. & DEVER, T. E. 2005. Mechanistic link between PKR dimerization, autophosphorylation, and eIF2α substrate recognition. *Cell,* 122**,** 901-913.

DIAZ, A., WANG, X. & AHLQUIST, P. 2010. Membrane-shaping host reticulon proteins play crucial roles in viral RNA replication compartment formation and function. *Proceedings of the National Academy of Sciences,* 107**,** 16291-16296.

DOLGANIUC, A., KODYS, K., KOPASZ, A., MARSHALL, C., DO, T., ROMICS, L., MANDREKAR, P., ZAPP, M. & SZABO, G. 2003. Hepatitis C virus core and nonstructural protein 3 proteins induce pro-and anti-inflammatory cytokines and inhibit dendritic cell differentiation. *The Journal of Immunology,* 170**,** 5615-5624.

DORE, G. J., HELLARD, M., MATTHEWS, G. V., GREBELY, J., HABER, P. S., PETOUMENOS, K., YEUNG, B., MARKS, P., VAN BEEK, I. & MCCAUGHAN, G. 2010. Effective treatment of injecting drug users with recently acquired hepatitis C virus infection. *Gastroenterology,* 138**,** 123-135. e2.

DORE, G. J., LAWITZ, E., HÃ©ZODE, C., SHAFRAN, S. D., RAMJI, A., TATUM, H. A., TALIANI, G., TRAN, A., BRUNETTO, M. R. & ZALTRON, S. 2015. Daclatasvir plus peginterferon and ribavirin is noninferior to peginterferon and ribavirin alone, and reduces the duration of treatment for HCV genotype 2 or 3 infection. *Gastroenterology,* 148**,** 355-366. e1.

DORNAN, J., TAYLOR, P. & WALKINSHAW, M. D. 2003. Structures of immunophilins and their ligand complexes. *Current topics in medicinal chemistry,* 3**,** 1392-1409.

DREUX, M., BOSON, B., RICARD-BLUM, S., MOLLE, J., LAVILLETTE, D., BARTOSCH, B., PÉCHEUR, E.-I. & COSSET, F.-L. 2007. The exchangeable apolipoprotein ApoC-I promotes membrane fusion of hepatitis C virus. *Journal of Biological Chemistry,* 282**,** 32357-32369.

DREUX, M., DAO THI, V. L., FRESQUET, J., GUÉRIN, M., JULIA, Z., VERNEY, G., DURANTEL, D., ZOULIM, F., LAVILLETTE, D. & COSSET, F.-L. 2009. Receptor complementation and mutagenesis reveal SR-BI as an essential HCV entry factor and functionally imply its intra-and extra-cellular domains. *PLoS pathogens,* 5**,** e1000310.

DREXLER, J. F., CORMAN, V. M., MÜLLER, M. A., LUKASHEV, A. N., GMYL, A., COUTARD, B., ADAM, A., RITZ, D., LEIJTEN, L. M. & VAN RIEL, D. 2013. Evidence for novel hepaciviruses in rodents. *PLoS pathogens,* 9**,** e1003438.

DUBUISSON, J. & COSSET, F.-L. 2014. Virology and cell biology of the hepatitis C virus life cycle–An update. *Journal of hepatology,* 61**,** S3-S13.

DUBUISSON, J., PENIN, F. O. & MORADPOUR, D. 2002. Interaction of hepatitis C virus proteins with host cell membranes and lipids. *Trends in cell biology,* 12**,** 517-523.

DUJARDIN, M., MADAN, V., GANDHI, N. S., CANTRELLE, F.-X., LAUNAY, H., HUVENT, I., BARTENSCHLAGER, R., LIPPENS, G. & HANOULLE, X. 2019. Cyclophilin A allows the allosteric regulation of a structural motif in the disordered domain 2 of NS5A and thereby fine-tunes HCV RNA replication. *Journal of Biological Chemistry,* 294**,** 13171-13185.

DUMOULIN, F. L., VON DEM BUSSCHE, A., LI, J., KHAMZINA, L., WANDS, J. R., SAUERBRUCH, T. & SPENGLER, U. 2003. Hepatitis C virus NS2 protein inhibits gene expression from different cellular and viral promoters in hepatic and nonhepatic cell lines. *Virology,* 305**,** 260-266.

DVORY-SOBOL, H., PANG, P. S. & GLENN, J. S. 2010. The future of HCV therapy: NS4B as an antiviral target. *Viruses,* 2**,** 2481-2492.

DZANANOVIC, E., MCKENNA, S. A. & PATEL, T. R. 2018. Viral proteins targeting host protein kinase R to evade an innate immune response: a mini review. *Biotechnology and Genetic Engineering Reviews,* 34**,** 33-59.

E KARANGELIS, D., KANAKIS, I., P ASIMAKOPOULOU, A., KAROUSOU, E., PASSI, A., D THEOCHARIS, A., TRIPOSKIADI, F., B TSILIMINGAS, N. & K KARAMANOS, N. 2010. Glycosaminoglycans as key molecules in atherosclerosis: the role of versican and hyaluronan. *Current medicinal chemistry,* 17**,** 4018-4026.

EGGER, D., WÖLK, B., GOSERT, R., BIANCHI, L., BLUM, H. E., MORADPOUR, D. & BIENZ, K. 2002. Expression of hepatitis C virus proteins induces distinct membrane alterations including a candidate viral replication complex. *Journal of virology,* 76**,** 5974-5984.

EHRENFELD, E. & HUNT, T. 1971. Double-stranded poliovirus RNA inhibits initiation of protein synthesis by reticulocyte lysates. *Proceedings of the National Academy of Sciences,* 68**,** 1075-1078.

EINAV, S., ELAZAR, M., DANIELI, T. & GLENN, J. S. 2004. A nucleotide binding motif in hepatitis C virus (HCV) NS4B mediates HCV RNA replication. *Journal of virology,* 78**,** 11288-11295.

ELAZAR, M., CHEONG, K. H., LIU, P., GREENBERG, H. B., RICE, C. M. & GLENN, J. S. 2003. Amphipathic helix-dependent localization of NS5A mediates hepatitis C virus RNA replication. *Journal of virology,* 77**,** 6055-6061.

ELAZAR, M., LIU, P., RICE, C. M. & GLENN, J. S. 2004. An N-terminal amphipathic helix in hepatitis C virus (HCV) NS4B mediates membrane association, correct localization of replication complex proteins, and HCV RNA replication. *Journal of virology,* 78**,** 11393-11400.

ENOMOTO, N., SAKUMA, I., ASAHINA, Y., KUROSAKI, M., MURAKAMI, T., YAMAMOTO, C., OGURA, Y., IZUMI, N., MARUMO, F. & SATO, C. 1996. Mutations in the nonstructural protein 5A gene and response to interferon in patients with chronic hepatitis C virus 1b infection. *New England Journal of Medicine,* 334**,** 77-82.

ERDTMANN, L., FRANCK, N., LERAT, H., LE SEYEC, J., GILOT, D., CANNIE, I., GRIPON, P., HIBNER, U. & GUGUEN-GUILLOUZO, C. 2003. The hepatitis C virus NS2 protein is an inhibitor of CIDE-B-induced apoptosis. *Journal of Biological Chemistry,* 278**,** 18256-18264.

EVANS, M. J., RICE, C. M. & GOFF, S. P. 2004. Phosphorylation of hepatitis C virus nonstructural protein 5A modulates its protein interactions and viral RNA replication. *Proceedings of the National Academy of Sciences,* 101**,** 13038-13043.

FEINSTONE, S. M., KAPIKIAN, A. Z., PURCELL, R. H., ALTER, H. J. & HOLLAND, P. V. 1975. Transfusion-associated hepatitis not due to viral hepatitis type A or B. *New England Journal of Medicine,* 292**,** 767-770.

FELS, D. R. & KOUMENIS, C. 2006. The PERK/eIF2α/ATF4 module of the UPR in hypoxia resistance and tumor growth. *Cancer biology & therapy,* 5**,** 723-728.

FENG, G. S., CHONG, K., KUMAR, A. & WILLIAMS, B. 1992. Identification of double-stranded RNA-binding domains in the interferon-induced double-stranded RNA-activated p68 kinase. *Proceedings of the National Academy of Sciences,* 89**,** 5447-5451.

FERNANDES, F., ANSARI, I.-U. H. & STRIKER, R. 2010. Cyclosporine inhibits a direct interaction between cyclophilins and hepatitis C NS5A. *PLoS One,* 5**,** e9815.

FERNANDES, F., POOLE, D. S., HOOVER, S., MIDDLETON, R., ANDREI, A. C., GERSTNER, J. & STRIKER, R. 2007. Sensitivity of hepatitis C virus to cyclosporine A depends on nonstructural proteins NS5A and NS5B. *Hepatology,* 46**,** 1026-1033.

FERRARIS, P., BEAUMONT, E., UZBEKOV, R., BRAND, D., GAILLARD, J., BLANCHARD, E. & ROINGEARD, P. 2013. Sequential biogenesis of host cell membrane rearrangements induced by hepatitis C virus infection. *Cellular and Molecular Life Sciences,* 70**,** 1297-1306.

FERRARIS, P., BLANCHARD, E. & ROINGEARD, P. 2010. Ultrastructural and biochemical analyses of hepatitis C virus-associated host cell membranes. *Journal of General Virology,* 91**,** 2230-2237.

FEUERSTEIN, S., SOLYOM, Z., ALADAG, A., FAVIER, A., SCHWARTEN, M., HOFFMANN, S., WILLBOLD, D. & BRUTSCHER, B. 2012. Transient structure and SH3 interaction sites in an intrinsically disordered fragment of the hepatitis C virus protein NS5A. *Journal of molecular biology,* 420**,** 310-323.

FIRTH, C., BHAT, M., FIRTH, M. A., WILLIAMS, S. H., FRYE, M. J., SIMMONDS, P., CONTE, J. M., NG, J., GARCIA, J. & BHUVA, N. P. 2014. Detection of zoonotic pathogens and characterization of novel viruses carried by commensal Rattus norvegicus in New York City. *MBio,* 5**,** e01933-14.

FLINT, M. & MCKEATING, J. A. 2000. The role of the hepatitis C virus glycoproteins in infection. *Reviews in medical virology,* 10**,** 101-117.

FOSTER, T. L., BELYAEVA, T., STONEHOUSE, N. J., PEARSON, A. R. & HARRIS, M. 2010. All three domains of the hepatitis C virus nonstructural NS5A protein contribute to RNA binding. *Journal of virology,* 84**,** 9267-9277.

FOSTER, T. L., GALLAY, P., STONEHOUSE, N. J. & HARRIS, M. 2011. Cyclophilin A interacts with domain II of hepatitis C virus NS5A and stimulates RNA binding in an isomerase-dependent manner. *Journal of virology,* 85**,** 7460-7464.

FRANCK, N., LE SEYEC, J., GUGUEN-GUILLOUZO, C. & ERDTMANN, L. 2005. Hepatitis C virus NS2 protein is phosphorylated by the protein kinase CK2 and targeted for degradation to the proteasome. *Journal of virology,* 79**,** 2700-2708.

FRICK, D. N., RYPMA, R. S., LAM, A. M. & GU, B. 2004. The nonstructural protein 3 protease/helicase requires an intact protease domain to unwind duplex RNA efficiently. *Journal of Biological Chemistry,* 279**,** 1269-1280.

FRIDELL, R. A., VALERA, L., QIU, D., KIRK, M. J., WANG, C. & GAO, M. 2013. Intragenic complementation of hepatitis C virus NS5A RNA replication-defective alleles. *Journal of virology,* 87**,** 2320-2329.

FRIDELL, R. A., WANG, C., SUN, J. H., O'BOYLE, D. R., NOWER, P., VALERA, L., QIU, D., ROBERTS, S., HUANG, X. & KIENZLE, B. 2011. Genotypic and phenotypic analysis of variants resistant to hepatitis C virus nonstructural protein 5A replication complex inhibitor BMS‐790052 in humans: in vitro and in vivo correlations. *Hepatology,* 54**,** 1924-1935.

FRIED, M. W. & HOOFNAGLE, J. H. Therapy of hepatitis C. Seminars in liver disease, 1995. Â© 1995 by Thieme Medical Publishers, Inc., 82-91.

FRIED, M. W., SHIFFMAN, M. L., REDDY, K. R., SMITH, C., MARINOS, G., GONÃ§ALES JR, F. L., HÃ¤USSINGER, D., DIAGO, M., CAROSI, G. & DHUMEAUX, D. 2002. Peginterferon alfa-2a plus ribavirin for chronic hepatitis C virus infection. *New England journal of medicine,* 347**,** 975-982.

FROMENTIN, R. M., MAJEAU, N., GAGNÃ©, M.-E. L., BOIVIN, A., DUVIGNAUD, J.-B. & LECLERC, D. 2007. A method for in vitro assembly of hepatitis C virus core protein and for screening of inhibitors. *Analytical biochemistry,* 366**,** 37-45.

GALE JR, M., BLAKELY, C. M., KWIECISZEWSKI, B., TAN, S.-L., DOSSETT, M., TANG, N. M., KORTH, M. J., POLYAK, S. J., GRETCH, D. R. & KATZE, M. G. 1998. Control of PKR protein kinase by hepatitis C virus nonstructural 5A protein: molecular mechanisms of kinase regulation. *Molecular and cellular biology,* 18**,** 5208-5218.

GALE JR, M. J., KORTH, M. J., TANG, N. M., TAN, S.-L., HOPKINS, D. A., DEVER, T. E., POLYAK, S. J., GRETCH, D. R. & KATZE, M. G. 1997. Evidence that hepatitis C virus resistance to interferon is mediated through repression of the PKR protein kinase by the nonstructural 5A protein. *Virology,* 230**,** 217-227.

GALLARDO-FLORES, C. E. & COLPITTS, C. C. 2021. Cyclophilins and their roles in hepatitis C virus and flavivirus infections: Perspectives for novel antiviral approaches. *Pathogens,* 10**,** 902.

GAO, L., AIZAKI, H., HE, J.-W. & LAI, M. M. 2004. Interactions between viral nonstructural proteins and host protein hVAP-33 mediate the formation of hepatitis C virus RNA replication complex on lipid raft. *Journal of virology,* 78**,** 3480-3488.

GARCIA, M., GIL, J., VENTOSO, I., GUERRA, S., DOMINGO, E., RIVAS, C. & ESTEBAN, M. 2006. Impact of protein kinase PKR in cell biology: from antiviral to antiproliferative action. *Microbiology and Molecular Biology Reviews,* 70**,** 1032-1060.

GARCIA, M., MEURS, E. & ESTEBAN, M. 2007. The dsRNA protein kinase PKR: virus and cell control. *Biochimie,* 89**,** 799-811.

GASTAMINZA, P., CHENG, G., WIELAND, S., ZHONG, J., LIAO, W. & CHISARI, F. V. 2008. Cellular determinants of hepatitis C virus assembly, maturation, degradation, and secretion. *Journal of virology,* 82**,** 2120-2129.

GASTAMINZA, P., DRYDEN, K. A., BOYD, B., WOOD, M. R., LAW, M., YEAGER, M. & CHISARI, F. V. 2010. Ultrastructural and biophysical characterization of hepatitis C virus particles produced in cell culture. *Journal of virology,* 84**,** 10999-11009.

GASTAMINZA, P., KAPADIA, S. B. & CHISARI, F. V. 2006. Differential biophysical properties of infectious intracellular and secreted hepatitis C virus particles. *Journal of virology,* 80**,** 11074-11081.

GAWLIK, K. & GALLAY, P. A. 2014. HCV core protein and virus assembly: what we know without structures. *Immunologic research,* 60**,** 1-10.

GEDDAWY, A., IBRAHIM, Y. F., ELBAHIE, N. M. & IBRAHIM, M. A. 2017. Direct acting anti-hepatitis C virus drugs: clinical pharmacology and future direction. *Journal of translational internal medicine,* 5**,** 8-17.

GENTZSCH, J., BROHM, C., STEINMANN, E., FRIESLAND, M., MENZEL, N., VIEYRES, G., PERIN, P. M., FRENTZEN, A., KADERALI, L. & PIETSCHMANN, T. 2013. Hepatitis C virus p7 is critical for capsid assembly and envelopment. *PLoS pathogens,* 9**,** e1003355.

GIL, J. & ESTEBAN, M. 2000. Induction of apoptosis by the dsRNA-dependent protein kinase (PKR): mechanism of action. *Apoptosis,* 5**,** 107-114.

GIL, J., GARCíA, M. A. & ESTEBAN, M. 2002. Caspase 9 activation by the dsRNA-dependent protein kinase, PKR: molecular mechanism and relevance. *FEBS letters,* 529**,** 249-255.

GIL, J., GARCÍA, M. A., GOMEZ-PUERTAS, P., GUERRA, S., RULLAS, J., NAKANO, H., ALCAMÍ, J. & ESTEBAN, M. 2004. TRAF family proteins link PKR with NF-κB activation. *Molecular and cellular biology,* 24**,** 4502-4512.

GOH, K. C., DEVEER, M. J. & WILLIAMS, B. R. 2000. The protein kinase PKR is required for p38 MAPK activation and the innate immune response to bacterial endotoxin. *The EMBO journal,* 19**,** 4292-4297.

GONG, Y. & CUN, W. 2019. The role of apoe in HCV infection and comorbidity. *International journal of molecular sciences,* 20**,** 2037.

GONZALEZ, M. E. & CARRASCO, L. 2003. Viroporins. *FEBS letters,* 552**,** 28-34.

GOONAWARDANE, N., GEBHARDT, A., BARTLETT, C., PICHLMAIR, A. & HARRIS, M. 2017. Phosphorylation of serine 225 in hepatitis C virus NS5A regulates protein-protein interactions. *Journal of virology,* 91**,** e00805-17.

GOSERT, R., EGGER, D., LOHMANN, V., BARTENSCHLAGER, R., BLUM, H. E., BIENZ, K. & MORADPOUR, D. 2003. Identification of the hepatitis C virus RNA replication complex in Huh-7 cells harboring subgenomic replicons. *Journal of virology,* 77**,** 5487-5492.

GOTO, K., WATASHI, K., MURATA, T., HISHIKI, T., HIJIKATA, M. & SHIMOTOHNO, K. 2006. Evaluation of the anti-hepatitis C virus effects of cyclophilin inhibitors, cyclosporin A, and NIM811. *Biochemical and biophysical research communications,* 343**,** 879-884.

GOUKLANI, H., BULL, R. A., BEYER, C., COULIBALY, F., GOWANS, E. J., DRUMMER, H. E., NETTER, H. J., WHITE, P. A. & HAQSHENAS, G. 2012. Hepatitis C virus nonstructural protein 5B is involved in virus morphogenesis. *Journal of virology,* 86**,** 5080-5088.

GOUTTENOIRE, J., CASTET, V., MONTSERRET, R., ARORA, N., RAUSSENS, V., RUYSSCHAERT, J.-M., DIESIS, E., BLUM, H. E., PENIN, F. & MORADPOUR, D. 2009a. Identification of a novel determinant for membrane association in hepatitis C virus nonstructural protein 4B. *Journal of virology,* 83**,** 6257-6268.

GOUTTENOIRE, J., MONTSERRET, R., KENNEL, A., PENIN, F. & MORADPOUR, D. 2009b. An amphipathic α-helix at the C terminus of hepatitis C virus nonstructural protein 4B mediates membrane association. *Journal of virology,* 83**,** 11378-11384.

GOUTTENOIRE, J., PENIN, F. & MORADPOUR, D. 2010a. Hepatitis C virus nonstructural protein 4B: a journey into unexplored territory. *Reviews in medical virology,* 20**,** 117-129.

GOUTTENOIRE, J., ROINGEARD, P., PENIN, F. & MORADPOUR, D. 2010b. Amphipathic α-helix AH2 is a major determinant for the oligomerization of hepatitis C virus nonstructural protein 4B. *Journal of virology,* 84**,** 12529-12537.

GRAKOUI, A., MCCOURT, D. W., WYCHOWSKI, C., FEINSTONE, S. M. & RICE, C. M. 1993a. A second hepatitis C virus-encoded proteinase. *Proceedings of the National Academy of Sciences,* 90**,** 10583-10587.

GRAKOUI, A., WYCHOWSKI, C., LIN, C., FEINSTONE, S. & RICE, C. 1993b. Expression and identification of hepatitis C virus polyprotein cleavage products. *Journal of virology,* 67**,** 1385-1395.

GREBELY, J., DORE, G. J., KIM, A. Y., LLOYD, A., SHOUKRY, N. H., PRINS, M. & PAGE, K. 2014. Genetics of spontaneous clearance of hepatitis C virus infection: a complex topic with much to learn. *Hepatology,* 60**,** 2127-2128.

GREBELY, J., MATTHEWS, G., PETOUMENOS, K. & DORE, G. 2010. Spontaneous clearance and the beneficial impact of treatment on clearance during recent hepatitis C virus infection. *Journal of viral hepatitis,* 17**,** 896-896.

GREEN, S. R. & MATHEWS, M. B. 1992. Two RNA-binding motifs in the double-stranded RNA-activated protein kinase, DAI. *Genes & development,* 6**,** 2478-2490.

GRETTON, S. N., TAYLOR, A. I. & MCLAUCHLAN, J. 2005. Mobility of the hepatitis C virus NS4B protein on the endoplasmic reticulum membrane and membrane-associated foci. *Journal of general virology,* 86**,** 1415-1421.

GRIFFIN, S., CLARKE, D., MCCORMICK, C., ROWLANDS, D. & HARRIS, M. 2005. Signal peptide cleavage and internal targeting signals direct the hepatitis C virus p7 protein to distinct intracellular membranes. *Journal of virology,* 79**,** 15525-15536.

GRIFFIN, S. D., BEALES, L. P., CLARKE, D. S., WORSFOLD, O., EVANS, S. D., JAEGER, J., HARRIS, M. P. & ROWLANDS, D. J. 2003. The p7 protein of hepatitis C virus forms an ion channel that is blocked by the antiviral drug, Amantadine. *FEBS letters,* 535**,** 34-38.

GRIFFIN, S. D., HARVEY, R., CLARKE, D. S., BARCLAY, W. S., HARRIS, M. & ROWLANDS, D. J. 2004. A conserved basic loop in hepatitis C virus p7 protein is required for amantadine-sensitive ion channel activity in mammalian cells but is dispensable for localization to mitochondria. *Journal of General Virology,* 85**,** 451-461.

GRISÉ, H., FRAUSTO, S., LOGAN, T. & TANG, H. 2012. A conserved tandem cyclophilin-binding site in hepatitis C virus nonstructural protein 5A regulates Alisporivir susceptibility. *Journal of virology,* 86**,** 4811-4822.

GUERRA, S., LÓPEZ-FERNÁNDEZ, L. A., GARCÍA, M. A., ZABALLOS, A. & ESTEBAN, M. 2006. Human gene profiling in response to the active protein kinase, interferon-induced serine/threonine protein kinase (PKR), in infected cells: Involvement of the transcription factor ATF-3 in PKR-induced apoptosis. *Journal of Biological Chemistry,* 281**,** 18734-18745.

GUO, M., PEI, R., YANG, Q., CAO, H., WANG, Y., WU, C., CHEN, J., ZHOU, Y., HU, X. & LU, M. 2015. Phosphatidylserine-specific phospholipase A1 involved in hepatitis C virus assembly through NS2 complex formation. *Journal of virology,* 89**,** 2367-2377.

HAJARIZADEH, B., GREBELY, J. & DORE, G. J. 2013. Epidemiology and natural history of HCV infection. *Nature reviews Gastroenterology & hepatology,* 10**,** 553-562.

HAMAMOTO, I., NISHIMURA, Y., OKAMOTO, T., AIZAKI, H., LIU, M., MORI, Y., ABE, T., SUZUKI, T., LAI, M. M. & MIYAMURA, T. 2005. Human VAP-B is involved in hepatitis C virus replication through interaction with NS5A and NS5B. *Journal of virology,* 79**,** 13473-13482.

HANDSCHUMACHER, R. E., HARDING, M. W., RICE, J., DRUGGE, R. J. & SPEICHER, D. W. 1984. Cyclophilin: a specific cytosolic binding protein for cyclosporin A. *Science,* 226**,** 544-547.

HANES, S. D. 2015. Prolyl isomerases in gene transcription. *Biochimica et Biophysica Acta (BBA)-General Subjects,* 1850**,** 2017-2034.

HANOULLE, X., BADILLO, A., WIERUSZESKI, J.-M., VERDEGEM, D., LANDRIEU, I., BARTENSCHLAGER, R., PENIN, F. & LIPPENS, G. 2009a. Hepatitis C virus NS5A protein is a substrate for the peptidyl-prolyl cis/trans isomerase activity of cyclophilins A and B. *Journal of Biological Chemistry,* 284**,** 13589-13601.

HANOULLE, X., VERDEGEM, D., BADILLO, A., WIERUSZESKI, J.-M., PENIN, F. & LIPPENS, G. 2009b. Domain 3 of non-structural protein 5A from hepatitis C virus is natively unfolded. *Biochemical and biophysical research communications,* 381**,** 634-638.

HARDING, H. P., ZHANG, Y., BERTOLOTTI, A., ZENG, H. & RON, D. 2000. Perk is essential for translational regulation and cell survival during the unfolded protein response. *Molecular cell,* 5**,** 897-904.

HARDING, M. W., HANDSCHUMACHER, R. & SPEICHER, D. 1986. Isolation and amino acid sequence of cyclophilin. *Journal of Biological Chemistry,* 261**,** 8547-8555.

HARRIS, H. J., DAVIS, C., MULLINS, J. G., HU, K., GOODALL, M., FARQUHAR, M. J., MEE, C. J., MCCAFFREY, K., YOUNG, S. & DRUMMER, H. 2010. Claudin association with CD81 defines hepatitis C virus entry. *Journal of Biological Chemistry,* 285**,** 21092-21102.

HARTLAGE, A. S., CULLEN, J. M. & KAPOOR, A. 2016. The strange, expanding world of animal hepaciviruses. *Annual review of virology,* 3**,** 53.

HASSAN, M., SELIMOVIC, D., GHOZLAN, H. & ABDELÂ€KADER, O. 2009. Hepatitis C virus core protein triggers hepatic angiogenesis by a mechanism including multiple pathways. *Hepatology,* 49**,** 1469-1482.

HDOUFANE, I., BJIJ, I., OUBAHMANE, M., SOLIMAN, M. E., VILLEMIN, D. & CHERQAOUI, D. 2022. In silico design and analysis of NS4B inhibitors against hepatitis C virus. *Journal of Biomolecular Structure and Dynamics,* 40**,** 1915-1929.

HE, L.-F., ALLING, D., POPKIN, T., SHAPIRO, M., ALTER, H. J. & PURCELL, R. H. 1987. Determining the size of non-A, non-B hepatitis virus by filtration. *Journal of Infectious Diseases,* 156**,** 636-640.

HE, Y., STASCHKE, K. A. & TAN, S.-L. 2006. HCV NS5A: a multifunctional regulator of cellular pathways and virus replication. *Hepatitis C viruses: genomes and molecular biology*.

HE, Y., TAN, S.-L., TAREEN, S. U., VIJAYSRI, S., LANGLAND, J. O., JACOBS, B. L. & KATZE, M. G. 2001. Regulation of mRNA translation and cellular signaling by hepatitis C virus nonstructural protein NS5A. *Journal of Virology,* 75**,** 5090-5098.

HEIM, M. H. & THIMME, R. 2014. Innate and adaptive immune responses in HCV infections. *Journal of hepatology,* 61**,** S14-S25.

HERBST, D. A. & REDDY, K. R. 2013. NS5A inhibitor, daclatasvir, for the treatment of chronic hepatitis C virus infection. *Expert opinion on investigational drugs,* 22**,** 1337-1346.

HERKER, E., HARRIS, C., HERNANDEZ, C., CARPENTIER, A., KAEHLCKE, K., ROSENBERG, A. R., FARESE, R. V. & OTT, M. 2010. Efficient hepatitis C virus particle formation requires diacylglycerol acyltransferase-1. *Nature medicine,* 16**,** 1295-1298.

HERKER, E. & OTT, M. 2011. Unique ties between hepatitis C virus replication and intracellular lipids. *Trends in Endocrinology & Metabolism,* 22**,** 241-248.

HIJIKATA, M., SHIMIZU, Y., KATO, H., IWAMOTO, A., SHIH, J., ALTER, H., PURCELL, R. & YOSHIKURA, H. 1993. Equilibrium centrifugation studies of hepatitis C virus: evidence for circulating immune complexes. *Journal of virology,* 67**,** 1953-1958.

HILLUNG, J., RUIZ-LOPEZ, E., BELLÓN-ECHEVERRÍA, I., CLEMENTE-CASARES, P. & MAS, A. 2012. Characterization of the interaction between hepatitis C virus NS5B and the human oestrogen receptor alpha. *Journal of general virology,* 93**,** 780-785.

HITTI, E. G., SALLACZ, N. B., SCHOFT, V. K. & JANTSCH, M. F. 2004. Oligomerization activity of a double-stranded RNA-binding domain. *FEBS letters,* 574**,** 25-30.

HNATYSZYN, H. J. 2005. Chronic hepatitis C and genotyping: the clinical significance of determining HCV genotypes. *Antiviral therapy,* 10**,** 1-11.

HOANG, H.-D., GRABER, T. E. & ALAIN, T. 2018. Battling for ribosomes: translational control at the forefront of the antiviral response. *Journal of molecular biology,* 430**,** 1965-1992.

HOFFMAN, B. & LIU, Q. 2011. Hepatitis C viral protein translation: mechanisms and implications in developing antivirals. *Liver International,* 31**,** 1449-1467.

HOFFMAN, B., SHI, Q. & LIU, Q. 2015. Arginine 112 is involved in HCV translation modulation by NS5A domain I. *Biochemical and Biophysical Research Communications,* 465**,** 95-100.

HOFFMANN, H. & SCHIENE-FISCHER, C. 2014. Functional aspects of extracellular cyclophilins. *Biological chemistry,* 395**,** 721-735.

HOPKINS, S., SCORNEAUX, B., HUANG, Z., MURRAY, M. G., WRING, S., SMITLEY, C., HARRIS, R., ERDMANN, F., FISCHER, G. & RIBEILL, Y. 2010. SCY-635, a novel nonimmunosuppressive analog of cyclosporine that exhibits potent inhibition of hepatitis C virus RNA replication in vitro. *Antimicrobial agents and chemotherapy,* 54**,** 660-672.

HORNER, S. M. & GALE, M. 2013. Regulation of hepatic innate immunity by hepatitis C virus. *Nature medicine,* 19**,** 879-888.

HORNG, T., BARTON, G. M. & MEDZHITOV, R. 2001. TIRAP: an adapter molecule in the Toll signaling pathway. *Nature immunology,* 2**,** 835-841.

HOURIOUX, C., AITÂ€GOUGHOULTE, M., PATIENT, R., FOUQUENET, D., ARCANGERÂ€DOUDET, F., BRAND, D., MARTIN, A. & ROINGEARD, P. 2007. Core protein domains involved in hepatitis C virusâ€like particle assembly and budding at the endoplasmic reticulum membrane. *Cellular microbiology,* 9**,** 1014-1027.

HSU, S.-C., TSAI, C.-N., LEE, K.-Y., PAN, T.-C., LO, C.-W. & YU, M.-J. 2018. Sequential S232/S235/S238 phosphorylation of the hepatitis C virus nonstructural protein 5A. *Journal of Virology,* 92**,** e01295-18.

HUANG, H., SUN, F., OWEN, D. M., LI, W., CHEN, Y., GALE JR, M. & YE, J. 2007. Hepatitis C virus production by human hepatocytes dependent on assembly and secretion of very low-density lipoproteins. *Proceedings of the National Academy of Sciences,* 104**,** 5848-5853.

HUEGING, K., WELLER, R., DOEPKE, M., VIEYRES, G., TODT, D., WÖLK, B., VONDRAN, F. W., GEFFERS, R., LAUBER, C. & KADERALI, L. 2015. Several human liver cell expressed apolipoproteins complement HCV virus production with varying efficacy conferring differential specific infectivity to released viruses. *PloS one,* 10**,** e0134529.

HUGHES, M., GRIFFIN, S. & HARRIS, M. 2009. Domain III of NS5A contributes to both RNA replication and assembly of hepatitis C virus particles. *Journal of general virology,* 90**,** 1329-1334.

HÜGLE, T., FEHRMANN, F., BIECK, E., KOHARA, M., KRÄUSSLICH, H.-G., RICE, C. M., BLUM, H. E. & MORADPOUR, D. 2001. The hepatitis C virus nonstructural protein 4B is an integral endoplasmic reticulum membrane protein. *Virology,* 284**,** 70-81.

HUGON, J., MOUTON-LIGER, F., DUMURGIER, J. & PAQUET, C. 2017. PKR involvement in Alzheimer's disease. *Alzheimer's research & therapy,* 9**,** 1-10.

HUGON, J., PAQUET, C. & CHANG, R. C.-C. 2009. Could PKR inhibition modulate human neurodegeneration? *Expert review of neurotherapeutics,* 9**,** 1455-1457.

IDE, Y., ZHANG, L., CHEN, M., INCHAUSPE, G., BAHL, C., SASAGURI, Y. & PADMANABHAN, R. 1996. Characterization of the nuclear localization signal and subcellular distribution of hepatitis C virus nonstructural protein NS5A. *Gene,* 182**,** 203-211.

IDREES, M. 2008. Development of an improved genotyping assay for the detection of hepatitis C virus genotypes and subtypes in Pakistan. *Journal of virological methods,* 150**,** 50-56.

IDREES, M. & RIAZUDDIN, S. 2008. Frequency distribution of hepatitis C virus genotypes in different geographical regions of Pakistan and their possible routes of transmission. *BMC infectious diseases,* 8**,** 1-9.

INOUE, K., SEKIYAMA, K., YAMADA, M., WATANABE, T., YASUDA, H. & YOSHIBA, M. 2003. Combined interferon α2b and cyclosporin A in the treatment of chronic hepatitis C: controlled trial. *Journal of gastroenterology,* 38**,** 567-572.

INOUE, K. & YOSHIBA, M. Interferon combined with cyclosporine treatment as an effective countermeasure against hepatitis C virus recurrence in liver transplant patients with end-stage hepatitis C virus related disease. Transplantation proceedings, 2005. Elsevier, 1233-1234.

INOUE, Y., AIZAKI, H., HARA, H., MATSUDA, M., ANDO, T., SHIMOJI, T., MURAKAMI, K., MASAKI, T., SHOJI, I. & HOMMA, S. 2011. Chaperonin TRiC/CCT participates in replication of hepatitis C virus genome via interaction with the viral NS5B protein. *Virology,* 410**,** 38-47.

ISHII, N., WATASHI, K., HISHIKI, T., GOTO, K., INOUE, D., HIJIKATA, M., WAKITA, T., KATO, N. & SHIMOTOHNO, K. 2006. Diverse effects of cyclosporine on hepatitis C virus strain replication. *Journal of virology,* 80**,** 4510-4520.

IVASHKINA, N., WÖLK, B., LOHMANN, V., BARTENSCHLAGER, R., BLUM, H. E., PENIN, F. & MORADPOUR, D. 2002. The hepatitis C virus RNA-dependent RNA polymerase membrane insertion sequence is a transmembrane segment. *Journal of virology,* 76**,** 13088-13093.

JACOBSON, I. M., GORDON, S. C., KOWDLEY, K. V., YOSHIDA, E. M., RODRIGUEZ-TORRES, M., SULKOWSKI, M. S., SHIFFMAN, M. L., LAWITZ, E., EVERSON, G. & BENNETT, M. 2013. Sofosbuvir for hepatitis C genotype 2 or 3 in patients without treatment options. *New England journal of medicine,* 368**,** 1867-1877.

JACOBSON, I. M., LAWITZ, E., GANE, E. J., WILLEMS, B. E., RUANE, P. J., NAHASS, R. G., BORGIA, S. M., SHAFRAN, S. D., WORKOWSKI, K. A. & PEARLMAN, B. 2017. Efficacy of 8 weeks of sofosbuvir, velpatasvir, and voxilaprevir in patients with chronic HCV infection: 2 phase 3 randomized trials. *Gastroenterology,* 153**,** 113-122.

JACOBSON, I. M., MCHUTCHISON, J. G., DUSHEIKO, G., DI BISCEGLIE, A. M., REDDY, K. R., BZOWEJ, N. H., MARCELLIN, P., MUIR, A. J., FERENCI, P. & FLISIAK, R. 2011. Telaprevir for previously untreated chronic hepatitis C virus infection. *New England Journal of Medicine,* 364**,** 2405-2416.

JIA, L., BETTERS, J. L. & YU, L. 2011. Niemann-pick C1-like 1 (NPC1L1) protein in intestinal and hepatic cholesterol transport. *Annual review of physiology,* 73**,** 239.

JIANG, J., WU, X., TANG, H. & LUO, G. 2013. Apolipoprotein E mediates attachment of clinical hepatitis C virus to hepatocytes by binding to cell surface heparan sulfate proteoglycan receptors. *PloS one,* 8**,** e67982.

JIRASKO, V., MONTSERRET, R., APPEL, N., JANVIER, A., EUSTACHI, L., BROHM, C., STEINMANN, E., PIETSCHMANN, T., PENIN, F. & BARTENSCHLAGER, R. 2008. Structural and functional characterization of nonstructural protein 2 for its role in hepatitis C virus assembly. *Journal of Biological Chemistry,* 283**,** 28546-28562.

JIRASKO, V., MONTSERRET, R., LEE, J. Y., GOUTTENOIRE, J., MORADPOUR, D., PENIN, F. & BARTENSCHLAGER, R. 2010. Structural and functional studies of nonstructural protein 2 of the hepatitis C virus reveal its key role as organizer of virion assembly. *PLoS pathogens,* 6**,** e1001233.

JONES, C. T., MURRAY, C. L., EASTMAN, D. K., TASSELLO, J. & RICE, C. M. 2007. Hepatitis C virus p7 and NS2 proteins are essential for production of infectious virus. *Journal of virology,* 81**,** 8374-8383.

JONES, D. M., PATEL, A. H., TARGETT-ADAMS, P. & MCLAUCHLAN, J. 2009. The hepatitis C virus NS4B protein can trans-complement viral RNA replication and modulates production of infectious virus. *Journal of virology,* 83**,** 2163-2177.

KALININA, O., NORDER, H., MUKOMOLOV, S. & MAGNIUS, L. O. 2002. A natural intergenotypic recombinant of hepatitis C virus identified in St. Petersburg. *Journal of virology,* 76**,** 4034-4043.

KALLEN, J., SPITZFADEN, C., ZURINI, M. G., WIDER, G., WIDMER, H., WÜTHRICH, K. & WALKINSHAW, M. D. 1991. Structure of human cyclophilin and its binding site for cyclosporin A determined by X-ray crystallography and NMR spectroscopy. *Nature,* 353**,** 276-279.

KANAZAWA, N., KUROSAKI, M., SAKAMOTO, N., ENOMOTO, N., ITSUI, Y., YAMASHIRO, T., TANABE, Y., MAEKAWA, S., NAKAGAWA, M. & CHEN, C.-H. 2004. Regulation of hepatitis C virus replication by interferon regulatory factor 1. *Journal of Virology,* 78**,** 9713-9720.

KANDANGWA, M. & LIU, Q. 2019. HCV NS5A hyperphosphorylation is involved in viral translation modulation. *Biochemical and Biophysical Research Communications,* 520**,** 192-197.

KANWAL, F., KRAMER, J. R., ILYAS, J., DUAN, Z. & ELÂ€SERAG, H. B. 2014. HCV genotype 3 is associated with an increased risk of cirrhosis and hepatocellular cancer in a national sample of US Veterans with HCV. *Hepatology,* 60**,** 98-105.

KAPOOR, A., SIMMONDS, P., GEROLD, G., QAISAR, N., JAIN, K., HENRIQUEZ, J. A., FIRTH, C., HIRSCHBERG, D. L., RICE, C. M. & SHIELDS, S. 2011. Characterization of a canine homolog of hepatitis C virus. *Proceedings of the National Academy of Sciences,* 108**,** 11608-11613.

KAPOOR, A., SIMMONDS, P., SCHEEL, T. K., HJELLE, B., CULLEN, J. M., BURBELO, P. D., CHAUHAN, L. V., DURAISAMY, R., SANCHEZ LEON, M. & JAIN, K. 2013. Identification of rodent homologs of hepatitis C virus and pegiviruses. *MBio,* 4**,** e00216-13.

KATTAKUZHY, S., LEVY, R., ROSENTHAL, E., TANG, L., WILSON, E. & KOTTILIL, S. 2016. Hepatitis C genotype 3 disease. *Hepatology international,* 10**,** 861-870.

KAUL, A., STAUFFER, S., BERGER, C., PERTEL, T., SCHMITT, J., KALLIS, S., ZAYAS LOPEZ, M., LOHMANN, V., LUBAN, J. & BARTENSCHLAGER, R. 2009. Essential role of cyclophilin A for hepatitis C virus replication and virus production and possible link to polyprotein cleavage kinetics. *PLoS pathogens,* 5**,** e1000546.

KE, P.-Y. & CHEN, S. S.-L. 2011. Activation of the unfolded protein response and autophagy after hepatitis C virus infection suppresses innate antiviral immunity in vitro. *The Journal of clinical investigation,* 121**,** 37-56.

KEATING, G. M. & VAIDYA, A. 2014. Sofosbuvir: first global approval. *Drugs,* 74**,** 273-282.

KHAN, I., KATIKANENI, D. S., HAN, Q., SANCHEZ-FELIPE, L., HANADA, K., AMBROSE, R. L., MACKENZIE, J. M. & KONAN, K. V. 2014. Modulation of hepatitis C virus genome replication by glycosphingolipids and four-phosphate adaptor protein 2. *Journal of virology,* 88**,** 12276-12295.

KIM, D. W., GWACK, Y., HAN, J. H. & CHOE, J. 1995. C-terminal domain of the hepatitis C virus NS3 protein contains an RNA helicase activity. *Biochemical and biophysical research communications,* 215**,** 160-166.

KIM, J., MORGENSTERN, K., LIN, C., FOX, T., DWYER, M., LANDRO, J., CHAMBERS, S., MARKLAND, W., LEPRE, C. & O'MALLEY, E. 1996. Crystal structure of the hepatitis C virus NS3 protease domain complexed with a synthetic NS4A cofactor peptide. *Cell,* 87**,** 343-355.

KIM, S., WELSCH, C., YI, M. & LEMON, S. M. 2011. Regulation of the production of infectious genotype 1a hepatitis C virus by NS5A domain III. *Journal of virology,* 85**,** 6645-6656.

KIRCHHOFF, S., KOROMILAS, A. E., SCHAPER, F., GRASHOFF, M., SONENBERG, N. & HAUSER, H. 1995. IRF-1 induced cell growth inhibition and interferon induction requires the activity of the protein kinase PKR. *Oncogene,* 11**,** 439-445.

KLEIN, K. C., DELLOS, S. R. & LINGAPPA, J. R. 2005. Identification of residues in the hepatitis C virus core protein that are critical for capsid assembly in a cell-free system. *Journal of virology,* 79**,** 6814-6826.

KLEVENS, R. M., HU, D. J., JILES, R. & HOLMBERG, S. D. 2012. Evolving epidemiology of hepatitis C virus in the United States. *Clinical infectious diseases,* 55**,** S3-S9.

KOHLWAY, A., PIRAKITIKULR, N., BARRERA, F. N., POTAPOVA, O., ENGELMAN, D. M., PYLE, A. M. & LINDENBACH, B. D. 2014a. Hepatitis C virus RNA replication and virus particle assembly require specific dimerization of the NS4A protein transmembrane domain. *Journal of virology,* 88**,** 628-642.

KOHLWAY, A., PIRAKITIKULR, N., DING, S. C., YANG, F., LUO, D., LINDENBACH, B. D. & PYLE, A. M. 2014b. The linker region of NS3 plays a critical role in the replication and infectivity of hepatitis C virus. *Journal of virology,* 88**,** 10970-10974.

KOLYKHALOV, A. A., MIHALIK, K., FEINSTONE, S. M. & RICE, C. M. 2000. Hepatitis C virus-encoded enzymatic activities and conserved RNA elements in the 3′ nontranslated region are essential for virus replication in vivo. *Journal of virology,* 74**,** 2046-2051.

KOPP, M., MURRAY, C. L., JONES, C. T. & RICE, C. M. 2010. Genetic analysis of the carboxy-terminal region of the hepatitis C virus core protein. *Journal of virology,* 84**,** 1666-1673.

KORENAGA, M., WANG, T., LI, Y., SHOWALTER, L. A., CHAN, T., SUN, J. & WEINMAN, S. A. 2005. Hepatitis C virus core protein inhibits mitochondrial electron transport and increases reactive oxygen species (ROS) production. *Journal of Biological Chemistry,* 280**,** 37481-37488.

KOUNTOURAS, J., ZAVOS, C. & CHATZOPOULOS, D. 2003. Apoptosis in hepatitis C. *Journal of Viral Hepatitis,* 10**,** 335-342.

KREY, T., THIEL, H.-J. R. & RÜMENAPF, T. 2005. Acid-resistant bovine pestivirus requires activation for pH-triggered fusion during entry. *Journal of virology,* 79**,** 4191-4200.

KUMAR, A., HAQUE, J., LACOSTE, J., HISCOTT, J. & WILLIAMS, B. 1994. Double-stranded RNA-dependent protein kinase activates transcription factor NF-kappa B by phosphorylating I kappa B. *Proceedings of the National Academy of Sciences,* 91**,** 6288-6292.

KUMAR, A., YANG, Y.-L., FLATI, V., DER, S., KADEREIT, S., DEB, A., HAQUE, J., REIS, L., WEISSMANN, C. & WILLIAMS, B. R. 1997. Deficient cytokine signaling in mouse embryo fibroblasts with a targeted deletion in the PKR gene: role of IRF-1 and NF-κB. *The EMBO journal,* 16**,** 406-416.

KUMARI, S., ROY, S., SINGH, P., SINGLA-PAREEK, S. & PAREEK, A. 2013. Cyclophilins: proteins in search of function. *Plant signaling & behavior,* 8**,** e22734.

KUNKEL, M. & WATOWICH, S. J. 2002. Conformational changes accompanying self-assembly of the hepatitis C virus core protein. *Virology,* 294**,** 239-245.

KUSAKAWA, T., SHIMAKAMI, T., KANEKO, S., YOSHIOKA, K. & MURAKAMI, S. 2007. Functional interaction of hepatitis C Virus NS5B with Nucleolin GAR domain. *Journal of biochemistry,* 141**,** 917-927.

KUSHIMA, Y., WAKITA, T. & HIJIKATA, M. 2010. A disulfide-bonded dimer of the core protein of hepatitis C virus is important for virus-like particle production. *Journal of virology,* 84**,** 9118-9127.

LAMBERT, S. M., LANGLEY, D. R., GARNETT, J. A., ANGELL, R., HEDGETHORNE, K., MEANWELL, N. A. & MATTHEWS, S. J. 2014. The crystal structure of NS5A domain 1 from genotype 1a reveals new clues to the mechanism of action for dimeric HCV inhibitors. *Protein Science,* 23**,** 723-734.

LAUCK, M., SIBLEY, S. D., LARA, J., PURDY, M. A., KHUDYAKOV, Y., HYEROBA, D., TUMUKUNDE, A., WENY, G., SWITZER, W. M. & CHAPMAN, C. A. 2013. A novel hepacivirus with an unusually long and intrinsically disordered NS5A protein in a wild Old World primate. *Journal of virology,* 87**,** 8971-8981.

LAVANCHY, D. 2009. The global burden of hepatitis C. *Liver international,* 29**,** 74-81.

LAVANCHY, D. 2011. Evolving epidemiology of hepatitis C virus. *Clinical Microbiology and Infection,* 17**,** 107-115.

LAWITZ, E., GANE, E., PEARLMAN, B., TAM, E., GHESQUIERE, W., GUYADER, D., ALRIC, L., BRONOWICKI, J.-P., LESTER, L. & SIEVERT, W. 2015. Efficacy and safety of 12 weeks versus 18 weeks of treatment with grazoprevir (MK-5172) and elbasvir (MK-8742) with or without ribavirin for hepatitis C virus genotype 1 infection in previously untreated patients with cirrhosis and patients with previous null response with or without cirrhosis (C-WORTHY): a randomised, open-label phase 2 trial. *The Lancet,* 385**,** 1075-1086.

LAWITZ, E., MANGIA, A., WYLES, D., RODRIGUEZ-TORRES, M., HASSANEIN, T., GORDON, S. C., SCHULTZ, M., DAVIS, M. N., KAYALI, Z. & REDDY, K. R. 2013. Sofosbuvir for previously untreated chronic hepatitis C infection. *New England Journal of Medicine,* 368**,** 1878-1887.

LE GUILLOU-GUILLEMETTE, H., VALLET, S., GAUDY-GRAFFIN, C., PAYAN, C., PIVERT, A., GOUDEAU, A. & LUNEL-FABIANI, F. 2007. Genetic diversity of the hepatitis C virus: impact and issues in the antiviral therapy. *World journal of gastroenterology: WJG,* 13**,** 2416.

LEE, J.-Y., CORTESE, M., HASELMANN, U., TABATA, K., ROMERO-BREY, I., FUNAYA, C., SCHIEBER, N. L., QIANG, Y., BARTENSCHLAGER, M. & KALLIS, S. 2019. Spatiotemporal coupling of the hepatitis C virus replication cycle by creating a lipid droplet-proximal membranous replication compartment. *Cell reports,* 27**,** 3602-3617. e5.

LEE, Y.-M. & LIM, C. 2008. Physical basis of structural and catalytic Zn-binding sites in proteins. *Journal of molecular biology,* 379**,** 545-553.

LEFÈVRE, M., FELMLEE, D. J., PARNOT, M., BAUMERT, T. F. & SCHUSTER, C. 2014. Syndecan 4 is involved in mediating HCV entry through interaction with lipoviral particle-associated apolipoprotein E. *PloS one,* 9**,** e95550.

LEROY, V., ANGUS, P., BRONOWICKI, J. P., DORE, G. J., HEZODE, C., PIANKO, S., POL, S., STUART, K., TSE, E. & MCPHEE, F. 2016. Daclatasvir, sofosbuvir, and ribavirin for hepatitis C virus genotype 3 and advanced liver disease: a randomized phase III study (ALLY‐3+). *Hepatology,* 63**,** 1430-1441.

LESBURG, C. A., CABLE, M. B., FERRARI, E., HONG, Z., MANNARINO, A. F. & WEBER, P. C. 1999. Crystal structure of the RNA-dependent RNA polymerase from hepatitis C virus reveals a fully encircled active site. *Nature structural biology,* 6**,** 937-943.

LEVIN, M. K., GURJAR, M. & PATEL, S. S. 2005. A Brownian motor mechanism of translocation and strand separation by hepatitis C virus helicase. *Nature structural & molecular biology,* 12**,** 429-435.

LI, G. & DE CLERCQ, E. 2017. Current therapy for chronic hepatitis C: The role of direct-acting antivirals. *Antiviral research,* 142**,** 83-122.

LI, H.-C., YANG, C.-H. & LO, S.-Y. 2021. Hepatitis C viral replication complex. *Viruses,* 13**,** 520.

LI, K., FOY, E., FERREON, J. C., NAKAMURA, M., FERREON, A. C., IKEDA, M., RAY, S. C., GALE JR, M. & LEMON, S. M. 2005. Immune evasion by hepatitis C virus NS3/4A protease-mediated cleavage of the Toll-like receptor 3 adaptor protein TRIF. *Proceedings of the National Academy of Sciences,* 102**,** 2992-2997.

LI, Q., AN, N., YIN, X., ZHANG, R., SHAO, H., YI, D. & CEN, S. 2022. MxB Disrupts Hepatitis C Virus NS5A–CypA Complex: Insights From a Combined Theoretical and Experimental Approach. *Frontiers in microbiology,* 13.

LI, S., PETERS, G. A., DING, K., ZHANG, X., QIN, J. & SEN, G. C. 2006. Molecular basis for PKR activation by PACT or dsRNA. *Proceedings of the National Academy of Sciences,* 103**,** 10005-10010.

LIANG, T. J. & GHANY, M. G. 2013. Current and future therapies for hepatitis C virus infection. *New England Journal of Medicine,* 368**,** 1907-1917.

LIANG, Y., YE, H., KANG, C. B. & YOON, H. S. 2007. Domain 2 of nonstructural protein 5A (NS5A) of hepatitis C virus is natively unfolded. *Biochemistry,* 46**,** 11550-11558.

LIAO, Y., LUO, D., PENG, K. & ZENG, Y. 2021. Cyclophilin A: a key player for etiological agent infection. *Applied microbiology and biotechnology,* 105**,** 1365-1377.

LIM, P. J., CHATTERJI, U., CORDEK, D., SHARMA, S. D., GARCIA-RIVERA, J. A., CAMERON, C. E., LIN, K., TARGETT-ADAMS, P. & GALLAY, P. A. 2012. Correlation between NS5A dimerization and hepatitis C virus replication. *Journal of Biological Chemistry,* 287**,** 30861-30873.

LIN, C.-C., TSAI, P., SUN, H.-Y., HSU, M.-C., LEE, J.-C., WU, I.-C., TSAO, C.-W., CHANG, T.-T. & YOUNG, K.-C. 2014. Apolipoprotein J, a glucose-upregulated molecular chaperone, stabilizes core and NS5A to promote infectious hepatitis C virus virion production. *Journal of hepatology,* 61**,** 984-993.

LIN, C., LINDENBACH, B. D., PRAGAI, B. M., MCCOURT, D. W. & RICE, C. M. 1994. Processing in the hepatitis C virus E2-NS2 region: identification of p7 and two distinct E2-specific products with different C termini. *Journal of virology,* 68**,** 5063-5073.

LIN, C., THOMSON, J. A. & RICE, C. M. 1995. A central region in the hepatitis C virus NS4A protein allows formation of an active NS3-NS4A serine proteinase complex in vivo and in vitro. *Journal of virology,* 69**,** 4373-4380.

LINDENBACH, B. & RICE, C. 2001. Flaviviridae: the viruses and their replication, vol. 1. Lippincott Williams & Wilkins, Philadelphia, PA.

LINDENBACH, B. D. 2013. Virion assembly and release. *Hepatitis C Virus: From Molecular Virology to Antiviral Therapy***,** 199-218.

LINDENBACH, B. D., EVANS, M. J., SYDER, A. J., WOLK, B., TELLINGHUISEN, T. L., LIU, C. C., MARUYAMA, T., HYNES, R. O., BURTON, D. R. & MCKEATING, J. A. 2005. Complete replication of hepatitis C virus in cell culture. *Science,* 309**,** 623-626.

LINDENBACH, B. D., PRÁGAI, B. M., MONTSERRET, R., BERAN, R. K., PYLE, A. M., PENIN, F. & RICE, C. M. 2007. The C terminus of hepatitis C virus NS4A encodes an electrostatic switch that regulates NS5A hyperphosphorylation and viral replication. *Journal of virology,* 81**,** 8905-8918.

LINDENBACH, B. D. & RICE, C. M. 2005. Unravelling hepatitis C virus replication from genome to function. *Nature,* 436**,** 933-938.

LINDENBACH, B. D. & RICE, C. M. 2013. The ins and outs of hepatitis C virus entry and assembly. *Nature Reviews Microbiology,* 11**,** 688-700.

LIU, J., FARMER JR, J. D., LANE, W. S., FRIEDMAN, J., WEISSMAN, I. & SCHREIBER, S. L. 1991. Calcineurin is a common target of cyclophilin-cyclosporin A and FKBP-FK506 complexes. *Cell,* 66**,** 807-815.

LIU, S., ANSARI, I. H., DAS, S. C. & PATTNAIK, A. K. 2006. Insertion and deletion analyses identify regions of non-structural protein 5A of Hepatitis C virus that are dispensable for viral genome replication. *Journal of general virology,* 87**,** 323-327.

LIU, W., LI, J., ZHENG, W., SHANG, Y., ZHAO, Z., WANG, S., BI, Y., ZHANG, S., XU, C. & DUAN, Z. 2017. Cyclophilin A-regulated ubiquitination is critical for RIG-I-mediated antiviral immune responses. *Elife,* 6**,** e24425.

LIU, Z., YANG, F., ROBOTHAM, J. M. & TANG, H. 2009. Critical role of cyclophilin A and its prolyl-peptidyl isomerase activity in the structure and function of the hepatitis C virus replication complex. *Journal of virology,* 83**,** 6554-6565.

LIVER, E. A. F. T. S. O. T. 2017. EASL recommendations on treatment of hepatitis C 2016. *Journal of hepatology,* 66**,** 153-194.

LIVER, E. A. F. T. S. O. T. 2018. EASL recommendations on treatment of hepatitis C 2018. *Journal of hepatology,* 69**,** 461-511.

LOHMANN, V. 2013. Hepatitis C virus RNA replication. *Hepatitis C virus: from molecular virology to antiviral therapy***,** 167-198.

LOHMANN, V., KORNER, F., KOCH, J.-O., HERIAN, U., THEILMANN, L. & BARTENSCHLAGER, R. 1999. Replication of subgenomic hepatitis C virus RNAs in a hepatoma cell line. *Science,* 285**,** 110-113.

LONG, G., HIET, M. S., WINDISCH, M. P., LEE, J. Y., LOHMANN, V. & BARTENSCHLAGER, R. 2011. Mouse hepatic cells support assembly of infectious hepatitis C virus particles. *Gastroenterology,* 141**,** 1057-1066.

LOVE, R. A., BRODSKY, O., HICKEY, M. J., WELLS, P. A. & CRONIN, C. N. 2009. Crystal structure of a novel dimeric form of NS5A domain I protein from hepatitis C virus. *Journal of virology,* 83**,** 4395-4403.

LOVE, R. A., PARGE, H. E., WICKERSHAM, J. A., HOSTOMSKY, Z., HABUKA, N., MOOMAW, E. W., ADACHI, T. & HOSTOMSKA, Z. 1996. The crystal structure of hepatitis C virus NS3 proteinase reveals a trypsin-like fold and a structural zinc binding site. *Cell,* 87**,** 331-342.

LUNDIN, M., MONNÉ, M., WIDELL, A., VON HEIJNE, G. & PERSSON, M. A. 2003. Topology of the membrane-associated hepatitis C virus protein NS4B. *Journal of virology,* 77**,** 5428-5438.

LUPBERGER, J., ZEISEL, M. B., XIAO, F., THUMANN, C., FOFANA, I., ZONA, L., DAVIS, C., MEE, C. J., TUREK, M. & GORKE, S. 2011. EGFR and EphA2 are host factors for hepatitis C virus entry and possible targets for antiviral therapy. *Nature medicine,* 17**,** 589-595.

MA, S., BOERNER, J. E., TIONGYIP, C., WEIDMANN, B., RYDER, N. S., COOREMAN, M. P. & LIN, K. 2006. NIM811, a cyclophilin inhibitor, exhibits potent in vitro activity against hepatitis C virus alone or in combination with alpha interferon. *Antimicrobial agents and chemotherapy,* 50**,** 2976-2982.

MA, Y., ANANTPADMA, M., TIMPE, J. M., SHANMUGAM, S., SINGH, S. M., LEMON, S. M. & YI, M. 2011. Hepatitis C virus NS2 protein serves as a scaffold for virus assembly by interacting with both structural and nonstructural proteins. *Journal of virology,* 85**,** 86-97.

MACKMAN, R. L., STEADMAN, V. A., DEAN, D. K., JANSA, P., POULLENNEC, K. G., APPLEBY, T., AUSTIN, C., BLAKEMORE, C. A., CAI, R. & CANNIZZARO, C. 2018. Discovery of a potent and orally bioavailable cyclophilin inhibitor derived from the sanglifehrin macrocycle. *Journal of Medicinal Chemistry,* 61**,** 9473-9499.

MADAN, V., PAUL, D., LOHMANN, V. & BARTENSCHLAGER, R. 2014. Inhibition of HCV replication by cyclophilin antagonists is linked to replication fitness and occurs by inhibition of membranous web formation. *Gastroenterology,* 146**,** 1361-1372. e9.

MAJEAU, N., GAGNE, V., BOIVIN, A., BOLDUC, M., MAJEAU, J.-A., OUELLET, D. & LECLERC, D. 2004. The N-terminal half of the core protein of hepatitis C virus is sufficient for nucleocapsid formation. *Journal of general virology,* 85**,** 971-981.

MAJUMDAR, A., KITSON, M. & ROBERTS, S. 2016. Systematic review: current concepts and challenges for the directâ€acting antiviral era in hepatitis C cirrhosis. *Alimentary pharmacology & therapeutics,* 43**,** 1276-1292.

MALANDRIS, K., KALOPITAS, G., THEOCHARIDOU, E. & GERMANIDIS, G. 2021. The role of RASs/RVs in the current management of HCV. *Viruses,* 13**,** 2096.

MANI, H., YEN, J.-H., HSU, H.-J., CHANG, C.-C. & LIOU, J.-W. 2022. Hepatitis C virus core protein: Not just a nucleocapsid building block, but an immunity and inflammation modulator. *Tzu-Chi Medical Journal,* 34**,** 139.

MARCELLIN, P. 1999. Hepatitis C: the clinical spectrum of the disease. *Journal of hepatology,* 31**,** 9-16.

MARTINEZ, M. A. & FRANCO, S. 2020. Therapy implications of hepatitis C virus genetic diversity. *Viruses,* 13**,** 41.

MASAKI, T., MATSUNAGA, S., TAKAHASHI, H., NAKASHIMA, K., KIMURA, Y., ITO, M., MATSUDA, M., MURAYAMA, A., KATO, T. & HIRANO, H. 2014. Involvement of hepatitis C virus NS5A hyperphosphorylation mediated by casein kinase I-α in infectious virus production. *Journal of virology,* 88**,** 7541-7555.

MASAKI, T., SUZUKI, R., MURAKAMI, K., AIZAKI, H., ISHII, K., MURAYAMA, A., DATE, T., MATSUURA, Y., MIYAMURA, T. & WAKITA, T. 2008. Interaction of hepatitis C virus nonstructural protein 5A with core protein is critical for the production of infectious virus particles. *Journal of virology,* 82**,** 7964-7976.

MAUGER, D. M., GOLDEN, M., YAMANE, D., WILLIFORD, S., LEMON, S. M., MARTIN, D. P. & WEEKS, K. M. 2015. Functionally conserved architecture of hepatitis C virus RNA genomes. *Proceedings of the National Academy of Sciences,* 112**,** 3692-3697.

MAYER, B. J. 2001. SH3 domains: complexity in moderation. *Journal of cell science,* 114**,** 1253-1263.

MAYO, C. B., WONG, C. J., LOPEZ, P. E., LARY, J. W. & COLE, J. L. 2016. Activation of PKR by short stem–loop RNAs containing single-stranded arms. *Rna,* 22**,** 1065-1075.

MCCORMACK, S. J., ORTEGA, L. G., DOOHAN, J. P. & SAMUEL, C. E. 1994. Mechanism of interferon action motif I of the interferon-induced, RNA-dependent protein kinase (PKR) is sufficient to mediate RNA-binding activity. *Virology,* 198**,** 92-99.

MCGIVERN, D. R., MASAKI, T., WILLIFORD, S., INGRAVALLO, P., FENG, Z., LAHSER, F., ASANTE-APPIAH, E., NEDDERMANN, P., DE FRANCESCO, R. & HOWE, A. Y. 2014. Kinetic analyses reveal potent and early blockade of hepatitis C virus assembly by NS5A inhibitors. *Gastroenterology,* 147**,** 453-462. e7.

MCLAUCHLAN, J. 2000. Properties of the hepatitis C virus core protein: a structural protein that modulates cellular processes. *Journal of viral hepatitis,* 7**,** 2-14.

MCLAUCHLAN, J., LEMBERG, M. K., HOPE, G. & MARTOGLIO, B. 2002. Intramembrane proteolysis promotes trafficking of hepatitis C virus core protein to lipid droplets. *The EMBO journal,* 21**,** 3980-3988.

MENZEL, N., FISCHL, W., HUEGING, K., BANKWITZ, D., FRENTZEN, A., HAID, S., GENTZSCH, J., KADERALI, L., BARTENSCHLAGER, R. & PIETSCHMANN, T. 2012. MAP-kinase regulated cytosolic phospholipase A2 activity is essential for production of infectious hepatitis C virus particles. *PLoS pathogens,* 8**,** e1002829.

MERZ, A., LONG, G., HIET, M.-S., BRÜGGER, B., CHLANDA, P., ANDRE, P., WIELAND, F., KRIJNSE-LOCKER, J. & BARTENSCHLAGER, R. 2011. Biochemical and morphological properties of hepatitis C virus particles and determination of their lipidome. *Journal of Biological Chemistry,* 286**,** 3018-3032.

MESSINA, J. P., HUMPHREYS, I., FLAXMAN, A., BROWN, A., COOKE, G. S., PYBUS, O. G. & BARNES, E. 2015. Global distribution and prevalence of hepatitis C virus genotypes. *Hepatology,* 61**,** 77-87.

MEUNIER, J.-C., RUSSELL, R. S., ENGLE, R. E., FAULK, K. N., PURCELL, R. H. & EMERSON, S. U. 2008. Apolipoprotein c1 association with hepatitis C virus. *Journal of virology,* 82**,** 9647-9656.

MEURS, E., CHONG, K., GALABRU, J., THOMAS, N. S. B., KERR, I. M., WILLIAMS, B. R. & HOVANESSIAN, A. G. 1990. Molecular cloning and characterization of the human double-stranded RNA-activated protein kinase induced by interferon. *Cell,* 62**,** 379-390.

MEURS, E. F., WATANABE, Y., KADEREIT, S., BARBER, G. N., KATZE, M. G., CHONG, K., WILLIAMS, B. & HOVANESSIAN, A. G. 1992. Constitutive expression of human double-stranded RNA-activated p68 kinase in murine cells mediates phosphorylation of eukaryotic initiation factor 2 and partial resistance to encephalomyocarditis virus growth. *Journal of virology,* 66**,** 5805-5814.

MEYER, K., BASU, A., SAITO, K., RAY, R. B. & RAY, R. 2005. Inhibition of hepatitis C virus core protein expression in immortalized human hepatocytes induces cytochrome c-independent increase in Apaf-1 and caspase-9 activation for cell death. *Virology,* 336**,** 198-207.

MEYLAN, E., CURRAN, J., HOFMANN, K., MORADPOUR, D., BINDER, M., BARTENSCHLAGER, R. & TSCHOPP, J. 2005. Cardif is an adaptor protein in the RIG-I antiviral pathway and is targeted by hepatitis C virus. *Nature,* 437**,** 1167-1172.

MICALLEF, J., KALDOR, J. & DORE, G. 2006. Spontaneous viral clearance following acute hepatitis C infection: a systematic review of longitudinal studies. *Journal of viral hepatitis,* 13**,** 34-41.

MICHALAK, J.-P., WYCHOWSKI, C., CHOUKHI, A. L., MEUNIER, J.-C., UNG, S., RICE, C. M. & DUBUISSON, J. 1997. Characterization of truncated forms of hepatitis C virus glycoproteins. *Journal of General Virology,* 78**,** 2299-2306.

MILLER, D. J., SCHWARTZ, M. D., DYE, B. T. & AHLQUIST, P. 2003. Engineered retargeting of viral RNA replication complexes to an alternative intracellular membrane. *Journal of virology,* 77**,** 12193-12202.

MILLER, M., AGARWAL, K., AUSTIN, A., BROWN, A., BARCLAY, S., DUNDAS, P., DUSHEIKO, G., FOSTER, G., FOX, R. & HAYES, P. 2014. 2014 UK consensus guidelinesâ€“hepatitis C management and directâ€acting antiâ€viral therapy. *Alimentary pharmacology & therapeutics,* 39**,** 1363-1375.

MILLER, S. & KRIJNSE-LOCKER, J. 2008. Modification of intracellular membrane structures for virus replication. *Nature Reviews Microbiology,* 6**,** 363-374.

MIYANARI, Y., ATSUZAWA, K., USUDA, N., WATASHI, K., HISHIKI, T., ZAYAS, M., BARTENSCHLAGER, R., WAKITA, T., HIJIKATA, M. & SHIMOTOHNO, K. 2007. The lipid droplet is an important organelle for hepatitis C virus production. *Nature cell biology,* 9**,** 1089-1097.

MIZUSHIMA, H., HIJIKATA, M., ASABE, S.-I., HIROTA, M., KIMURA, K. & SHIMOTOHNO, K. 1994. Two hepatitis C virus glycoprotein E2 products with different C termini. *Journal of Virology,* 68**,** 6215-6222.

MOHD HANAFIAH, K., GROEGER, J., FLAXMAN, A. D. & WIERSMA, S. T. 2013. Global epidemiology of hepatitis C virus infection: new estimates of age-specific antibody to HCV seroprevalence. *Hepatology,* 57**,** 1333-1342.

MOHSEN, W. & LEVY, M. T. 2017. Hepatitis A to E: what's new? *Internal Medicine Journal,* 47**,** 380-389.
MORADPOUR, D., BRASS, V., BIECK, E., FRIEBE, P., GOSERT, R., BLUM, H. E., BARTENSCHLAGER, R., PENIN, F. & LOHMANN, V. 2004a. Membrane association of the RNA-dependent RNA polymerase is essential for hepatitis C virus RNA replication. *Journal of virology,* 78**,** 13278-13284.
MORADPOUR, D., BRASS, V. & PENIN, F. 2005. Function follows form: the structure of the N-terminal domain of HCV NS5A. Wiley Online Library.
MORADPOUR, D., EVANS, M. J., GOSERT, R., YUAN, Z., BLUM, H. E., GOFF, S. P., LINDENBACH, B. D. & RICE, C. M. 2004b. Insertion of green fluorescent protein into nonstructural protein 5A allows direct visualization of functional hepatitis C virus replication complexes. *Journal of virology,* 78**,** 7400-7409.
MORADPOUR, D. & PENIN, F. 2013. Hepatitis C virus proteins: from structure to function. *Hepatitis C virus: from molecular virology to antiviral therapy***,** 113-142.
MORADPOUR, D., PENIN, F. & RICE, C. M. 2007. Replication of hepatitis C virus. *Nature reviews microbiology,* 5**,** 453-463.
MORIKAWA, K., LANGE, C., GOUTTENOIRE, J., MEYLAN, E., BRASS, V., PENIN, F. & MORADPOUR, D. 2011. Nonstructural protein 3-4A: the Swiss army knife of hepatitis C virus. *Journal of viral hepatitis,* 18**,** 305-315.
MORIYA, K., FUJIE, H., SHINTANI, Y., YOTSUYANAGI, H., TSUTSUMI, T., ISHIBASHI, K., MATSUURA, Y., KIMURA, S., MIYAMURA, T. & KOIKE, K. 1998. The core protein of hepatitis C virus induces hepatocellular carcinoma in transgenic mice. *Nature medicine,* 4**,** 1065-1067.
MORIYA, K., YOTSUYANAGI, H., SHINTANI, Y., FUJIE, H., ISHIBASHI, K., MATSUURA, Y., MIYAMURA, T. & KOIKE, K. 1997. Hepatitis C virus core protein induces hepatic steatosis in transgenic mice. *Journal of general virology,* 78**,** 1527-1531.
MUNAKATA, T., NAKAMURA, M., LIANG, Y., LI, K. & LEMON, S. M. 2005. Down-regulation of the retinoblastoma tumor suppressor by the hepatitis C virus NS5B RNA-dependent RNA polymerase. *Proceedings of the National Academy of Sciences,* 102**,** 18159-18164.
MURPHY, D. G., SABLON, E., CHAMBERLAND, J., FOURNIER, E., DANDAVINO, R. & TREMBLAY, C. L. 2015. Hepatitis C virus genotype 7, a new genotype originating from central Africa. *Journal of clinical microbiology,* 53**,** 967-972.
MURRAY, C. L., JONES, C. T. & RICE, C. M. 2008. Architects of assembly: roles of Flaviviridae non-structural proteins in virion morphogenesis. *Nature reviews microbiology,* 6**,** 699-708.
NADERI, M., GHOLIPOUR, N., ZOLFAGHARI, M. R., BINABAJ, M. M., MOGHADAM, A. Y. & MOTALLEB, G. 2014. Hepatitis C virus and vaccine development. *International journal of molecular and cellular medicine,* 3**,** 207.
NAG, A., ROBOTHAM, J. M. & TANG, H. 2012. Suppression of viral RNA binding and the assembly of infectious hepatitis C virus particles in vitro by cyclophilin inhibitors. *Journal of virology,* 86**,** 12616-12624.
NAGGIE, S. 2019. Treating HCV infection: it doesn't get much better than this. *Topics in Antiviral Medicine,* 26**,** 104.
NAKABAYASHI, H., TAKETA, K., MIYANO, K., YAMANE, T. & SATO, J. 1982. Growth of human hepatoma cell lines with differentiated functions in chemically defined medium. *Cancer research,* 42**,** 3858-3863.
NAKAGAWA, M., SAKAMOTO, N., ENOMOTO, N., TANABE, Y., KANAZAWA, N., KOYAMA, T., KUROSAKI, M., MAEKAWA, S., YAMASHIRO, T. & CHEN, C.-H. 2004. Specific inhibition of hepatitis C virus replication by cyclosporin A. *Biochemical and biophysical research communications,* 313**,** 42-47.
NAKAGAWA, M., SAKAMOTO, N., TANABE, Y., KOYAMA, T., ITSUI, Y., TAKEDA, Y., CHEN, C. H., KAKINUMA, S., OOOKA, S. & MAEKAWA, S. 2005. Suppression of hepatitis C virus replication by cyclosporin a is mediated by blockade of cyclophilins. *Gastroenterology,* 129**,** 1031-1041.

NAKAI, K., OKAMOTO, T., KIMURA-SOMEYA, T., ISHII, K., LIM, C. K., TANI, H., MATSUO, E., ABE, T., MORI, Y. & SUZUKI, T. 2006. Oligomerization of hepatitis C virus core protein is crucial for interaction with the cytoplasmic domain of E1 envelope protein. *Journal of virology,* 80**,** 11265-11273.

NANDA, S. K., HERION, D. & LIANG, T. J. 2006. Src homology 3 domain of hepatitis C virus NS5A protein interacts with Bin1 and is important for apoptosis and infectivity. *Gastroenterology,* 130**,** 794-809.

NANDURI, S., CARPICK, B. W., YANG, Y., WILLIAMS, B. R. & QIN, J. 1998. Structure of the double-stranded RNA-binding domain of the protein kinase PKR reveals the molecular basis of its dsRNA-mediated activation. *The EMBO journal,* 17**,** 5458-5465.

NANDURI, S., RAHMAN, F., WILLIAMS, B. R. & QIN, J. 2000. A dynamically tuned double-stranded RNA binding mechanism for the activation of antiviral kinase PKR. *The EMBO journal,* 19**,** 5567-5574.

NAOUMOV, N. V. 2014. Cyclophilin inhibition as potential therapy for liver diseases. *Journal of hepatology,* 61**,** 1166-1174.

NELSON, D. R., COOPER, J. N., LALEZARI, J. P., LAWITZ, E., POCKROS, P. J., GITLIN, N., FREILICH, B. F., YOUNES, Z. H., HARLAN, W. & GHALIB, R. 2015. All‐oral 12‐week treatment with daclatasvir plus sofosbuvir in patients with hepatitis C virus genotype 3 infection: ALLY‐3 phase III study. *Hepatology,* 61**,** 1127-1135.

NGURE, M., ISSUR, M., SHKRIABAI, N., LIU, H.-W., COSA, G., KVARATSKHELIA, M. & GÖTTE, M. 2016. Interactions of the disordered domain II of hepatitis C virus NS5A with cyclophilin A, NS5B, and viral RNA show extensive overlap. *ACS Infectious Diseases,* 2**,** 839-851.

NIELSEN, S. U., BASSENDINE, M. F., BURT, A. D., MARTIN, C., PUMEECHOCKCHAI, W. & TOMS, G. L. 2006. Association between hepatitis C virus and very-low-density lipoprotein (VLDL)/LDL analyzed in iodixanol density gradients. *Journal of virology,* 80**,** 2418-2428.

NIGRO, P., POMPILIO, G. & CAPOGROSSI, M. 2013. Cyclophilin A: a key player for human disease. *Cell death & disease,* 4**,** e888-e888.

NITTA, S., ASAHINA, Y., MATSUDA, M., YAMADA, N., SUGIYAMA, R., MASAKI, T., SUZUKI, R., KATO, N., WATANABE, M. & WAKITA, T. 2016. Effects of resistance-associated NS5A mutations in hepatitis C virus on viral production and susceptibility to antiviral reagents. *Scientific reports,* 6**,** 1-9.

NKONTCHOU, G., ZIOL, M., AOUT, M., LHABADIE, M., BAAZIA, Y., MAHMOUDI, A., ROULOT, D., GANNE‐CARRIE, N., GRANDO‐LEMAIRE, V. & TRINCHET, J. C. 2011. HCV genotype 3 is associated with a higher hepatocellular carcinoma incidence in patients with ongoing viral C cirrhosis. *Journal of viral hepatitis,* 18**,** e516-e522.

NOUROZ, F., SHAHEEN, S., MUJTABA, G. & NOREEN, S. 2015. An overview on hepatitis C virus genotypes and its control. *Egyptian Journal of Medical Human Genetics,* 16**,** 291-298.

OGAWA, K., HISHIKI, T., SHIMIZU, Y., FUNAMI, K., SUGIYAMA, K., MIYANARI, Y. & SHIMOTOHNO, K. 2009. Hepatitis C virus utilizes lipid droplet for production of infectious virus. *Proceedings of the Japan Academy, Series B,* 85**,** 217-228.

OLIVER KOCH, J. & BARTENSCHLAGER, R. 1999. Modulation of hepatitis C virus NS5A hyperphosphorylation by nonstructural proteins NS3, NS4A, and NS4B. *Journal of virology,* 73**,** 7138-7146.

ORGANIZATION, W. H. 2017. Global hepatitis report 2017: World Health Organization. *Accessed October,* 23**,** 2020.

ORGANIZATION, W. H. 2021. Global progress report on HIV, viral hepatitis and sexually transmitted infections, 2021: accountability for the global health sector strategies 2016â€“2021: actions for impact: web annex 2: data methods.

ORLAND, J. R., WRIGHT, T. L. & COOPER, S. 2001. Acute hepatitis C. *Hepatology (Baltimore, Md.),* 33**,** 321-327.

PAGE-SHAFER, K., PAPPALARDO, B. L., TOBLER, L. H., PHELPS, B. H., EDLIN, B. R., MOSS, A. R., WRIGHT, T. L., WRIGHT, D. J., O'BRIEN, T. R. & CAGLIOTI, S. 2008. Testing strategy to identify cases of acute hepatitis C virus (HCV) infection and to project HCV incidence rates. *Journal of clinical microbiology,* 46**,** 499-506.

PAGE, K., HAHN, J. A., EVANS, J., SHIBOSKI, S., LUM, P., DELWART, E., TOBLER, L., ANDREWS, W., AVANESYAN, L. & COOPER, S. 2009. Acute hepatitis C virus infection in young adult injection drug users: a prospective study of incident infection, resolution, and reinfection. *The Journal of infectious diseases,* 200**,** 1216-1226.

PALLAORO, M., LAHM, A., BIASIOL, G., BRUNETTI, M., NARDELLA, C., ORSATTI, L., BONELLI, F., ORRÙ, S., NARJES, F. & STEINKÜHLER, C. 2001. Characterization of the hepatitis C virus NS2/3 processing reaction by using a purified precursor protein. *Journal of virology,* 75**,** 9939-9946.

PALOMARES-JEREZ, M. F., NEMESIO, H. & VILLALAÍN, J. 2012. Interaction with membranes of the full C-terminal domain of protein NS4B from hepatitis C virus. *Biochimica et Biophysica Acta (BBA)-Biomembranes,* 1818**,** 2536-2549.

PANG, P. S., JANKOWSKY, E., PLANET, P. J. & PYLE, A. M. 2002. The hepatitis C viral NS3 protein is a processive DNA helicase with cofactor enhanced RNA unwinding. *The EMBO journal,* 21**,** 1168-1176.

PAUL, D. & BARTENSCHLAGER, R. 2015. Flaviviridae replication organelles: oh, what a tangled web we weave. *Annu Rev Virol,* 2**,** 289-310.

PAUL, D., HOPPE, S., SAHER, G., KRIJNSE-LOCKER, J. & BARTENSCHLAGER, R. 2013. Morphological and biochemical characterization of the membranous hepatitis C virus replication compartment. *Journal of virology,* 87**,** 10612-10627.

PAUL, D., MADAN, V. & BARTENSCHLAGER, R. 2014. Hepatitis C virus RNA replication and assembly: living on the fat of the land. *Cell host & microbe,* 16**,** 569-579.

PAUL, D., ROMERO-BREY, I., GOUTTENOIRE, J., STOITSOVA, S., KRIJNSE-LOCKER, J., MORADPOUR, D. & BARTENSCHLAGER, R. 2011. NS4B self-interaction through conserved C-terminal elements is required for the establishment of functional hepatitis C virus replication complexes. *Journal of virology,* 85**,** 6963-6976.

PAVLOVIĆ, D., NEVILLE, D. C., ARGAUD, O., BLUMBERG, B., DWEK, R. A., FISCHER, W. B. & ZITZMANN, N. 2003. The hepatitis C virus p7 protein forms an ion channel that is inhibited by long-alkyl-chain iminosugar derivatives. *Proceedings of the National Academy of Sciences,* 100**,** 6104-6108.

PENE, V., HERNANDEZ, C., VAULOUPÂ€FELLOUS, C., GARAUDÂ€AUNIS, J. & ROSENBERG, A. 2009. Sequential processing of hepatitis C virus core protein by host cell signal peptidase and signal peptide peptidase: a reassessment. *Journal of viral hepatitis,* 16**,** 705-715.

PENIN, F., BRASS, V., APPEL, N., RAMBOARINA, S., MONTSERRET, R., FICHEUX, D., BLUM, H. E., BARTENSCHLAGER, R. & MORADPOUR, D. 2004a. Structure and function of the membrane anchor domain of hepatitis C virus nonstructural protein 5A. *Journal of Biological Chemistry,* 279**,** 40835-40843.

PENIN, F., DUBUISSON, J., REY, F. A., MORADPOUR, D. & PAWLOTSKY, J. M. 2004b. Structural biology of hepatitis C virus. *Hepatology,* 39**,** 5-19.

PEYROU, M., CLÉMENT, S., MAIER, C., BOURGOIN, L., BRANCHE, E., CONZELMANN, S., KADDAI, V., FOTI, M. & NEGRO, F. 2013. PTEN protein phosphatase activity regulates hepatitis C virus secretion through modulation of cholesterol metabolism. *Journal of hepatology,* 59**,** 420-426.

PFLUGHEBER, J., FREDERICKSEN, B., SUMPTER JR, R., WANG, C., WARE, F., SODORA, D. L. & GALE JR, M. 2002. Regulation of PKR and IRF-1 during hepatitis C virus RNA replication. *Proceedings of the National Academy of Sciences,* 99**,** 4650-4655.

PHAM, A. M., SANTA MARIA, F. G., LAHIRI, T., FRIEDMAN, E., MARIÉ, I. J. & LEVY, D. E. 2016. PKR transduces MDA5-dependent signals for type I IFN induction. *PLoS pathogens,* 12**,** e1005489.

PHAN, T., BERAN, R. K., PETERS, C., LORENZ, I. C. & LINDENBACH, B. D. 2009. Hepatitis C virus NS2 protein contributes to virus particle assembly via opposing epistatic interactions with the E1-E2 glycoprotein and NS3-NS4A enzyme complexes. *Journal of virology,* 83**,** 8379-8395.

PHAN, T., KOHLWAY, A., DIMBERU, P., PYLE, A. M. & LINDENBACH, B. D. 2011. The acidic domain of hepatitis C virus NS4A contributes to RNA replication and virus particle assembly. *Journal of virology,* 85**,** 1193-1204.

PIETSCHMANN, T., KAUL, A., KOUTSOUDAKIS, G., SHAVINSKAYA, A., KALLIS, S., STEINMANN, E., ABID, K., NEGRO, F., DREUX, M. & COSSET, F.-L. 2006. Construction and characterization of infectious intragenotypic and intergenotypic hepatitis C virus chimeras. *Proceedings of the National Academy of Sciences,* 103**,** 7408-7413.

PIÑEIRO, D. & MARTINEZ-SALAS, E. 2012. RNA structural elements of hepatitis C virus controlling viral RNA translation and the implications for viral pathogenesis. *Viruses,* 4**,** 2233-2250.

PIVER, E., BOYER, A., GAILLARD, J., BULL, A., BEAUMONT, E., ROINGEARD, P. & MEUNIER, J.-C. 2017. Ultrastructural organisation of HCV from the bloodstream of infected patients revealed by electron microscopy after specific immunocapture. *Gut,* 66**,** 1487-1495.

PLOEN, D., HAFIRASSOU, M. L., HIMMELSBACH, K., SAUTER, D., BINIOSSEK, M. L., WEISS, T. S., BAUMERT, T. F., SCHUSTER, C. & HILDT, E. 2013. TIP47 plays a crucial role in the life cycle of hepatitis C virus. *Journal of hepatology,* 58**,** 1081-1088.

POLYAK, S. J., KLEIN, K. C., SHOJI, I., MIYAMURA, T. & LINGAPPA, J. R. 2006. Assemble and interact: pleiotropic functions of the HCV core protein. *Hepatitis C viruses: genomes and molecular biology*.

POLYAK, S. J., PASCHAL, D. M., MCARDLE, S., JR, M. J., MORADPOUR, D. & GRETCH, D. R. 1999. Characterization of the effects of hepatitis C virus nonstructural 5A protein expression in human cell lines and on interferon‐sensitive virus replication. *Hepatology,* 29**,** 1262-1271.

POORDAD, F. & DIETERICH, D. 2012. Treating hepatitis C: current standard of care and emerging direct‐acting antiviral agents. *Journal of viral hepatitis,* 19**,** 449-464.

POORDAD, F., MCCONE JR, J., BACON, B. R., BRUNO, S., MANNS, M. P., SULKOWSKI, M. S., JACOBSON, I. M., REDDY, K. R., GOODMAN, Z. D. & BOPARAI, N. 2011. Boceprevir for untreated chronic HCV genotype 1 infection. *New England Journal of Medicine,* 364**,** 1195-1206.

POPESCU, C.-I., CALLENS, N., TRINEL, D., ROINGEARD, P., MORADPOUR, D., DESCAMPS, V., DUVERLIE, G., PENIN, F., HÉLIOT, L. & ROUILLÉ, Y. 2011. NS2 protein of hepatitis C virus interacts with structural and non-structural proteins towards virus assembly. *PLoS pathogens,* 7**,** e1001278.

POPESCU, C. I. & DUBUISSON, J. 2010. Role of lipid metabolism in hepatitis C virus assembly and entry. *Biology of the Cell,* 102**,** 63-74.

PREMKUMAR, A., WILSON, L., EWART, G. & GAGE, P. 2004. Cation-selective ion channels formed by p7 of hepatitis C virus are blocked by hexamethylene amiloride. *FEBS letters,* 557**,** 99-103.

PRENTOE, J., SERRE, S. B., RAMIREZ, S., NICOSIA, A., GOTTWEIN, J. M. & BUKH, J. 2014. Hypervariable region 1 deletion and required adaptive envelope mutations confer decreased dependency on scavenger receptor class B type I and low-density lipoprotein receptor for hepatitis C virus. *Journal of virology,* 88**,** 1725-1739.

PRENTOE, J., VELÁZQUEZ‐MOCTEZUMA, R., FOUNG, S. K., LAW, M. & BUKH, J. 2016. Hypervariable region 1 shielding of hepatitis C virus is a main contributor to genotypic differences in neutralization sensitivity. *Hepatology,* 64**,** 1881-1892.

QUAN, P.-L., FIRTH, C., CONTE, J. M., WILLIAMS, S. H., ZAMBRANA-TORRELIO, C. M., ANTHONY, S. J., ELLISON, J. A., GILBERT, A. T., KUZMIN, I. V. & NIEZGODA, M. 2013. Bats are a major natural reservoir for hepaciviruses and pegiviruses. *Proceedings of the National Academy of Sciences,* 110**,** 8194-8199.

QUINTAVALLE, M., SAMBUCINI, S., SUMMA, V., ORSATTI, L., TALAMO, F., DE FRANCESCO, R. & NEDDERMANN, P. 2007. Hepatitis C virus NS5A is a direct substrate of casein kinase I-α, a cellular kinase identified by inhibitor affinity chromatography using specific NS5A hyperphosphorylation inhibitors. *Journal of Biological Chemistry,* 282**,** 5536-5544.

RAMASAMY, I. 2014. Recent advances in physiological lipoprotein metabolism. *Clinical Chemistry and Laboratory Medicine (CCLM),* 52**,** 1695-1727.

RAMIREZ, S., MIKKELSEN, L. S., GOTTWEIN, J. M. & BUKH, J. 2016. Robust HCV genotype 3a infectious cell culture system permits identification of escape variants with resistance to sofosbuvir. *Gastroenterology,* 151**,** 973-985. e2.

RANEY, K. D., SHARMA, S. D., MOUSTAFA, I. M. & CAMERON, C. E. 2010. Hepatitis C virus non-structural protein 3 (HCV NS3): a multifunctional antiviral target. *Journal of Biological Chemistry,* 285**,** 22725-22731.

REISS, S., REBHAN, I., BACKES, P., ROMERO-BREY, I., ERFLE, H., MATULA, P., KADERALI, L., POENISCH, M., BLANKENBURG, H. & HIET, M.-S. 2011. Recruitment and activation of a lipid kinase by hepatitis C virus NS5A is essential for integrity of the membranous replication compartment. *Cell host & microbe,* 9**,** 32-45.

ROBIDA, J. M., NELSON, H. B., LIU, Z. & TANG, H. 2007. Characterization of hepatitis C virus subgenomic replicon resistance to cyclosporine in vitro. *Journal of virology,* 81**,** 5829-5840.

ROCCASECCA, R., ANSUINI, H., VITELLI, A., MEOLA, A., SCARSELLI, E., ACALI, S., PEZZANERA, M., ERCOLE, B. B., MCKEATING, J. & YAGNIK, A. 2003. Binding of the hepatitis C virus E2 glycoprotein to CD81 is strain specific and is modulated by a complex interplay between hypervariable regions 1 and 2. *Journal of virology,* 77**,** 1856-1867.

ROCKSTROH, J. R. K. 2015. HCV cure for everyone or which challenges remain? *Journal of Virus Eradication,* 1**,** 55-58.

ROMERO-BREY, I., BERGER, C., KALLIS, S., KOLOVOU, A., PAUL, D., LOHMANN, V. & BARTENSCHLAGER, R. 2015. NS5A domain 1 and polyprotein cleavage kinetics are critical for induction of double-membrane vesicles associated with hepatitis C virus replication. *MBio,* 6**,** e00759-15.

ROMERO-BREY, I., MERZ, A., CHIRAMEL, A., LEE, J.-Y., CHLANDA, P., HASELMAN, U., SANTARELLA-MELLWIG, R., HABERMANN, A., HOPPE, S. & KALLIS, S. 2012. Three-dimensional architecture and biogenesis of membrane structures associated with hepatitis C virus replication. *PLoS pathogens,* 8**,** e1003056.

ROSA, D., CAMPAGNOLI, S., MORETTO, C., GUENZI, E., COUSENS, L., CHIN, M., DONG, C., WEINER, A. J., LAU, J. & CHOO, Q.-L. 1996. A quantitative test to estimate neutralizing antibodies to the hepatitis C virus: cytofluorimetric assessment of envelope glycoprotein 2 binding to target cells. *Proceedings of the National Academy of Sciences,* 93**,** 1759-1763.

ROSS-THRIEPLAND, D., AMAKO, Y. & HARRIS, M. 2013. The C terminus of NS5A domain II is a key determinant of hepatitis C virus genome replication, but is not required for virion assembly and release. *The Journal of general virology,* 94**,** 1009.

ROSS-THRIEPLAND, D. & HARRIS, M. 2015. Hepatitis C virus NS5A: enigmatic but still promiscuous 10 years on! *Journal of General Virology,* 96**,** 727-738.

ROY, A., KUCUKURAL, A. & ZHANG, Y. 2010. I-TASSER: a unified platform for automated protein structure and function prediction. *Nature protocols,* 5**,** 725-738.

RYFFEL, B., WOERLY, G., GREINER, B., HAENDLER, B., MIHATSCH, M. & FOXWELL, B. 1991. Distribution of the cyclosporine binding protein cyclophilin in human tissues. *Immunology,* 72**,** 399.

SABARIEGOS, R., ALBENTOSA-GONZÁLEZ, L., PALMERO, B., CLEMENTE-CASARES, P., RAMÍREZ, E., GARCÍA-CRESPO, C., GALLEGO, I., DE ÁVILA, A. I., PERALES, C. & DOMINGO, E. 2021. Akt Phosphorylation of Hepatitis C Virus NS5B Regulates Polymerase Activity and Hepatitis C Virus Infection. *Frontiers in Microbiology***,** 3043.

SADLER, A. J. & WILLIAMS, B. R. G. 2007. Structure and function of the protein kinase R. *Interferon: The 50th Anniversary***,** 253-292.

SAEED, M., GONDEAU, C., HMWE, S., YOKOKAWA, H., DATE, T., SUZUKI, T., KATO, T., MAUREL, P. & WAKITA, T. 2013. Replication of hepatitis C virus genotype 3a in cultured cells. *Gastroenterology,* 144**,** 56-58. e7.

SAEED, M., SCHEEL, T. K., GOTTWEIN, J. M., MARUKIAN, S., DUSTIN, L. B., BUKH, J. & RICE, C. M. 2012. Efficient replication of genotype 3a and 4a hepatitis C virus replicons in human hepatoma cells. *Antimicrobial agents and chemotherapy,* 56**,** 5365-5373.

SALLOUM, S., WANG, H., FERGUSON, C., PARTON, R. G. & TAI, A. W. 2013. Rab18 binds to hepatitis C virus NS5A and promotes interaction between sites of viral replication and lipid droplets. *PLoS pathogens,* 9**,** e1003513.

SANTOLINI, E., MIGLIACCIO, G. & LA MONICA, N. 1994. Biosynthesis and biochemical properties of the hepatitis C virus core protein. *Journal of virology,* 68**,** 3631-3641.

SANTOLINI, E., PACINI, L., FIPALDINI, C., MIGLIACCIO, G. & MONICA, N. 1995. The NS2 protein of hepatitis C virus is a transmembrane polypeptide. *Journal of virology,* 69**,** 7461-7471.

SCARSELLI, E., ANSUINI, H., CERINO, R., ROCCASECCA, R. M., ACALI, S., FILOCAMO, G., TRABONI, C., NICOSIA, A., CORTESE, R. & VITELLI, A. 2002. The human scavenger receptor class B type I is a novel candidate receptor for the hepatitis C virus. *The EMBO journal,* 21**,** 5017-5025.

SCHALLER, T., APPEL, N., KOUTSOUDAKIS, G., KALLIS, S., LOHMANN, V., PIETSCHMANN, T. & BARTENSCHLAGER, R. 2007. Analysis of hepatitis C virus superinfection exclusion by using novel fluorochrome gene-tagged viral genomes. *Journal of virology,* 81**,** 4591-4603.

SCHEEL, T. K. & RICE, C. M. 2013. Understanding the hepatitis C virus life cycle paves the way for highly effective therapies. *Nature medicine,* 19**,** 837-849.

SCHINDELIN, J., ARGANDA-CARRERAS, I., FRISE, E., KAYNIG, V., LONGAIR, M., PIETZSCH, T., PREIBISCH, S., RUEDEN, C., SAALFELD, S. & SCHMID, B. 2012. Fiji: an open-source platform for biological-image analysis. *Nature methods,* 9**,** 676-682.

SCHMEDT, C., GREEN, S. R., MANCHE, L., TAYLOR, D. R., MA, Y. & MATHEWS, M. B. 1995. Functional characterization of the RNA-binding domain and motif of the double-stranded RNA-dependent protein kinase DAI (PKR). *Journal of molecular biology,* 249**,** 29-44.

SCHMIDT-MENDE, J., BIECK, E., HÜGLE, T., PENIN, F. O., RICE, C. M., BLUM, H. E. & MORADPOUR, D. 2001. Determinants for membrane association of the hepatitis C virus RNA-dependent RNA polymerase. *Journal of Biological Chemistry,* 276**,** 44052-44063.

SCHULZ, O., PICHLMAIR, A., REHWINKEL, J., ROGERS, N. C., SCHEUNER, D., KATO, H., TAKEUCHI, O., AKIRA, S., KAUFMAN, R. J. & E SOUSA, C. R. 2010. Protein kinase R contributes to immunity against specific viruses by regulating interferon mRNA integrity. *Cell host & microbe,* 7**,** 354-361.

SECCI, E., LUCHINAT, E. & BANCI, L. 2016. The Casein Kinase 2‐Dependent Phosphorylation of NS5A Domain 3 from Hepatitis C Virus Followed by Time‐Resolved NMR Spectroscopy. *ChemBioChem,* 17**,** 328-333.

SEEFF, L. B. 2009. The history of the â€œnatural historyâ€ of hepatitis C (1968â€“2009). *Liver International,* 29**,** 89-99.

SEREBROV, V. & PYLE, A. M. 2004. Periodic cycles of RNA unwinding and pausing by hepatitis C virus NS3 helicase. *Nature,* 430**,** 476-480.

SESMERO, E. & THORPE, I. F. 2015. Using the hepatitis C virus RNA-dependent RNA polymerase as a model to understand viral polymerase structure, function and dynamics. *Viruses,* 7**,** 3974-3994.

SHAH, R., AHOVEGBE, L., NIEBEL, M., SHEPHERD, J. & THOMSON, E. C. 2021. Non-epidemic HCV genotypes in low-and middle-income countries and the risk of resistance to current direct-acting antiviral regimens. *Journal of hepatology,* 75**,** 462-473.

SHARMA, N. R., MATEU, G., DREUX, M., GRAKOUI, A., COSSET, F.-L. & MELIKYAN, G. B. 2011. Hepatitis C virus is primed by CD81 protein for low pH-dependent fusion. *Journal of Biological Chemistry,* 286**,** 30361-30376.

SHAVINSKAYA, A., BOULANT, S., PENIN, F., MCLAUCHLAN, J. & BARTENSCHLAGER, R. 2007. The lipid droplet binding domain of hepatitis C virus core protein is a major determinant for efficient virus assembly. *Journal of Biological Chemistry,* 282**,** 37158-37169.

SHEPARD, C. W., SIMARD, E. P., FINELLI, L., FIORE, A. E. & BELL, B. P. 2006. Hepatitis B virus infection: epidemiology and vaccination. *Epidemiologic reviews,* 28**,** 112-125.

SHERRY, B., YARLETT, N., STRUPP, A. & CERAMI, A. 1992. Identification of cyclophilin as a proinflammatory secretory product of lipopolysaccharide-activated macrophages. *Proceedings of the National Academy of Sciences,* 89**,** 3511-3515.

SHI, Q., JIANG, J. & LUO, G. 2013. Syndecan-1 serves as the major receptor for attachment of hepatitis C virus to the surfaces of hepatocytes. *Journal of virology,* 87**,** 6866-6875.

SHI, S. T., POLYAK, S. J., TU, H., TAYLOR, D. R., GRETCH, D. R. & LAI, M. M. 2002. Hepatitis C virus NS5A colocalizes with the core protein on lipid droplets and interacts with apolipoproteins. *Virology,* 292**,** 198-210.

SHIMOIKE, T., MCKENNA, S. A., LINDHOUT, D. A. & PUGLISI, J. D. 2009. Translational insensitivity to potent activation of PKR by HCV IRES RNA. *Antiviral research,* 83**,** 228-237.

SIEVERT, W., ALTRAIF, I., RAZAVI, H. A., ABDO, A., AHMED, E. A., ALOMAIR, A., AMARAPURKAR, D., CHEN, C. H., DOU, X. & EL KHAYAT, H. 2011. A systematic review of hepatitis C virus epidemiology in Asia, Australia and Egypt. *Liver international,* 31**,** 61-80.

SIMMONDS, P. 2001. 2000 Fleming Lecture. The origin and evolution of hepatitis viruses in humans. *Journal of General Virology,* 82**,** 693-712.

SIMMONDS, P., HOLMES, E., CHA, T.-A., CHAN, S.-W., MCOMISH, F., IRVINE, B., BEALL, E., YAP, P., KOLBERG, J. & URDEA, M. 1993. Classification of hepatitis C virus into six major genotypes and a series of subtypes by phylogenetic analysis of the NS-5 region. *Journal of general virology,* 74**,** 2391-2399.

SIMMONDS, P., SMITH, D., MCOMISH, F., YAP, P., KOLBERG, J., URDEA, M. & HOLMES, E. 1994. Identification of genotypes of hepatitis C virus by sequence comparisons in the core, E1 and NS-5 regions. *Journal of General Virology,* 75**,** 1053-1061.

SIMONS, J. N., PILOT-MATIAS, T. J., LEARY, T. P., DAWSON, G. J., DESAI, S. M., SCHLAUDER, G. G., MUERHOFF, A. S., ERKER, J. C., BUIJK, S. L. & CHALMERS, M. L. 1995. Identification of two flavivirus-like genomes in the GB hepatitis agent. *Proceedings of the National academy of Sciences,* 92**,** 3401-3405.

SINGH, S., MALHOTRA, V. & SARIN, S. K. 2004. Distribution of hepatitis C virus genotypes in patients with chronic hepatitis C infection in India. *INDIAN JOURNAL OF MEDICAL RESEARCH.,* 119**,** 145-148.

SIR, D., KUO, C.-F., TIAN, Y., LIU, H. M., HUANG, E. J., JUNG, J. U., MACHIDA, K. & OU, J.-H. J. 2012. Replication of hepatitis C virus RNA on autophagosomal membranes. *Journal of Biological Chemistry,* 287**,** 18036-18043.

SIU, G. K. Y., ZHOU, F., YU, M. K., ZHANG, L., WANG, T., LIANG, Y., CHEN, Y., CHAN, H. C. & YU, S. 2016. Hepatitis C virus NS5A protein cooperates with phosphatidylinositol 4-kinase IIIα to induce mitochondrial fragmentation. *Scientific reports,* 6**,** 1-13.

SMITH, D., MAGRI, A., BONSALL, D., IP, C. L., TREBES, A., BROWN, A., PIAZZA, P., BOWDEN, R., NGUYEN, D. & ANSARI, M. A. 2019. Resistance analysis of genotype 3 hepatitis C virus indicates subtypes inherently resistant to nonstructural protein 5A inhibitors. *Hepatology,* 69**,** 1861-1872.

SMITH, D. B., BUKH, J., KUIKEN, C., MUERHOFF, A. S., RICE, C. M., STAPLETON, J. T. & SIMMONDS, P. 2014. Expanded classification of hepatitis C virus into 7 genotypes and 67 subtypes: updated criteria and genotype assignment web resource. *Hepatology,* 59**,** 318-327.

SÓLYOM, Z., MA, P., SCHWARTEN, M., BOSCO, M., POLIDORI, A., DURAND, G., WILLBOLD, D. & BRUTSCHER, B. 2015. The disordered region of the HCV protein NS5A: conformational dynamics, SH3 binding, and phosphorylation. *Biophysical journal,* 109**,** 1483-1496.

SONG, Y., FRIEBE, P., TZIMA, E., JUÌˆNEMANN, C., BARTENSCHLAGER, R. & NIEPMANN, M. 2006. The hepatitis C virus RNA 3â€²-untranslated region strongly enhances translation directed by the internal ribosome entry site. *Journal of virology,* 80**,** 11579-11588.

SOOD, A., SARIN, S. K., MIDHA, V., HISSAR, S., SOOD, N., BANSAL, P. & BANSAL, M. 2012. Prevalence of hepatitis C virus in a selected geographical area of northern India: a population based survey. *Indian Journal of Gastroenterology,* 31**,** 232-236.

SORRENTINO, V., NELSON, J. K., MASPERO, E., MARQUES, A. R., SCHEER, L., POLO, S. & ZELCER, N. 2013. The LXR-IDOL axis defines a clathrin-, caveolae-, and dynamin-independent endocytic route for LDLR internalization and lysosomal degradation. *Journal of lipid research,* 54**,** 2174-2184.

SOURISSEAU, M., MICHTA, M. L., ZONY, C., ISRAELOW, B., HOPCRAFT, S. E., NARBUS, C. M., PARRA MARTÍN, A. & EVANS, M. J. 2013. Temporal analysis of hepatitis C virus cell entry with occludin directed blocking antibodies. *PLoS pathogens,* 9**,** e1003244.

SPIK, G., HAENDLER, B., DELMAS, O., MARILLER, C., CHAMOUX, M., MAES, P., TARTAR, A., MONTREUIL, J., STEDMAN, K. & KOCHER, H. 1991. A novel secreted cyclophilin-like protein (SCYLP). *Journal of Biological Chemistry,* 266**,** 10735-10738.

STAMNES, M. A., RUTHERFORD, S. L. & ZUKER, C. S. 1992. Cyclophilins: a new family of proteins involved in intracellular folding. *Trends in cell biology,* 2**,** 272-276.

STAPLEFORD, K. A. & LINDENBACH, B. D. 2011. Hepatitis C virus NS2 coordinates virus particle assembly through physical interactions with the E1-E2 glycoprotein and NS3-NS4A enzyme complexes. *Journal of virology,* 85**,** 1706-1717.

STAPLETON, J. T., FOUNG, S., MUERHOFF, A. S., BUKH, J. & SIMMONDS, P. 2011. The GB viruses: a review and proposed classification of GBV-A, GBV-C (HGV), and GBV-D in genus Pegivirus within the family Flaviviridae. *Journal of general virology,* 92**,** 233-246.

STEWART, H., BARTLETT, C., ROSS-THRIEPLAND, D., SHAW, J., GRIFFIN, S. & HARRIS, M. 2015. A novel method for the measurement of hepatitis C virus infectious titres using the IncuCyte ZOOM and its application to antiviral screening. *Journal of virological methods,* 218**,** 59-65.

SU, J., BROOK, R. A., KLEINMAN, N. L. & COREY‐LISLE, P. 2010. The impact of hepatitis C virus infection on work absence, productivity, and healthcare benefit costs. *Hepatology,* 52**,** 436-442.

SUDA, G., KIMURA, M., SHIGESAWA, T., SUZUKI, K., NAKAMURA, A., OHARA, M., KAWAGISHI, N., NAKAI, M., SHO, T. & MAEHARA, O. 2019. Effects of resistance‐associated variants in genotype 2 hepatitis C virus on viral replication and susceptibility to antihepatitis C virus drugs. *Hepatology Research,* 49**,** 1275-1285.

SUDHAKAR, A., RAMACHANDRAN, A., GHOSH, S., HASNAIN, S. E., KAUFMAN, R. J. & RAMAIAH, K. V. 2000. Phosphorylation of serine 51 in initiation factor 2α (eIF2α) promotes complex formation between eIF2α (P) and eIF2B and causes inhibition in the guanine nucleotide exchange activity of eIF2B. *Biochemistry,* 39**,** 12929-12938.

SUMPTER JR, R., LOO, Y.-M., FOY, E., LI, K., YONEYAMA, M., FUJITA, T., LEMON, S. M. & GALE JR, M. 2005. Regulating intracellular antiviral defense and permissiveness to hepatitis C virus RNA replication through a cellular RNA helicase, RIG-I. *Journal of virology,* 79**,** 2689-2699.

SUN, S., GUO, M., ZHANG, J. B., HA, A., YOKOYAMA, K. K. & CHIU, R. H. 2014. Cyclophilin A (CypA) interacts with NF-κB subunit, p65/RelA, and contributes to NF-κB activation signaling. *PloS one,* 9**,** e96211.

SUN, S., WANG, Q., GIANG, A., CHENG, C., SOO, C., WANG, C.-Y., LIAU, L. M. & CHIU, R. 2011. Knockdown of CypA inhibits interleukin-8 (IL-8) and IL-8-mediated proliferation and tumor growth of glioblastoma cells through down-regulated NF-κB. *Journal of neuro-oncology,* 101**,** 1-14.

SUNDARAM, M. & YAO, Z. 2012. Intrahepatic role of exchangeable apolipoproteins in lipoprotein assembly and secretion. *Arteriosclerosis, thrombosis, and vascular biology,* 32**,** 1073-1078.

SUZUKI, J., JIN, Z.-G., MEOLI, D. F., MATOBA, T. & BERK, B. C. 2006. Cyclophilin A is secreted by a vesicular pathway in vascular smooth muscle cells. *Circulation research,* 98**,** 811-817.

SUZUKI, R., MATSUURA, Y., SUZUKI, T., ANDO, A., CHIBA, J., HARADA, S., SAITO, I. & MIYAMURA, T. 1995. Nuclear localization of the truncated hepatitis C virus core protein with its hydrophobic C terminus deleted. *Journal of General Virology,* 76**,** 53-61.

SUZUKI, R., SAKAMOTO, S., TSUTSUMI, T., RIKIMARU, A., TANAKA, K., SHIMOIKE, T., MORIISHI, K., IWASAKI, T., MIZUMOTO, K. & MATSUURA, Y. 2005. Molecular determinants for subcellular localization of hepatitis C virus core protein. *Journal of virology,* 79**,** 1271-1281.

SWEENEY, Z. K., FU, J. & WIEDMANN, B. 2014. From chemical tools to clinical medicines: nonimmunosuppressive cyclophilin inhibitors derived from the cyclosporin and sanglifehrin scaffolds. *Journal of medicinal chemistry,* 57**,** 7145-7159.

SY, T. & JAMAL, M. M. 2006. Epidemiology of hepatitis C virus (HCV) infection. *International journal of medical sciences,* 3**,** 41-46.

TAI, A. W., BENITA, Y., PENG, L. F., KIM, S.-S., SAKAMOTO, N., XAVIER, R. J. & CHUNG, R. T. 2009. A functional genomic screen identifies cellular cofactors of hepatitis C virus replication. *Cell host & microbe,* 5**,** 298-307.

TAI, C.-L., CHI, W.-K., CHEN, D.-S. & HWANG, L.-H. 1996. The helicase activity associated with hepatitis C virus nonstructural protein 3 (NS3). *Journal of virology,* 70**,** 8477-8484.

TAKADA, Y., ICHIKAWA, H., PATAER, A., SWISHER, S. & AGGARWAL, B. 2007. Genetic deletion of PKR abrogates TNF-induced activation of IκBα kinase, JNK, Akt and cell proliferation but potentiates p44/p42 MAPK and p38 MAPK activation. *Oncogene,* 26**,** 1201-1212.

TAMAI, K., SHIINA, M., TANAKA, N., NAKANO, T., YAMAMOTO, A., KONDO, Y., KAKAZU, E., INOUE, J., FUKUSHIMA, K. & SANO, K. 2012. Regulation of hepatitis C virus secretion by the Hrs-dependent exosomal pathway. *Virology,* 422**,** 377-385.

TAN, S.-L., NAKAO, H., HE, Y., VIJAYSRI, S., NEDDERMANN, P., JACOBS, B. L., MAYER, B. J. & KATZE, M. G. 1999. NS5A, a nonstructural protein of hepatitis C virus, binds growth factor receptor-bound protein 2 adaptor protein in a Src homology 3 domain/ligand-dependent manner and perturbs mitogenic signaling. *Proceedings of the National Academy of Sciences,* 96**,** 5533-5538.

TANIGUCHI, T., OGASAWARA, K., TAKAOKA, A. & TANAKA, N. 2001. IRF family of transcription factors as regulators of host defense. *Annual review of immunology,* 19**,** 623.

TANIUCHI, S., MIYAKE, M., TSUGAWA, K., OYADOMARI, M. & OYADOMARI, S. 2016. Integrated stress response of vertebrates is regulated by four eIF2α kinases. *Scientific reports,* 6**,** 1-11.

TANJI, Y., HIJIKATA, M., SATOH, S., KANEKO, T. & SHIMOTOHNO, K. 1995a. Hepatitis C virus-encoded nonstructural protein NS4A has versatile functions in viral protein processing. *Journal of virology,* 69**,** 1575-1581.

TANJI, Y., KANEKO, T., SATOH, S. & SHIMOTOHNO, K. 1995b. Phosphorylation of hepatitis C virus-encoded nonstructural protein NS5A. *Journal of Virology,* 69**,** 3980-3986.

TARGETT-ADAMS, P., BOULANT, S., DOUGLAS, M. W. & MCLAUCHLAN, J. M. 2010. Lipid metabolism and HCV infection. *Viruses,* 2**,** 1195-1217.

TARGETT-ADAMS, P., BOULANT, S. & MCLAUCHLAN, J. 2008a. Visualization of double-stranded RNA in cells supporting hepatitis C virus RNA replication. *Journal of virology,* 82**,** 2182-2195.

TARGETT-ADAMS, P., HOPE, G., BOULANT, S. & MCLAUCHLAN, J. 2008b. Maturation of hepatitis C virus core protein by signal peptide peptidase is required for virus production. *Journal of Biological Chemistry,* 283**,** 16850-16859.

TARGETT-ADAMS, P. & MCLAUCHLAN, J. 2005. Development and characterization of a transient-replication assay for the genotype 2a hepatitis C virus subgenomic replicon. *Journal of general virology,* 86**,** 3075-3080.

TAYLOR, D. R., SHI, S. T., ROMANO, P. R., BARBER, G. N. & LAI, M. M. 1999. Inhibition of the interferon-inducible protein kinase PKR by HCV E2 protein. *Science,* 285**,** 107-110.

TAYLOR, D. R., TIAN, B., ROMANO, P. R., HINNEBUSCH, A. G., LAI, M. M. & MATHEWS, M. B. 2001. Hepatitis C virus envelope protein E2 does not inhibit PKR by simple competition with autophosphorylation sites in the RNA-binding domain. *Journal of Virology,* 75**,** 1265-1273.

TEDBURY, P., WELBOURN, S., PAUSE, A., KING, B., GRIFFIN, S. & HARRIS, M. 2011. The subcellular localization of the hepatitis C virus non-structural protein NS2 is regulated by an ion channel-independent function of the p7 protein. *The Journal of general virology,* 92**,** 819.

TELLINGHUISEN, T. L., FOSS, K. L. & TREADAWAY, J. 2008a. Regulation of hepatitis C virion production via phosphorylation of the NS5A protein. *PLoS pathogens,* 4**,** e1000032.

TELLINGHUISEN, T. L., FOSS, K. L., TREADAWAY, J. C. & RICE, C. M. 2008b. Identification of residues required for RNA replication in domains II and III of the hepatitis C virus NS5A protein. *Journal of virology,* 82**,** 1073-1083.

TELLINGHUISEN, T. L., MARCOTRIGIANO, J., GORBALENYA, A. E. & RICE, C. M. 2004. The NS5A protein of hepatitis C virus is a zinc metalloprotein. *Journal of Biological Chemistry,* 279**,** 48576-48587.

TELLINGHUISEN, T. L., MARCOTRIGIANO, J. & RICE, C. M. 2005. Structure of the zinc-binding domain of an essential component of the hepatitis C virus replicase. *Nature,* 435**,** 374-379.

TERAOKA, S., MISHIRO, S., EBIHARA, K., SANAKA, T., YAMAGUCHI, Y., NAKAJIMA, I., KAWAI, T., YAGISAWA, T., HONDA, H. & FUCHINOUE, S. Effect of cyclosporine on proliferation of non-A, non-B hepatitis virus. Transplantation Proceedings, 1988. 868-876.

THAPAR, R. 2015. Roles of prolyl isomerases in RNA-mediated gene expression. *Biomolecules,* 5**,** 974-999.

THOMPSON, A. A., ZOU, A., YAN, J., DUGGAL, R., HAO, W., MOLINA, D., CRONIN, C. N. & WELLS, P. A. 2009. Biochemical characterization of recombinant hepatitis C virus nonstructural protein 4B: evidence for ATP/GTP hydrolysis and adenylate kinase activity. *Biochemistry,* 48**,** 906-916.

THOMSSEN, R., BONK, S., PROPFE, C., HEERMANN, K.-H., KÖCHEL, H. & UY, A. 1992. Association of hepatitis C virus in human sera with β-lipoprotein. *Medical microbiology and immunology,* 181**,** 293-300.

TOKUMOTO, Y., HIASA, Y., HORIIKE, N., MICHITAKA, K., MATSUURA, B., CHUNG, R. T. & ONJI, M. 2007. Hepatitis C virus expression and interferon antiviral action is dependent on PKR expression. *Journal of medical virology,* 79**,** 1120-1127.

TORONEY, R., NALLAGATLA, S. R., BOYER, J. A., CAMERON, C. E. & BEVILACQUA, P. C. 2010. Regulation of PKR by HCV IRES RNA: importance of domain II and NS5A. *Journal of molecular biology,* 400**,** 393-412.

TRIPATHI, L. P., KAMBARA, H., CHEN, Y.-A., NISHIMURA, Y., MORIISHI, K., OKAMOTO, T., MORITA, E., ABE, T., MORI, Y. & MATSUURA, Y. 2013. Understanding the biological context of NS5A–host interactions in HCV infection: a network-based approach. *Journal of proteome research,* 12**,** 2537-2551.

TSCHERNE, D. M., JONES, C. T., EVANS, M. J., LINDENBACH, B. D., MCKEATING, J. A. & RICE, C. M. 2006. Time-and temperature-dependent activation of hepatitis C virus for low-pH-triggered entry. *Journal of virology,* 80**,** 1734-1741.

TU, Z., HAMALAINEN-LAANAYA, H. K., NISHITANI, C., KUROKI, Y., CRISPE, I. N. & ORLOFF, M. S. 2012. HCV core and NS3 proteins manipulate human blood-derived dendritic cell development and promote Th 17 differentiation. *International immunology,* 24**,** 97-106.

URBAN, S., NEUMANN-HAEFELIN, C. & LAMPERTICO, P. 2021. Hepatitis D virus in 2021: virology, immunology and new treatment approaches for a difficult-to-treat disease. *Gut,* 70**,** 1782-1794.

URBANI, A., BAZZO, R., NARDI, M. C., CICERO, D. O., DE FRANCESCO, R., STEINKÜHLER, C. & BARBATO, G. 1998. The metal binding site of the hepatitis C virus NS3 protease: A spectroscopic investigation. *Journal of Biological Chemistry,* 273**,** 18760-18769.

VALERO, M. L., SABARIEGOS, R., CIMAS, F. J., PERALES, C., DOMINGO, E., SÁNCHEZ-PRIETO, R. & MAS, A. 2016. Hepatitis C virus RNA-dependent RNA polymerase interacts with the Akt/PKB kinase and induces its subcellular relocalization. *Antimicrobial agents and chemotherapy,* 60**,** 3540-3550.

VERDEGEM, D., BADILLO, A., WIERUSZESKI, J.-M., LANDRIEU, I., LEROY, A., BARTENSCHLAGER, R., PENIN, F., LIPPENS, G. & HANOULLE, X. 2011. Domain 3 of NS5A protein from the hepatitis C virus has intrinsic α-helical propensity and is a substrate of cyclophilin A. *Journal of Biological Chemistry,* 286**,** 20441-20454.

VIEYRES, G., BROHM, C., FRIESLAND, M., GENTZSCH, J., WÖLK, B., ROINGEARD, P., STEINMANN, E. & PIETSCHMANN, T. 2013. Subcellular localization and function of an epitope-tagged p7 viroporin in hepatitis C virus-producing cells. *Journal of virology,* 87**,** 1664-1678.

VIEYRES, G., DUBUISSON, J. & PIETSCHMANN, T. 2014. Incorporation of hepatitis C virus E1 and E2 glycoproteins: the keystones on a peculiar virion. *Viruses,* 6**,** 1149-1187.

VIEYRES, G., THOMAS, X., DESCAMPS, V. R., DUVERLIE, G., PATEL, A. H. & DUBUISSON, J. 2010. Characterization of the envelope glycoproteins associated with infectious hepatitis C virus. *Journal of virology,* 84**,** 10159-10168.

VOGT, D. A., CAMUS, G., HERKER, E., WEBSTER, B. R., TSOU, C.-L., GREENE, W. C., YEN, T.-S. B. & OTT, M. 2013. Lipid droplet-binding protein TIP47 regulates hepatitis C Virus RNA replication through interaction with the viral NS5A protein. *PLoS pathogens,* 9**,** e1003302.

VON RORETZ, C. & GALLOUZI, I.-E. 2010. Protein kinase RNA/FADD/caspase-8 pathway mediates the proapoptotic activity of the RNA-binding protein human antigen R (HuR). *Journal of Biological Chemistry,* 285**,** 16806-16813.

VOTTELER, J. & SUNDQUIST, W. I. 2013. Virus budding and the ESCRT pathway. *Cell host & microbe,* 14**,** 232-241.

WANG, H., PERRY, J. W., LAURING, A. S., NEDDERMANN, P., DE FRANCESCO, R. & TAI, A. W. 2014. Oxysterol-binding protein is a phosphatidylinositol 4-kinase effector required for HCV replication membrane integrity and cholesterol trafficking. *Gastroenterology,* 146**,** 1373-1385. e11.

WANG, P. & HEITMAN, J. 2005. The cyclophilins. *Genome biology,* 6**,** 1-6.

WANG, Y., JIE, W., LING, J. & YUANSHUAI, H. 2021. HCV core antigen plays an important role in the fight against HCV as an alternative to HCV‐RNA detection. *Journal of Clinical Laboratory Analysis,* 35**,** e23755.

WARD, J. C., BOWYER, S., CHEN, S., CAMPOS, G. R. F., RAMIREZ, S., BUKH, J. & HARRIS, M. 2020. Insights into the unique characteristics of hepatitis C virus genotype 3 revealed by development of a robust sub-genomic DBN3a replicon. *The Journal of General Virology,* 101**,** 1182.

WATANABE, T., IMAMURA, T. & HIASA, Y. 2018. Roles of protein kinase R in cancer: Potential as a therapeutic target. *Cancer science,* 109**,** 919-925.

WATASHI, K., HIJIKATA, M., HOSAKA, M., YAMAJI, M. & SHIMOTOHNO, K. 2003. Cyclosporin A suppresses replication of hepatitis C virus genome in cultured hepatocytes. *Hepatology,* 38**,** 1282-1288.

WATASHI, K., ISHII, N., HIJIKATA, M., INOUE, D., MURATA, T., MIYANARI, Y. & SHIMOTOHNO, K. 2005. Cyclophilin B is a functional regulator of hepatitis C virus RNA polymerase. *Molecular cell,* 19**,** 111-122.

WEBB, G. W., KELLY, S. & DALTON, H. R. 2020. Hepatitis A and Hepatitis E: Clinical and epidemiological features, diagnosis, treatment, and prevention. *Clinical microbiology newsletter,* 42**,** 171-179.

WEINER, A. J., BRAUER, M. J., ROSENBLATT, J., RICHMAN, K. H., TUNG, J., CRAWFORD, K., BONINO, F., SARACCO, G., CHOO, Q.-L. & HOUGHTON, M. 1991. Variable and hypervariable domains are found in the regions of HCV corresponding to the flavivirus envelope and NS1 proteins and the pestivirus envelope glycoproteins. *Virology,* 180**,** 842-848.

WEK, R. C. 1994. eIF-2 kinases: regulators of general and gene-specific translation initiation. *Trends in biochemical sciences,* 19**,** 491-496.

WELBOURN, S., GREEN, R., GAMACHE, I., DANDACHE, S., LOHMANN, V., BARTENSCHLAGER, R., MEEROVITCH, K. & PAUSE, A. 2005. Hepatitis C virus NS2/3 processing is required for NS3 stability and viral RNA replication. *Journal of Biological Chemistry,* 280**,** 29604-29611.

WELSCH, S., MÜLLER, B. & KRÄUSSLICH, H.-G. 2007. More than one door–budding of enveloped viruses through cellular membranes. *Febs Letters,* 581**,** 2089-2097.

WELZEL, T. M., BHARDWAJ, N., HEDSKOG, C., CHODAVARAPU, K., CAMUS, G., MCNALLY, J., BRAINARD, D., MILLER, M. D., MO, H. & SVAROVSKAIA, E. 2017. Global epidemiology of HCV subtypes and resistance-associated substitutions evaluated by sequencing-based subtype analyses. *Journal of hepatology,* 67**,** 224-236.

WESTBROOK, R. H. & DUSHEIKO, G. 2014. Natural history of hepatitis C. *Journal of hepatology,* 61**,** S58-S68.

WILKINS, T., AKHTAR, M., GITITU, E., JALLURI, C. & RAMIREZ, J. 2015. Diagnosis and management of hepatitis C. *American family physician,* 91**,** 835-842.

WITTEVELDT, J., MARTIN-GANS, M. & SIMMONDS, P. 2016. Enhancement of the replication of hepatitis C virus replicons of genotypes 1 to 4 by manipulation of CpG and UpA dinucleotide frequencies and use of cell lines expressing SECL14L2 for antiviral resistance testing. *Antimicrobial agents and chemotherapy,* 60**,** 2981-2992.

WÖLK, B., SANSONNO, D., KRÄUSSLICH, H.-G., DAMMACCO, F., RICE, C. M., BLUM, H. E. & MORADPOUR, D. 2000. Subcellular localization, stability, and trans-cleavage competence of the hepatitis C virus NS3-NS4A complex expressed in tetracycline-regulated cell lines. *Journal of virology,* 74**,** 2293-2304.

WONG, A. H.-T., TAM, N. W. N., YANG, Y.-L., CUDDIHY, A. R., LI, S., KIRCHHOFF, S., HAUSER, H., DECKER, T. & KOROMILAS, A. E. 1997. Physical association between STAT1 and the interferon-inducible protein kinase PKR and implications for interferon and double-stranded RNA signaling pathways. *The EMBO Journal,* 16**,** 1291-1304.

WRENSCH, F., CROUCHET, E., LIGAT, G., ZEISEL, M. B., KECK, Z.-Y., FOUNG, S. K., SCHUSTER, C. & BAUMERT, T. F. 2018. Hepatitis C virus (HCV)–apolipoprotein interactions and immune evasion and their impact on HCV vaccine design. *Frontiers in immunology,* 9**,** 1436.

XU, G., XIN, X. & ZHENG, C. 2013. GPS2 is required for the association of NS5A with VAP-A and hepatitis C virus replication. *PLoS One,* 8**,** e78195.

XU, R., RONG, X., ARANDAY-CORTES, E., VATTIPALLY, S., HUGHES, J., MCLAUCHLAN, J. & FU, Y. 2022. The transmission route and selection pressure in HCV subtype 3a and 3b Chinese infections: evolutionary kinetics and selective force analysis. *Viruses,* 14**,** 1514.

XU, Y., MARTINEZ, P., SÉRON, K., LUO, G., ALLAIN, F., DUBUISSON, J. & BELOUZARD, S. 2015. Characterization of hepatitis C virus interaction with heparan sulfate proteoglycans. *Journal of virology,* 89**,** 3846-3858.

YAMAGA, A. K. & OU, J.-H. 2002. Membrane topology of the hepatitis C virus NS2 protein. *Journal of Biological Chemistry,* 277**,** 33228-33234.

YAMANE, D., FENG, H., RIVERA-SERRANO, E. E., SELITSKY, S. R., HIRAI-YUKI, A., DAS, A., MCKNIGHT, K. L., MISUMI, I., HENSLEY, L. & LOVELL, W. 2019. Basal expression of interferon regulatory factor 1 drives intrinsic hepatocyte resistance to multiple RNA viruses. *Nature microbiology,* 4**,** 1096-1104.

YAMASHITA, T., KANEKO, S., SHIROTA, Y., QIN, W., NOMURA, T., KOBAYASHI, K. & MURAKAMI, S. 1998. RNA-dependent RNA polymerase activity of the soluble recombinant hepatitis C virus NS5B protein truncated at the C-terminal region. *Journal of Biological Chemistry,* 273**,** 15479-15486.

YAN, X.-B., BATTAGLIA, S., BOUCREUX, D., CHEN, Z., BRECHOT, C. & PAVIO, N. 2007. Mapping of the interacting domains of hepatitis C virus core protein and the double-stranded RNA-activated protein kinase PKR. *Virus research,* 125**,** 79-87.

YANG, F., ROBOTHAM, J. M., GRISE, H., FRAUSTO, S., MADAN, V., ZAYAS, M., BARTENSCHLAGER, R., ROBINSON, M., GREENSTEIN, A. E. & NAG, A. 2010. A major determinant of cyclophilin dependence and cyclosporine susceptibility of hepatitis C virus identified by a genetic approach. *PLoS pathogens,* 6**,** e1001118.

YANG, F., ROBOTHAM, J. M., NELSON, H. B., IRSIGLER, A., KENWORTHY, R. & TANG, H. 2008. Cyclophilin A is an essential cofactor for hepatitis C virus infection and the principal mediator of cyclosporine resistance in vitro. *Journal of virology,* 82**,** 5269-5278.

YANG, J. & ZHANG, Y. 2015. I-TASSER server: new development for protein structure and function predictions. *Nucleic acids research,* 43**,** W174-W181.

YASUI, K., WAKITA, T., TSUKIYAMA-KOHARA, K., FUNAHASHI, S.-I., ICHIKAWA, M., KAJITA, T., MORADPOUR, D., WANDS, J. R. & KOHARA, M. 1998. The native form and maturation process of hepatitis C virus core protein. *Journal of virology,* 72**,** 6048-6055.

YEUNG, M. C., LIU, J. & LAU, A. S. 1996. An essential role for the interferon-inducible, double-stranded RNA-activated protein kinase PKR in the tumor necrosis factor-induced apoptosis in U937 cells. *Proceedings of the National Academy of Sciences,* 93**,** 12451-12455.

YIN, C., GOONAWARDANE, N., STEWART, H. & HARRIS, M. 2018. A role for domain I of the hepatitis C virus NS5A protein in virus assembly. *PLoS pathogens,* 14**,** e1006834.

ZAJĄC, M., MUSZALSKA, I., SOBCZAK, A., DADEJ, A., TOMCZAK, S. & JELIŃSKA, A. 2019. Hepatitis C–New drugs and treatment prospects. *European journal of medicinal chemistry,* 165**,** 225-249.

ZAMANIAN-DARYOUSH, M., MOGENSEN, T. H., DIDONATO, J. A. & WILLIAMS, B. R. 2000. NF-κB activation by double-stranded-RNA-activated protein kinase (PKR) is mediated through NF-κB-inducing kinase and IκB kinase. *Molecular and cellular biology,* 20**,** 1278-1290.

ZAYAS, M., LONG, G., MADAN, V. & BARTENSCHLAGER, R. 2016. Coordination of hepatitis C virus assembly by distinct regulatory regions in nonstructural protein 5A. *PLoS pathogens,* 12**,** e1005376.

ZEIN, N. N. 2000. Clinical significance of hepatitis C virus genotypes. *Clinical microbiology reviews,* 13**,** 223-235.

ZHANG, P. & SAMUEL, C. E. 2008. Induction of protein kinase PKR-dependent activation of interferon regulatory factor 3 by vaccinia virus occurs through adapter IPS-1 signaling. *Journal of Biological Chemistry,* 283**,** 34580-34587.

ZHANG, X. & ZHANG, K. 2012. Endoplasmic reticulum stress-associated lipid droplet formation and type II diabetes. *Biochemistry research international,* 2012.

ZHU, H. & BRIGGS, J. M. 2011. Mechanistic role of NS4A and substrate in the activation of HCV NS3 protease. *Proteins: Structure, Function, and Bioinformatics,* 79**,** 2428-2443.

ZONA, L., LUPBERGER, J., SIDAHMED-ADRAR, N., THUMANN, C., HARRIS, H. J., BARNES, A., FLORENTIN, J., TAWAR, R. G., XIAO, F. & TUREK, M. 2013. HRas signal transduction promotes hepatitis C virus cell entry by triggering assembly of the host tetraspanin receptor complex. *Cell host & microbe,* 13**,** 302-313.

ZYDOWSKY, L. D., ETZKORN, F. A., CHANG, H. Y., FERGUSON, S. B., STOLZ, L. A., HO, S. I. & WALSH, C. T. 1992. Active site mutants of human cyclophilin A separate peptidyl‐prolyl isomerase activity from cyclosporin A binding and calcineurin inhibition. *Protein Science,* 1**,** 1092-1099.

Chapter 9: Appendix

Mutants	Backbones
WT	mSGR-Luc-JFH1, mJFH1, SGR-Luc-DBN3a, pET28a-sumo-NS5A Domain I
I52A	mSGR-Luc-JFH1, mJFH1, pET28a-sumo-NS5A Domain I
V52A	SGR-Luc-DBN3a
V67A	mSGR-Luc-JFH1, SGR-Luc-DBN3a
G70A	mSGR-Luc-JFH1, mJFH1, SGR-Luc-DBN3a
S71A	mSGR-Luc-JFH1, mJFH1
M72A	mSGR-Luc-JFH1, mJFH1, SGR-Luc-DBN3a,
P102A	mSGR-Luc-JFH1
Y106A	mSGR-Luc-JFH1
W111A	mSGR-Luc-JFH1
P141A	mSGR-Luc-JFH1, mJFH1, SGR-Luc-DBN3a,
C142A	mSGR-Luc-JFH1, mJFH1, pET28a-sumo-NS5A DomianI
Q143A	mSGR-Luc-JFH1, mJFH1,
P145A	mSGR-Luc-JFH1, SGR-Luc-DBN3a
P147A	mSGR-Luc-JFH1, mJFH1,
E148A	mSGR-Luc-JFH1, mJFH1, SGR-Luc-DBN3a
F149A	mSGR-Luc-JFH1
C190A	mSGR-Luc-JFH1, mJFH1, pET28a-sumo-NS5A Domain I
E191A	mSGR-Luc-JFH1, mJFH1, pET28a-sumo-NS5A Domain I

Appendix Table 9.1 List of mutants generated in the course of this study.

Host factors	Backbones
CypA	pGEX-4T-1, pHIV-SIREN
CypA-H126Q	pGEX-4T-1
CypB	pHIV-SIREN
PKR	pcDNA 3.1 (+), pLentiCRISPRv2
RIG-I	pLentiCRISPRv2
IRF1	pLentiCRISPRv2

Appendix Table 9.2 List of host factors used in the course of this study.

Mutants		Quickchange Primer
I52A	Forward	GGCACTGGCGCGATGACCACGCGCT
	Reverse	GGCCCACACACCCTTGTACCCCTT
G70A	Forward	CGCCTGGCGTCTATGAGGATCACAGGGCC
	Reverse	GACATTGCCAGAGATGTTGGCGC
S71A	Forward	CTGGGCGCGATGAGGATCACAGGGCC
	Reverse	GCGGACATTGCCAGAGATGTTGGCG
M72A	Forward	CTGGGCTCTGCGAGGATCACAGGGCC
	Reverse	GCGGACATTGCCAGAGATGTTGGCG
P102A	Forward	GCGCCGAAAGCGCCCACGAACTACAA
	Reverse	GCACTGGCCCTCCGTGTAGCAAT
Y106A	Forward	CCCCCCACGAACGCGAAGACCGCCA
	Reverse	TTTCGGCGCGCACTGGCCCTC
W111A	Forward	GCCATCGCGAGGGTGGCGGCCTC
	Reverse	GGTCTTGTAGTTCGTGGGGGGTTTC
P141A	Forward	TGAAAATTGCGTGCCAACTACCTTCTCT
	Reverse	ATTGTCAGTGGTCAGTCCTGTTAC
C142A	Forward	CTGAAAATTCCTGCGCAACTACCTTCTCCAG
	Reverse	ATTGTCAGTGGTCAGTCCTGTTAC
Q143A	Forward	CCTTGCGCGCTACCTTCTCCAGAGTTT
	Reverse	AATTTTCAGATTGTCAGTGGTCAGTC
P147A	Forward	CCTTCTGCGGAGTTTTTCTCCTGGG
	Reverse	TAGTTGGCAAGGAATTTTCAGATTGTC
E148A	Forward	CCTTCTCCAGCGTTTTTCTCCTGGGTGG
	Reverse	TAGTTGGCAAGGAATTTTCAGATTGTC
F149A	Forward	CCAGAGGCGTTCTCCTGGGTGGACGG
	Reverse	AGAAGGTAGTTGGCAAGGAATTTTCAG
C190A	Forward	CAGCTTCCCGCGGAACCTGAGCCCGA
	Reverse	GGACCCGACAGCATAGGAATTAAG
E191A	Forward	CAGCTTCCCTGTGCGCCTGAGCCCGA
	Reverse	GGACCCGACAGCATAGGAATTAAG

Appendix Table 9.3 List of oligonucleotide primers used to generate mutations in mJFH1 NS5A Domain I.

Mutants		Quickchange Primer
V52A	Forward	GGGGACGGTGCGATGTCA ACGCGCTG
	Reverse	CGTTGACATCGCACCGTCCCCC
V67A	Forward	GCCGGCCATGCGAAGAATGGGTC
	Reverse	CCCATTCTTCGCATGGCCGGCTATTG
G70A	Forward	GTGAAGAATGCGTCCATGCGGCTTG
	Reverse	CCGCATGGACGCATTCTTCACATGG
M72A	Forward	GAATGGGTCCGCGCGGCTTGCGGGGCCGC
	Reverse	CAAGCCGCGCGGACCCATTCTTCACATGGCCGGC
P141A	Forward	CTCAAGTGTGCGTGCCAAGTGCCG
	Reverse	CACTTGGCACGCACACTTGAGCTCAT
P145A	Forward	CAAGTGGCGGCTGCTGAGTTCTTTACTG
	Reverse	CAGCAGCCGCCACTTGGCAC
E148A	Forward	GCCGGCTGCTGCGTTCTTTACTG
	Reverse	AAAGAACGCAGCAGCCGGCAC

Appendix Table 9.4 List of oligonucleotide primers used to generate mutations in SGR-Luc-DBN3a NS5A Domain I.

Mutants		Quickchange Primer
His-Sumo-NS5A DI 35-215	Forward	CTGCCCGGATCCCCCTTCATCTCTTGTCAAAAGGG
	Reverse	CGTGCCCTCGAGTTACGCCGCAGTCTCCGCCGTG
His-Sumo-NS5A DI 35-249	Forward	CTGCCCGGATCCCCCTTCATCTCTTGTCAAAAGGG
	Reverse	CGTGCCCTCGAGTTAGGTGTTGCTGTGGGTGGTGCAGG
PCDNA3.1-PKR	Forward	CGCGGATCCATGGCTGGTGATCTTTCAGCA
	Reverse	CCGCTCGAGCTAACATGTGTGTCGTTCATTTT

Appendix Table 9.5 List of oligonucleotide primers used to generate His tagged NS5A Domain I and PKR for GST-pulldown and His-pulldown assay.

NS5A domain I fragment with mutations was PCR amplified using different templates (mJFH1 WT, I52A ,C142A, C190A and E191A)a nd then cloned into PET-28a-sumo vector via *BamHI/XhoI* restriction sites. PKR was amplified from Huh7 RNA and cloned into pcDNA3.1 vector using *BamHI/XhoI* restriction sites to construct pcDNA3.1-PKR.